TABLE OF CONTENTS

Page

LIST OF TABLES

LIST OF FIGURES

LIST OF ABREVIATIONS

ETS	École de Technologie Supérieure
MMR	Mobile Manipulator Robot
GREPCI	Groupe de Recherche en Électronique de Puissance et Commande Industrielle
VDC	Virtual Decomposition Control
DoF	Degree of Freedom
APF	Artificial Potential Field
RAMP	Real Time Adaptive Motion Planning
RTW	Real-Time Workshop
FVP	Flow of Virtual Power

LISTE OF SYMBOLS AND UNITS OF MEASUREMENTS

UNITS OF MEASUREMENT

m	meter
rad	radian
Nm	Newton meter
s or sec	second
deg	degree
N	Newton

SYMBOLS

XYZ	Cartesian coordinate system main axes
$X_oY_oZ_o$	center of gravity coordinate object axes
X_o	position of the object
V_o	linear/angular velocity of the object
X_e	position of the mobile manipulator end-effectors
V_e	linear/angular velocity of the mobile manipulator end-effector
${}^{A}U_B$	force/moment transformation matrix from frame A to frame B
${}^{*}F_r$	required net force/moment vector
τ^*	net torque for the joint
τ_B	link force/moment vector
τ	control torque

M	the symmetric positive definite inertia matrix
C	Coriolis and centrifugal matrix terms
G	gravitational vector terms
Y	regressor matrix
θ_B	link parameters vector
θ_{ai}	joint parameters vector
$\hat{\theta}_B$	estimated link parameters vector
$\hat{\theta}_{ai}$	estimated joint parameters vector
J_o	Jacobian matrix from the object frame to the mobile manipulator end-effectors
J_e	Jacobian matrix
F_I	Internal forces vector
λ_I	Lagrange multiplier

INTRODUCTION

Robotics as it is known today is an interdisciplinary science encompassing vast fields of research: vision, planning, motion / control, locomotion, design, and so on. The objective of the creation of robots in the early sixties was to relieve man of some tedious work such as: handling, repetitive tasks that are often tiring or even sometimes infeasible manually. Following this situation, several kinds of manipulators were created (Siciliano and Khatib (2016)).

Historically, the first more manufactured robots were the manipulator arms, which are widely used in industry. These robotic systems have the ability to act on the environment through the realization of manipulation tasks such as the grasping of objects, the assembly of pieces, etc. They are nevertheless very limited in their operational workspace and in the type of work that can be done. This is why mobile platforms, characterized by their ability to evolve in larger size environments, have appeared. These mobile platforms were first developed for navigation, maintenance or surveillance operations, in particular in hostile environments, by equipping them with various sensors (cameras, gas detectors, radioactivity detectors, etc.). For missions in a hostile, spatial environment, or simply those requiring combined locomotion and manipulation capabilities, these platforms had to be equipped with a manipulator arm to become mobile manipulators. The well known examples of mobile manipulators, more or less automated, are the truck-mounted cranes, satellite arms, submarines exploring the seabed or extra-planetary exploration vehicles. Basically, the exploitation of such systems relies on the implementation of a series of sequences:

a. A transport phase, where only the degrees of mobility of the platform are used, in order to bring the manipulator arm to the manipulation site;

b. A manipulation phase during which the base remains fixed, and where only the degrees of mobility of the arm are used;

c. A phase of coordination or transporting an object where both the degrees of mobility of the platforms and the degrees of mobility of the arm are used.

Some tasks requiring the handling of a heavy object are difficult to achieve by only one mobile manipulator. Multiple mobile manipulators can complete tasks in coordination which are difficult or impossible for a single robot. However, one of the most important problems remains the cooperation, planning and coordination of movements within a control / command architecture in a multi-robot context. The study of multi-robot systems has become a major concern in the field of robotic research, because whatever the capabilities of a single robot, it remains spatially limited. However, this significantly complicates the robotic system as its control design complexity increases greatly. The problem of controlling the mechanical system forming a closed kinematic chain mechanism lies in the fact that it imposes a set of kinematic constraints on the coordination of the position and velocity of the mobile manipulator. Therefore, there is a reduction in the degrees of freedom for the entire system. Further, the internal forces of the object produced by all mobile manipulators must be controlled. Few research works have been proposed to solve the control problem of these robotic systems, which have high degrees of freedom and are tightly interconnected because all their manipulators are in contact with the object.

The aim of this thesis is to propose and validate experimentally a nonlinear control approach for a group of manipulator arms mounted on mobile platforms transporting a rigid object in coordination. The idea is to develop a nonlinear control law (decentralized, adaptive, by sliding mode or control by virtual decomposition,...) ensuring stability of the interconnected robotic systems.

The organization of this thesis is given as follows: Chapter 1 presents the research objectives, the literature review, the methodology objectives and the originality of the work. Subsequently, Chapters 2, 3, 4, 5, and 6 present the main results of the work in the form of papers, submitted

for (Chapters 2, 5 and 6) or accepted and published (Chapters 3 and 4). The main contributions of this works are summarized as follows:

The first chapter of this thesis outlines the problem of research. First, the identification and justification of the research problem are detailed in this chapter, where the problematic that validates the present work is presented. A state-of-the-art of the existing literature in this area of research is given. Then, the objectives of this work, general and more specific, are declared. Finally, an overview of the methodology used is given.

In chapter 2, a model of the complete system is given, this model was used in the numerical simulation and experimental validation. In this chapter, a general formulation and stability analysis of the different approach of control developed and implemented in this thesis are given to help understand the chapters based on the papers published or submitted.

Chapter 3 presents an experimental validation of a novel adaptive control based on the virtual decomposition approach applied for formation control of virtual leader-follower mobile robots formation. In this work, we propose a kinematic control law based on the choice of a potential function, combined with an adaptive dynamic control scheme based on virtual decomposition control (VDC) for the leader-follower formation. The leader is a virtual robot represented by its dynamic model and is considered as a leader, and the followers are real robots.

Chapter 4 presents a numerical simulation and an experimental validation of a novel adaptive control based on the virtual decomposition approach applied for multiple mobile manipulator robots transporting rigid object in coordination. In this work, all parameters of the robotic system were considered uncertain and were estimated by using the virtual decomposition approach. The global asymptotic stability of the entire system was proved by the principle of the virtual stability of each subsystem.

Chapter 5 presents a numerical simulation and an experimental validation of a novel adaptive control based on the Lyapunov technique applied for multiple mobile manipulator robots cooperatively handling a common rigid object in coordination. In this work, the parameter uncertainties are estimated using the virtual decomposition approach and the controller was developed based on the appropriate choice of Lyapunov function. The global stability of the system was proved based on the Lyapunov approach.

Chapter 6 presents a real time coordinated adaptive control based on the virtual decomposition approach combined with the backstepping approach. It was applied for multiple mobile manipulator robots handling rigid object. In this work, the parameter uncertainties are estimated using the virtual decomposition approach and the controller was developed based on the backstepping control. The stability of the entire system was proved by choosing an appropriate Lyapunov function and by using the virtual work method.

Chapter 7 presents an adaptive coordinated control based on the sliding mode approach applied for multiple mobile manipulator robots transporting a rigid object. In this work, we were designed an adaptive control in which the parameters uncertainties and the perturbations were estimated by using the adaptive update techniques. The proposed control schemes ensure a good tracking errors of the system under which these errors converge to zero and the tracking error of the internal force stays bounded. All through this work, the designed control law and the global stability analysis were carried out based on the appropriate choice of the candidate Lyapunov function.

CHAPTER 1

RESEARCH PROBLEM

The objective of the creation of robots in the early sixties was to relieve human of some tedious work such as: manipulation and repetitive tasks which are often tiring or even sometimes infeasible manually. Following this situation, several kinds of robots were created. For some tasks the use of a single robot is impossible which necessitates the coordination of multiple robots to execute correctly these tasks.

In order to control and coordinate a multi-agent systems, various architectures and approaches have been developed (Wen *et al.* (2014), Wen *et al.* (2016), Aranda *et al.* (2015)). Many contributed works on multi-agent formation control have been performed using mobile robots (Panagou *et al.* (2016), Yu and Liu (2016a), Khan *et al.* (2016)), helicopter (Shaw *et al.* (2007)), underwater vehicles (Yin *et al.* (2016), Li *et al.* (2016)) and quadcopters (Vargas-Jacob *et al.* (2016), Kang and Ahn (2016)). The multiple mobile manipulators are one of the most important categories of these robotic systems. The coordinated control of multiple mobile manipulators has attracted the attention of many researchers (Tanner *et al.* (2003), Chinelato and de Siqueira Martins-Filho (2013), Khatib *et al.* (1996b) and Sugar and Kumar (2002)). Interest in these systems is due to the greater capability of mobile manipulators in performing more complex tasks requiring skills that cannot be accomplished by a single mobile manipulator, which significantly complicates the robotic system, and greatly increases its control design complexity. The problem with controlling a mechanical system forming a closed kinematic chain mechanism is that it imposes a set of kinematic constraints on the coordination of the position and velocity of the mobile manipulator, thus leading to a reduction in the degrees of freedom of the entire system. Although the object internal forces produced by all mobile manipulators must be controlled, few works have been proposed to solve this control problem for this category of robotic systems, which have high degrees of freedom and are tightly interconnected because all manipulators are in contact with the object. The aim of the proposed

nonlinear approaches is to be able to control multiple mobile manipulator robots transporting a rigid object in coordination under parameters uncertainties and disturbances.

1.1 Literature review

Most research works in this field of the robotic system have thus far focused on the three main coordination mechanisms involved: motion planning, the leader-follower control approach and centralized/decentralized control.

1.1.1 Motion planning

Motion planning is one of the fundamental problems in robotics, this approach has been covered in some studies from the perspective of a group of MMRs (which is another fundamental problem in robotics, especially in multi-robot systems), where several robots perform the task of transporting an object in cooperation, in a known or unknown environment.

These studies include those presented in (LaValle (2006), Latombe (2012), Khatib (1985)). Morn Benewitz in (Bennewitz *et al.* (2001)) proposed a planning technique based on a "hill-climb" coast algorithm to optimize the robot trajectory. Another structure for planning optimal trajectories was introduced in (Desai and Kumar (1997)) for two mobile manipulators pushing a common object to a desired location. The authors in (Yamamoto and Fukuda (2002), Guozheng *et al.* (2002)) proposed a control method for multiple mobile manipulators holding a common object. The measures of kinematic and dynamic manipulability are given, taking into account collision avoidance. However, the dynamics of the object are ignored. In Guozheng *et al.* (2002) the authors have proposed a real-time trajectory planning approach for multiple mobile robots. In this approach, the robot considers only the problem of collision with the robot that has a higher priority.

In Furuno *et al.* (2003), a trajectory planning method for a group of mobile manipulator robots in cooperation, which takes into consideration the dynamic characteristics of mobile manipulators and the object to be grasped, was proposed. The dynamics are composed of equations

of the motion of mobile manipulators, the movements of the object, the non-holonomic constraints of mobile platforms and the geometric constraints between the end-effectors and the object. In Sun and Gong (2004b), Zhu and Yang (2003), a planning approach based on genetic algorithms was proposed. A navigation approach of non-holonomic mobile robots in a dynamic environment was proposed in Gakuhari *et al.* (2004). In this study, the information about the environment and the robots are fed back into the system in real time. The global motion planning is executed cyclically.

These approaches are mainly used in the case where the environment is known, which means that the robots have prior knowledge of the environment. Planning motion in an unknown environment for a group of mobile robots is rarely reported in the literature. Khatib (1986) proposed a novel motion planning approach based on the artificial potential field (APF) method applied for an unknown environment. It has been used successfully in trajectory planning for mobile robots and manipulator robots. However, some of the researchers have applied the APF in motion planning for a group of mobile robots in an unknown environment such as in (Zheng and Zhao (2006)).

However, none of the previous works has studied this problem of motion planning in the case of high degree of freedom mobile manipulators tightly interconnected and performing tasks in coordination in the presence of dynamic obstacles. In fact, there is relatively little research on motion planning in an unknown dynamic environment, even for a single mobile manipulator. Only a few researchers have examined the avoidance of local obstacles by a mobile manipulator as those given in (Mbede *et al.* (2004), Brock *et al.* (2002), Tan and Xi (2001)) and (Ogren *et al.* (2000b), Ogren *et al.* (2000a)).

Vannoy and Jung in (Vannoy and Xiao (2007a)) discussed the problem of motion planning for a pair of mobile manipulators moving a common object, thus forming a closed chain in an unknown dynamic environment. They presented a new approach to planning the high-dimensional movements of the robot team in real time with a dynamic "leader-helpers" architecture where the leader is selected according to the situations using a "Switch" selector. This

approach was based on the Real Time Adaptive Motion Planning (RAMP) paradigm introduced in (Vannoy and Xiao (2007b)) and (Vannoy and Xiao (2006)), in order to plan the leader's movement. In Bolandi and Ehyaei (2011), Hekmatfar *et al.* (2014) the authors were interested in the problem of trajectory planning for two MMs transporting a payload in presence of obstacles. This work represents a control strategy to successfully complete the cooperative transport of the object while avoiding obstacles. In addition to what was discussed above, many other research works have been proposed such as (Desai and Kumar (1997), Furuno *et al.* (2003), Tzafestas *et al.* (1998), Iwamura *et al.* (2000)).

1.1.2 The leader-follower approach

The leader-follower architecture is the second approach used for the coordination of multiple mobile manipulators. In this approach, a single or a group of MMRs is designated as a leader trying to follow a desired trajectory, while the other group members follow the leaders. This control approach was addressed in (Chen and Li (2006), Hirata *et al.* (2004a), Tang *et al.* (2009)). In Fujii *et al.* (2007), the authors introduced the notion of virtual leader, in which every follower considers the rest of the team (leader and other followers) as constituting the virtual leader. The trajectory of the follower robot converges towards the trajectory of the leader if: Each follower is controlled by the desired trajectory of his virtual leader (as a reference) once the trajectory of the virtual leader is estimated accurately and as long as each follower estimates the trajectory of his virtual leader with precision all the followers finally estimate the real trajectory of the leader.

All that has been seen in the literature on the problem of the cooperation of multiple mobile manipulators carrying an object was studied under the assumption that the manipulators are rigidly attached to the object, that is to say that no relative movement exists between the object and the end-effectors. But in this study (Fujii *et al.* (2007)), the authors used a "lead-followers" control algorithm under constraint that the manipulators do not hold the object rigidly, but there is a slip effect because of the effector used, this phenomenon is known as "Loose handling" or free handling, using a hook effector.

In Li *et al.* (2007) and (Li *et al.* (2009), the authors propose a method that can be applied for tasks requiring a relative motion between the handled object and the effector of the manipulators such as assembly of parts or in an operation of welding where the object is held rigidly (closed) on one side by a manipulator and on the other side there will be movement between the object and the end-effector of the second manipulator. In Kosuge and Oosumi (1996) and Kosuge *et al.* (1999), a leader-follower approach was applied for mobile robots transporting a single object. In these works, sub-groups consisting of the real leader and the other followers were represented by a "virtual leader". The followers estimate the position of the virtual-leader online, then move according to this estimated position. Then this idea was extended and implemented to control a group of mobile manipulators (Kume *et al.* (2007)). Differently with what was used in (Kosuge and Oosumi (1996), Kosuge *et al.* (1999)), in this work the force was estimated by using the robot dynamics where they consider that the robot parameters are accurately identified. In Hirata *et al.* (2004b), a leader–follower approach of multiple mobile manipulators handling a rigid object was proposed. In this algorithm, the representative point of each robot was controlled as a caster-like dynamics in three-dimensional space.

1.1.3 Hybrid centralized/decentralized control

In this approach the position and the internal force are controlled in a given direction of the workspace. The first one is the centralized control, in which the robotic system is regarded as one system and the controller is designed for the full system. The second one is the decentralized control, in which the robotic system is decomposed into several subsystems forming the full system, then controllers for each subsystem are designed separately and no coupling is considered. In Tanner *et al.* (2003) and Tanner *et al.* (1998), modelling and centralized coordinating control were applied for a group of mobile manipulator robots transporting a deformable object in presence of obstacles. In Chinelato and de Siqueira Martins-Filho (2013), modelling and control law were developed for two mobile manipulators robots to execute performed tasks, where subtasks were simulated including transport and manipulations tasks.

Khatib *et al.* (1996b) and Khatib *et al.* (1996a) proposed an extension of the four methods developed initially for a manipulator arms mounted on a fixed-base including : 1) the formulation of the operational space is focused on robot motion tasks and force control, 2) Of a macro / mini structure to increase the mechanical bandwidth of the robotic system; 3) the augmented object model for manipulating objects in a multiple arm robot systems; and 4) the model of a virtual link for the characterization and control of internal forces in a multi-arm system to manipulator arm mounted on holonomic bases, with a novel command for decentralized cooperation tasks.The authors in (Sugar and Kumar (2002)) addressed the coordinated feedback control applied to a small team of collaborative mobile manipulators performing tasks, such as grasping a large flexible object and transporting it in a two-dimensional environment in the presence of obstacles. Under the assumption that each mobile manipulator is equipped with a specific effector, that allows it to exercise controlled forces in the plane. In other words, the effector can only push the object.

(Kosuge *et al.* (1999), Kosuge and Oosumi (1996), Hirata *et al.* (1999)) proposed a control algorithm based on the geometric constraints between the contact points and the point representing the object which reduces the effect of sensor noise. Then this algorithm was extended to a decentralized control algorithm and applied for multiple mobile robots moving a rigid object in coordination. Based on what was done in Kosuge and Oosumi (1996),Kosuge *et al.* (1999), Kume *et al.* (2007) proposed a decentralized control law, in which they introduced the notion without a torque / force sensor. In Shao *et al.* (2015) a distributed control combined with observer state was designed for multi-agent robotic systems. In Sayyaadi and Babaee (2014) a decentralized approach based input-output linearisation method is proposed to design an independent controller for each robot, each robot has a three degrees of freedom manipulator arm mounted on platform mobile. A partially and fully decentralized controller applied to cooperating control of load manipulation by a team of mobile manipulators robots were proposed in Petitti *et al.* (2016). This approach was numerically simulated in presence of sensor noise. In Dai and Liu (2016) the authors proposed a distributed coordination/cooperation control for interconnected mobile manipulators with time delays, the decoupled dynamics is considered in

which the task and the null space of the mobile manipulators were designed to achieve different missions.

Most of these proposed approaches of control explained above have been designed under the assumption that the geometric relations between the robots are known with precision. But, in practice it is difficult to know these geometrical relations between the robots precisely, especially when the robots manipulate an unknown common object. There may be errors in the position / orientation of each mobile robot detected by a navigation system due to slippage between the wheels and the ground. Even if the geometric relationships between the robots are measured, these geometric relationships could not be more precise because of the errors included in the orientation/position information of each robot. To overcome these problems, a coordinated motion control algorithm of multiple mobile robots, which is robust against positioning errors, was designed by Kume *et al.* (2001). In this paper, the authors propose a decentralized control law of several mobile manipulators manipulating a single object in coordination without using the geometrical relations between them. The proposed control algorithm is experimentally applied to three manipulator arms mounted on holonomic platform mobile.

In Farivarnejad *et al.* (2016), a decentralized control approach based on sliding mode control was applied for multiple robots, differently from the previous cited works. In this paper, the authors assumed that the controllers do not require knowledge of the load dynamics and geometry of the handling load.

1.2 Research objectives and methodology

As discussed above, all studies based on the classical methods such as the Lagrangian or the Newton/Euler approaches, require a good knowledge of the parameters of the system. In practical terms, this is not true, and the resulting model is generally uncertain. The parameters' uncertainties, the high nonlinearity, and the interconnected kinematics and dynamics coupling of these categories of robotic systems greatly complicate the control problem and make it difficult to solve by using only the known classical approaches explained earlier. A group of many

mobile manipulators holding an object in coordination is one of the most important in these classes of robotic systems. Many research works in this area were proposed and developed, such as in (Chen (2015), Zhao *et al.* (2016), Liu *et al.* (2016), Li and Ge (2013)). This is due to the fact that such robotic systems have been implemented in most modern manufacturing applications. To overcome this serious problem of uncertainties, the adaptive control of robotic systems with high degrees of freedom has been receiving increasing attention in recent years. Some researchers have proposed an adaptive control approach (Karray and Feki (2014)), and others have proposed and intelligent adaptive control based on a neural networks scheme (Liu *et al.* (2014), Liu and Zhang (2013),Liu *et al.* (2013), Li and Su (2013)) and a fuzzy logic approach (Mai and Wang (2014), Wang *et al.* (2014), Li *et al.* (2013)).

The main objective of this project is to develop a nonlinear adaptive coordinated control for a group of mobile manipulator robots transporting a rigid object. Differently to what was done in the literature, in this work, the developed decentralized adaptive controls are not based on the full dynamic of the interconnected robotic systems. The robotic systems with high number of degrees of freedom were decomposed into many simple subsystems. This decomposition simplified the control and the adaptation of the parameters and made them very easy. To achieve this main objective, two identical mobile manipulator robots were used. The mechanical part and the electronic hardware were developed in the first part of this project, then all the developed control laws were implemented in real time.

1.2.1 Development of an experimental platform

To achieve our objective, two identical mobile manipulator robots were developed, the mechanical part was mounted in the GRÉPCI/ÉTS laboratory as illustrated in Figure 1 b. For the electronic part, the platform of each mobile manipulator has four wheels, where only the two front wheels are actuated by two HN-GH12-2217Y DC motors (DC-12V-200RPM 30:1), and the angular positions were given using encoder sensors (E4P-100-079-D-H-T-B). All joints of the manipulator arm were actuated by Dynamixel motors (MX-64T). As low level control an Atmega 32 micro-controller is used is shown in Figure 1.1 a. All developed nonlinear control

schemes were implemented in real time using of Mathworks® Real-Time Workshop (RTW). A Zigbee technology communication system was used between the mobile manipulator robots and the application program implemented in Simulink Mathworks®.

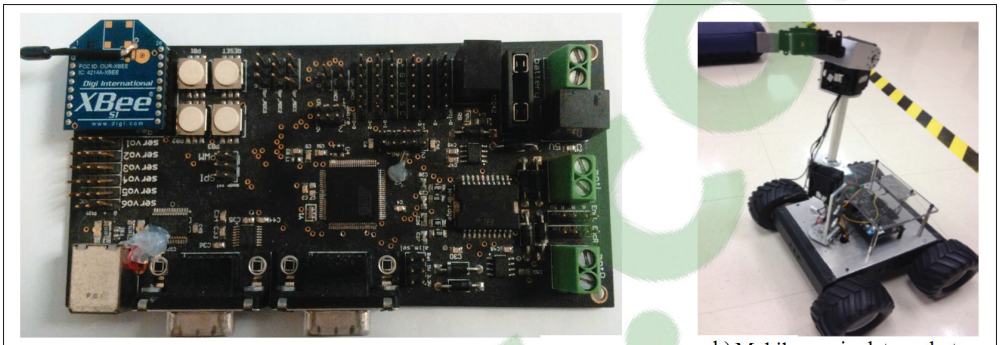

Figure 1.1 Experimental platform

1.2.2 Development of the nonlinear control laws

Different control approaches were studied. The uncertainties, the high nonlinearity, and the tight kinematics and dynamics coupling characterizing such systems greatly complicate the control problem and make it difficult to solve using the classical approaches explained earlier. To solve this serious problem many adaptive coordinated control laws were proposed and implemented in real time. These approaches can be summarized as follows:

a. An adaptive coordinated control applied to leader-follower formation of mobile robots was developed. A kinematic control law of the formation was developed based on the choice of potential function, and combined with the virtual decomposition approach to ensure a good formation tracking and parameters adaptation;

b. An adaptive decentralized control based on the virtual decomposition was developed and applied to a 7 DoF manipulator robot named ANAT robot (Brahmi *et al.* (2013b)), and then this approach was applied for mobile manipulators (Brahmi *et al.* (2016b)). The

proposed approach was extended and applied to a group of mobile manipulator robots handling a rigid object in coordination (chapter 4);

c. A novel decentralized adaptive control based on the approach proposed in chapter 4 was applied to tracking control of mobile manipulators (Brahmi *et al.* (2016b)) and then extended to multiple mobile manipulators transporting a rigid object. In this work, the stability analysis and the control law were designed based on the appropriate choice of Laypunov function where the virtual decomposition approach was used to simplify the parameters' adaptation of the robotic systems (chapter 5);

d. An adaptive backstepping control was developed and implemented for the tracking control of mobile manipulators (Brahmi *et al.* (2016a), Brahmi *et al.* (2017)) and then this approach was extended and applied to control a group of mobile manipulators moving an object in coordination. In this work the virtual decomposition approach was combined with the backstepping method to ensure the stability and tracking control (chapter 6);

e. Finally, an adaptive coordinated control based on the sliding mode approach combined to the potential field function was designed and applied to a group of mobile manipulator robots transporting a rigid object in coordination (chapter 7). This novel adaptive coordinated control scheme ensures a good position/force trajectory tracking, under parameters uncertainties and disturbances. This proposed control law can also minimize greatly the chattering phenomena when the sliding surface is close to zero which is not possible with the conventional sliding mode.

1.3 Originality of the research and contribution

This research focuses on the development of nonlinear control laws to ensure the stability of tracking error dynamics for multiple mobile manipulator robots transporting a rigid object in coordination. Following the literature review, although several studies deal with the control of multiple mobile manipulators executing tasks in coordination, few of them take a precise look on the high nonlinearity and uncertainties of the parameters where the majority of them

consider that the dynamic model of the interconnected system is known. In practical terms, this is difficult, and the resulting model is generally uncertain. To solve this problem of modelling and dynamic control in the presence of uncertainty, some researchers have proposed an adaptive control approach based on the complete dynamic of the robotic system. In this project, we propose different adaptive decentralized approaches. In contrast with what appears in the cited works, this thesis enriches the knowledge in the field through the following contributions:

a. By using the virtual decomposition approach, several major advantages are obtained, with the main ones being that:

   - The whole dynamics of the system can easily be found based on the individual dynamics of each subsystem, even in the presence of a change in the system configuration. In this case, adding a new robot or removing a faulty one from the system does not require a recalculation of the full dynamics of the system;
   - the schemes render the system control design very flexible and greatly facilitate the calculation of the dynamic system, with respect to changes in the system configuration;
   - They render the adaptation of the uncertain parameters very simple and systematic.

b. The global stability of the complete system is proven based on the appropriate choice of Lyapunov functions using the virtual stability of each subsystem, based on the principle of virtual work. Contrary to the original VDC stability analysis, in this works, all parameters are estimated and considered completely unknown, with unknown limits;

c. To solve the problem of parameter adaptation and modelling of systems using standard approaches; Firstly, a VDC approach based on an appropriate choice of Lyapunov function was proposed, then this approach (VDC) was combined with backstepping control to ensure a good workspace position tracking;

d. We designed an adaptive coordinated control based on the sliding mode approach in which the parameters uncertainties and the perturbation are estimated by the adaptive update

techniques. The proposed control ensures good tracking errors of the system under which these errors converge to zero and the tracking error of the internal force stays bounded; in addition, this controller limits perfectly the chattering phenomena when the sliding surface is close to zero;

e. To achieve our objective an experimental platform was developed in which all designed control laws were implemented.

CHAPTER 2

MODELLING SYSTEM AND APPROACH OF CONTROL

The dynamic model of a mechanical system establishes the relationship between the forces applied to the system and its coordinates, velocities and generalized accelerations. Depending on the application, this model may take different forms. The first is called explicit and one of the most explicit formalism used is the Lagrangian formalism. The model can also take an implicit form. This is the case of the Newton-Euler formalism which, furthermore, takes a recursive form. The explicit form permits the study of the properties of the model of a system and can be obtained in a systematic method. The second form is rather adapted to the real time calculations of the quantities describing the evolution of the system with time. We are interested here in two formalisms, Lagrange, which, in addition to describing the dynamics of the system in the form of simple (non-recursive) equations, is very general and permits, for example, non-holonomic links, and to the virtual decomposition approach that is based on the Newton-Euler method, which makes it possible to simplify the modelling of systems with many degrees of freedom.

2.1 Modelling system

We recall that the general equation of the dynamics of a mechanical system is given by:

$$\frac{d}{dt}\left(\frac{\partial L(q,\dot{q},t)}{\partial \dot{q}_i}\right) - \left(\frac{\partial L(q,\dot{q},t)}{\partial q_i}\right) = Q_i, \qquad (1 \leq i \leq n) \tag{2.1}$$

This result is the expression of the principle of the virtual powers, expressed in terms of the kinetic energy $L(q,\dot{q},t)$ of the system.

Q_i is called the power coefficient for the generalized real force associated with the parameter q_i. It is a force when q_i is a displacement and a torque when q_i is an angle. $q_i, \dot{q}_i, \ddot{q}_i \in \mathbb{R}^n$ are respectively the generalized coordinates vector, the joint velocity and the acceleration.

Wheeled mobile manipulators are nonholonomic systems and therefore incompletely parameterized. The dynamic expression given in (2.1) can be rewritten as:

$$\frac{d}{dt}\left(\frac{\partial L(q,\dot{q},t)}{\partial \dot{q}_i}\right) - \left(\frac{\partial L(q,\dot{q},t)}{\partial q_i}\right) = Q_i + J(q) f_i, \tag{2.2}$$

where f is the constraint force corresponding to holonomic and nonholonomic constraints and J is the jacobian matrix. The dynamic model of the the i-*th* mobile manipulator robot based on (2.2) can be obtained as follow:

$$M_i(q_i)\ddot{q}_i + C_i(q_i,\dot{q}_i)\dot{q}_i + G_i(q_i) = E_i\tau_i + J_{ie}(q_i) f_i, \tag{2.3}$$

where $M_i(q_i) \in \mathbb{R}^{n\times n}$ is the inertia matrix, $C_i(q_i,\dot{q}_i) \in \mathbb{R}^{n\times n}$ represents the Centripetal and Coriolis terms, $G_i(q_i) \in \mathbb{R}^n$ is the vector of gravity, $q_i = \begin{bmatrix} q_{iv} & q_{ia} \end{bmatrix}^T \in \mathbb{R}^n$ with $q_{iv} \in \mathbb{R}^{n_v}$ and $q_{ia} \in \mathbb{R}^{n_a}$ are the generalized coordinates vector of the platform and the manipulator arm respectively, $\tau_i \in \mathbb{R}^k$ the input torques and $E_i \in \mathbb{R}^{n\times k}$ is input transformation matrix. f_i is the constraints forces corresponding to holonomic and nonholonomic constraints and $J_{ie}^T \in \mathbb{R}^{n\times n}$ is the Jacobian matrix and are represented as:

$$M_i = \begin{bmatrix} M_{iv} & M_{iva} \\ M_{iav} & M_{ia} \end{bmatrix}, C_i = \begin{bmatrix} C_{iv} & C_{iva} \\ C_{iav} & C_{ia} \end{bmatrix}, G_i = \begin{bmatrix} G_{iv} \\ G_{ia} \end{bmatrix}, J_{ie} = \begin{bmatrix} A_i & 0 \\ J_{iv} & J_{ia} \end{bmatrix}, E_i = \begin{bmatrix} E_{iv} & 0 \\ 0 & E_{ia} \end{bmatrix},$$

$$f_i = \begin{bmatrix} f_{iv} \\ f_{ie} \end{bmatrix} \text{ and } \tau_i = \begin{bmatrix} \tau_{iv} \\ \tau_{ia} \end{bmatrix}.$$

2.1.1 Elimination of Lagrange multipliers

As defined above the mobile manipulator robot is subjected to nonholonomic constraints, in which the m independent velocity constraints are presented by the given expression:

$$A_i(q_{iv})\dot{q}_{iv} = 0 \tag{2.4}$$

where A_i is the constraint matrix of the mobile platform. Define a matrix $R_i(q_{iv}) \in \mathbb{R}^{n_v \times (n-m)}$, for which $R_i^T(q_{iv})R_i(q_{iv})$ is a full rank matrix to be a basis of the null space of $A_i(q_{iv})$, we obtain the following result:

$$R_i^T(q_{iv})A_i^T(q_{iv}) = 0 \tag{2.5}$$

where m is the number of the non integrable and independent velocity constraints on the mobile platform.

There is an auxiliary input vector $\vartheta_{iv} \in \mathbb{R}^{(n_v-m)}$ that satisfies:

$$\dot{q}_{iv} = R_i \vartheta_{iv} \tag{2.6}$$

$$\ddot{q}_{iv} = R_i \dot{\vartheta}_{iv} + \dot{R}_i \vartheta_{iv} \tag{2.7}$$

Let us define the vector $\eta_i = \begin{bmatrix} \vartheta_{iv} & q_{ia} \end{bmatrix}^T \in \mathbb{R}^{n-m}$, based on (2.6) and (2.7) the dynamics expression of the i-th mobile manipulator (2.3) can be given as follows:

$$M_i^1(\eta_i)\ddot{\eta}_i + C_i^1(\eta_i, \dot{\eta}_i)\dot{\eta}_i + G_i^1(\eta_i) + p_i^1 = E_i^1 \tau_i + J_{ie}^T f_{ie} \tag{2.8}$$

where, $M_i^1 = \begin{bmatrix} R_i^T M_{iv} R_i & R_i^T M_{iva} \\ M_{iav} R_i & M_{ia} \end{bmatrix}$, $G_i^1 = \begin{bmatrix} R_i^T G_{iv} \\ G_{ia} \end{bmatrix}$, $C_i^1 = \begin{bmatrix} R_i^T M_{iv}\dot{R}_i + R_i^T C_{iv} R_i & R_i^T C_{iva} \\ M_{iav}\dot{R}_i + C_{iav} R_i & C_{ia} \end{bmatrix}$,

$J_{ie} = \begin{bmatrix} 0 & 0 \\ J_{iv} R_i & J_{ia} \end{bmatrix}$, $p_i^1 = \begin{bmatrix} R_i^T p_{iv} \\ p_{ia} \end{bmatrix}$, and $E_i^1 = \begin{bmatrix} R_i^T E_{iv} & 0 \\ 0 & E_{ia} \end{bmatrix}$.

The dynamics expression of the N mobile manipulator robots from (2.8) can be written as:

$$M\ddot{\eta} + C\dot{\eta} + G + P = E\tau + J_e^T F_e \tag{2.9}$$

where $M = diag(M_1^1, .., M_N^1) \in \mathbb{R}^{N(n-m)\times N(n-m)}$, $C = diag(C_1^1, .., C_N^1) \in \mathbb{R}^{N(n-m)\times N(n-m)}$, $G = [G_1^{1T}, .., G_N^{1T}]^T \in \mathbb{R}^{N(n-m)}$, $F_e = [f_{1e}^T, .., f_{Ne}^T]^T \in \mathbb{R}^{(n-m)N}$, $J_e^T = diag(J_{1e}^T, .., J_{Ne}^T) \in \mathbb{R}^{N(n-m)\times N(n-m)}$, $P = [p_1^{1T}, .., p_N^{1T}]^T \in \mathbb{R}^{N(n-m)}$, $\eta = [\eta_1^{1T}, .., \eta_N^{1T}]^T \in \mathbb{R}^{N(n-m)}$, and $E\tau = [(E_1\tau_1)^T, .., (E_N\tau_N)^T]^T \in \mathbb{R}^{N(n-m)}$.

2.1.2 Dynamics of the handled object

The object is considered rigid and it was tightly handled and transported by N mobile manipulator robots in coordination. The dynamics of movement of the object in space can be expressed as follows:

$$M_o(x_o)\dot{V}_o + C_o V_o + G_o = F_o \tag{2.10}$$

where $x_o \in \mathbb{R}^{n_o}$ denotes the coordinates of the objects center of gravity and $V_o \in \mathbb{R}^{n_o}$ denotes its linear/angular velocity. $M_o \in \mathbb{R}^{n_o \times n_o}$ is the inertia matrix, $C_o \in \mathbb{R}^{n_o \times n_o}$ is defined as the Centrifugal and Coriolis terms, $G_o \in \mathbb{R}^{n_o}$ is the vector of gravity and $F_o \in \mathbb{R}^{n_o}$ represent the vector of forces applied to the object.

From the configuration of the robotic system including the N mobile manipulator robots and the handled object, the relationship between the object force $F_o \in \mathbb{R}^{n_o}$ and the end-effector forces $F_e \in \mathbb{R}^{N(n-m)}$ is given by:

$$F_o = -J_o(x_o)^T F_e \tag{2.11}$$

where $J_o(x_o)$ is the Jacobian matrix relating the two forces F_e and F_o. Furthermore, the end-effector force F_e can be decomposed into two orthogonal components: the first one denotes the internal force where the second contributes to the movement of the handled object. This representation is given by the following form:

$$F_e = -J_o(x_o)^{T+} F_o - F_I \tag{2.12}$$

where $J_o(x_o)^{T+}$ is the pseudo-inverse of $J_o(x_o)^T$ and is given by $J_o(J_o^T J_o)^{-1}$. $F_I = \left[F_{1I}^T, ..., F_{NI}^T\right]^T \in \mathbb{R}^{N(n-m)}$ are defined as the internal forces in the null space of J_o^T. These internal forces are also parametrized by the Lagrangian multiplier vector λ_I as follows:

$$F_I = \rho^T \lambda_I \tag{2.13}$$

where ρ is the Jacobian matrix for internal force, and verifies the following property:

$$J_o^T \rho^T = 0 \tag{2.14}$$

2.1.3 Dynamics of the entire robotic system

Before calculating the dynamics of the complete interconnected robotic system, a brief kinematic description will be given in this subsection. Let us define $V_{ie} \in \mathbb{R}^{(n-m)}$ as a linear/angular velocity of the i-*th* mobile manipulator robot. Then this velocity is related to the joint velocity coordinate $\dot{\eta}_i \in \mathbb{R}^{(n-m)}$ by the Jacobian matrix $J_{ie} \in \mathbb{R}^{(n-m)\times(n-m)}$as:

$$V_{ie} = J_{ie}(\eta_i)\dot{\eta}_i \tag{2.15}$$

and the relationship between the i-*th* end-effector velocity $V_{ie} \in \mathbb{R}^{(n-m)}$ and the velocity of the object V_o is given by the following:

$$V_{ie} = J_{io}(x_{io})V_o \tag{2.16}$$

From (2.15), the joint velocity of the N mobile manipulators $\dot{\eta} \in \mathbb{R}^{N(n-m)}$ is related to the linear/angular velocity of the end-effectors $V_e \in \mathbb{R}^{N(n-m)}$ by the following expression:

$$V_e = J_e(\eta)\dot{\eta} \tag{2.17}$$

$$V_e = J_o(x_o)V_o \tag{2.18}$$

where $J_e = blockdiag(J_{1e}, ..., J_{Ne}) \in \mathbb{R}^{N(n-m)\times N(n-m)}$ and $J_o = \left[J_{1o}^T, ..., J_{No}^T\right]^T \in \mathbb{R}^{N(n-m)\times n_o}$. Assuming that the object is rigidly handled by the N mobile manipulator robots so all the robots are acting on this object at the same time, based on (2.17) and (2.18), the joint velocity can be given as:

$$\dot{\eta} = \Im V_o \tag{2.19}$$

where $\Im = J_e^{-1}(\eta)J_o(x_o)$. Differentiating (2.19) with respect to time, we obtain:

$$\ddot{\eta} = \Im \dot{V}_o + \dot{\Im} V_o \tag{2.20}$$

multiplying both side of (2.12) by J_e^T we obtain:

$$J_e^T F_e = -\Im^T F_o - J_o^T F_I \tag{2.21}$$

Based on (2.19) and (2.20) the dynamics of the N mobile manipulator robots coupled with the dynamic model of the handled object (2.10), using (2.21), can be expressed in the Cartesian space by the following:

$$M_e \dot{V}_o + C_e V_o + G_e + P_e = U + J_o^T F_e \tag{2.22}$$

where $M_e = \Im^T M \Im$, $C_e = \Im^T (M\dot{\Im} + C\Im)$, $G_e = \Im^T G$, $P_e = \Im^T P$ and $U = \Im^T E\tau$. Based on (2.11) the force applied to the grasped object can be calculated from (2.22) as follows:

$$F_o = U - \left(M_e \dot{V}_o + C_e V_o + G_e + P_e\right) \tag{2.23}$$

Substituting the object dynamics (2.10) into (2.23), the dynamics of the robotic system (2.23) can be written as:

$$\mathbb{M}\dot{V}_o + \mathbb{C}V_o + \mathbb{G} + P_e = U \tag{2.24}$$

where $\mathbb{M} = M_o + M_e$, $\mathbb{C} = C_o + C_e$ and $\mathbb{G} = G_o + G_e$. The obtained dynamics (2.24) has the following important properties, that are often used in the control design and in the stability analysis of the robotic systems.

Property 2.1: The matrix $\mathbb{M}$ is symmetric, positive definite and are bounded, There $\lambda_{min} I \leq \mathbb{M} \leq \lambda_{max} I$, where λ_{min} and λ_{max} are defined as the minimum and the maximum eigenvalues of $\mathbb{M}$ and I is the identity matrix.

Property 2.2: The matrix $\dot{\mathbb{M}} - 2\mathbb{C}$ is skew symmetric, that verifies, $x^T(\dot{\mathbb{M}} - 2\mathbb{C})x = 0$ for any vector $x \in \mathbb{R}^{(n_o)}$.

Property 2.3: All Jacobian matrices are uniformly continuous and uniformly bounded if the position trajectories X_e and x_o are uniformly continuous and uniformly bounded.

2.2 Approach of control

The virtual decomposition control (VDC) approach was used in this thesis to control and to simplify the estimation of the uncertainty parameters of the system. In this chapter, a general formulation of this approach will be given.

2.2.1 Virtual decomposition approach

2.2.1.1 General formulation

The VDC approach consists in breaking down the complete robotic system into a graph comprised of several objects and open chains. An object is a rigid body and an open chain consists of a series of rigid links connected one-by-one by a hinge, and having a certain degrees of freedom. The dynamic coupling between the subsystems can be represented by the flow of virtual power (FVP) at the cutting point; this is the principle of virtual decomposition. The principal use of the VDC approach is to resolve the problem of adaptation and modelling of systems with several degrees of freedom using classical approaches, which makes control of the robotic system more flexible when its configuration changes. In this case, adding a new robot or removing a faulty one from the robotics system does not require a recalculation of the full dynamics of the system. Before giving the rationale behind the virtual decomposition approach, we start by giving a brief formulation of the kinematics and dynamics modelling of the robot under consideration. The decomposition is illustrated in figure 2.1 (Zhu (2010)).

2.2.1.2 Kinematics

The kinematics model is obtained based on the modified Denavit-Hartenberg parameters for the decomposition illustrated in figure 2.2,

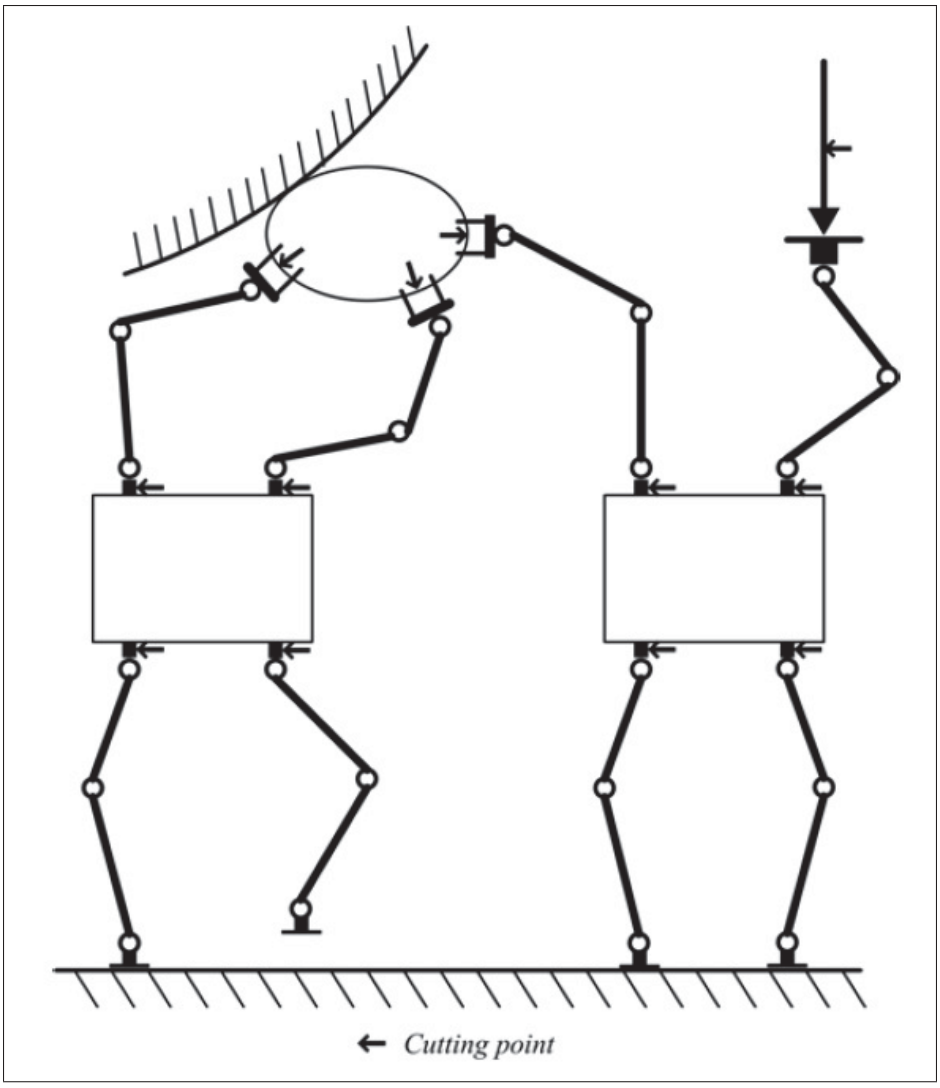

Figure 2.1 A interconnected robotic system
Taken from Zhu (2010)

The homogeneous transformation matrices can be used to calculate the force/moment transformations between successive frames B_i , identified as ${}^{B_i}U_{B_{i+1}}$ for $i = 1,..,n$ and is given as follows:

$$ {}^{B_i}U_{B_{i+1}} = \begin{bmatrix} {}^{B_i}R_{B_{i+1}} & 0_{3\times 3} \\ ({}^{B_i}r_{B_i}\times) & {}^{B_i}R_{B_{i+1}} \end{bmatrix} \tag{2.25} $$

where ${}^{B_i}R_{B_{i+1}} \in \mathbb{R}^{3\times 3}$ is the rotation matrix between frame B_i and the frame B_{i+1}, $({}^{B_i}r_{B_{i+1}}\times) \in \mathbb{R}^{3\times 3}$ is a skew symmetric matrix built from the vector $({}^{B_i}r_{B_{i+1}}) \in \mathbb{R}^3$ linking the origins of

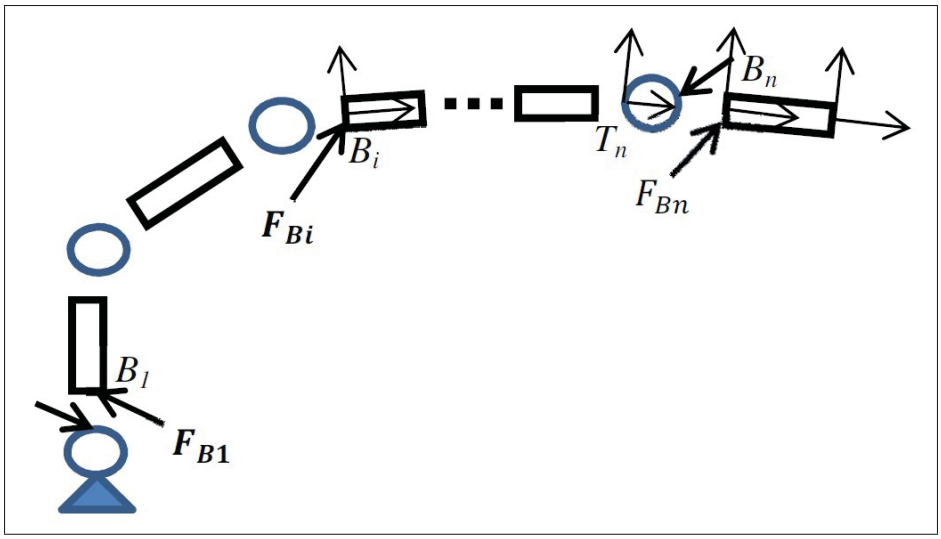

Figure 2.2 A serial manipulator robot
Taken from Zhu (2010)

frame B_i and the frame B_{i+1} assumed to be located at centre of mass, expressed in the coordinates of frame B_{i+1} and is given by the following expression:

$$({}^{B_i}r_{B_i}\times) = \begin{bmatrix} 0 & -{}^{B_i}r_{B_{i+1}}(3) & {}^{B_i}r_{B_{i+1}}(2) \\ {}^{B_i}r_{B_{i+1}}(3) & 0 & -{}^{B_i}r_{B_{i+1}}(1) \\ -{}^{B_i}r_{B_{i+1}}(2) & {}^{B_i}r_{B_{i+1}}(1) & 0 \end{bmatrix} \tag{2.26}$$

where ${}^{B_i}r_{B_{i+1}}(j)$ is defined as the j-*th* element of the ${}^{B_i}r_{B_{i+1}}$ vector.
Let us define the velocity vector by the following vector:

$$V_n = \begin{bmatrix} \dot{q}_1 & \dots & \dot{q}_n & V_{B_1}^T & \dots & V_{B_n}^T \end{bmatrix}^T \tag{2.27}$$

where $\dot{q}_i$ is the joint velocity, and the $V_{B_i} \in \mathbb{R}^6$ vectors represents the velocity of each frame B_i. The following relates the velocity propagation along the structure:

$$V_{B_{i+1}} = Z\dot{q}_{i+1} + {}^{B_i}U_{B_{i+1}}^T V_{B_i} \tag{2.28}$$

where the vector Z is defined as $Z = \begin{bmatrix} 0 & 0 & 1 & 0 & 0 & 0 \end{bmatrix}^T$ for prismatic axes and as $Z = \begin{bmatrix} 0 & 0 & 0 & 0 & 0 & 1 \end{bmatrix}^T$, for revolute axes.

In general, we can write the system in matrix form by using the virtual decomposition Jacobian matrix:

$$V_n = J_n \dot{q} \tag{2.29}$$

where $\dot{q} = \begin{bmatrix} \dot{q}_1 & \dots & \dot{q}_n \end{bmatrix}^T$, and the Jacobian is defined by:

$$J_n = \begin{bmatrix} I_{n\times n} \\ \Xi \end{bmatrix} \tag{2.30}$$

with,

$$\Xi = \begin{bmatrix} Z & 0_6 & \cdots & 0_6 \\ {}^{B_1}U_{B_2}^T Z & Z & \cdots & 0_6 \\ \vdots & \vdots & \cdots & \vdots \\ {}^{B_1}U_{B_n}^T Z & \dots & {}^{B_{n-1}}U_{B_n}^T & Z \end{bmatrix} \tag{2.31}$$

2.2.1.3 Dynamics and control of the i-*th* link

The dynamics of the i-*th* rigid body is given in the linear form by the following equation:

$$F_{B_i}^* = M_{B_i}\dot{V}_{B_i} + C_{B_i}V_{B_i} + G_{B_i} = Y_{B_i}\theta_{B_i} \tag{2.32}$$

where $M_{B_i} \in \mathbb{R}^{6\times 6}$ is the matrix of inertial terms, $C_{B_i} \in \mathbb{R}^{6\times 6}$ represents the matrix of Centrifugal/Coriolis terms, $G_{B_i} \in \mathbb{R}^6$ is the vector related to the gravity that are given by:

$$M_{B_i} = \begin{bmatrix} m_{B_i} I_3 & -m_{B_i}({}^{B_i}r_{B_iA}\times) \\ m_{B_i}({}^{B_i}r_{B_iA}\times) & I_{B_i} - m_{B_i}({}^{B_i}r_{B_iA}\times)^2 \end{bmatrix}, \quad G_{B_i} = \begin{bmatrix} m_{B_i}.{}^{B_i}R_I\mathfrak{g} \\ m_{B_i}({}^{B_i}r_{B_iA}\times)\mathfrak{g} \end{bmatrix}, \text{ and}$$

$$C_{B_i}(w_{B_i}\times) = \begin{bmatrix} m_{B_i}(w_{B_i}\times) & -m_{B_i}(w_{B_i}\times)({}^{B_i}r_{B_iA}\times) \\ m_{B_i}(w_{B_i}\times)({}^{B_i}r_{B_iA}\times) & (w_{B_i}\times)I_{B_i} + I_{B_i}(w_{B_i}\times) - m_{B_i}({}^{B_i}r_{B_iA}\times)(w_{B_i}\times)({}^{B_i}r_{B_iA}\times) \end{bmatrix}$$

where m_{B_i} is the mass of the link, $I_3 \in \mathbb{R}^{3\times3}$ is an identity matrix, $I_{B_i} = {}^{B_i}R_I I_o(t) {}^{I}R_{B_i}$ is defined as a time varying moment of inertia matrix, $I_o(t) \in \mathbb{R}^{3\times3}$ is called the moment of inertia matrix, ${}^{B_i}R_I \in \mathbb{R}^{3\times3}$ is the rotation matrix between frame B_i and the inertial frame, $({}^{B_i}r_{B_iA}\times) \in \mathbb{R}^{3\times3}$ is a skew symmetric matrix built from the vector $({}^{B_i}r_{B_iA}) \in \mathbb{R}^3$ linking the origins of frame B_i and the frame A assumed to be located at centre of mass, expressed in the coordinates of frame B_i, $\mathfrak{g} = [0,0,9.81]^T$, $\theta_{B_i} \in \mathbb{R}^{13}$ is the parameters vector, and finally $Y_{B_i} \in \mathbb{R}^{6\times13}$ is the dynamic regressor matrix built from the vectors V_{B_i}, w_{B_i}, q_i and their derivatives, defined in Appendix I. The vector of resulting forces/moments acting on the rigid body is computed by an iterative process as follows.

$$\begin{aligned} F_{B_n} &= F^*_{B_n} \\ F_{B_{n-1}} &= F^*_{B_{n-1}} + {}^{B_{n-1}}U_{B_n} F^*_{B_n} \\ &\vdots \\ F_{B_1} &= F^*_{B_1} + {}^{B_1}U_{B_2} F^*_{B_2} + \ldots + {}^{B_1}U_{B_n} F^*_{B_n} \end{aligned} \tag{2.33}$$

The dynamics of the i-*th* rigid body based on its required velocity $V^r_{B_i} \in \mathbb{R}^6$ is expressed in the linear form by the following equation:

$$F^{*r}_{B_i} = M_{B_i}\dot{V}^r_{B_i} + C_{B_i}V^r_{B_i} + G_{B_i} = Y_{B_i}\theta_{B_i} \tag{2.34}$$

Since the physical parameters of the i-*th* rigid body are assumed to be unknown and should be estimated, then the vector $\hat{\theta}_{B_i} \in \mathbb{R}^{13}$ is used and its equation of control becomes:

$$F^{*r}_{B_i} = Y_{B_i}\hat{\theta}_{B_i} + K_{B_i}(V^r_{B_i} - V_{B_i}) \tag{2.35}$$

where, $\dot{\hat{\theta}}_{B_i} = \rho_{B_i} Y_{B_i}^T S_{B_i}$ is the parameters adaptation function, and is chosen to ensure system stability, $S_{B_i} = (V_{B_i}^r - V_{B_i})$ and $\rho_{B_i} \in \mathbb{R}^{13\times13}$ is diagonal positive definite matrix. The vector of resulting forces / moments acting on the i-*th* rigid body is given by an iterative process. We begin by computing the vector of forces in the different cutting points:

$$\begin{aligned}
F_{B_n}^r &= Y_{B_n}\hat{\theta}_{B_n} + K_{B_n}(V_{B_n}^r - V_{B_n}) \\
F_{B_{n-1}} &= Y_{B_{n-1}}\hat{\theta}_{B_{n-1}} + K_{B_{n-1}}(V_{B_{n-1}}^r - V_{B_{n-1}}) + {}^{B_{n-1}}U_{B_n} F_{B_n}^r \\
&\vdots \\
F_{B_i} &= Y_{B_i}\hat{\theta}_{B_i} + K_{B_i}(V_{B_i}^r - V_{B_i}) + {}^{B_i}U_{B_{i+1}} F_{B_{i+1}}^r \\
&\vdots \\
F_{B_1} &= Y_{B_1}\hat{\theta}_{B_1} + K_{B_1}(V_{B_1}^r - V_{B_1}) + {}^{B_1}U_{B_2} F_{B_2}^r + \ldots + {}^{B_1}U_{B_n} F_{B_n}^r
\end{aligned} \tag{2.36}$$

2.2.1.4 Dynamics and control of the actuator

The dynamics of the i-*th* actuator can be expressed by the following dynamics:

$$\tau_{ai} = J_{m_{ai}}\ddot{q}_i + \xi(q_i, \dot{q}_i) \tag{2.37}$$

where $\xi(q_i, \dot{q}_i)$ represents the friction and gravitation force / torque terms and $J_{m_{ai}}$ is the moment of inertia of the motor driving this joint. According to the property of linearity in the parameters, these dynamics can be written in linear form as:

$$\tau_{ai} = Y_{ai}\theta_{ai} \tag{2.38}$$

where, $\theta_{ai} \in \mathbb{R}^4$ are the column vectors of the dynamic parameters of the motor driving the i-*th* joint and $Y_{ai} \in \mathbb{R}^4$ are the dynamic regressor (row) vectors, also defined in the Appendix II.
The dynamics of the i-*th* joint actuator based on its required velocity q_i^r is expressed in the linear form by the following equation:

$$J_{m_{ai}}\ddot{q}_i^r + \xi(q_i^r, \dot{q}_i^r) = Y_{ai}\theta_{ai} \tag{2.39}$$

Since the physical parameters of the i-*th* actuator are unknown and need to be estimated, then the vector $\hat{\theta}_{ai}$ is used and its equation of control is given by the following expression:

$$\tau_{ai}^{r} = Y_{ai}\hat{\theta}_{ai} + K_{ai}(\dot{q}_{i}^{r} - \dot{q}_{i}) \tag{2.40}$$

where $\dot{\hat{\theta}}_{ai} = \rho_{ai} y_{ai}^{T} S_{ai}$ is the parameters adaptation function, and is chosen to ensure system stability; $S_{ai} = \dot{q}_{i}^{r} - \dot{q}_{i}$, and ρ_{ai}, K_{ai} are positive gains. Y_{ai} is the dynamic regressor (row) vectors, defined in Appendix I and given with more details in (Zhu *et al.* (1997), Zhu (2010)). Finally, the input control torque at the i-th articulation is calculated from the desired torque τ_{i}^{r} obtained from (2.40), and the required force at cutting point B_i, identified $F_{B_i}^{r}$ as:

$$\tau_{i} = \tau_{ai}^{r} + Z^{T} F_{B^{I}}^{r} \tag{2.41}$$

with $Z = [0 \;\; 0 \;\; 0 \;\; 0 \;\; 0 \;\; 1]^{T}$ for the revolute joints and $Z = [0 \;\; 0 \;\; 1 \;\; 0 \;\; 0 \;\; 0]^{T}$ for the prismatic joints.

2.2.2 Virtual stability analysis

The global stability of the system's VDC is proven through the virtual stability of each subsystem based on the virtual work approach. It will be proven that each of the i-*th* links combined with its control equations and each joint combined with its control equations qualifies to be virtually stable. Consequently, the entire robotics system is stable virtually .

2.2.2.1 Virtual stability of the i-*th* link

Let us consider the non-negative Lyapunov candidate function as:

$$v_{i} = \frac{1}{2}(V_{B_i}^{r} - V_{B_i})^{T} M_{B_i} (V_{B_i}^{r} - V_{B_i}) + \frac{1}{2}\sum_{\gamma=1}^{13} \left(\theta_{i\gamma} - \hat{\theta}_{i\gamma}\right)^{2} / \rho_{i\gamma} \tag{2.42}$$

where $\theta_{i\gamma}, \hat{\theta}_{i\gamma}$ denotes the γ-*th* element of $\theta_{i\gamma}$ and $\hat{\theta}_{i\gamma}$ respectively. $\rho_{i\gamma} > 0$ is a parameter update gain. Then from the dynamics of the i-*th* link (2.32), (2.33), and by using its equation

of control in appendix (AII-16), (AII-5) and the update control law given after (AII-16), the first derivative of (2.42) along time can be given by the following expression:

$$\dot{v}_i \leq -(V_{B_i}^r - V_{B_i})^T K_{B_i}(V_{B_i}^r - V_{B_i}) + (V_{B_i}^r - V_{B_i})^T (F_{B_i}^{*r} - F_{B_i}^*) \tag{2.43}$$

2.2.2.2 Virtual stability of the i-*th* actuator

Let us define the positive Lyapunov candidate function as follows:

$$v_{ai} = \frac{1}{2} J_{m_{ai}} (\dot{q}_i^r - \dot{q}_i)^2 + \frac{1}{2} \sum_{i=1}^{4} \left(\theta_{ai\gamma} - \hat{\theta}_{ai\gamma}\right)^2 / \rho_{ai\gamma} \tag{2.44}$$

where $\theta_{ai\gamma}, \hat{\theta}_{ai\gamma}$ denote the γ-*th* element of $\theta_{ai\gamma}$ and $\hat{\theta}_{ai\gamma}$ respectively. $\rho_{ai\gamma} > 0$ is a parameter update gain. Then from the dynamics of the i-*th* actuator (2.37), (2.39), and by using its equation of control (2.40) and the update control law given after (2.40), the first derivative of (2.44) along time is given by:

$$\dot{v}_{ai} = -(\dot{q}_i^r - \dot{q}_i) J_{m_{ai}} (\ddot{q}_i^r - \ddot{q}_i) - \sum_{\gamma=1}^{4} \left(\theta_{ai\gamma} - \hat{\theta}_{ai\gamma}\right) \frac{\dot{\hat{\theta}}_{ai}}{\rho_{ai\gamma}} \tag{2.45}$$

$$\dot{v}_{ai} \leq -K_{ai}(\dot{q}_i^r - \dot{q}_i)^2 + (\dot{q}_i^r - \dot{q}_i)(\tau_{ai}^r - \tau_{ai}) \tag{2.46}$$

2.2.2.3 Stability of the entire system

Using the same method given above, a definite positive Lyapunov candidate function is chosen as:

$$v = \sum_{i=1}^{n} v_i + \sum_{i=1}^{n} v_{ai} \tag{2.47}$$

Based on (2.45), (2.46) and (Appendix II) the time derivative of v is given as follow:

$$\dot{v}_{ai} \leq -\sum_{i=1}^{n} (V_{B_i}^r - V_{B_i})^T K_{B_i}(V_{B_i}^r - V_{B_i}) - \sum_{i=1}^{n} K_{ai}(\dot{q}_i^r - \dot{q}_i)^2 \tag{2.48}$$

The details of the proof is given in Appendix II, and the reader can also found more details in (Zhu (2010)).

2.3 Adaptive backstepping approach

The backstepping technique was combined with the virtual decomposition approach and used to control a robotic system with n-DoF. This approach was used to control the links where the actuators are controlled based on the virtual decomposition approach.

2.3.1 Controller design

A general formulation is given in this section where more details are given in Chapter 6. Let US define the error variables for the robotic system at the cutting points as follows:

$$\begin{cases} e_1^{B_i} = Z(q_i - q_i^d) \\ e_2^{B_i} = (V_{B_i} - \alpha_{B_i}) \end{cases} \tag{2.49}$$

where α_{B_i} is a virtual input, to guaranty the stability of the system, this virtual input control can be chosen as follows:

$$\alpha_{B_i} = Z\dot{q}_i^d - K_1^{B_i} e_1^{B_i} - {}^{B_i}U_{B_{i-1}}^T V_{B_{i-1}} \tag{2.50}$$

The control law of the i-*th* rigid body (link) (2.34) based on the virtual input (2.50) and the linear parametrization form is given by the following expression:

$$F_{B_i}^{*r} = M_{B_i}\dot{\alpha}_{B_i} + C_{B_i}\alpha_{B_i} + G_{B_i} - e_1^{B_i} - K_2^{B_i} e_2^{B_i} \tag{2.51}$$

Nevertheless, since the physical parameters of the i-*th* rigid body (link) are supposed to be unknown but constant and need to be estimated, then the estimated vector of parameters $\hat{\theta}_{B_i}$ is

used and the required force/moment of the i-*th* link is chosen as follows:

$$F_{B_i}^{*r} = Y_{B_i}\hat{\theta}_{B_i} - e_1^{B_i} - K_2^{B_i}e_2^{B_i} - K_3^{B_i}sign(e_2^{B_i}) \tag{2.52}$$

where, $\dot{\hat{\theta}}_{B_i} = \rho_{B_i}Y_{B_i}^T S_{B_i}$ is the adaptation function that can ensure convergence and stability of the system, $S_{B_i} = V_{B_i}^d - V_{B_i}$ and ρ_{B_i}, $K_1^{B_i}$, $K_2^{B_i}$ and $K_3^{B_i}$ are a positive controller gains. The vector of resulting forces/moments acting at the different rigid body is calculated by using an iterative process (Zhu (2010)) as in (2.36). Subsequently the vector of forces at the different cutting point is obtained as follows:

$$\begin{aligned}
F_{B_n}^r &= F_{B_n}^{*r} \\
F_{B_{n-1}}^r &= F_{B_{n-1}}^{*r} + {}^{B_{n-1}}U_{B_n}F_{B_n}^{*r} \\
&\cdot \\
F_{B_i}^r &= F_{B_i}^{*r} + {}^{B_i}U_{B_{i+1}}F_{B_{i+1}}^{*r} \\
&\cdot \\
F_{B_1}^r &= F_{B_1}^{*r} + {}^{B_1}U_{B_2}F_{B_2}^{*r} + \ldots + {}^{B_1}U_{B_n}F_{B_n}^{*r}
\end{aligned} \tag{2.53}$$

The control equation of the i-*th* actuator (2.39) based on the required velocity is given as follows:

$$\tau_{ai}^r = Y_{ai}\hat{\theta}_{ai} + K_{ai}(\dot{q}_i^r - \dot{q}_i) \tag{2.54}$$

where $\dot{\hat{\theta}}_{ai} = \rho_{ai}y_{ai}^T S_{ai}$ is the parameters adaptation function, and chosen to ensure the system stability; $S_{ai} = \dot{q}_i^r - \dot{q}_i$, and ρ_{ai}, K_{ai} are positive gains. Y_{ai} is the dynamic regressor (row) vectors, defined in Appendix I (Zhu *et al.* (1997),Zhu (2010)). Finally, the i-*th* input joint control torque τ_i is calculated based on the suitable torque obtained from (2.54) and the required force at the i-*th* cutting point $F_{B_i}^{*r}$, is obtained as:

$$\tau_i = \tau_{ai}^r + Z^T F_{B_i}^r \tag{2.55}$$

2.3.2 Stability analysis

Consider the i-*th* rigid body dynamics (2.32) and the joint actuator dynamics (2.37), under the control design (2.52) and (2.54). The stability of the entire system is proved based on the virtual stability of each subsystem explained above. The control objective is satisfied and the error tracking states are asymptotically stable.

2.3.2.1 Stability of i-*th* link

Consider the non-negative Lyapunov candidate function:

$$v_i = \frac{1}{2} e_1^{B_i T} e_1^{B_i} + \frac{1}{2} e_2^{B_i T} M_{B_i} e_2^{B_i} + \frac{1}{2} \sum_{\gamma=1}^{13} \left(\theta_{i\gamma} - \hat{\theta}_{i\gamma}\right)^2 / \rho_{i\gamma} \tag{2.56}$$

Then based on the dynamics of the i-*th* link (2.32), (2.33), its equation of control (2.50), (2.52) and the update control law given after (AII-5). By knowing that $e_2^{B_i T} sign(e_2^{B_i}) = \left\| e_2^{B_i} \right\|$, the first time derivative of (2.56) is given by:

$$\dot{v}_i = -e_1^{B_i T} K_1^{B_i} e_1^{B_i} - e_2^{B_i T} K_2^{B_i} e_2^{B_i} - K_3^{B_i} \left\| e_2^{B_i} \right\| + (V_{B_i}^r - V_{B_i})^T (F_{B_i}^{*r} - F_{B_i}^*) \tag{2.57}$$

2.3.2.2 Stability of i-*th* actuator

For the actuator the same method based on the virtual decomposition approach explained previously will be used to prove the stability of the dynamics of the i-*th* actuator. Let define the positive Lyapunov candidate function as follow:

$$v_{ai} = \frac{1}{2} J_{m_{ai}} (\dot{q}_i^r - \dot{q}_i)^2 + \frac{1}{2} \sum_{i=1}^{4} \left(\theta_{ai\gamma} - \hat{\theta}_{ai\gamma}\right)^2 / \rho_{ai\gamma} \tag{2.58}$$

where $\theta_{ai\gamma}, \hat{\theta}_{ai\gamma}$ denotes the γ-*th* element of θ_{ai} and $\hat{\theta}_{ai}$ respectively. $\rho_{ai\gamma} > 0$ is a parameter update gain. Then based on the dynamics of the i-*th* actuator (2.37), its equation of control

(2.54) and the update control law given after (2.54) , the time derivative of (2.58) is given by:

$$\dot{v}_{ai} = -(\dot{q}_i^r - \dot{q}_i) J_{m_{ai}} (\ddot{q}_i^r - \ddot{q}_i) - \sum_{\gamma=1}^{4} \left(\theta_{ai\gamma} - \hat{\theta}_{ai\gamma}\right) \frac{\dot{\hat{\theta}}_{ai}}{\rho_{ai\gamma}} \tag{2.59}$$

$$\dot{v}_{ai} \leq -K_{ai} (\dot{q}_i^r - \dot{q}_i)^2 + (\dot{q}_i^r - \dot{q}_i)(\tau_{ai}^r - \tau_{ai}) \tag{2.60}$$

2.3.2.3 Stability of the entire system

Based on the Lyapunov functions of the i-*th* link and the i-*th* actuator, then the non negative Lyapunov function of the entire system is chosen as follows:

$$v = \sum_{i=1}^{n} v_i + \sum_{i=1}^{n} v_{ai} \tag{2.61}$$

Using the principle of the virtual decomposition approach (Zhu (2010)), the definition of the virtual power and the choice of the parameter function adaptation as in (2.40) and (2.54), details are given also in Appendix II; it is straightforward to prove that $\dot{v}$ is always decreasing and is given as follows;

$$\dot{v} = \sum_{i=1}^{n} \dot{v}_i + \sum_{i=1}^{n} \dot{v}_{ai} \tag{2.62}$$

$$\dot{v} \leq -\sum_{i=1}^{n} \left(e_1^{B_i T} K_1^{B_i} e_1^{B_i} + e_2^{B_i T} K_2^{B_i} e_2^{B_i} + K_3^{B_i} \left\| e_2^{B_i} \right\| + K_{ai} (\dot{q}_i^r - \dot{q}_i)^2 \right) \tag{2.63}$$

This approach was developed and applied to a group of mobile manipulator robots transporting a rigid object in coordination, more details are given in chapter 6.

2.4 Adaptive sliding mode control

2.4.1 Control design

Based on (2.19) and (2.20), the dynamics of the N mobile manipulator robots coupled with the dynamic model of the handled object (2.10), using (2.21) can be expressed in Cartesian space

by the following:

$$M_e\dot{V}_e + C_eV_e + G_e + P_e = U - J_o^{T+}F_o - F_I \tag{2.64}$$

where $M_e = J_e^{+T}MJ_e^+$, $C_e = J_e^{+T}(M\dot{J}_e^+ + CJ_e^+)$, $G_e = J_e^{+T}G$,$P_e = J_e^{+T}P$ and $U = J_e^{+T}E\tau$. Substituting the object dynamic (2.10) into (2.18) and using (2.12) and (2.21), the dynamics of the robotic system (2.64) can be given in suitable form for control as follows:

$$\mathbf{M}\dot{V}_e + \mathbf{C}V_e + \mathbf{P} + \mathbf{G} = U - \rho^T\lambda_I \tag{2.65}$$

where $\mathbf{M} = M_e + J_o^{+T}MJ_o^+$, $\mathbf{C} = C_e + J_o^{+T}(M_o\dot{J}_o^+ + C_oJ_o^+)$, $\mathbf{G} = G_e + J_o^{+T}G$ and $\mathbf{P} = J_o^{+T}P$. This dynamics satisfies the properties 2.1 and 2.2, that are used in the control stability and in the prove of stability.

Assumption 2.1: The desired trajectory of the object and the end-effector defined as x_{od}, X_{ed} and its derivatives up to third order are assumed to be bounded and uniformly continuous. The desired internal force is assumed also to be bounded and uniformly continuous.

Let define the errors as: $e = X_e - X_{ed}$ and $e_f = \lambda_I - \lambda_{Id}$, then the required internal force and velocity based on their desired values and the errors are given by the following expressions:

$$\lambda_{Ir} = \lambda_{Id} - K_\lambda e_f \tag{2.66}$$

$$V_{er} = V_{ed} - K_p e \tag{2.67}$$

Then the sliding surface is computed as:

$$s = V_e - V_{er} = \dot{e} + K_p e \tag{2.68}$$

where K_λ, K_p are diagonal positive definite gains matrices and V_{ed}, λ_{Id} are the desired end-effector velocity and internal force respectively.

Based on Assumption 2.1, the dynamic expression (2.65) can be written as follow:

$$\mathbf{M}\dot{s} = -A_m\psi_m + U - \mathbf{C}s - J_e^T\rho^T\lambda_I \tag{2.69}$$

where $A_m = \begin{bmatrix}\mathbf{M} & \mathbf{C} & \mathbf{G} & \mathbf{P}\end{bmatrix}^T$, and $\psi_m = \begin{bmatrix}\dot{V}_e & V_e & 1 & 1\end{bmatrix}^T$.

Assumption 2.2: There exist some finite positive constants, $a_i \geq 0, \quad 1 \leq i \leq 4$ and finite positive constants $a_5 \geq 0$ such that $\forall X_e \in \mathbb{R}^{6N}$, $\forall V_e \in \mathbb{R}^{6N}$, $\|\mathbf{M}\| \leq a_1$, $\|\mathbf{C}\| \leq a_2 + a_3\|V_e\|$, $\|\mathbf{G}\| \leq a_4$ and $\|P\| \leq a_5$. Since $a_i \geq 0$ are considered unknown, then the adaptive laws are developed to estimate the unknown upper bounds. Let consider the following control law:

$$U = -\sum_{i=1}^{5}\frac{s\hat{a}_i\psi_i^2}{\|s\|\psi_i + \delta_i} - K_s s - \frac{Ksign(s)}{H(s)} + \rho^T\lambda_{Ir} \tag{2.70}$$

where δ_i is a time varying positive function that converges to zeros as $t \to \infty$ and that satisfies: $\lim_{t\to\infty}\int_0^t \delta_i(r)dr = \alpha_i < \infty$, with α_i is a finite constant (Wang *et al.* (2004)) and $H(s)$ is given by the following expression:

$$H(s) = \beta + (1-\beta)h(|s|, 0, s_q) \tag{2.71}$$

where s_q is an upper limit positive constant, $0 < \beta < 1$ and $h(x,a,b)$ is referred to be a p-time differential bump function that satisfies the following properties (Do (2008),Do (2010)):

- $h(x,0,b) = 0$, if $x = 0$;
- $h(x,0,b) = 1$, if $x \geq b$;
- $0 < h(x,0,b) < 1$, if $0 < x < b$;
- $h(x,0,b)$ is p-time differentiable with respect to x;
- $\frac{\partial h(x,0,b)}{\partial x} > 0$ if $x \in (0,b)$.

Let $h(x,a,b)$ be defined as follows:

$$h(x,a,b) = \frac{\int_0^x g(\sigma)g(b-\sigma)d\sigma}{\int_0^b g(\sigma)g(b-\sigma)d\sigma}$$

where g is such that: $g(z) = 0$ if $z \leq 0$ and $g(z) = z^l$ if $z \geq 0$, and l is a positive constant integer.

Remark 2.1: The term $-\frac{Ksign(s)}{H(s)}$ is added to the proposed control law compared with the controller proposed in (Wang *et al.* (2004); Li *et al.* (2008)). Thus, more robust control performance can be obtained and fast convergence when the system states are closed to the surface $s = 0$ can be ensured.

Note that the term $H(s)$ added to the control law (2.70) does not affect the stability of the control because $H(s)$ is always strictly positive. From the definition of the potential function (2.71), one can see that if $|s|$ increases, $H(s)$ approaches β, and therefore, $\frac{K}{H(s)}$ converges to $\frac{K}{\beta}$,which is greater than K. This means that $\frac{K}{H(s)}$ increases in reaching phase, and consequently, the attraction of the sliding surface will be faster. On the other hand, if $|s|$ decreases, then $H(s)$ approaches one, and $\frac{K}{H(s)}$ converges to K. This means that, when the system approaches the sliding surface, $\frac{K}{H(s)}$ progressively decreases, which minimize sorely the chattering. Consequently, the proposed law let the controller to dynamically adjust to the changes in the switching function by making $\frac{K}{H(s)}$ vary between K and $\frac{K}{\beta}$.

Remark 2.2: If β is chosen to be equal to one, the reaching law of (2.70) becomes identical to that of conventional sliding mode control. Therefore, the conventional reaching law becomes a particular case of the proposed approach.

2.4.2 Stability analysis

The chosen Lyapunov candidate function can be given as follows:

$$V = \frac{1}{2}s^T\mathbf{M}s + \frac{1}{2}\tilde{A}_m^T\Gamma_a^{-1}\tilde{A}_m \tag{2.72}$$

where $\tilde{A}_m = A_m - \hat{A}_m$, $A_m = [a_1 \;\; a_2 \;\; a_3 \;\; a_4 \;\; a_5]^T$, $\hat{A}_m$ denoted the estimate constants of A_m, $\Gamma_a = diag(\gamma_1, .., \gamma_5)$ and $\gamma_i \geq 0$ are constants. The first time derivative of (2.71) is given by:

$$\dot{V} = s^T \mathbf{M}\dot{s} + \frac{1}{2} s^T \dot{\mathbf{M}} s + \tilde{A}_m^T \Gamma_a^{-1} \dot{\hat{A}}_m \tag{2.73}$$

Based on the assumption 2.2 , the dynamics model (2.70) and the closed loop (2.66), then (2.73) can be simplified as follow:

$$\dot{V} \leq s^T (\|\mathbf{M}\|\|\dot{V}_e\| + \|\mathbf{C}\|\|V_e\| + \|\mathbf{G}\| + \|P\| + U - \rho^T \lambda_I) + \tilde{A}_m^T \Gamma_a^{-1} \dot{\hat{A}}_m \tag{2.74}$$

Based on the control law (2.70) under the assumption 2.2, the first time derivative (2.74) can simplified as follows: Using the control law (2.70) under the assumption 2.2, the first derivative (2.74) can be written as follows

$$\dot{V} \leq -s^T K_s s - K\|s\| + \sum_{i=1}^{5} \|s\| a_i \psi_i$$

$$- \sum_{i=1}^{5} \frac{\|s\|^2 \hat{a}_i \psi_i^2}{\|s\| \psi_i + \delta_i} - \sum_{i=1}^{5} \tilde{a}_i \gamma_i^{-1} \dot{\hat{a}}_i \tag{2.75}$$

Consider the update law as:

$$\dot{\hat{a}}_i = \gamma_i \left(\frac{\|s\|^2 \psi_i^2}{\|s\| \psi_i + \delta_i} - \gamma_i^{'} \hat{a}_i \right) \tag{2.76}$$

with $\gamma_i \geq 0$; $\gamma_i^{'} \geq 0$ and $\delta_i \geq 0$ verifying the following expressions:

$$\begin{cases} \int_0^\infty \gamma_i^{'}(r) dr = \alpha_{i\gamma'} < \infty \\ \\ \int_0^\infty \delta_i(r) dr = \alpha_{i\delta} < \infty \end{cases} \tag{2.77}$$

Substituting the update law (2.76) into (2.75) with some simplifications,it is straightforward to obtain the following:

$$\dot{V} \leq -\lambda_{min}(K_s \|s\|^2) + \sigma \tag{2.78}$$

where $\sigma = \sum_{i=1}^{5} a_i \delta_i + \sum_{i=1}^{5} \frac{1}{4} \gamma_i' a_i^2 \rightarrow 0$ as $t \rightarrow \infty$, from above, s converges to a small set containing the origin when $t \rightarrow \infty$. All details are given in chapter 7.

To complete the proof of the stability, substituting the control law (2.70) and (2.66) into the reduced order dynamic expression (2.65) yields:

$$\rho^T (\lambda_{Ir} - \lambda_I) = A_m \psi_m + \sum_{i=1}^{5} \frac{s \hat{a}_i \psi_i^2}{\|s\| \psi_i + \delta_i} + \frac{K sign(s)}{H(s)} + K_s s$$

$$\rho^T e_f = (K_\lambda + I)^{-1} \mu \tag{2.79}$$

with $\mu = A_m \psi_m + \sum_{i=1}^{5} \frac{s \hat{a}_i \psi_i^2}{\|s\| \psi_i + \delta_i} + \frac{K sign(s)}{H(s)} + K_s s$, All terms on the right hand of (2.79) are bounded, therefore the internal force tracking error are bounded and can be adjusted by tuning the feedback gain K_λ.

This approach of control was applied to control a group of two mobile manipulator robots transporting a rigid object in coordination. Numerical simulation and experimental results are given in chapter 7, more details about the stability analysis can be also found in this chapter.

CHAPTER 3

REAL-TIME FORMATION CONTROL OF VIRTUAL-LEADER REAL-FOLLOWER MOBILE ROBOTS USING POTENTIAL FUNCTION

Abdelkrim Brahmi[1], Maarouf Saad[1], Guy Gauthier[2], Wen-Hong Zhu[3]
and Jawhar Ghommam[4]

[1] Département of Electrical Engineering, École de Technologie Supérieure,
[2] Département of automated manufacturing Engineering, École de Technologie Supérieure,
1100 Notre-Dame Ouest, Montréal, Québec, Canada H3C 1K3
[3] Space Exploration,Canadian Space Agency,
6767 Route de l'Aéroport, Longueuil (St-Hubert), Québec, Canada J3Y 8Y9
[4] Research Unit on Mechatronics and Automation Systems,
Ecole National d'Ingenieurs de Sfax, BPW,3038 Sfax, Tunisia,

Accepted in Part I: Journal of Systems and Control Engineering, September 14, 2017

Abstract

In this paper, the problem of leader-follower formation control taking into account the measurement of the velocities of the leader and followers, as well as the dynamic uncertainties in the robots' models was considered. As a solution, this paper proposes a kinematic control law based on the choice of potential function, combined with an adaptive dynamic control scheme based on virtual decomposition control (VDC) to estimate the nonlinearity and the dynamic uncertainties in the robots model, for the leader-follower formation. A virtual robot represented by its dynamic model is considered as a leader. This leader is able to move along a predefined trajectory. The follower robots are separated by a predefined distance range from the leader, with a desired relative bearing angle region compared to the leader. The proposed scheme is validated experimentally on real-time robots. The obtained results show the effectiveness of the proposed controller.

Keywords: Leader-follower formation, potential function, virtual decomposition control.

3.1 Introduction

The idea of using a group of mobile robots in one environment is attracting a large number of robotics researchers, particularly in the area of control. The interest in this area of investigation is justified since the space and variety of tasks that can be explored by a group of mobile robots are broader, when compared to those explorable by a single robot. Technological advances in communications systems have greatly contributed to the results that have been obtained thus far. Typical applications include space exploration, formation maintenance, transport of objects, rescue and navigation. To date, the bulk of the research carried out in this area has focused on two mechanisms of coordination: centralized and decentralized control. In the first approach, as its name suggests, the control of multi-mobile robots is centralized over the physical structure of the robot, and is located at a central unit that manages and ensures the execution of the task. The central unit has a global information environment, which is an important asset for decision support and the coordination of actions. For this scheme, the central unit also constitutes the main limitation of this approach, because the group of mobile robots depends entirely on this unit, which means that a faulty central supervisor implies a complete shutdown. In the decentralized approach, the resources (sensors, computation units, etc.) are distributed over all the elements of the group. Each robot then uses its own individual resources and control unit, and may communicate its information to other robots. With this decentralization, the functional faults are better managed, and the failure of a single robot does not mean the complete cessation of the group. In order to control and coordinate a multi agents system, various architectures and approaches have been developed (Wen *et al.* (2014, 2016); Aranda *et al.* (2015)). Many contributed works on multi-agent formation control have been performed using mobile robots (Panagou *et al.* (2016); Yu and Liu (2016a); Khan *et al.* (2016)), helicopter (Shaw *et al.* (2007)), underwater vehicles (Yin *et al.* (2016); Li *et al.* (2016)) and quadcopters (Vargas-Jacob *et al.* (2016); Kang and Ahn (2016)). The conventional formation control approaches include virtual structure approach (Lewis and Tan (1997); Ren and Beard (2004); Mehrjerdi *et al.* (2011)), leader-follower approach (Qian *et al.* (2015); Dai and Lee (2012); Xiao *et al.* (2016); Li and Xiao (2005); Fujimori *et al.* (2014)) and behaviour-based

approach (Lawton *et al.* (2003); Li and Yang (2003)). The virtual structure approach considers the group of mobile robots as a single rigid object. The desired trajectory is assigned to the whole virtual structure, rather than to each robot of the formation. However, it is easy to maintain such a formation and control the behavior of the entire group. In the leader-follower strategy, one or some robots of the formation are designed as leaders, while others are assigned as followers. The leader moves along the desired trajectory and the followers maintain desired relative positions with respect to the leader. There is no explicit feedback from the follower to the leader, which represents an inherent disadvantage of this approach. In the behaviour-based approach, several desired behaviors are considered for each robot, but the final action or the group behavior is obtained by weighting the relative importance of each behavior. The main disadvantage of this approach is that its mathematical analysis is complex, which makes it difficult to ensure precise formation control. Therefore, the convergence of the group to a desired configuration cannot be guaranteed. The authors in (Das *et al.* (2002)) propose a leader-follower control based on an input-output linearization approach. It is assumed that the velocity of the leader is measured, and to overcome this problem, an estimator using robust filtering techniques was proposed in (Ghommam *et al.* (2013)). While this method is robust to perturbations, it does however suffer from slow convergence of the estimated velocity to the real value. During the last years, many contributed works based on the consensus theory, have been developed; consensus approach has been simulated and applied to achieve the formation of multiple mobile robots. In (Jadbabaie *et al.* (2003)) a formal mathematical analysis for consensus was presented. Some research on the consensus problem was extended to the case of directed topology as in Wen *et al.* (2014); Yu and Wang (2012). A consensus analysis and design control of multiple non-holonomic mobile based on the virtual leader-follower strategy was proposed in (Peng *et al.* (2015)). However, these cited works focus on the kinematics of all mobile robots and consider that the robot systems are linear. In practice, the robots have a non-holonomic constraint and are nonlinear. The approach proposed in this paper has the following advantages. In this paper, the formation problem is formulated as follows: a formation of three mobile robots is used, with two of them being real mobile robots named EtsRob, and considered as followers. The third one is replaced by a dynamic model of the robot and is considered as a

leader. The leader mobile robot is firstly considered as capable of moving along a predefined trajectory, and then the follower robots are separated by a predefined distance range from the leader, with a desired relative bearing angle region compared to the leader. Motivated by the previous observations, the main contributions of this paper are:

a. Most existing techniques employ more complicated controllers and focus on providing the solution to the leader-follower formation problem, convergence to an absolute desired distance, and a fixed desired relative bearing angle (Desai *et al.* (1998); Lawton *et al.* (2003)). It is worth noting that there are just a few of the proposed approaches in which the convergence of this formation to the desired distance range and desired relative bearing angle region are discussed. As examples, a circular formation control of multiple nonholonomic vehicle was studied and numerically simulated in (Ceccarelli *et al.* (2008); Yu and Liu (2017, 2016b)) to show the effectiveness of the developed control and the convergence of the circular formation motion. In Zheng *et al.* (2015) a bearing-based target enclosing problem using a group of mobile robots was proposed. In this work, the authors developed a control scheme for multiple mobiles robots to enclose a target with only relative bearing measurement, and assume that the position information is not available. Therefore, in our paper, a simple controller is developed and implemented;

b. Each follower must maintain a desired distance range and a given bearing region from the leader, and that there is no interaction or information exchange among the followers but the inter-collision problem between them is ensured by only the leader robot. The advantage of this strategy can be summarized as;

   - this approach uses minimum information compared to the other methods that solve the problem of inter-collision by using more sophisticated sensors for measurement and communication;
   - Compared to the cited works, since the leader is a virtual robot we do not have the problem of a failure of the leader robot and the failure of a follower robot does not mean the complete cessation of the group.

c. To guarantee collision avoidance and position tracking, we include a potential function, based on the p-time differential bump function introduced in (Do (2010)) as a kinematic control. This kinematic control is combined with an adaptive dynamic control based on the virtual decomposition approach (VDC) (Zhu (2010); Brahmi *et al.* (2013b,a)), and used to move the follower robots into the desired region;

d. Since the parameters of the follower robots are considered uncertain, the controllers' design is based on kinematic and dynamic models with unknown parameters. The proposed virtual decomposition approach helps simplify the problem of the parameters' adaptation of the complete systems since the problem is converted into an estimation problem for each subsystem.

Finally, the formation tracking control problem is resolved and implemented in real time on the leader mobile robot and two identical mobile robots called EtsRob.
The rest of the paper is organized as follows. Section 3.2 presents the modelling of the mobile robot, while section 3.3 presents the leader-follower formation formulation. Section 3.4 explains the control design, and experimental results are given in section 3.5 to illustrate the effectiveness of the proposed approach. Finally, a conclusion is given in section 3.6.

3.2 Modeling of the mobile robot

In this section, the kinematics and the dynamics of the i-th mobile robot are briefly described (Das *et al.* (2002); Ghommam *et al.* (2010)) using the VDC approach (Zhu (2010)).

3.2.1 Kinematics Model

Figure 3.1 illustrates a nonholonomic mobile robot. The frame (X,Y) is the world frame and (X_B, Y_B) is the body frame.
L is the distance between the left and the right wheels, R is the radius of the wheel, and CG is the centre of gravity, where the body frame is located. The kinematic equations of the i-th

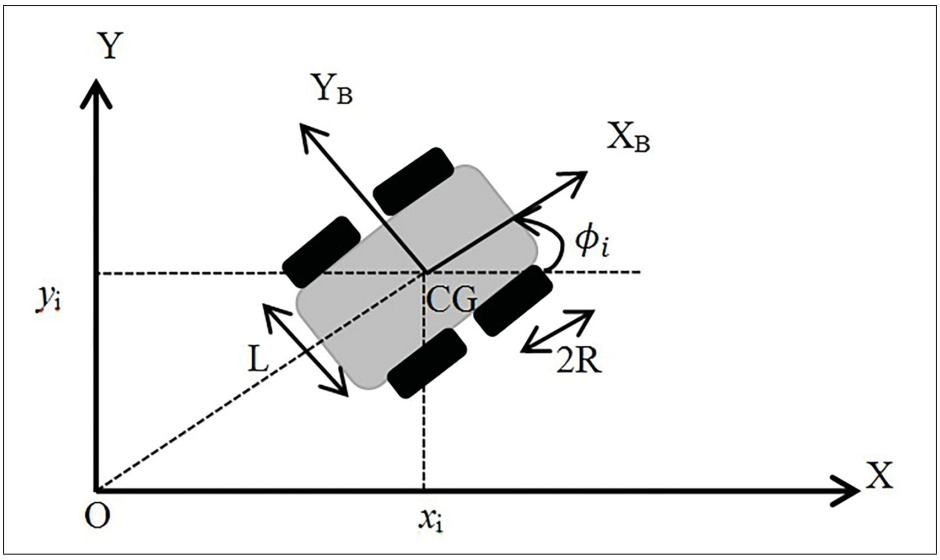

Figure 3.1 Nonholonomic mobile robots

mobile robot are given as follows (Das *et al.* (2002); Ghommam *et al.* (2011)):

$$\begin{cases} \dot{x}_i = v_i \cos(\phi_i) \\ \dot{y}_i = v_i sin(\phi_i) \\ \dot{\phi}_i = w_i, \end{cases} \tag{3.1}$$

where v_i and w_i are the linear and angular velocities of the i-th robot of the group, $i \in \{l, f\}$ (respectively the leader and follower mobile robot) and $P_i = \begin{bmatrix} x_i & y_i & \phi_i \end{bmatrix}^T$ denote its position and orientation, respectively. The right and left wheel angular velocities and are obtained by the following expressions:

$$\begin{cases} \dot{q}_{iR} = \frac{1}{R}\left(v_i + \frac{L}{2} w_i\right) \\ \\ \dot{q}_{iL} = \frac{1}{R}\left(v_i - \frac{L}{2} w_i\right) \end{cases} \tag{3.2}$$

The mobile robot is subjected to the nonholonomic constraints expressed by the following equation:

$$\dot{y}_i \cos(\phi_i) - \dot{x}_i \sin(\phi_i) = 0 \tag{3.3}$$

Defining the augmented velocity vector, $V_B = \begin{bmatrix} V_{io} & V_{i_R} & V_{i_L} \end{bmatrix}^T$, and is given as follows:

$$V_B = J\, V_{io} \tag{3.4}$$

where J is the VDC Jacobian matrix of the mobile robot, $V_{io} = \begin{bmatrix} \dot{x}_i & \dot{y}_i & 0 & 0 & 0 & \dot{\phi}_i \end{bmatrix}^T$ is the velocity vector of the platform, V_{i_R} and V_{i_L} are the right and the left velocities of the mobile platform respectively.

3.2.2 Dynamic Model

In this section, the dynamic model of the i-th mobile robot is briefly described using the VDC approach (Zhu (2010)). The decomposition of the i-th mobile robot is illustrated in Figure 3.2.

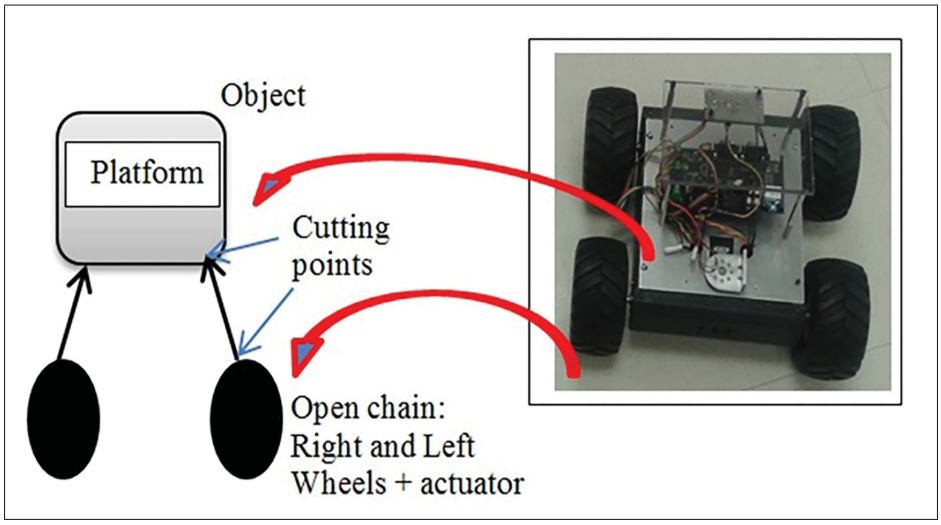

Figure 3.2 The virtual decomposition of the i-th mobile robot

The dynamics of the platform considered as a rigid object the right and the left wheels, based on the velocity vectors V_{io}, V_{iR} and V_{iL}, is expressed by the following equation:

$$F_{ij} = M_{ij}\dot{V}_{ij} + C_{ij}V_{ij} + G_{ij} = Y_{ij}\theta_{ij} \tag{3.5}$$

where $M_{ij} \in \mathbb{R}^{6\times6}$ is the matrix of inertial terms, $C_{ij} \in \mathbb{R}^{6\times6}$ the matrix of centrifugal/Coriolis terms, $G_{ij} \in \mathbb{R}^6$ the vector related to gravity, $F_{ij} \in \mathbb{R}^6$ the required forces, $\theta_{ij} \in \mathbb{R}^{13}$ the parameters vector, $Y_{ij} \in \mathbb{R}^{6\times13}$ the dynamic regressor matrix and $j \in \left\{o, R, L\right\}$, as given in (Zhu (2010)). The vector of resulting forces/moments acting on the i-th rigid body is given by an iterative process. We begin by computing the vector of forces in the different cutting points, as shown in Figure 3.2:

$$F_{iw} = F_{iw}^{*}; \quad w = R, L$$

$$F_{io} = F_{io}^{*} + \sum_{w=R}^{L} {}^{iw}U_{io} F_{iw}^{*} + f_n \tag{3.6}$$

where f_n are the generalized constraint forces for the nonholonomic constraints that can be given by:

$$f_n = A^T \lambda_n \tag{3.7}$$

where A is the kinematic-constraint matrix, λ_n the Lagrangian multiplier, and ${}^{iw}U_{io}$ is computed by using the transformation matrix of force/moment vectors from frame B to frame A, defined by:

$${}^{A}U_{B} = \begin{bmatrix} {}^{A}R_{B} & 0_{3\times3} \\ \\ S({}^{A}r_{AB}){}^{A}R_{B} & {}^{A}R_{B} \end{bmatrix} \tag{3.8}$$

where ${}^{A}R_{B}$ is the rotation matrix between frames A and B, and $S({}^{A}r_{AB})$ is a skew symmetric matrix built from the vector ${}^{A}r_{AB}$ linking the origins of frames A and B, expressed in the coordinates of frame A. From (3.5) and (3.6), the forward dynamic model of the i-th mobile robot can be written as follows:

$$F_{io} = J^T M_{iv} \dot{V}_B + J^T C_{iv} V_B + J^T G_{iv} + f_n \tag{3.9}$$

where $M_{iv} = diag(M_{io}, M_{iR}, M_{iL})$ is the matrix of inertial terms, $C_{iv} = diag(C_{io}, C_{iR}, C_{iL})$ the matrix of centrifugal/Coriolis terms, and $G_{iv} = \left[G_{io}^T, G_{iR}^T, G_{iL}^T\right]^T$ the vector related to gravity.

Using (3.4), this dynamic (3.9) can be given by the following formula:

$$F_{io} = \mathscr{M}_i \dot{V}_{io} + \mathscr{C}_i V_{io} + \mathscr{G}_i + f_n \tag{3.10}$$

where $\mathscr{M}_i = J^T M_{iv} J$,$\mathscr{C}_i = J^T M_{iv} \dot{J} + J^T C_{iv} J$,$\mathscr{G}_i = J^T G_{iv}$ and V_{io} is defined in (3.4).
Then, the system represented by the dynamic (3.10) is transformed into general form, which is used in the control.

The objective is to eliminate the term of constraint $f_n = A^T \lambda_n$, using (3.1-3.2) and the right and left wheels' angular velocities $\dot{q}_{iR}$ and $\dot{q}_{iR}$ that are obtained by the following expression:

$$V_{io} = S(q)\dot{q}_i \tag{3.11}$$

where $\dot{q}_i = [\dot{q}_{iR}, \dot{q}_{iL}]^T$ are the generalized coordinate right/left angular velocities and $S(q)$ is in the null space of the kinematic constraint matrix $A(q)$. Therefore, we obtain:

$$S^T(q)A^T(q) = 0 \tag{3.12}$$

Substituting (3.11), and its first derivative in the dynamic (3.10), and then multiplying both sides of the resulting equation by $S^T(q)$, then using the (3.12), the reduced dynamic model is given by:

$$\tau_{ic} = \bar{\mathscr{M}}_i \ddot{q}_i + \bar{\mathscr{C}}_i \dot{q}_i + \bar{\mathscr{G}}_i \tag{3.13}$$

with $\tau_{ic} = S^T F_{io}$, $\bar{\mathscr{M}}_i = S^T \mathscr{M}_i S$, $\bar{\mathscr{C}}_i = S^T(\mathscr{M}_i \dot{S} + \mathscr{C}_i S)$, and $\bar{\mathscr{G}}_i = S^T \mathscr{G}_i$.
The dynamics of the w-th wheel actuator based on its angular velocity $\dot{q}_{iw}$ is expressed in linear form by the following equation:

$$\tau^*_{aiw} = J_{aiw}\ddot{q}_{iw} + \xi(q_{iw}, \dot{q}_{iw}) = Y_{aiw}\theta_{aiw} \tag{3.14}$$

where $\xi(q_{iw}, \dot{q}_{iw})$ represents the friction and gravitation force/torque terms, J_{aiw} is the moment of inertia of the motor driving this joint, $w \in \left\{R, L\right\}$ (the right and the left wheels), and τ^*_{aiw} is the actuator torque.

Finally, the input control torque at the i-th mobile wheel actuator is calculated from the torque τ^*_{aiw} obtained in (3.14) and the force at cutting point B_i, identified F_{io}, as:

$$\tau_i = \tau^*_{ai} + \tau_{ic} \tag{3.15}$$

where $\tau^*_{ai} = [\tau_{aiR}, \tau_{aiL}]^T$.

3.3 Leader-Follower formation formulation

The leader-follower control problem can be divided into two different strategies; the first strategy is called the $l-\psi$ control problem, where the formation is based on knowledge of the separation distance and bearing between two robots in the group, and in the second control strategy, called the $l-l$ control problem, another robot is added to the first configuration on which the $l-\psi$ scheme resides, based on knowledge of the three separation distances between the robots and the two relative bearings between the leader and the two follower robots. In this work, the leader-follower problem is examined based on (Das *et al.* (2002); Ghommam *et al.* (2013)), with a few modifications brought in: the leader mobile robot moves along a reference trajectory and the follower mobile robots are separated at a predefined distance from the leader at a relative bearing angle from the leader.

We consider a basic leader-follower configuration (Figure 3.3) called the $l-\psi$ formation scheme, in which mobile robot R_f, follows a leader robot R_l with distance separation l_{lf} and a relative bearing angle ψ_{lf}. As in (Das *et al.* (2002); Ghommam *et al.* (2011)), these two values are obtained as follows:

$$\begin{cases} l_{lf} = \sqrt{\left(x_l - x_f - dcos(\phi_f)\right)^2 + \left(y_l - y_f - dsin(\phi_f)\right)^2} \\ \psi_{lf} = \pi + \varphi_{lf} - \phi_l, \end{cases} \tag{3.16}$$

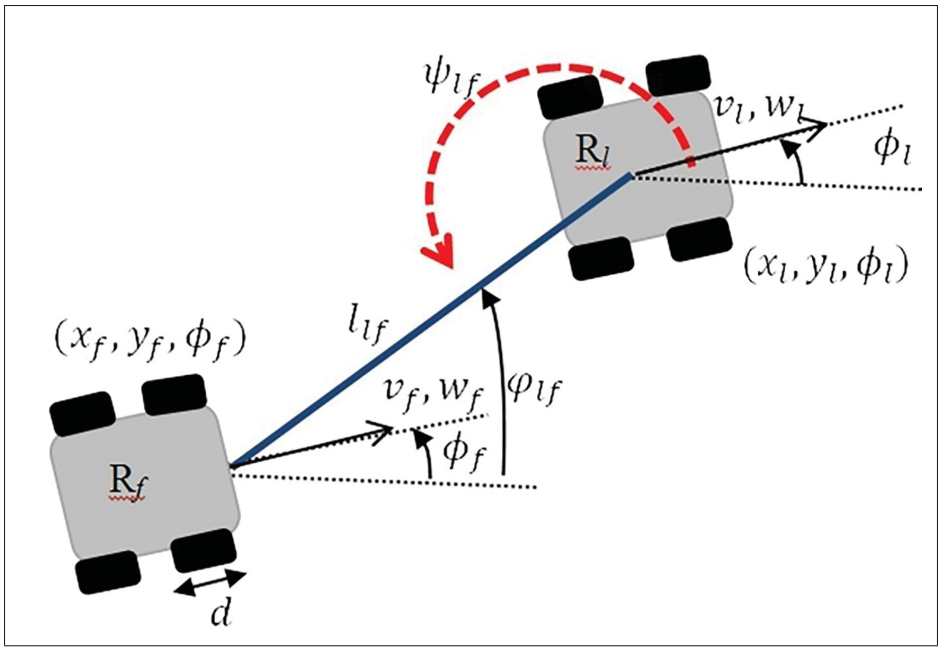

Figure 3.3 $l-\psi$ Formation scheme

where d is the distance between the front and the center of gravity of the robot, and φ_{lf} is given by

$$\varphi_{lf} = tan^{-1}\left(\frac{(y_l - y_f - dsin(\phi_f)}{(x_l - x_f - dcos(\phi_f)}\right) \tag{3.17}$$

Let $e_{lf} = [l_{lf}, \psi_{lf}]^T$, from the derivative of (3.16) and (3.17) with respect to time, the kinematics of the formation is obtained as follows (Das *et al.* (2002),Ghommam *et al.* (2011)):

$$\dot{e}_{lf} = Fu_f + Hu_l \tag{3.18a}$$

$$\dot{\psi}_{lf} = w_l - w_f \tag{3.18b}$$

where $u_f = [v_f, w_f]^T$ and $u_l = [v_l, w_l]^T$ are the input vectors of the follower and the leader robot, respectively. $F = \begin{bmatrix} cos(\beta_{lf}) & dsin(\beta_{lf}) \\ -\frac{sin(\beta_{lf})}{l_{lf}} & \frac{dsin(\beta_{lf})}{l_{lf}} \end{bmatrix}$, $H = \begin{bmatrix} -cos(\psi_{lf}) & 0 \\ \frac{sin(\psi_{lf})}{l_{lf}} & -1 \end{bmatrix}$. The angle β_{lf} is defined as the sum of the difference between the robot's heading and the bearing angle, i.e.:

$$\beta_{lf} = \psi_{lf} + (\phi_l - \phi_f) \tag{3.19}$$

The objective is to design u_f such that e_{lf} converges to the desired distance/bearing of the leader robot while guaranteeing that l_{lf} and ψ_{lf} are confined within a defined range: i.e., $l_{lf}^{min} \leqslant l_{lf} \leqslant l_{lf}^{max}$ and $\psi_{lf}^{min} \leqslant \psi_{lf} \leqslant \psi_{lf}^{max}$. In this paper, a leader-follower formation control using a potential function is proposed to solve the $l-\psi$ scheme problem, as explained in the following section.

3.4 Control design

Before starting the leader-follower formation control design, let us consider the following assumption and definitions, which will be used in the control design:

Assumption 3.4.1: The velocities of of the leader and the followers' are considered available for feedback, which are assumed to be bounded.

Definition 3.4.1: A scalar function $h(x,a,b)$ is referred to as a p-time differential bump function if the following properties are verified (Do (2008)):

- $h(x,a,b) = 0$, if $x \leq a$
- $h(x,a,b) = 1$, if $x \geq b$
- $0 < h(x,a,b) < 1$, if $a < x < b$
- $h(x,a,b)$ is p-time differentiable with respect to x.
- $\frac{\partial h(x,a,b)}{\partial x} > 0$ if $x \in (a,b)$.

Let $h(x,a,b)$ be defined as follows:

$$h(x,a,b) = \frac{\int_a^x g(\sigma - a)g(b-\sigma)d\sigma}{\int_a^b g(\sigma - a)g(b-\sigma)d\sigma} \tag{3.20}$$

where g is such that: $g(z) = 0$ if $z \leq 0$ and $g(z) = z^p$ if $z \geq 0$. and p is a positive constant integer. These functions are used in the case of limited communication between multiple mobile robots in the formation control.

Definition 3.4.2: To guarantee collision avoidance and position tracking, we need to define the potential function $V_x(x,a,b)$ such that:

$$V_x(x,a,b) \to \infty \ \text{ as } \ x \to a \ \ (\text{and} \, x \to b) \tag{3.21}$$

when $x = \frac{(b-a)}{2}$, V_x gets the only minimum value. Interested readers are referred to (Do (2010)) for the particular potential function $V_{e_{lf}}(e_{lf}, \underline{e_{lf}}, \overline{e_{lf}})$ satisfying these properties. In this paper, the potential function is chosen as follows:

$$V_{e_{lf}} = \begin{bmatrix} V_{l_{lf}}(l_{lf}, \underline{l_{lf}}, \overline{l_{lf}}) \\ \\ V_{\psi_{lf}(\psi_{lf}, \underline{\psi_{lf}}, \overline{\psi_{lf}})} \end{bmatrix}$$

$$V_{e_{lf}} = \begin{bmatrix} \frac{-1}{\pi} Ln\left(cos\left(\frac{\pi}{2}\left(1 - 2h(l_{lf}, \underline{l_{lf}}, \overline{l_{lf}})\right)\right)\right) \\ \\ \frac{-1}{\pi} Ln\left(cos\left(\frac{\pi}{2}\left(1 - 2h(\psi_{lf}, \underline{\psi_{lf}}, \overline{\psi_{lf}})\right)\right)\right) \end{bmatrix} \tag{3.22}$$

where $\underline{e_{lf}} = [\underline{l_{lf}}, \underline{\psi_{lf}}]^T = [l_{lf}^{min}, \psi_{lf}^{min}]^T$, $\overline{e_{lf}} = [\overline{l_{lf}}, \overline{\psi_{lf}}]^T = [l_{lf}^{max}, \psi_{lf}^{max}]^T$ are defined in the previous section, and $h(e_{lf}, \underline{e_{lf}}, \overline{e_{lf}})$ is defined in Definition 3.4.1. The first derivative of $V_{e_{lf}}$ with to respect to h is calculated as follows:

$$\frac{\partial V_{e_{lf}}}{\partial h} = \begin{bmatrix} -tan\left(\frac{\pi}{2}\left(1 - 2h(l_{lf}, \underline{l_{lf}}, \overline{l_{lf}}\right)\right) \\ \\ -tan\left(\frac{\pi}{2}\left(1 - 2h(\psi_{lf}, \underline{\psi_{lf}}, \overline{\psi_{lf}}\right)\right) \end{bmatrix} \tag{3.23}$$

3.4.1 Kinematic control design

Before presenting the controller design, we consider the formation scheme and formation setup shown in Figure 3.3. We want to confine l_{lf} and ψ_{lf} within a range such that:

$$l_{lf}^{min} \leq l_{lf} \leq l_{lf}^{max}, \;\; \psi_{lf}^{min} \leq \psi_{lf} \leq \psi_{lf}^{max} \tag{3.24}$$

where $l_{lf}^{min}, l_{lf}^{max}$ are the minimum and the maximum distances between the leader and the follower, and $\psi_{lf}^{min}, \psi_{lf}^{max}$ are the minimum and maximum relative bearing angles compared to the leader.

Based on the kinematic of the formation (3.18a), and the choice of potential function (3.22-3.23), the proposed controller, which ensures convergence and stability of the formation, is designed as follows:

$$u_f = F^{-1}\left(\dot{e}_{lf}^{d} - Hu_l\right) \tag{3.25}$$

with

$$\dot{e}_{lf}^{d} = -K_{lf}\frac{\partial V_{e_{lf}}}{\partial h} \tag{3.26}$$

where $K_{lf} \in \mathbb{R}^{2\times 2}$ is a diagonal positive gain matrix, u_l is the linear/angular velocity of the leader, and $V_{e_{lf}} = [V_{l_{lf}}, V_{\psi_{lf}}]^T$ is the potential field function defined in Definition 2.4.2.
The potential function $V_{e_{lf}}$ and the dynamics $\dot{e}_{lf}$ described by (3.22) and (3.26) respectively indicate that when $e_{lf} > \overline{e_{lf}}$, then $\dot{e}_{lf} > 0$ and the robots are attractive, and when $e_{lf} < \underline{e_{lf}}$, then $\dot{e}_{lf} < 0$, and the robots are repulsive, and when $\frac{(\overline{e_{lf}} - e_{lf})}{2}$, that is, $\dot{e}_{lf} = 0$, the force between the robots reaches an equilibrium, and $V_{e_{lf}}$is minimized. Equation (3.26) acts in (3.18a) as a potential field control, such that the closed loops dynamics become:

$$\begin{cases} \dot{e}_{lf}^{d} = -K_{lf}\frac{\partial V_{e_{lf}}}{\partial h} \\ \\ \phi_{lf} = w_l - w_f \end{cases} \tag{3.27}$$

Proposition 3.4.1: Let us suppose that $v_l > 0$ and $|w_l| < w_{lmax}$ under Assumption 3.4.1, the kinematic control, based on the choice of the potential function (3.25-3.27), stabilizes the system dynamics (3.18a-3.18b) and ensures that all the following objective formation controls are satisfied, in the sense that:

$$l_{lf}^{min} \leq l_{lf} = l_{lf}^{d} \leq l_{lf}^{max}, \quad \psi_{lf}^{min} \leq \psi_{lf} = \psi_{lf}^{d} \leq \psi_{lf}^{max}$$

Proof: Consider the Lyapunov candidate function:

$$V = V_{l_{lf}} + V_{\psi_{lf}} \tag{3.28}$$

From the first derivative of this function with respect to time, we obtain:

$$\dot{V} = \frac{\partial V_{l_{lf}}}{\partial h}\frac{\partial h}{\partial l_{lf}}\frac{\partial l_{lf}}{\partial t} + \frac{\partial V_{\psi_{lf}}}{\partial h}\frac{\partial h}{\partial \psi_{lf}}\frac{\partial \psi_{lf}}{\partial t} \tag{3.29}$$

Substituting (3.26) in (3.29), the following relation can be obtained:

$$\dot{V} = -\left(\frac{\partial h}{\partial e_{lf}}\right)^{T} K_{lf} \left(\frac{\partial V_{e_{lf}}}{\partial h}\right)^{2} \tag{3.30}$$

From the properties of the function $h(e_{lf}, \underline{e_{lf}}, \overline{e_{lf}}) = \begin{bmatrix} h(l_{lf}, \underline{l_{lf}}, \overline{l_{lf}}) & h(\psi_{lf}, \underline{\psi_{lf}}, \overline{\psi_{lf}}) \end{bmatrix}^{T}$ we know that $\frac{\partial h}{\partial e_{lf}} > 0$. Considering the properties of the potential function $V_{e_{lf}}$, under proposition 3.4.1 and (3.25), we have: $u_{fmin} \leqslant u_f \ll u_l$ when the robot is repulsive and $u_l \leqslant u_f \ll u_{fmax}$ when the robot is attractive, where $[u_{fmin}, u_{fmax}]^T$ are the minimum and the maximum linear/angular velocities of the follower, respectively. The first time derivative of (3.28) is $\dot{V} \leq 0$ and, $\dot{V} = 0$ for $e_{lf} \to \frac{(\overline{e_{lf}} - \underline{e_{lf}})}{2}$, which implies that $l_{lf} \to \frac{(l_{lf}^{max} - l_{lf}^{min})}{2}$ and $\psi_{lf} \to \frac{(\psi_{lf}^{max} - \psi_{lf}^{min})}{2}$. This proves that l_{lf}, ψ_{lf} stay within the ranges defined above. Consequently, the closed-loop system is asymptotically stable. To complete the stability study, the stability of the internal dynamics of the formation should be ensured. The internal dynamics is computed from its expression in (3.18a). The expression of w_f is the second element of the vector of the follower velocity u_f.

This expression is then substituted into (3.18b) to obtain:

$$\dot{e}_\phi = -\frac{v_l}{d} sin(e_\phi) + \Gamma\left(w_l, l_{lf}, \dot{l}_{lf}, \dot{\psi}_{lf}, e_\phi\right) \tag{3.31}$$

with $\Gamma = -\frac{1}{d}\left[\dot{l}_{lf} sin\left(e_\phi + \psi_{lf}\right) + \dot{\psi}_{lf} sin\left(e_\phi + \psi_{lf}\right)\right] + w_l\left(1 - \frac{l_{lf}}{d} cos\left(e_\phi + \psi_{lf}\right)\right)$ and $e_\phi = \phi_l - \phi_f$ is the angular error between the leader and the follower. To analyse the stability of the internal dynamics, we need to show that the orientation error is bounded. The nominal system with ($\Gamma = 0$) is given by:

$$\dot{e}_\phi = -\frac{v_l}{d} sin(e_\phi) \tag{3.32}$$

If the linear velocity of the leader mobile robot $v_l > 0$ and $\left\|e_\phi\right\| < \pi$, then the internal dynamics of the system is (locally) exponentially stable. Since the angular velocity of the leader w_l is bounded, we can show that $\|\Gamma\| \leq \alpha$. Using stability theory and the condition $\left|e_\phi(0)\right| < \varepsilon\pi$ gives (Das *et al.* (2002));

$$\left\|e_\phi\right\| < \rho, \ \forall t \geq t_1 \tag{3.33}$$

for some finite time t_1 and a positive number ρ. As shown in (Ghommam *et al.* (2013)), there exists a Lyapunov function $V_{e_\phi} \in [0,\infty) \times T$ where $T = \left\{e_\phi \in R \left\|e_\phi\right\| < c\right\}, c > 0$, such that $\dot{V}_{e_\phi} \leq 0$.

3.4.2 Dynamic control design

An adaptive dynamic control scheme based on the virtual decomposition approach is combined with the kinematic control developed above and used to move each follower to the desired distance range and relative bearing angle region. Firstly, the desired linear and angular velocities of the followers (v_f^d, w_f^d) are calculated from the kinematic control (3.25), (3.2), and then the required velocity $V_f^r = [\dot{x}_f^d, \dot{y}_f^d, 0, 0, 0, w_f^d]^T$ of the mobile platform and that of the two wheels are computed as follows:

$$\dot{q}_{fw}^r = \dot{q}_{fw}^d + \lambda_f\left(\dot{q}_{fw}^d - \dot{q}_{fw}\right) \tag{3.34}$$

where $\dot{q}^d_{fw}$ are the desired right and left wheel angular velocities of the follower robots, λ_f is a positive constant, $w \in \{R,L\}$ the right and left wheels, and f are the follower mobile robots. Since the physical parameters of the platform (object) and the wheels are unknown, the dynamic of the platform (3.5) based on the estimated parameters $\hat{\theta}_{fj} \in \mathbb{R}^{13}$ and the required velocity $V^r_{fj} \in \mathbb{R}^6$, can then be written as:

$$F^{*r}_{fj} = Y_{fj}\hat{\theta}_{fj} + K_{fj}\left(V^r_{fj} - V_{fj}\right) \tag{3.35}$$

where $\dot{\hat{\theta}}_{fj} = -\rho_{fj}Y^T_{fj}s_{fj}$ is the adaptation function, and is chosen to ensure system stability, as in (Zhu (2010)), $s_{fj} = V^r_{fj} - V_{fj}$, $\rho_{fj} \in \mathbb{R}^{13\times 13}$ is a diagonal positive matrix and $j \in \{o,R,L\}$ are the platform (object), the right and left wheels. The vector of the resulting forces/moments acting on the *i*-th rigid body is given by an iterative process. We begin by computing the vector of the required forces at the different cutting points:

$$F^r_{fw} = F^{*r}_{fw}; \quad w = R,L$$

$$F^r_{fo} = F^{*r}_{fo} + \sum_{w=R}^{L} {}^{fw}U_{fo}F^{*r}_{fw} \tag{3.36}$$

where ${}^{fw}U_{fo}$ is defined in (3.8).

The dynamics of the wheel actuators based on their desired velocity $\dot{q}^d_f = [\dot{q}^d_{fR}, \dot{q}^d_{fL}]^T$ is expressed in linear form, and since the physical parameters of the actuators are unknown and need to be estimated, the vector $\hat{\theta}_{af} = [\hat{\theta}_{afR}, \hat{\theta}_{afL}]^T \in \mathbb{R}^8$ is then used, and its dynamics becomes:

$$\tau^{*r}_{af} = Y_{af}\hat{\theta}_{af} + K_{af}\left(\dot{q}^d_f - \dot{q}_f\right) \tag{3.37}$$

where $Y_{af} = diag(Y_{afR}, Y_{afL})$, $\tau^{*r}_{af} = [\tau^{*r}_{afR}, \tau^{*r}_{afL}]^T$ and $\hat{\theta}_{af} = [\hat{\theta}_{afR}, \hat{\theta}_{afL}]^T$, in which $\dot{\hat{\theta}}_{af} = -\rho_{af}Y^T_{af}s_{af}$ is the adaptation function, and is chosen to ensure system stability (Zhu (2010)), $s_{af} = \dot{q}^d_f - \dot{q}_f$, $\rho_{af} = [\rho_{afR}, \rho_{afL}]^T$ and K_{af} are positive constant gains.

Finally, the input control torque at the follower mobile robot actuator is calculated based on the

desired torque obtained from (3.37) and the force at the cutting point B_i, identified F_{fo}^r, as:

$$\tau_f = \tau_{af}^{*r} + \tau_{fc} \tag{3.38}$$

where $\tau_{fc} = S_T F_{fo}^r$ and S^T is defined in (3.11).

Proposition 3.4.2: Assuming that the follower velocities are bounded, consider the mobile robot dynamics (3.6) and the wheels' actuator dynamics (3.14), under the control design (3.38). Then, the systems' states are bounded, in particular, the control objective as in proposition 3.4.1 is satisfied and the error tracking states are asymptotically stable (Zhu (2010)), in the sense that:

$$\lim_{t\to\infty} \left\| x_f^d - x_f \right\| = 0, \ \lim_{t\to\infty} \left\| y_f^d - y_f \right\| = 0$$

$$\lim_{t\to\infty} \left\| \phi_f^d - \phi_f \right\| = 0$$

The virtual decomposition approach ensures that these objectives are achieved, and the reader can find the proof of stability in (Zhu (2010); Brahmi *et al.* (2013b)). In contrast with existing works, the current work presents the following advantages. Firstly, we include a potential function, based on the p-time differential bump function introduced in (Do (2010)) as a kinematic control of the formation. Secondly, since the parameters of the follower robots are considered uncertain, this kinematic control is combined with an adaptive dynamic control scheme based on the VDC to move the follower robots into the desired region.

3.5 Experimental results

Figure 3.4 shows the complete system design of the two control levels, the trajectory generation and the coordination of the group of mobile robots used in our experimental tests. In this section, we discuss the results of the control of different coordinated trajectories of one leader mobile robot and two mobile robots named Ets_Rob, as illustrated in Figure 3.4. A Zigbee technology communication device is used between the application program with 115200 baud rate, implemented in Mathworks® Simulink, and the mobile robots. The mobile robots used

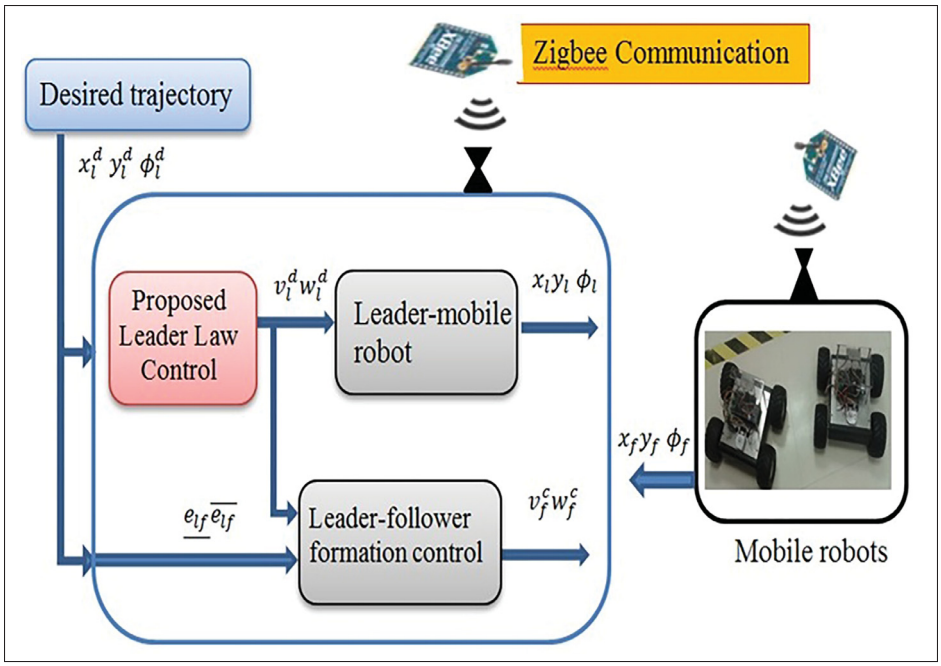

Figure 3.4 Control design for group

in the experimental setup have four wheels, with only the two front wheels being DC-motor actuated. The two wheels of the mobile platform are actuated by two HN-GH12-2217Y DC-motors (DC-12V-200RPM 30:1) and the angular positions are given using encoder sensors (E4P-100-079-D-H-T-B). Specific wheels are used to minimize slips and kinematic errors of the robot. Firstly, a second order filter is used to compute the right and left velocity, then the linear and angular velocities are computed using the kinematic property of the mobile robot (3.1-3.2). The distance between the followers and the leader is calculated using (3.16). The controls gains of the controller are chosen to be $K_{af} = diag(5), K_{of} = diag(2), K_{fw} = diag(2)$, $\rho_{of} = 0.7, \rho_{afw} = 0.8$. The sampling time is set at 0.005 seconds. In the first test, sinusoidal trajectories are discussed. In this scenario, the leader mobile robot moves along the X-axis with a sinusoidal trajectory along the Y-axis. The starting point is $P_i = [x_l, y_l, \phi_l]^T = [0, 1.05, 0.69]^T$ and the arrival point is $P_f = [x_l, y_l, \phi_l]^T = [4.05, 1.05, 0.69]^T$. The two other robots follow the leader at a desired distance and desired relative bearing angle. The two robots are initially placed as follows: $P_{f1} = [x_f, y_f, \phi_f]^T = [0, 0.5, 0]^T$. $P_{f2} = [x_f, y_f, \phi_f]^T = [0, 1.5, 0]^T$. The

desired distance and relative bearing angle for each follower robot are chosen as follows:

$$\begin{cases} 1 \leq l_{lf1}^{d} \leq 1.4 \quad (\text{m}), \quad 4 \leq \psi_{lf1}^{d} \leq 4.2 \quad (\text{rad}) \\ \\ 0.8 \leq l_{lf2}^{d} \leq 1.1 \quad (\text{m}), \quad 1.6 \leq \psi_{lf2}^{d} \leq 1.8 \quad (\text{rad}) \end{cases} \tag{3.39}$$

As can be seen from the experimental results in Figures 3.5-3.6, the trajectory tracking objective for the desired distance range and the relative bearing angle region for a group of mobile robot is achieved. Figure 3.5 shows that the two followers presented with red and green lines

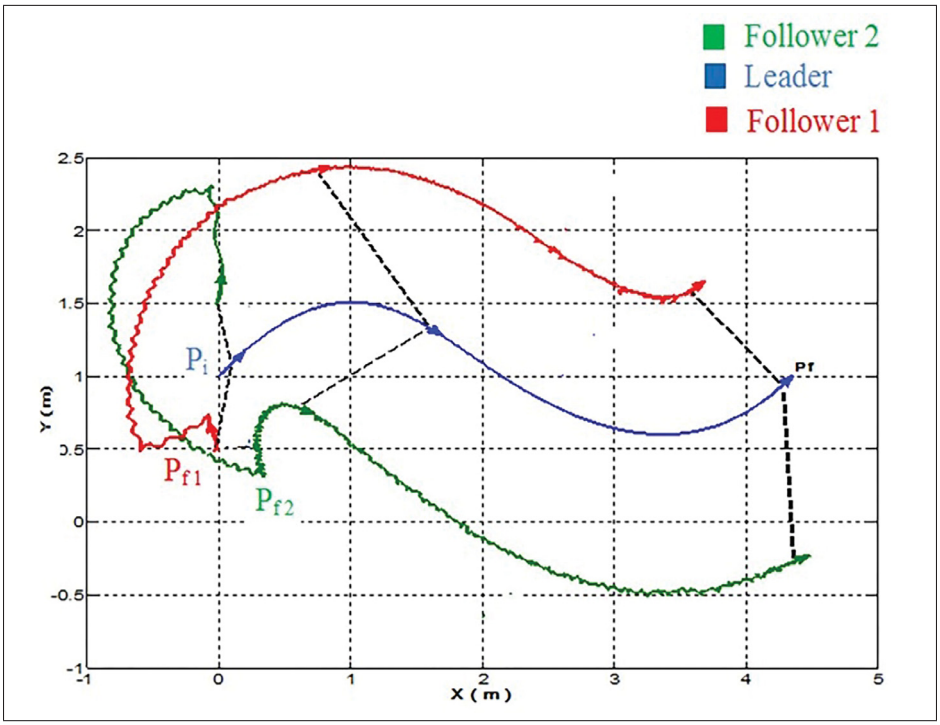

Figure 3.5 Trajectory tracking of the leader-follower formation

placed initially in arbitrary position follow their desired generated trajectory in less than 10 seconds. The good convergence to the desired distance range and the relative bearing angle region is clearly presented in Figure 3.6. In the second test, a linear trajectory is applied with a passage in a known corridor position, which shows the reconfiguration of the formation, thereby avoiding any collision. In this scenario, the leader mobile robot moves along the X-axis. The

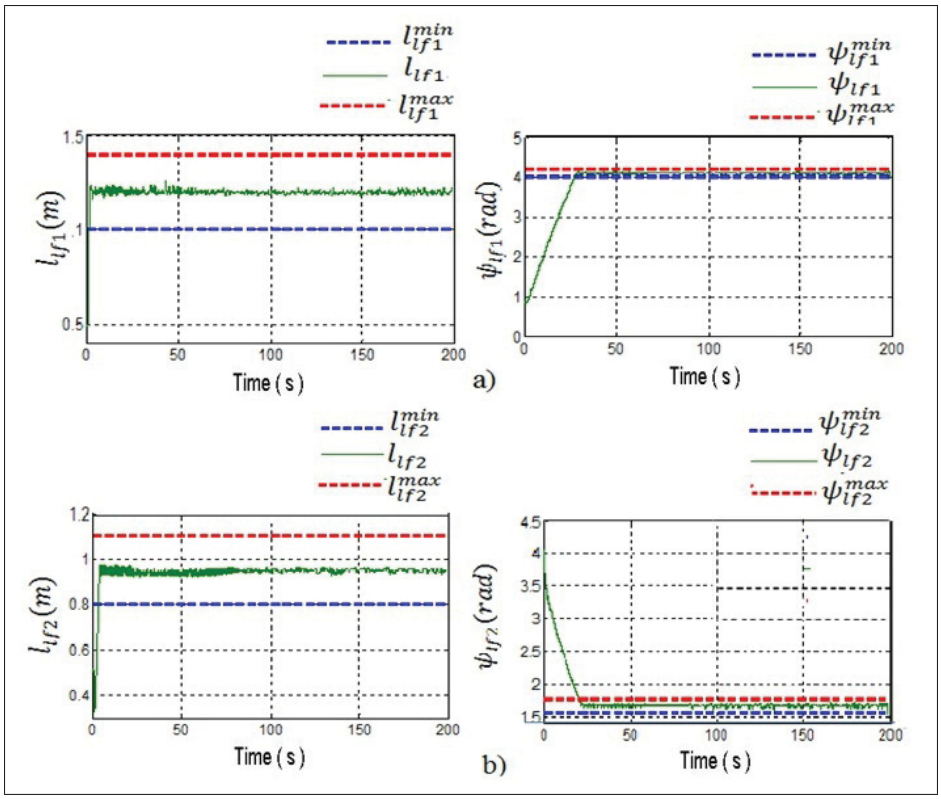

Figure 3.6 Desired and real distances and relative bearing of the two follower robots

starting point is $P_i = [x_l, y_l, \phi_l]^T = [2,2,0]^T$ and it arrives at $P_f = [x_l, y_l, \phi_l]^T = [10,2,0]^T$. The two other robots follow the leader, with a desired distance range and a desired relative bearing angle region outside of the corridor, and with another desired distance and relative bearing angle inside the corridor. The two robots are initially placed as follows:

$P_{f1} = [x_f, y_f, \phi_f]^T = [1.5,1,0]^T$. $P_{f2} = [x_f, y_f, \phi_f]^T = [1.5,3,0]^T$. The desired distance range and relative bearing angle region for each follower robot outside of the corridor are chosen as follows:

$$\begin{cases} 1.2 \le l_{lf1}^d \le 1.4 \quad (\text{m}), \quad 3.8 \le \psi_{lf1}^d \le 4 \quad (\text{rad}) \\ \\ 1 \le l_{lf2}^d \le 1.2 \quad (\text{m}), \quad 1.8 \le \psi_{lf2}^d \le 2.1 \quad (\text{rad}) \end{cases} \tag{3.40}$$

And inside the corridor, these desired values are given as follows:

$$\begin{cases} 1 \leq l_{lf1}^{d} \leq 1.2 \quad (\text{m}), \quad 3.09 \leq \psi_{lf1}^{d} \leq 3.19 \quad (\text{rad}) \\ \\ 0.5 \leq l_{lf2}^{d} \leq 0.7 \quad (\text{m}), \quad 3.09 \leq \psi_{lf2}^{d} \leq 3.19 \quad (\text{rad}) \end{cases} \tag{3.41}$$

In this scenario, a known environment is considered, where the position of the corridor is predefined for the leader mobile robot. Outside of the corridor, the leader moves along a linear predefined trajectory and the followers move at a predefined desired distance and relative bearing angle from the leader (3.40). Inside the corridor, the leader maintains the same predefined trajectory and the followers move at the other predefined desired distance and relative bearing angle (3.41). This change of configuration inside/outside of the corridor is chosen such as to avoid any collision with the corridor and between the follower mobile robots. As can be seen from the experimental results in Figures 3.7-3.8, the trajectory tracking objective for the desired distance range and relative bearing angle region of the two followers is achieved.

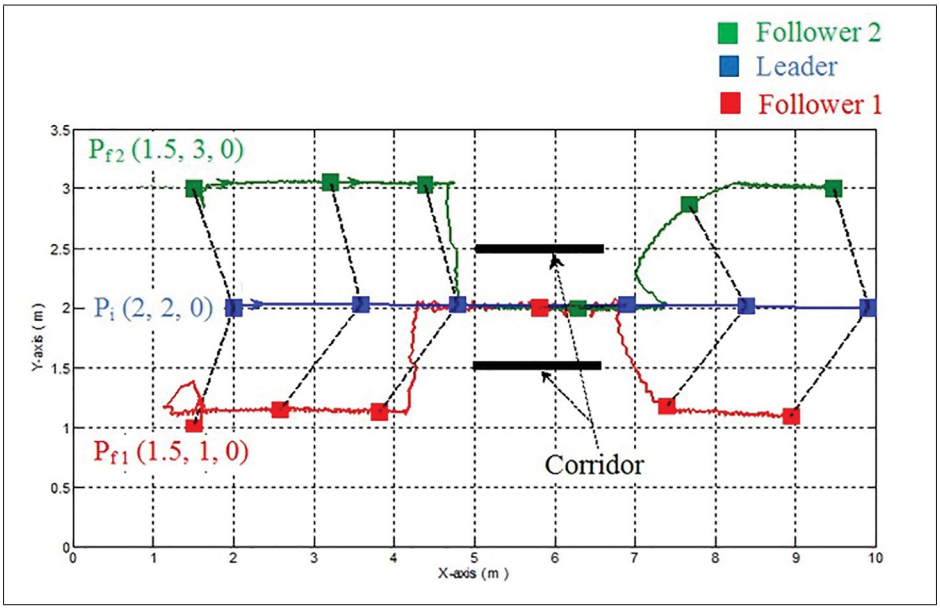

Figure 3.7 Trajectory tracking of the leader-follower formation

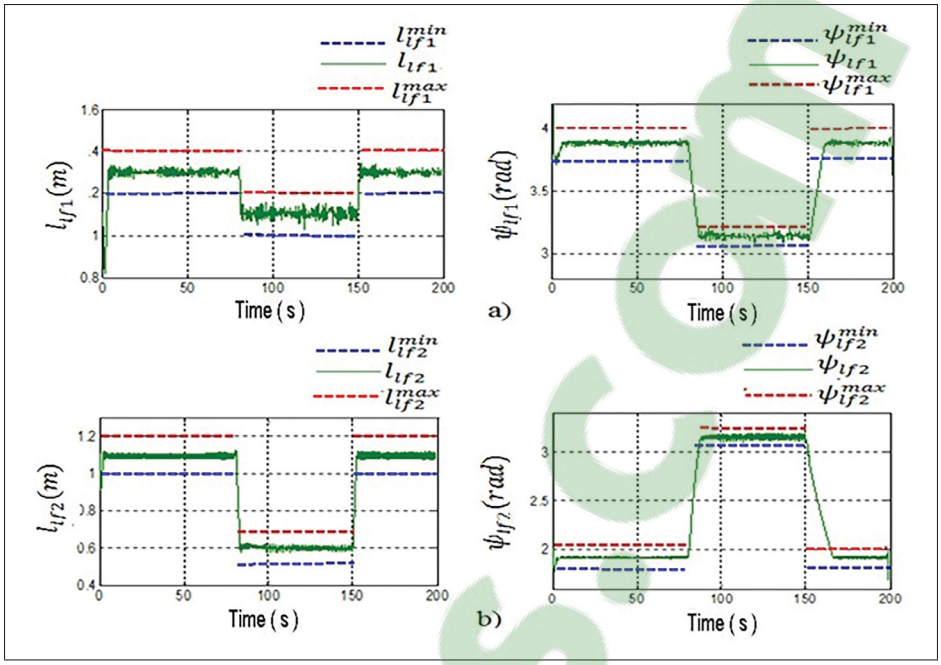

Figure 3.8 Desired and real distances and relative bearing:
a) follower 1 and b) follower 2

For this second experiment, we tested the rapidity of followers to follow the leader. It was decided to change the configuration just before entering inside the corridor forcing the two followers to react faster to avoid a collision with the walls of the corridor. But when they exit the corridor, the most secured way for followers is to follow a reasonable curve as it is illustrated in Figure 3.7.

Figure 3.8 shows a good trajectory tracking and change of configuration of the leader-follower formation outside and inside the corridor.

3.6 Conclusion

In this paper, a combination of the Lyapunov technique, based on the choice of the appropriate potential field function and the virtual decomposition adaptive control approach, has been presented and applied to the leader-follower formation control problem. A multi-level architecture control based on adaptive and PI controllers was designed to have the leader mobile robot move along a predefined trajectory, with the other mobile robots following it at a desired

distance range and a relative bearing angle region within a leader-follower scheme. A high level controller uses the potential function technique as the kinematic control of the formation; this kinematic control is combined with an adaptive control law based on a virtual decomposition approach to move the formation into the desired region. A low level PI controller for the left and right motors is implemented. The obtained real-time results show the effectiveness of the proposed control algorithm, and prove that all the control objectives set in this paper are achieved successfully. In a future work, the leader mobile robot will be replaced by a real mobile robot, and the non-availability of the leader and follower velocity measurements will be considered.

CHAPTER 4

ADAPTIVE COORDINATED CONTROL OF MULTI-MOBILE MANIPULATOR SYSTEMS

Abdelkrim Brahmi[1], Maarouf Saad[1], Guy Gauthier[2], Wen-Hong Zhu[3]
and Jawhar Ghommam[4]

[1] Département of Electrical Engineering, École de Technologie Supérieure,
[2] Département of automated manufacturing Engineering, École de Technologie Supérieure,
1100 Notre-Dame Ouest, Montréal, Québec, Canada H3C 1K3
[3] Space Exploration,Canadian Space Agency,
6767 Route de l'Aéroport, Longueuil (St-Hubert), Québec, Canada J3Y 8Y9
[4] Research Unit on Mechatronics and Automation Systems,
Ecole National d'Ingenieurs de Sfax, BPW,3038 Sfax, Tunisia,

Published in International Journal of Digital Signal and Smart System, August 04, 2017

Abstract

This paper presents an adaptive coordinated control scheme for multiple mobile manipulator robots (MMR) moving a rigid object in coordination. The dynamic parameters of the object handled and of the mobile manipulators are considered unknown but constant. The control law and the adaptation of uncertain parameters are designed using the virtual decomposition (VDC) approach. This control approach was originally applied to multiple manipulator robot systems. The proposed control design ensures that the position error in the workspace converges to zero, and that the external force error is bounded. The global stability of the system using VDC is proven through the virtual stability of each subsystem. Numerical simulations and an experimental validation are carried out for two mobile manipulators transporting an object, and are compared with the results obtained using the computed torque approach in order to show the effectiveness of the proposed controller.

Keywords: Adaptive control, coordinated control, virtual decomposition control, multi-mobile manipulator.

4.1 Introduction

The need for robots capable of locomotion and manipulation has led to the design of mobile manipulator robot (MMR) platforms. Typical examples of MMR include satellite arms, underwater robots in seabed exploration, and vehicles used in extra-planetary exploration. However, the most popular mobile manipulators are semi-automated cranes mounted on trucks. Some operations requiring the handling of heavy objects are very difficult for single mobile manipulators, and require the use and coordination of multiple mobile manipulators, which significantly complicates the robotic system, and greatly increases its control design complexity. The problem with controlling a mechanical system forming a closed kinematic chain mechanism is that it imposes a set of kinematic constraints on the coordination of the position and velocity of the mobile manipulator, thus leading to a reduction in the degrees of freedom of the entire system. Although the object internal forces produced by all mobile manipulators must be controlled, few works have been proposed to solve this control problem for the robotic systems, which have high degrees of freedom and are tightly interconnected because all manipulators are in contact with the object. Most research works in this field have thus far focused on the three main coordination mechanisms involved: decentralized control, the leader-follower control approach and motion planning. In (Kume *et al.* (2007)), a motion coordination control not involving the use of a torque/force sensor is proposed and applied to a multi-holonomic mobile manipulator. To reduce the effect of the sensor noise at the end-effector, a control scheme using constraints between the contact points and the point representing the handled object was proposed in (Kosuge and Oosumi (1996); Hirata *et al.* (1999); Kosuge *et al.* (1999)). The authors then extended and applied this approach on multiple omnidirectional mobile robots manipulating a rigid object in coordination. A further extension of the method applied to manipulators with bases attached to a holonomic mobile manipulator, engaged in novel decentralized cooperation tasks, was proposed in (Khatib *et al.* (1996b); Park and Khatib (2008)).

In another approach, a single or a group of MMR is designated as a leader capable of moving a desired trajectory, while the other group members follow this leader. Many papers, including (Chen and Li (2006); Hirata *et al.* (2004c); Tang *et al.* (2009); Fujii *et al.* (2007)), have cov-

ered this approach. Finally, the third approach deals with the motion planning strategy, which is another fundamental problem in robotics, especially in multi-robot systems. This approach has been covered in a limited number of research works in the case of multiple mobile manipulator robots, where several robots execute the task of transporting an object in coordination, in a known/unknown environment. These studies include those presented in (Desai and Kumar (1997); Pajak *et al.* (2004); Sun and Gong (2004b); LaValle (2006); Latombe (2012); Furuno *et al.* (2003); Zhu and Yang (2003)). In (Desai and Kumar (1997)), an optimal trajectory was proposed for two mobile manipulators pushing a common object to a desired location; the authors in (Pajak *et al.* (2004)) proposed a control method for multiple mobile manipulators holding a common object. Here, the measures of kinematic and dynamic manipulability were given, taking into account collision avoidance, but the dynamics of the object was however ignored. In (Sun and Gong (2004b); LaValle (2006)), a planning approach based on genetic algorithms was proposed.

Over the past few years, increased attention has been paid to the adaptive control of robotic systems with high degrees of freedom, with many research works developed based on the approach, including those in (Chen (2015); Zhao *et al.* (2016); Liu *et al.* (2016); Andaluz *et al.* (2012); Yan *et al.* (2014); Karray and Feki (2014)). This is due to the fact that this type of robotic system can be implemented in complex applications with unknown parameters. The kinematics and dynamics of these systems are characterized by uncertainty, high nonlinearity, and tight coupling, which in turn renders the control problem very complicated and difficult to solve using the classical approaches developed and explained above. One of the categories of complex robotic systems involves multiple-mobile manipulator systems holding an object. The constraints imposed on a system forming a closed kinematic chain will often cause the degrees of freedom of motion to be less than the number of actuators. In this case, not only the motions, but also the internal forces, need to be controlled. To overcome these problems, a novel adaptive control based on the virtual decomposition approach is proposed in this work.
All previous studies based on Lagrangian or Newton/Euler approaches require knowledge of the exact parameters of the system. In practice, this is difficult, and using them, the model

obtained is usually uncertain. To overcome the problem of dynamic modelling and control, some researchers have proposed an adaptive control based on neural network control (Liu *et al.* (2014); Liu and Zhang (2013); Liu *et al.* (2013)) and fuzzy logic approaches (Mai and Wang (2014); Yoshimura (2015); Baklouti *et al.* (2016)). For instance, non-model-based techniques have been developed for a different type of mobile manipulator robot with dynamic parameter uncertainties. Another problem with existing approaches is that with them, the dynamics of the whole system are complicated. Any change in the structure of the group requires a new dynamic modeling (removal of a faulty robot or addition of a new robot to the system). Finally, for these types of tightly coupled systems with a high degree of freedom, adapting the parameters using methods based on full dynamics is very complicated due to the huge number of parameters involved.

Based on the preceding observations, in this paper, we intend to extend the work proposed in (Brahmi *et al.* (2016a)) by using the adaptive decentralized control of a single mobile manipulator robot based on virtual decomposition control (VDC) (Zhu *et al.* (1997); Al-Shuka *et al.* (2014); Zhu (2010); Ochoa Luna *et al.* (2015)) originally designed for fixed-base robotic systems with high degrees of freedom. Furthermore, diverging from what is seen in the available works in the literature, we propose an adaptive coordinated control based on the VDC approach. The main contributions of this paper are summarized as follows.

a. Most approaches cited previously are fundamentally based on the Lagrangian formulation in calculating the dynamic model of robotic systems in closed form. It is known that the complexity of the dynamic expression obtained is proportional to the fourth power of the number of degrees of freedom of the robotic systems (Hollerbach (1980); Craig (2005)). This fact challenges both the numerical simulation and real-time control of robots with high degrees of freedom. To overcome this difficulty, an adaptive decentralized approach based on an extension of the virtual decomposition control (VDC) is proposed in this paper;

b. To overcome the problem of adaptation and modeling of systems using classical approaches, a VDC approach is implemented, which makes the control system more flexible in meeting changes to its configuration. In this case, adding a new robot or removing a faulty one from the system does not require a recalculation of the full dynamics of the system.

c. Using the VDC approach means that changing the dynamics of a subsystem only affects the respective local equations associated with that subsystem, while the equations associated with the rest of the system remain unchanged;

d. The global stability of the system's VDC is proven through the virtual stability of each subsystem. Contrary to the original VDC stability, in this paper, all parameters are considered completely unknown, in addition to there being no known limit for the estimated parameters;

- The whole dynamics of the system can easily be found based on the individual dynamics of each subsystem (rigid object and open chains);
- The schemes render the system control design very flexible and greatly facilitate the calculation of the dynamic system, with respect to changes in the system configuration, and
- They greatly simplify the adaptation of the physical parameters, which they make systematic.

The rest of the paper is organized as follows. Section 4.2 presents the modeling of the system, while section 4.3 presents the problem control statement. Section 4.4 explains the control design. Simulation results are given in section 4.5. Section 4.6 presents an experimental validation of the developed approach. Finally, a conclusion is given in section 4.7.

4.2 Modelling system and description

Figure 4.1 shows the N (MMR) handling a common rigid object, with P_{ie} being the position/orientation vector of the *i*-th MMR effector and the position/orientation vector of the object. Before presenting the developed adaptive control law based on the virtual decomposition approach, we will briefly formulate the kinematic and dynamic modeling of the *i*-th mobile manipulator robot and the handled object.

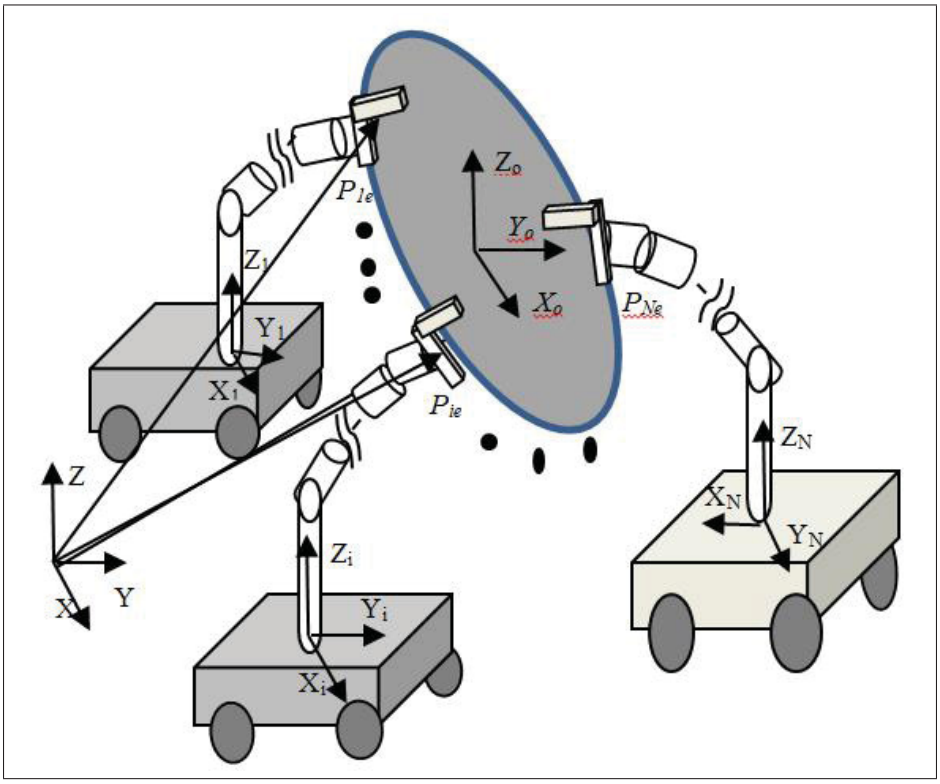

Figure 4.1 Multiple MMR handling a rigid object

The VDC approach consists in breaking down the robotic system into a graph comprised of several objects and open chains. An object is a rigid body and an open chain consists of a series of rigid links connected one-by-one by a hinge, and having a certain degree of freedom. The dynamic coupling between the subsystems can be represented by the flow of virtual power (FVP) at the cutting point; this is the principle of virtual work (Zhu *et al.* (1997); Al-Shuka *et al.* (2014); Zhu (2010)). The decomposition is illustrated in Figure 4.2 as follows:

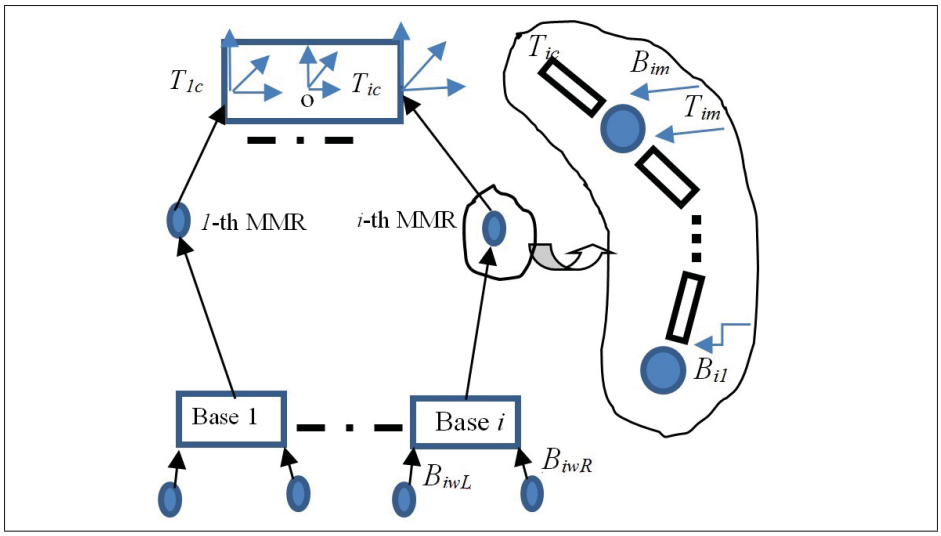

Figure 4.2 Virtual decomposition of the robotic system

4.2.1 Kinematics and dynamics of the object

4.2.1.1 Kinematics and dynamics of the object

Since the frames o and T_{ic} for all $i \in \{1,N\}$ are rigidly attached, it follows that:

$$V_c = \begin{bmatrix} V_{1c} \\ . \\ . \\ . \\ V_{Nc} \end{bmatrix} = {}^oU_{T_c}^T \Gamma^T {}^oV = J_o {}^oV \tag{4.1}$$

where ${}^oV = [v_o^T \; w_o^T]^T$ with v_o and w_o being the linear and angular velocities of the center of gravity of the object, respectively. $V_c = \begin{bmatrix} V_{1c}^T & . & . & . & V_{Nc}^T \end{bmatrix}^T$ are the velocities at the contact points between the end-effectors and the object , T_{ic} , $i \in \{1,N\}$ and J_o is the Jacobian matrix given as follows:

${}^oU_{T_c} = diag[{}^oU_{T_{1c}}, ..., {}^oU_{T_{ic}}, ..., {}^oU_{T_{Nc}}] \in \mathbb{R}^{6N \times 6N}$ and $\Gamma = [I_6, ..., I_6]^T \in \mathbb{R}^{6 \times 6N}$

where I_6 is the 6×6 identity matrix, and the transformation matrix of force/moment and lin-

ear/angular velocity vectors from frame B to frame A is defined by:

$$ {}^{A}U_{B} = \begin{bmatrix} {}^{A}R_{B} & 0_{3\times 3} \\ S({}^{A}r_{AB}){}^{A}R_{B} & {}^{A}R_{B} \end{bmatrix} \tag{4.2} $$

where ${}^{A}R_{B}$ is the rotation matrix between frames A and B, and $S({}^{A}r_{AB})$ is a skew symmetric matrix built from the vector ${}^{A}r_{AB}$ linking the origins of frames A and B, expressed in the coordinates of frame A.

4.2.1.2 Dynamics model of the object

The object handled by N mobile manipulators is rigid. The equation of motion of the effort based on the linear parameterization form is given by the following equation:

$$ \begin{aligned} {}^{o}F &= M_o {}^{o}\dot{V} + C_o {}^{o}V + G_o \\ &= Y_o \theta_o \end{aligned} \tag{4.3} $$

where, v_o and w_o being respectively the linear and angular velocities of the object.${}^{o}F \in \mathbb{R}^6$ is the vector of forces applied on the object, $M_o \in \mathbb{R}^{6\times 6}$ is the mass matrix, $C_o \in \mathbb{R}^{6\times 6}$ represents the centrifugal and Coriolis matrix and $G_o \in \mathbb{R}^6$ is the vector of gravity, $Y_o \in \mathbb{R}^{6\times 13}$ is the dynamic regressor matrix and $\theta_o \in \mathbb{R}^{13}$ is known parameter vector, defined in (Zhu *et al.* (1997); Al-Shuka *et al.* (2014); Zhu (2010)).

The net force/moment vector is given by:

$$ \begin{aligned} {}^{o}F^{*} &= \sum_{i=1}^{N} {}^{o}U_{T_{ic}}^{T} {}^{T_{ic}}F \\ &= \Gamma {}^{o}U_{T_c} {}^{T_c}F \end{aligned} \tag{4.4} $$

where, ${}^{T_c}F = \begin{bmatrix} {}^{T_1 c}F^{T} & . & . & . & {}^{T_N c}F^{T} \end{bmatrix}^{T}$ denotes the force/moment vectors in frame T_{ic} at the contact (cutting) point for $i \in \{1, N\}$. By introducing the internal force vector $F_{int} \in \mathbb{R}^{6\times(N-1)}$,

the force/moment vectors at the contact point T_{ic} can be computed from (4.4) as:

$$ {}^{T_c}F = {}^{T_c}U_o \begin{bmatrix} \Phi_m & \Phi_f \end{bmatrix} \begin{bmatrix} {}^{o}F^* \\ F_{\text{int}} \end{bmatrix} \tag{4.5} $$

where ${}^{T_c}U_o = {}^{o}U_{T_c}^{-1}$ and the matrices $\Phi_m \in \mathbb{R}^{6N\times 6}$ and $\Phi_f \in \mathbb{R}^{6N\times(6N-6)}$ are governed by:

$$ \begin{cases} \Gamma\Phi_m = I_6 \\ \Gamma\Phi_f = 0 \end{cases} \tag{4.6} $$

Note that the matrix $\begin{bmatrix} \Phi_m & \Phi_f \end{bmatrix}$ is of full rank. There exists a matrix Ω that verifies:

$$ \begin{bmatrix} \Gamma \\ \Omega \end{bmatrix} = \begin{bmatrix} \Phi_m & \Phi_f \end{bmatrix}^{-1} \tag{4.7} $$

Therefore, the internal force coordinates can be calculated from (4.5) based on the force/moment at the N end-effectors as follows:

$$ F_{\text{int}} = \Omega {}^{o}U_{T_c} {}^{T_c}F \tag{4.8} $$

4.2.2 Kinematics and dynamics of the i-th mobile manipulator

Figure 4.3 shows the *i*-th holonomic manipulator arm mounted on a nonholonomic mobile platform where the manipulator has ***p***-DOF, the mobile platform has ***m***-DOF, and the full robotic system has ***n=m+p***-DOF.

4.2.2.1 Kinematics of the *i*-th mobile manipulator

The augmented linear/angular velocities vector of each frame B_{ij} is defined as $V_{iB} = [\dot{q}_{ij}, V_{iv}, V_{B_{iwR}}^T, V_{B_{iwL}}^T, V_{B_{i1}}^T, ..., V_{B_{im}}^T]^T$, where $\dot{q}_{ij} = [\dot{q}_{iwR}, \dot{q}_{iwL}, \dot{q}_{i1} ..., \dot{q}_{im}]$ are the right/left wheels velocities and the *j*-th joint velocities of the manipulator arm, $V_{B_{ij}} \in \mathbb{R}^6$ is the linear

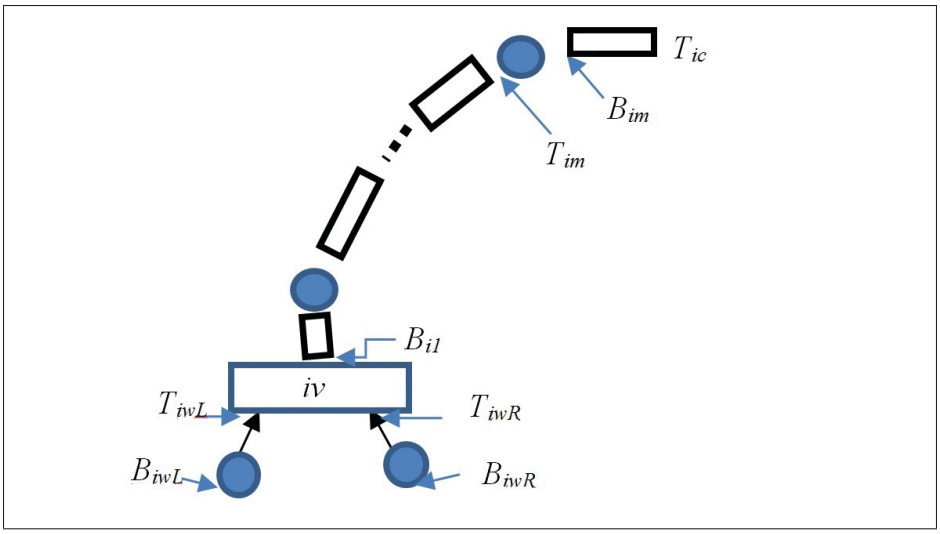

Figure 4.3 Virtual decomposition of the i-th MMR

and angular velocity vector of the corresponding frame B_{ij},and $V_{iv} \in \mathbb{R}^6$ is the linear/angular velocity vector of the mobile platform of the i-th mobile manipulator robot.

In general, we can write the system in matrix form by using the Jacobian matrix:

$$\begin{cases} V_{iB} = J_{in}\dot{q}_{ij} \\ V_{ic} = J_{iq}\dot{q}_{ij} \end{cases} \tag{4.9}$$

where V_{ic} is the velocity at the contact points attached to the object and J_{in}, J_{iq} are the Jacobian matrices.

4.2.2.2 Dynamics of the i-th mobile manipulator

The dynamics of the j-th rigid body of the i-th manipulator arm based on the linear parameterization form is given by the following equation:

$$\begin{aligned} {}^{*}F_{B_{ij}} &= M_{B_{ij}}\dot{V}_{B_{ij}} + C_{B_{ij}}V_{B_{ij}} + G_{B_{ij}} \\ &= Y_{B_{ij}}\theta_{B_{ij}} \end{aligned} \tag{4.10}$$

where $M_{B_{ij}}$ is the matrix of inertial term, $C_{B_{ij}}$ is the matrix of centrifugal/Coriolis term, $G_{B_{ij}}$ is the vector related to the gravity, $Y_{B_{ij}} \in \mathbb{R}^{6\times 13}$ is the dynamic regressor matrix and $\theta_{B_{ij}} \in \mathbb{R}^{13}$

is known parameter vector, defined in (Zhu *et al.* (1997); Al-Shuka *et al.* (2014); Zhu (2010)), and $j = wR, wL, 1, .., m$ represents the right/left wheels and the m joints of the arm manipulator. The dynamics of the mobile platform (object) based on the linear parametrization form is given by the following equation:

$$\begin{aligned} F_{iv}^{*} &= M_{iv}\dot{V}_{iv} + C_{iv}V_{iv} + G_{iv} \\ &= Y_{iv}\theta_{iv} \end{aligned} \tag{4.11}$$

where M_{iv} is the matrix of inertial term, C_{iv} is the matrix of centrifugal/Coriolis term, G_{iv} is the vector related to the gravity, $Y_{iv} \in \mathbb{R}^{6\times 13}$ is the dynamic regressor matrix and $\theta_{iv} \in \mathbb{R}^{13}$ is known parameter vector, defined in appendix I.

The vector of resulting forces/moments acting on the rigid body is computed by an iterative process as follows:

$$\begin{aligned} F_{B_{im}} &= F_{B_{im}}^{*} + {}^{B_{im}}U_{T_{ie}}\,{}^{T_{ie}}F \\ F_{B_{im-1}} &= F_{B_{im-1}}^{*} + {}^{B_{im-1}}U_{B_{im}}F_{B_{im}} \\ &\vdots \\ F_{iv} = F_{iv}^{*} &= {}^{iv}U_{T_{iwR}}F_{T_{iwR}} + {}^{iv}U_{T_{iwL}}F_{T_{iwL}} + {}^{iv}U_{B_{i1}}F_{B_{i1}} \\ F_{B_{iwR}} &= F_{B_{iwR}}^{*} + {}^{B_{iwR}}U_{T_{iwR}}F_{T_{iwR}} \\ F_{B_{iwL}} &= F_{B_{iwL}}^{*} + {}^{B_{iwL}}U_{T_{iwL}}F_{T_{iwL}} \end{aligned} \tag{4.12}$$

The dynamics of the j-th joint actuator of the manipulator arm and that of the right/left driving motors of the platform are expressed based on the linear parameterization form by the following equation:

$$\begin{aligned} \tau_{a_{ij}}^{*} &= J_{m_{ij}}\ddot{q}_{ij} + \xi_{ij}(t) \\ &= Y_{a_{ij}}\theta_{a_{ij}} \end{aligned} \tag{4.13}$$

where, $J_{m_{ij}}$ denotes the moment of inertia of j-th joint motor, $\xi_{ij}(t) \in \mathbb{R}$ denotes the friction force/torque, $j = wR, wL, 1, .., m$ is defined in (4.10) and $Y_{a_{ij}} \in \mathbb{R}^{1\times 4}$ is the dynamic regressor matrix and $\theta_{a_{ij}} \in \mathbb{R}^{4}$ is known parameter vector, defined in (Zhu *et al.* (1997); Al-Shuka *et al.* (2014); Zhu (2010)).

Finally, from (4.10) and (4.13), the dynamics of the i-th mobile manipulator robot can be written as follows:

$$\tau_{a_{ij}} = \tau^*_{a_{ij}} + z^T F_{B_{ij}} \tag{4.14}$$

with, $Z = [0\ 0\ 0\ 0\ 0\ 1]^T$ for the revolute joints and $Z = [0\ 0\ 1\ 0\ 0\ 0]^T$ for the prismatic joints.

4.3 Control problem statement

To simplify the control formulation, the following assumptions are made:

Assumption 3.1: The desired object trajectory is assumed to be smooth, and there exists ε_1 , ε_2 and ε_3 such that

$$\left\| \frac{\partial X_o^d}{\partial x} \right\| \leq \varepsilon_1, \left\| \frac{\partial^2 X_o^d}{\partial x^2} \right\| \leq \varepsilon_2, \left\| \frac{\partial^3 X_o^d}{\partial x^3} \right\| \leq \varepsilon_3,$$

Assumption 4.2: The object is rigid, and all end-effectors are attached rigidly to it. As a result, there is no relative motion between the end-effector and the object.

Assumption 4.3: The parameters of the object and the mobile manipulators are unknown, but constant.

Assumption 4.4: All the joint velocities of the mobile manipulator robots are available for feedback as well as for the measurement of external forces.

The control objective is to generate a set of torque inputs such that the position tracking error of the transported object in the workspace converges asymptotically to zero. Formally speaking, the control problem is to design the control input:

$$U = f\left(V_c, \dot{V}_c, X_o, {}^oV\right)$$

such that the following limits hold:

$$-\lim_{t\to\infty} \left\| X_o - X_o^d \right\| = 0, \lim_{t\to\infty} \left\| {}^oV - {}^oV^d \right\| = 0$$

$$-\lim_{t\to\infty}\left\|F_{\text{int}}^{d}-F_{\text{int}}\right\|=bounded.$$

where, $X_o^d \in \mathbb{R}^6, {}^oV^d \in \mathbb{R}^6$ are the desired position and velocity of the object generated in the workspace, and $F_{\text{int}}^d \in \mathbb{R}^{6N}$ and $F_{\text{int}} \in \mathbb{R}^{6N}$ are the desired and measured internal forces/moment coordinates.

4.4 Control design

4.4.1 Methodology

The overall control system is designed using the following steps:

- The required velocities of the object ${}^oV^r \in \mathbb{R}^6$ as well as the velocities of the end-effector are first computed, and then the required velocity of the n fixed body frames illustrated in Figure 4.2, are calculated;
- The VDC approach is used to simplify the problem of adaptation of the parameters of the complete systems, with this problem converted into a problem of estimation of the parameters of each subsystem. From the velocities computed in the first step, the estimated parameters are calculated;
- The control law of each mobile manipulator is finally designed.

4.4.2 Design

Step 1. The required velocity ${}^oV^r \in \mathbb{R}^6$ of the object is calculated based on the desired object velocity ${}^oV^d \in \mathbb{R}^6$:

$${}^oV^r = {}^oV^r + K_\lambda e_o \tag{4.15}$$

where $e_o = X_o^d - X_o$ is the position/orientation error vector and K_λ is a scalar.
constant. The desired velocity at the contact point of the N mobile manipulators with the object

${}^{c}V^{r} \in \mathbb{R}^{6}$ is calculated from the required velocity of the object ${}^{o}V^{r} \in \mathbb{R}^{6}$:

$$V_c^r = \begin{bmatrix} V_{1c}^r \\ . \\ . \\ . \\ V_{Nc}^r \end{bmatrix} = {}^{o}U_{T_c}^{T}(\Gamma^{T\,o}V^r + \Omega^T K_f(\tilde{F}_{\text{int}}^d - \tilde{F}_{\text{int}})) \tag{4.16}$$

where Γ, Ω are defined in (4.6),(4.7), K_f is a diagonal positive definite matrix, and $\tilde{F}_{int}^d, \tilde{F}_{int}$ are the filtered internal force/moment coordinates, which are obtained as:

$$\begin{cases} \dot{\tilde{F}}_{int}^d = \lambda_f(F_{\text{int}}^d - \tilde{F}_{\text{int}}^d) \\ \dot{\tilde{F}}_{\text{int}} = \lambda_f(F_{int} - \tilde{F}\text{int}) \end{cases} \tag{4.17}$$

with λ_f being a diagonal positive definite matrix.

Step 2. In this step, the goal is to virtually decompose (Zhu *et al.* (1997)) the robotic system into several parts and open chain elements. Each part is a rigid body, and an open chain consists of a series of rigid links connected one-by-one.

Assumption 4.4.1: In this paper, the manipulators are operating away from any singularity. The required velocity in any frame is given by:

$$\begin{cases} V_{ic}^r = J_{iq}\dot{q}_{ij}^r \\ V_{iB}^r = J_{in}\dot{q}_{ij}^r \end{cases} \tag{4.18}$$

with $V_{iB}^r = [\dot{q}_{ij}^r, V_{iv}^r, V_{B_{iwR}}^{rT}, V_{B_{iwL}}^{rT}, V_{B_{i1}}^{rT}, ..., V_{B_{im}}^{rT}]^T$, J_{iq}, J_{in} being the Jacobian matrix, and $\dot{q}_{ij}^r = [\dot{q}_{iwR}^r, \dot{q}_{iwL}^r, \dot{q}_{i1}^r ..., \dot{q}_{im}^r]^T$ being the required joint angular velocities.
The dynamics of the object (4.3) based on its required velocity ${}^{o}V^{r} \in \mathbb{R}^{6}$ and their estimated parameter is expressed in linear form by the following equation:

$${}^{o}F^{*r} = Y_o\hat{\theta}_o + K_o({}^{o}V^r - {}^{o}V) \tag{4.19}$$

where ${}^{o}F^{*r} \in \mathbb{R}^6$ is the required object force, $\dot{\hat{\theta}}_o = \rho_o Y_o s_o \in \mathbb{R}^{13}$ is the adaptation function, and is chosen to ensure system stability, $s_o = ({}^{o}V^{r} - {}^{o}V)$, ρ_o, K_o are positive gains, and $Y_o \in \mathbb{R}^{6\times 13}$ is the dynamic regressor matrix, defined in (Zhu *et al.* (1997); Al-Shuka *et al.* (2014); Zhu (2010)).

The required force/moment vectors at the N end-effectors are computed from (4.10) as:

$$ {}^{T_c}F^{r} = {}^{T_e}U_o \begin{bmatrix} \Phi_m & \Phi_f \end{bmatrix} \begin{bmatrix} {}^{o}F^{*r} \\ F^{d}_{\text{int}} \end{bmatrix} \tag{4.20} $$

The control equation of the *j*-th rigid body of the *i*-th manipulator (4.10), based on its required velocity and its estimated parameters, is given in linear form by the following equation:

$$ F^{*r}_{B_{ij}} = Y_{B_{ij}} \hat{\theta}_{B_{ij}} + K_{B_{ij}} (V^{r}_{B_{ij}} - V_{B_{ij}}) \tag{4.21} $$

where $\dot{\hat{\theta}}_{B_{ij}} = \rho_{B_{ij}} Y_{B_{ij}} s_{B_{ij}} \in \mathbb{R}^{13}$ is the adaptation function, and is chosen to ensure system stability; $s_{B_{ij}} = (V^{r}_{B_{ij}} - V_{B_{ij}})$, $\rho_{B_{ij}}$, $K_{B_{ij}}$ are positive gains, and is the dynamic regressor matrix, defined in (Zhu *et al.* (1997); Al-Shuka *et al.* (2014); Zhu (2010)).

The vector of resulting forces/moments acting on the *j*-th rigid body is given by an iterative process (Al-Shuka *et al.* (2014)). We begin by computing the vector of forces at the different cutting points:

$$ \begin{aligned} F^{r}_{B_{im}} &= F^{r*}_{B_{im}} + {}^{B_{im}}U_{T_{ie}} {}^{T_{ic}}F^{r} \\ F^{r}_{B_{im-1}} &= F^{r*}_{B_{im-1}} + {}^{B_{im-1}}U_{B_{im}} F^{r}_{B_{im}} \\ &\vdots \\ F^{r}_{iv} = F^{r*}_{iv} &= {}^{iv}U_{T_{iwR}} F^{r}_{T_{iwR}} + {}^{iv}U_{T_{iwL}} F^{r}_{T_{iwL}} + {}^{iv}U_{B_{i1}} F^{r}_{B_{i1}} \\ F^{r}_{B_{iwR}} &= F^{r*}_{B_{iwR}} + {}^{B_{iwR}}U_{T_{iwR}} F^{r}_{T_{iwR}} \\ F^{r}_{B_{iwL}} &= F^{r*}_{B_{iwL}} + {}^{B_{iwL}}U_{T_{iwL}} F^{r}_{T_{iwL}} \end{aligned} \tag{4.22} $$

The control equation of the j-th joint actuator of the manipulator arm and the mobile platform driving motor (4.13) are expressed by the following expression:

$$\tau_{a_{ij}}^{r*} = Y_{a_{ij}}\hat{\theta}_{a_{ij}} + K_{a_{ij}}(\dot{q}_{ij}^{r} - \dot{q}_{ij}) \tag{4.23}$$

where $\dot{\hat{\theta}}_{a_{ij}} = \rho_{a_{ij}} Y_{a_{ij}}^{T} s_{a_{ij}}$ is the adaptation function, and is chosen to ensure system stability; $s_{a_{ij}} = (\dot{q}_{ij}^{r} - \dot{q}_{ij})$,$\rho_{a_{ij}}$, $K_{a_{ij}}$ are positive gains, and $Y_{a_{ij}}$ is the dynamic regressor (row) vectors, defined in (Zhu *et al.* (1997); Al-Shuka *et al.* (2014); Zhu (2010)) and $j = wR, wL, 1, ..., m$. Finally, from (4.21),(4.22) and (4.23), the control equation of the i-th mobile manipulator mobile robot can be written as follows:

$$\tau_{a_{ij}} = \tau_{a_{ij}}^{r*} + z^{T} F_{B_{ij}}^{r} \tag{4.24}$$

with $j = wR, wL, 1, ..., m$ and z defined in (4.10). The block diagram in Figure 4.4 shows the different control law calculation and implementation steps.

4.4.3 Stability analysis

Consider the j-th rigid dynamics (4.10-4.12) and the joint actuator dynamics (4.13), under the control design (4.21-4.23). The control objective is satisfied and the error tracking states are asymptotically stable.

Remark 4.1: The global stability of the system using the VDC approach is proven through the virtual stability of each subsystem (Brahmi *et al.* (2016a); Al-Shuka *et al.* (2014)).

Proof: To prove the stability, we consider the following Lyapunov function:

$$V = \sum_{i=1}^{N} \left(\sum_{j=1}^{n} V_{ij} + \sum_{j=1}^{n} V_{a_{ij}} + V_{iv} \right) + V_{ob} + V_{f} \tag{4.25}$$

where $V_{ij}, V_{a_{ij}}, V_{ip}, V_{ob}$ and V_f are non-negative Lyapunov candidate functions related to the j-th rigid link, the j-th joint, the mobile platform of the i-th mobile manipulator robot, the handled

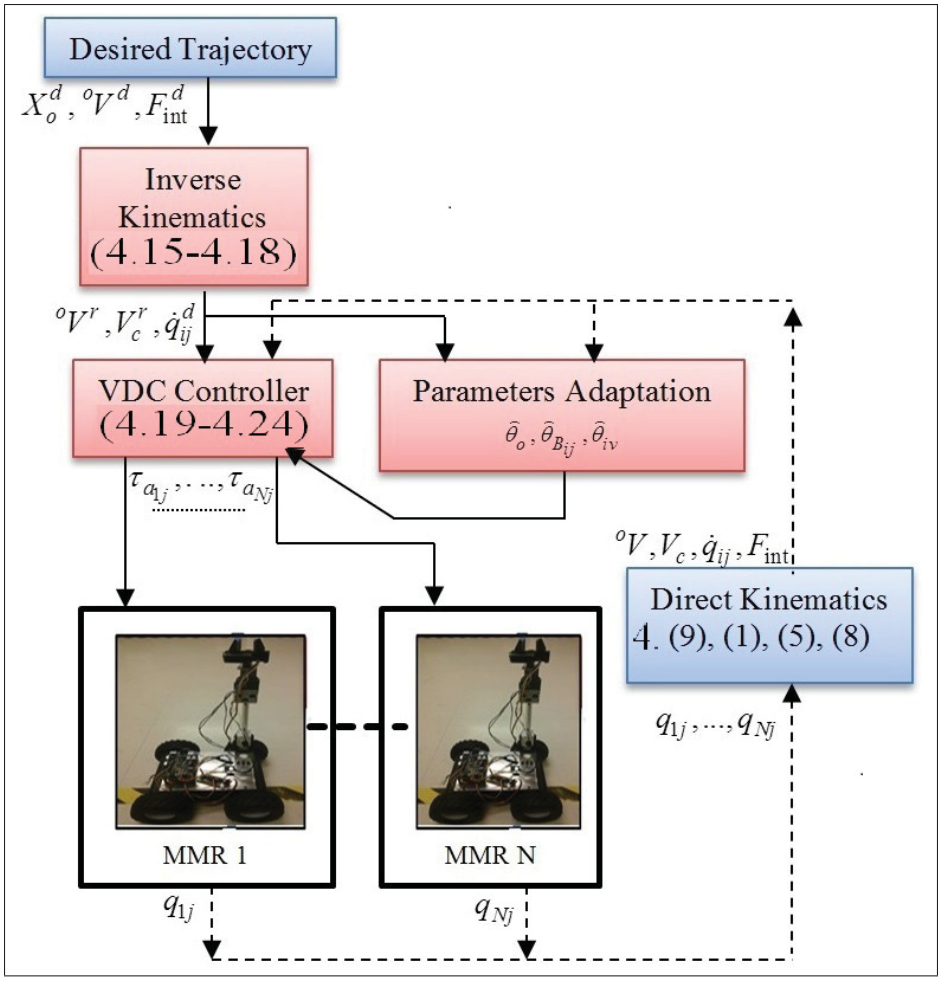

Figure 4.4 Adaptive coordinated control of N MMRs

object and the internal force, respectively. These Lyapunov candidate functions are chosen as follows:

$$\begin{cases} V_{ij} = \frac{1}{2}\left(V_{B_{ij}}^r - V_{B_{ij}}\right)^T M_{B_{ij}}\left(V_{B_{ij}}^r - V_{B_{ij}}\right) + \frac{1}{2}\sum_{k=1}^{13}\frac{\left(\theta_{B_{ijk}} - \hat{\theta}_{B_{ijk}}\right)^2}{\rho_{B_{ijk}}} \\ V_{a_{ij}} = \frac{1}{2}J_{m_{ij}}\left(\dot{q}_{ij}^r - \dot{q}_{ij}\right)^2 + \frac{1}{2}\sum_{k=1}^{4}\frac{\left(\theta_{a_{ijk}} - \hat{\theta}_{a_{ijk}}\right)^2}{\rho_{a_{ijk}}} \\ V_{iv} = \frac{1}{2}\left(V_{iv}^r - V_{iv}\right)^T M_{iv}\left(V_{iv}^r - V_{iv}\right) + \frac{1}{2}\sum_{k=1}^{13}\frac{\left(\theta_{iv_k} - \hat{\theta}_{iv_k}\right)^2}{\rho_{iv_k}} \\ V_{ob} = \frac{1}{2}\left({}^oV^r - {}^oV\right)^T M_o\left({}^oV^r - {}^oV\right) + \frac{1}{2}\sum_{k=1}^{13}\frac{\left(\theta_{ok} - \hat{\theta}_{ok}\right)^2}{\rho_{ok}} \\ V_f = \frac{1}{2}\left(\tilde{F}_{\text{int}}^d - \tilde{F}_{\text{int}}\right)^T K_f \lambda_f^{-1}\left(\tilde{F}_{\text{int}}^d - \tilde{F}_{\text{int}}\right) \end{cases} \tag{4.26}$$

The first derivative of the Lyapunov candidate function (4.25) is given as follows:

$$\dot{V} = \sum_{i=1}^{N} \left(\sum_{j=1}^{n} \dot{V}_{ij} + \sum_{j=1}^{n} \dot{V}_{a_{ij}} + \dot{V}_{iv} \right) + \dot{V}_{ob} + \dot{V}_{f} \tag{4.27}$$

By using the definition of the virtual power and the choice of the parameter function adaptation as in (4.20),(4.21) and (4.23), it is straightforward to prove that $\dot{V}$ is always decreasing, and is given as follows:

$$\begin{aligned} \dot{V} = -\sum_{i=1}^{N} \left(\sum_{j=1}^{n} \left(V_{B_{ij}}^{r} - V_{B_{ij}} \right)^{T} K_{B_{ij}} \left(V_{B_{ij}}^{r} - V_{B_{ij}} \right) + \left(V_{iv}^{r} - V_{iv} \right)^{T} K_{iv} \left(V_{iv}^{r} - V_{iv} \right) \right) \\ -K_{a_{ij}} \left(\dot{q}_{ij}^{r} - \dot{q}_{ij} \right)^{2} - \left({}^{o}V^{r} - {}^{o}V \right)^{T} K_{o} \left({}^{o}V^{r} - {}^{o}V \right) - \left(\tilde{F}_{\text{int}}^{d} - \tilde{F}_{\text{int}} \right) \end{aligned} \tag{4.28}$$

The stability analysis shows that $\dot{V}$ is always decreasing, and that the system is asymptotically stable in the sense of Lyapunov. Using Barbalat's lemma (Spong *et al.* (2006)) we prove that the error tracking states are asymptotically stable. The reader can find the detailed proof of stability in (Zhu *et al.* (1997); Al-Shuka *et al.* (2014); Zhu (2010)).

4.5 Simulation results

The block diagram in Fig. 4.5 shows the different control law development and simulation steps. Numerical simulations are carried out on two identical 6DoF MMRs handling a rigid object in coordination, as illustrated in Fig. 4.6, The desired trajectory of the center of gravity of the object is generated in the Cartesian space. The object displacement is along the X-axis, with a sinusoidal trajectory along the Y-axis, and no rotation along the Z-axis. In this case, there is no displacement along the Z-axis, and no rotation along the X-axis and the Y-axis. The starting point is $P_o = (x_o, y_o, z_o, \beta_o) = (2, 0.5, 1, 0)$ and the final point is $P_f = (x_o, y_o, z_o, \beta_o) = (5, 0.5, 1, 0)$. The controls gains of the controller are chosen to be $K_{B_{ij}} = 25, K_{a_{ij}} = 15, K_o = 50, K_\lambda = 5, \rho_o = 0.7, \rho_{\text{ffl}B_{ij}} = 0.8$ and $\rho_{a_{ij}} = 0.8$. The trajectory tracking is presented in Figure 4.7 and Figure 4.8. A good position and orientation tracking can be observed. The convergence

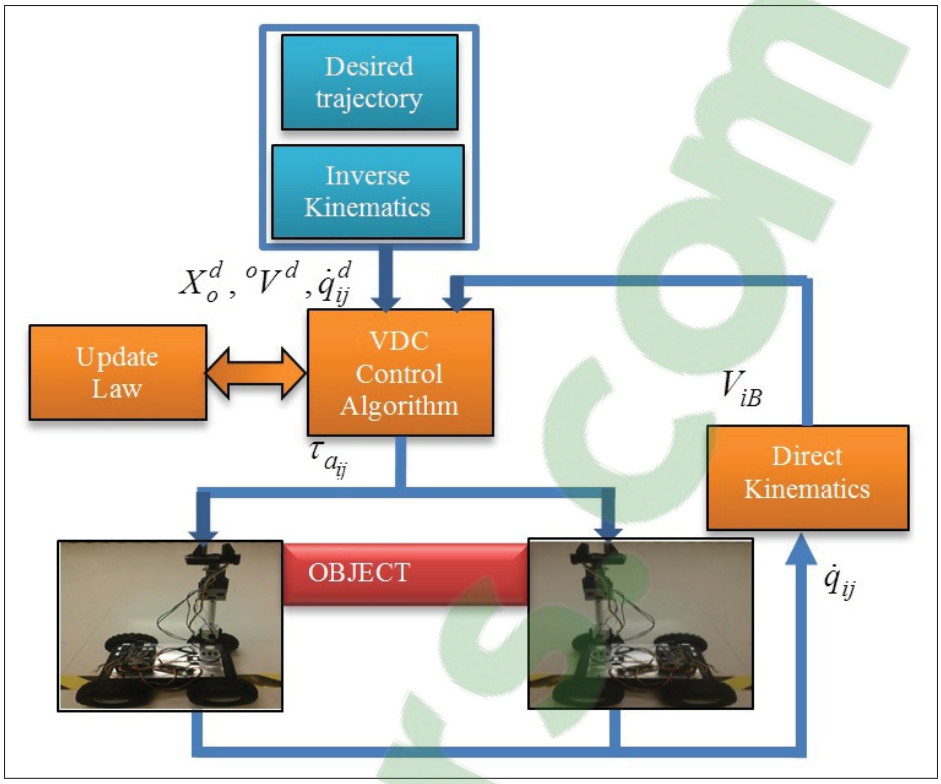

Figure 4.5 Adaptive control of N MMRs transporting a rigid object

of the error to zero along the XYZ positions and the moment along the Z-axis are presented in Figure 4.8.

4.6 Experimental validation

In this section, the proposed control scheme is implemented in real time on two identical mobile manipulator robots named Mob_ETS located in the GREPCI laboratory. In this experimental test, a Zigbee technology communication is used between the application program implemented in Matlab® Simulink and the mobile manipulator robots. The adaptive control developed and simulated in the previous section is implemented and compared to the computed torque approach in real time using Real-Time Workshop (RTW) by Mathworks®. Since the external end-effector force is unavailable for measurement, we use an end-effector observer proposed in (Alcocer *et al.* (2003)) to estimate it in this section. Figure 4.9 shows the complete structure design of the control. The two wheels of the *j*-th mobile manipulator robot platform

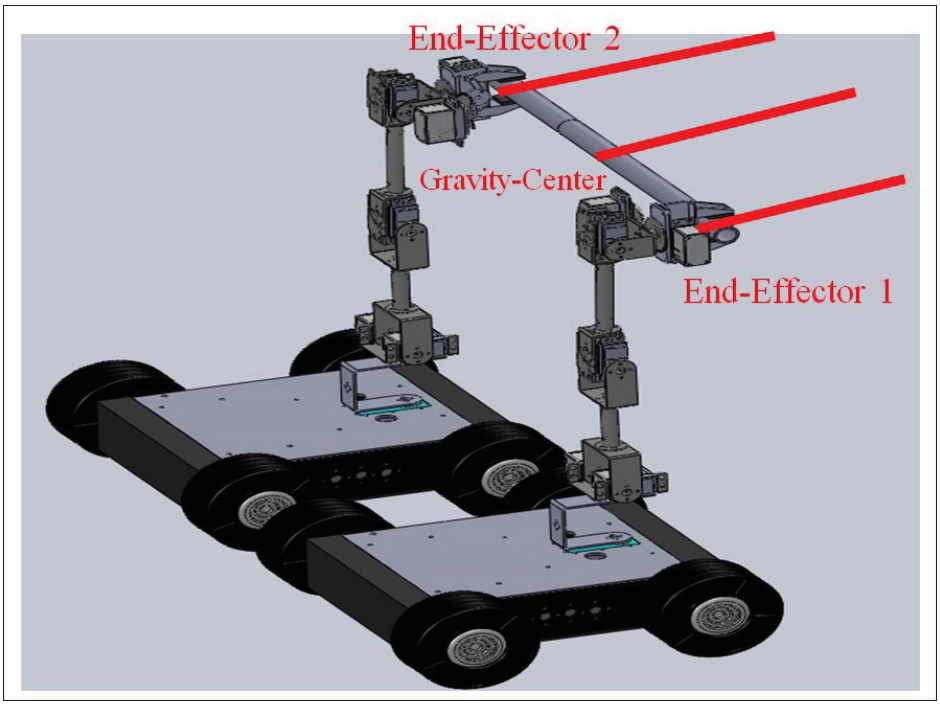

Figure 4.6 Two identical 6DoF mobile manipulators

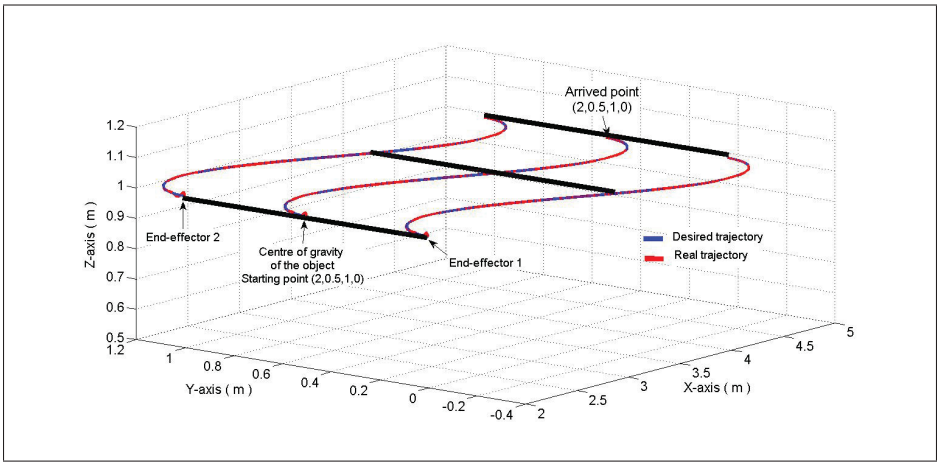

Figure 4.7 Desired and real trajectories of the object

are actuated by two DC motors, HN-GH12-2217Y (DC-12V-200RPM 30:1), and its angular positions are given by using encoder sensors (E4P-100-079-D-H-T-B). All the joints of the manipulator arm are actuated by a Dynamixel motor (MX-64T).

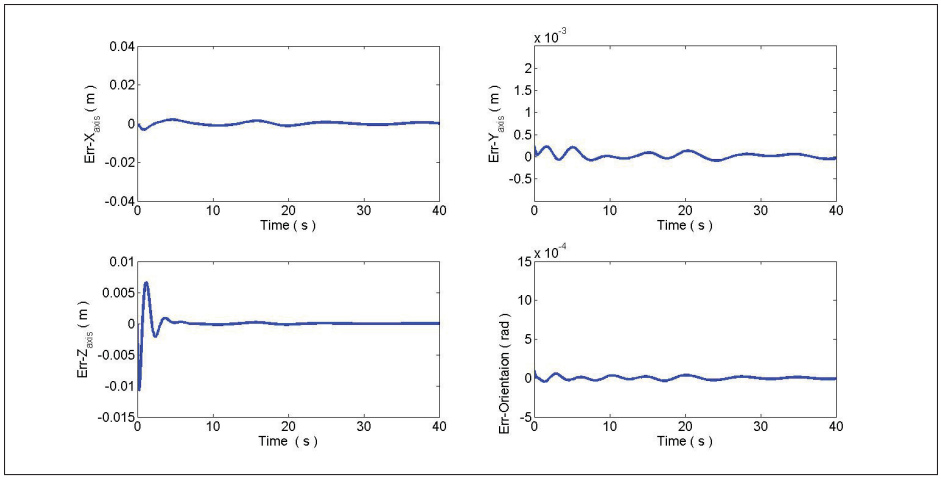

Figure 4.8 Error in X-axis, in Y- axis, in Z-axis and in orientation

The desired trajectory of the center of gravity of the object is generated in the Cartesian space. The object displacement is along the X-axis, with a sinusoidal trajectory along the Y-axis. The starting point is $P_o = (x_o, y_o, z_o, \beta_o) = (0.1, -0.1, 0.42, 0)$ and the final point is $P_f = (x_o, y_o, z_o, \beta_o) = (3, -0.1, 0.47, 0)$. The control gains of the controller are chosen to be $K_{B_{ij}} = 2.5, K_{a_{ij}} = 1.5, K_o = 5, K_\lambda = 5, \rho_o = 0.7, \rho_{B_{ij}} = 0.8$ and $\rho_{a_{ij}} = 0.8$ .The sampling time is set to 0.015 seconds.

The trajectory tracking is presented in Figure 4.10 and Figure 4.11. A good position and orientation tracking can be observed. The convergence of the errors to zero along the XYZ positions and the moment along the Z-axis are presented in Figure 4.11, and the convergence of the parameters of the first mobile manipulator during the adaptive control is illustrated in Figure 4.12 as an example, where Figure 4.12(a) represents the convergence of all estimated parameters of the first manipulator robot $\hat{\theta}_{B_{1j}}$ with $j = w_R, w_L, 1, .., m$ and Figure 4.12(b-c) shows the convergence of the parameters of only two links $\hat{\theta}_{B_{1j}}, \hat{\theta}_{B_{2j}}$ of this manipulator mobile robot. To show the effectiveness of the control strategy tested above, the computed torque is used for the same mobile manipulators. Figures 4.13-4.14 show the experimental results for the computed torque approach using the same desired trajectories. For purposes of comparison, the multi-mobile manipulators handling the object are controlled by applying the computed torque method, using the same desired trajectory. The tracking of the position

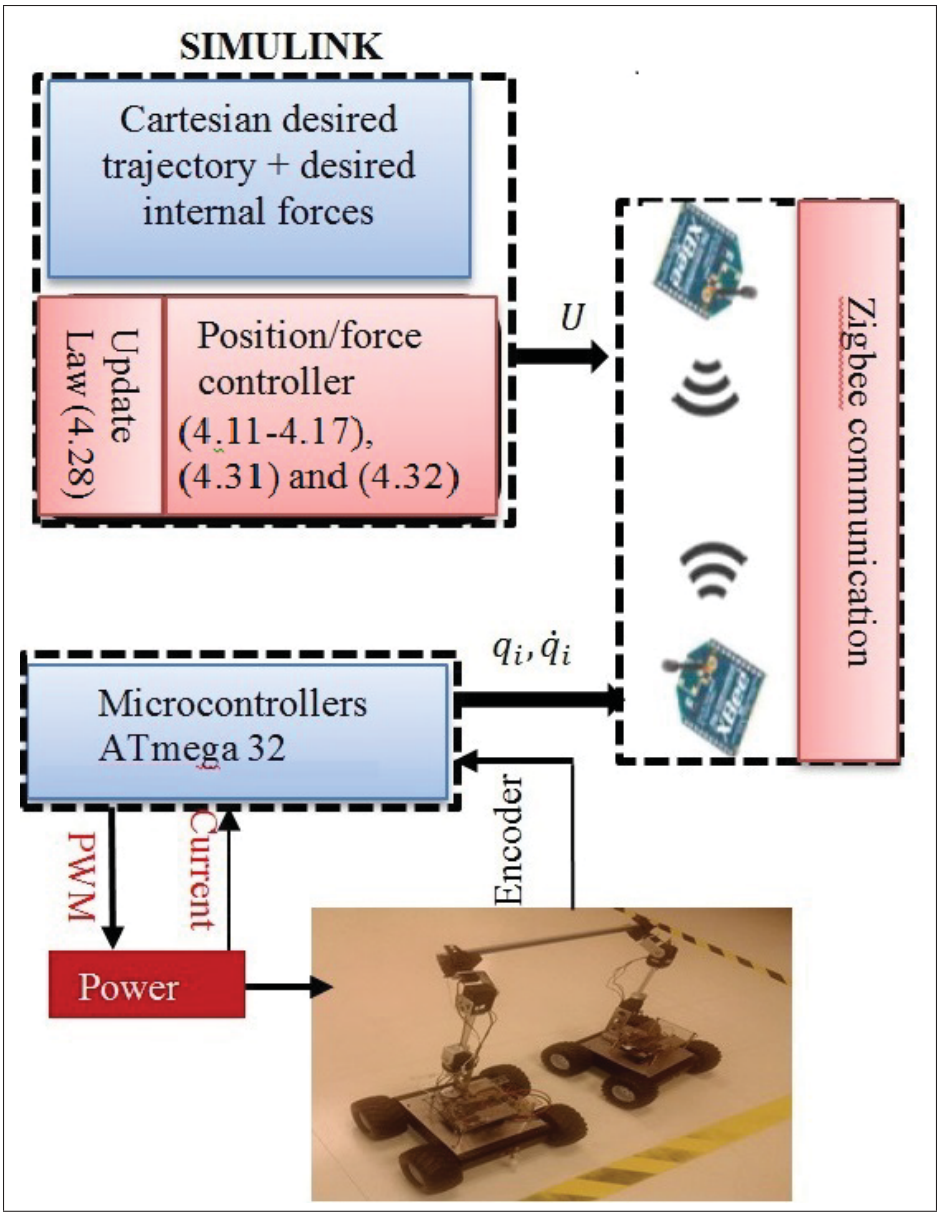

Figure 4.9 Real-time setup

and orientation in the workspace is shown in Figure 4.13, and errors along the XYZ positions and the moment along the Z-axis are presented in Figure 4.14. According to the experimental results shown in Figure 4.15, the resulting tracking errors of the proposed control strategy (dashed line) are smaller than those found using the computed torque method (solid line). This illustrates the effectiveness of the adaptive coordinated approach developed in this paper.

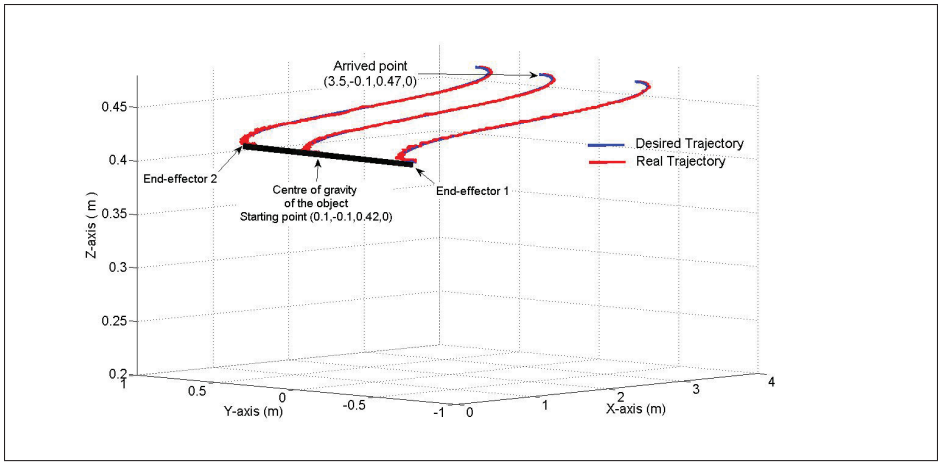

Figure 4.10 Desired and real trajectories of the object

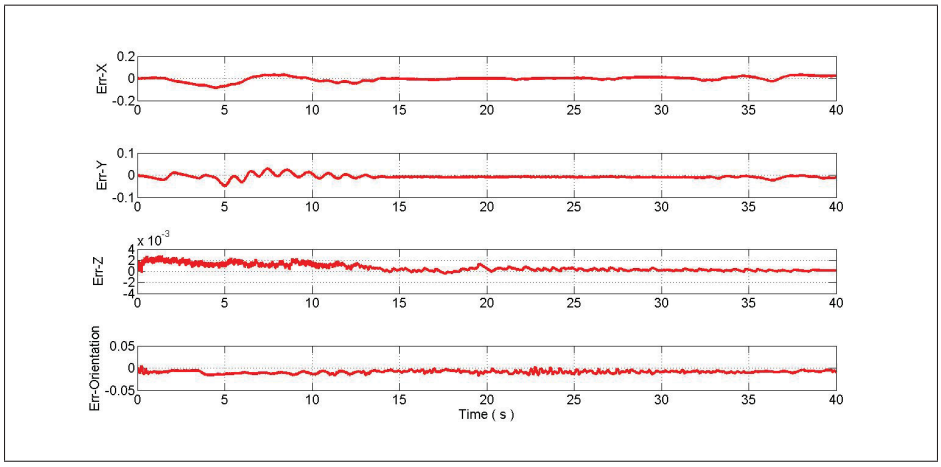

Figure 4.11 Error in X-axis, in Y- axis, in Z-axis and in orientation

4.7 Conclusions

In this paper, a coordinated control scheme for multiple mobile manipulator robots transporting a rigid object in coordination has been presented. The desired trajectory of the object is generated in the workspace and the parameters of the handling object and that of the mobile manipulators are estimated online using the virtual decomposition approach. In this study, the external forces are considered available. The control law is designed based on the virtual decomposition approach, and the global stability of the system is proven through the virtual stability of each subsystem. The proposed control design ensures that the workspace position

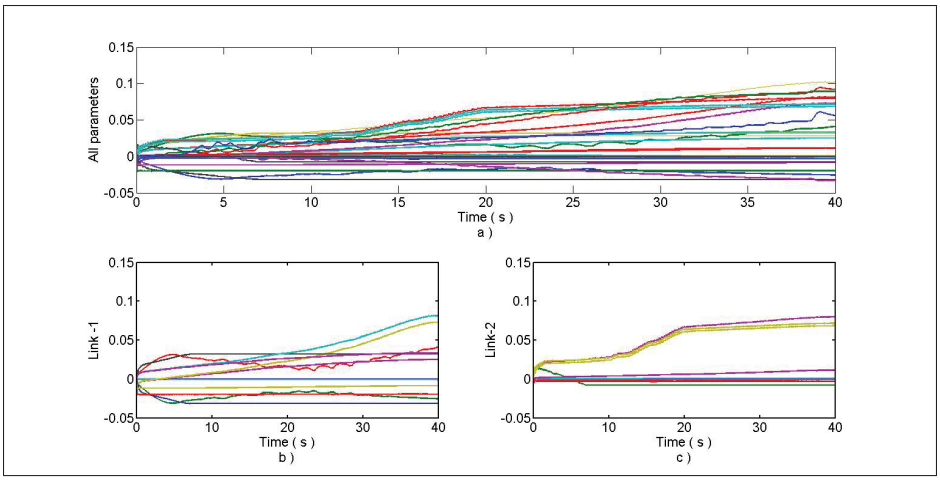

Figure 4.12 Parameter convergence of: a) the MMR 1, b) the link 1 of the MMR 1, c) the link 2 of the MMR 1

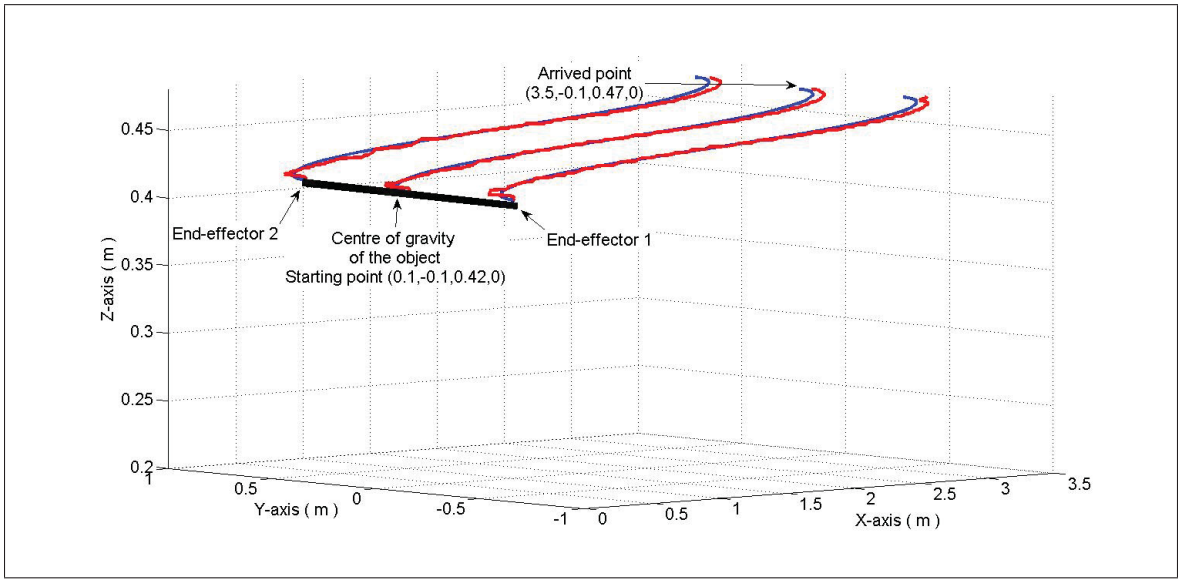

Figure 4.13 Desired and real trajectories of the object

error converges to zero asymptotically. This controller is tested and is compared with the computed torque approach. The simulation and experimental results show the effectiveness of the proposed control and illustrate the validation of the theoretical development.

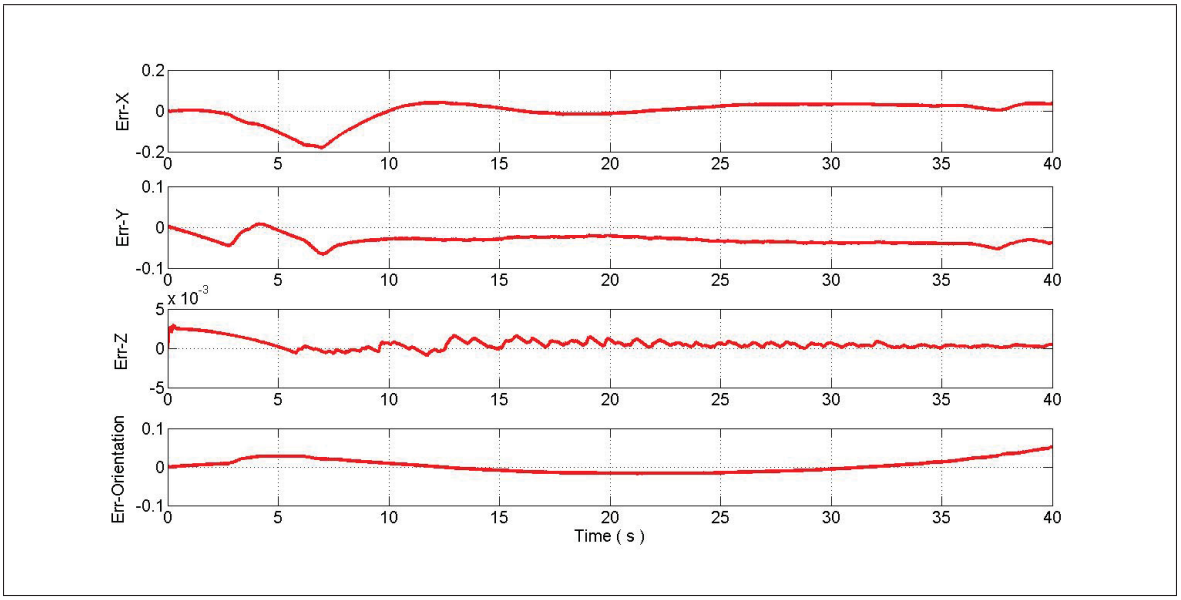

Figure 4.14 Error in X-axis, in Y- axis, in Z-axis and in orientation

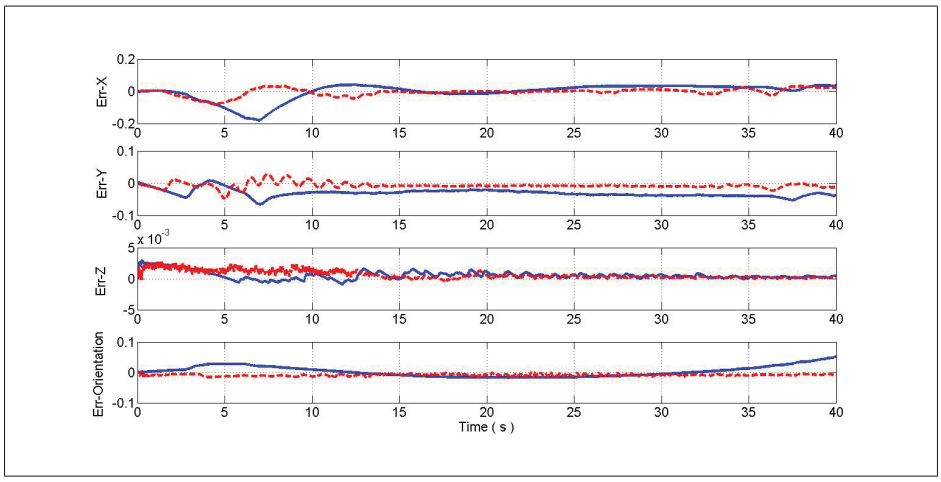

Figure 4.15 Errors: adaptive control (dashed red line), computed torque (solid blue line)

CHAPTER 5

ADAPTIVE CONTROL OF MULTIPLE MOBILE MANIPULATORS TRANSPORTING A RIGID OBJECT

Abdelkrim Brahmi[1], Maarouf Saad[1], Guy Gauthier[2], Wen-Hong Zhu[3]
and Jawhar Ghommam[4]

[1] Département of Electrical Engineering, École de Technologie Supérieure,
[2] Département of automated manufacturing Engineering, École de Technologie Supérieure,
1100 Notre-Dame Ouest, Montréal, Québec, Canada H3C 1K3
[3] Space Exploration,Canadian Space Agency,
6767 Route de l'Aéroport, Longueuil (St-Hubert), Québec, Canada J3Y 8Y9
[4] Research Unit on Mechatronics and Automation Systems,
Ecole National d'Ingénieurs de Sfax, BPW,3038 Sfax, Tunisia,

Published in the International Journal of Control Automation and System, June 5, 2017

Abstract

This paper presents a nonlinear control scheme for multiple mobile manipulator robots (MMR) moving a rigid object in coordination. The dynamic parameters of the handled object and the mobile manipulators are estimated online using the virtual decomposition approach. The control law is designed based on an appropriate choice of the Lyapunov function candidate. The proposed control design ensures that the position error in the workspace converges to zero, and the external force error is bounded. Numerical simulations and an experimental validation are carried out for two mobile manipulators transporting an object in order to show the effectiveness of the proposed controller.

Keywords: Mobile manipulator; Virtual decomposition approach; Coordination; Nonlinear control.

5.1 Introduction

The need for robots capable of locomotion and manipulation has led to the design of mobile manipulator robot (MMR) platforms. Typical examples of MMR include satellite arms, un-

derwater robots used in seabed exploration, and vehicles used in extra-planetary exploration. The most popular mobile manipulators, which are somewhat automated, are cranes mounted on trucks. Some operations requiring the handling of heavy objects become very difficult for single mobile manipulators, and require cooperation among multiple mobile manipulators. However, this significantly complicates the robotic system as its control design complexity increases greatly. The problem of controlling the mechanical system forming a closed kinematic chain mechanism lies in the fact that it imposes a set of kinematic constraints on the coordination of the position and velocity of the mobile manipulator. Therefore, there is a reduction in the degrees of freedom for the entire system. Further, the internal forces of the object produced by all mobile manipulators must be controlled. Few works have been proposed to solve the control problem of these robotic systems, which have high degrees of freedom and are tightly interconnected because all their manipulators are in contact with the object.

5.1.1 Previous works

Most research works in this area have thus far focused on three major mechanisms of coordination: decentralized control, the leader-follower control approach, and motion planning. In the first approach, the position and the internal force of the object are controlled in a given direction of the workspace. Khatib (Khatib *et al.* (1996b); Park and Khatib (2008)) proposed an extension of a method developed for manipulators with bases fixed to holonomic mobile manipulator robots, with a new command for decentralized cooperation tasks. In (Kosuge and Oosumi (1996); Hirata *et al.* (1999); Kosuge *et al.* (1999)), the authors proposed a control algorithm using geometric constraints between the contact points and the point representing the object, reducing the effect of sensor noise. They then extended and implemented this algorithm on multiple omnidirectional mobile robots handling a single object in coordination. A motion coordination control proposed by (Kume *et al.* (2007)) is applied to a group of holonomic mobile manipulators transporting an object in coordination without using torque/force sensors.

The leader-follower architecture is the second approach used for the coordination of multiple mobile manipulators. In this approach, a single or a group of MMRs is designated as a leader

trying to follow a desired trajectory, while the other group members follow the leaders. This control approach was addressed in (Chen and Li (2006); Hirata *et al.* (2004c)), and (Tang *et al.* (2009)). In (Fujii *et al.* (2007)), the authors introduced the notion of virtual leader, in which every follower considers the rest of the team (leader and other followers) as constituting the virtual leader.

Finally, the motion planning approach has been covered in a few studies from the perspective of a group of MMRs (which is another fundamental problem in robotics, especially in multi-robot systems), where several robots perform the task of transporting an object in cooperation, in a known or unknown environment. These studies include those presented in (LaValle (2006); Latombe (2012)). Another structure for planning optimal trajectories was introduced in (Desai and Kumar (1997)) for two mobile manipulators pushing a common object to a desired location. The authors in (Yamamoto and Fukuda (2002)) proposed a control method for multiple mobile manipulators holding a common object. The measures of kinematic and dynamic manipulability are given, taking into account collision avoidance. However, the dynamics of the object are ignored. In (Furuno *et al.* (2003)), a trajectory planning method for mobile manipulator groups in cooperation, which takes into consideration the dynamic characteristics of mobile manipulators and the object to be grasped, was proposed. The dynamics are composed of equations of the motion of mobile manipulators, the movements of the object, the non-holonomic constraints of mobile platforms and the geometric constraints between the end-effectors and the object. In (Sun and Gong (2004b); Zhu and Yang (2003)), a planning approach based on genetic algorithms was proposed. The adaptive control of robotic systems with high degrees of freedom has been receiving increasing attention in recent years. Many contributions in this area have been developed, such as in (Chen (2015); Zhao *et al.* (2016); Liu *et al.* (2016)). This is due to the fact that such robotic systems have been implemented in most modern manufacturing applications. The uncertainties, the high nonlinearity, and the tight kinematics and dynamics coupling of these systems greatly complicate the control problem and make it difficult to solve by using the classical approaches explained previously. A system formed of many mobile manipulators holding an object, is one of the most important in

these class of robotic systems. The constraints, imposed by the kinematic closed-chains system, make the motion degrees of freedom often less than the number of actuators. In this case, not only the motion needs to be controlled but the internal forces as well. To overcome these problems, a novel adaptive control based on the virtual decomposition approach is proposed in this work.

5.1.2 Main contribution

All previous studies based on Lagrangian or Newton/Euler approaches require knowledge of the exact parameters of the system. In practice, this is difficult, and the obtained model is usually uncertain. To overcome the problem of dynamic modeling and dynamic control, some researchers have proposed adaptive control based on neural network control (Liu *et al.* (2014); Liu and Zhang (2013); Liu *et al.* (2013)) and fuzzy logic approaches (Mai and Wang (2014)). For instance, non-model-based techniques have been developed for a different type of mobile manipulator robot with uncertain parameters. Another problem is that the dynamics of the whole system are complicated. Any change in the structure of the group requires a new dynamics modelling (removal of a faulty robot or addition of a new robot to the system). Finally, for these types of systems with a large degree of freedom, and which are tightly coupled, adapting the parameters using methods based on full dynamics is very complicated due to the huge number of parameters involved. To overcome these problems, we propose in this paper an adaptive decentralized approach based on an extension of the virtual decomposition control (VDC) methodology presented in Zhu *et al.* (1997); Al-Shuka *et al.* (2014), originally designed for fixed-base robotic systems with large degrees of freedom. This approach will be used in this paper for a group of holonomic mobile manipulators moving without considering the slipping effect. Some of the many advantages of this approach are: 1) the whole dynamics of the system can easily be found based on the individual dynamics of each subsystem; 2) it makes the system control design very flexible and the calculation of the dynamic system, with respect to the changes in the system configuration, very easy, and 3) it makes the adaptation

of the physical parameters very simple and systematic. Contrary to what was done in previous works, our contributions in this paper present the following characteristics:

a. The use of the VDC approach to overcome the problem of adaptation and modelling of systems using classical approaches, which makes the system more control-flexible when its configuration changes. In this case, adding a new robot or removing a faulty one from the system does not require a recalculation of the full dynamics of the system;
b. Using the VDC approach means that changing the dynamics of a subsystem only affects the respective local equations associated with that subsystem, while keeping the equations associated with the rest of the system unchanged;
c. The global stability of the system's VDC is proven through the virtual stability of each subsystem. Contrary to the original VDC stability and control, in this paper, the stability analysis and the control law are designed based on an appropriate choice of a candidate Lyapunov function of the entire system.

The rest of the paper is organized as follows. Section 5.2 presents the modelling of the system, while section 5.3 presents the problem control statement. Section 5.4 explains the control design, and simulation results are given in section 5.5. Section 5.6 presents an experimental validation of the proposed approach. Finally, the conclusion is given in section 5.7.

5.2 System modelling

Figure 5.1 shows the N MMR handling a common rigid object, with P_{ie} being the position/orientation vector of the i-th MMR effector and X_o the position/orientation vector of the object.

This section will briefly describe the kinematics and dynamic models of the i-th MMR, the dynamic model for handling the object, and then provide the dynamics of the entire system.

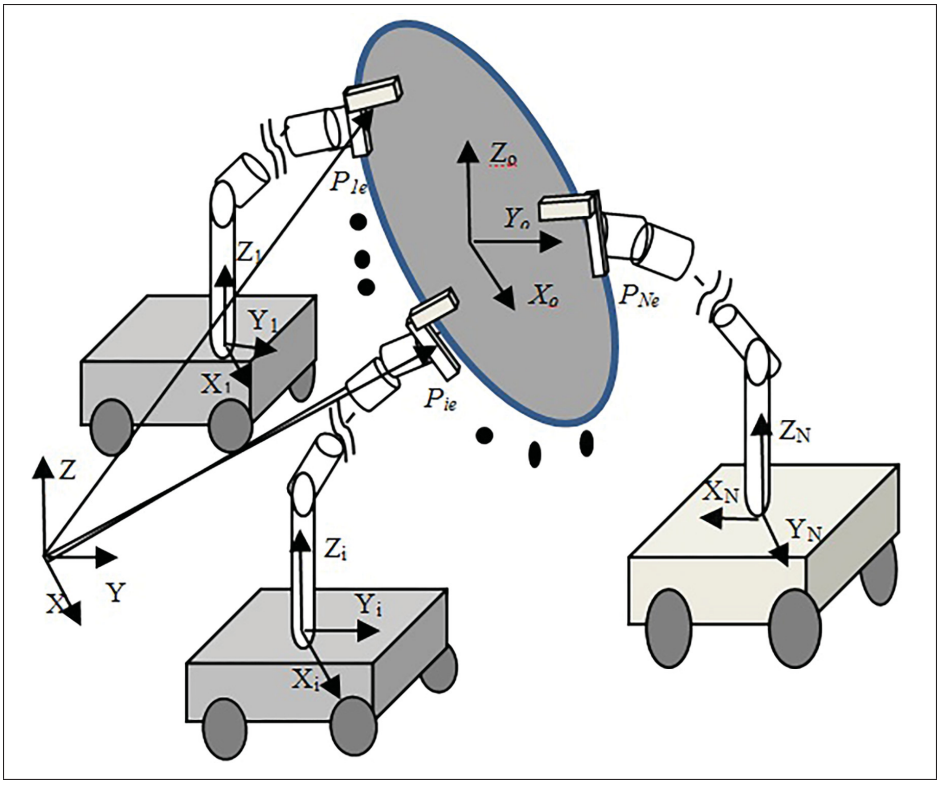

Figure 5.1 Multiple MMR handling a rigid object

5.2.1 Kinematics

The relationship between the effector velocity $V_{ie} \in \mathbb{R}^6$ of the i-th mobile manipulator and the object velocity $V_o \in \mathbb{R}^6$ is given by:

$$V_{ie} = J_{io}^T V_o \tag{5.1}$$

where $J_{io} \in \mathbb{R}^{6\times 6}$ is the Jacobian matrix from the center of gravity of the object to the i-th mobile manipulator end-effector.

5.2.2 The *i*-th mobile manipulator dynamics

The dynamic model of the i-th mobile manipulator without an object is given in the joint space by the following equation:

$$M_i(q_i)\ddot{q}_i + C_i(q_i,\dot{q}_i)\dot{q}_i + G_i(q_i) = U_i + A_i^T f_i \tag{5.2}$$

where $M_i(q) \in \mathbb{R}^{n\times n}$ is the mass matrix; $C_i(q_i,\dot{q}_i) \in \mathbb{R}^{n\times n}$ represents the Coriolis and centrifugal terms; $G_i(q_i) \in \mathbb{R}^n$ is the vector of gravity; $q_i,\dot{q}_i,\ddot{q}_i \in \mathbb{R}^n$ are respectively the coordinate generalized vector, the joint velocity, and the acceleration, and $U_i \in \mathbb{R}^n$is the input control vector; $A_i \in \mathbb{R}^{n\times m}$ is the Jacobian matrix and $f_i \in \mathbb{R}^m$ is the constraint force corresponding to the holonomic constraints. The mobile platform is subject to the holonomic constraints.

Remark 5.1: In this paper, the mobile manipulator robot is considered as a fully actuated arm mounted on the holonomic mobile platform.

In the presence of the object, the dynamic equation of the i-th mobile manipulator in the workspace is given by:

$$ {}^iM\dot{V}_{ie} + {}^iCV_{ie} + {}^iG = {}^iU + F_{ie} \tag{5.3}$$

where ${}^iM \in \mathbb{R}^{6\times 6}$is the mass matrix, ${}^iC \in \mathbb{R}^{6\times 6}$ represents the Coriolis and centrifugal terms,${}^iG \in \mathbb{R}^6$ is the vector of gravity, and $F_{ie} \in \mathbb{R}^6$ is the external end-effector force caused by the handling of the object. This force is assumed to be measurable.

5.2.3 Dynamics of the object

The object handled by N mobile manipulators is rigid. To find the dynamic model that characterizes this manipulated object, the Newton Euler method is used. The equation of motion of the effort is given by:

$$ M_o(X_o)\dot{V}_o + C_o(X_o,\dot{X}_o)V_o + G_o(X_o) = F_o \tag{5.4}$$

where $V_o = \begin{bmatrix} v_o^T & w_o^T \end{bmatrix}^T$ with $v_o \in \mathbb{R}^3$ and $w_o \in \mathbb{R}^3$ being the linear and angular velocities of the object, respectively; $F_o \in \mathbb{R}^6$ is the vector of forces applied to the object, $M_o \in \mathbb{R}^{6\times 6}$ is the mass matrix, $C_o \in \mathbb{R}^{6\times 6}$ represents the centrifugal and Coriolis matrix and $G_o \in \mathbb{R}^6$ is the vector of gravity.

5.2.4 Total dynamics

From the general form of the i-th mobile manipulator (5.3), the dynamics of N MMRs is given by

$$M\dot{V}_e + CV_e + G = U + F_e \tag{5.5}$$

with:
$V_e = \left[V_{1e}^T \quad V_{2e}^T \quad .. \quad V_{Ne}^T\right]^T$, $M = blockdiag\left[{}^1M \quad .. \quad {}^NM\right]$, $F_e = \left[F_{1e}^T \quad ... \quad F_{Ne}^T\right]^T$
$C = blockdiag\left[{}^1C \quad .. \quad {}^NC\right]$, $G = \left[{}^1G^T \quad .. \quad {}^NG^T\right]^T$,$U = \left[{}^1U^T \quad .. \quad {}^NU^T\right]^T$.
The dynamic given in (5.5) has the following properties:

Property 5.1: The matrix M is symmetric positive definite.

Property 5.2: The matrix $S = \dot{M} - 2C$ is skew symmetric, that is, for any vector x, we have $x^T(\dot{M} - 2C)x = 0$.

The end-effector forces F_e are related to the object force as follows:

$$F_o = -J_o(X_o)F_e \tag{5.6}$$

where $J_o \in \mathbb{R}^{6\times 6N}$ is the Jacobian matrix relating the two forces. Furthermore, the end-effector force F_e is divided into two orthogonal components: the first contributes to the movement of the object and the second gives the internal force. This representation is given in (Jean and Fu (1993)), and has the following form:

$$F_e = -(J_o(X_o))^+ F_o - F_I \tag{5.7}$$

where $(J_o)^+$ is the pseudo-inverse of (J_o) given by $(J_o)^+ = J_o^T(J_oJ_o^T)^{-1}$ and $F_I = \left[{}^1F_I^T \quad .. \quad {}^NF_I^T\right]^T \in \mathbb{R}^{6N}$ are the internal forces in the null space of (J_o). From (Kume *et al.* (2007)), F_I can be parameterized by the Lagrangian multiplier vector λ_I as follows:

$$F_I = \left(I - (J_o(X_o)^T)^+ J_o(X_o)^T\right)\lambda_I = \rho^T\lambda_I \tag{5.8}$$

where ρ^T is the Jacobian matrix for the internal force, and is restricted to:

$$J_o(X_o)\rho^T = 0 \tag{5.9}$$

To simplify the control formulation, the following assumptions are made:

Assumption 5.1: The desired trajectory is assumed to be smooth, and there exists ε_1, ε_2 and ε_3 such that:

$$\left\| \frac{\mathrm{d}X_o^d}{\mathrm{d}x} \right\| \leq \varepsilon_1, \left\| \frac{\mathrm{d}^2X_o^d}{\mathrm{d}x^2} \right\| \leq \varepsilon_1, \left\| \frac{\mathrm{d}^3X_o^d}{\mathrm{d}x^3} \right\| \leq \varepsilon_3$$

Assumption 5.2: The object is rigid and all end-effectors are rigidly attached to it. As a result, there is no relative motion between the end-effector and the object.

Assumption 5.3:The parameters of the object and the mobile manipulators are unknown, but constant.

Assumption 5.4:All the velocities of the joints of the mobile manipulator robots are available for feedback as well as for the measurement of external forces.

5.3 Control problem statement

The control objective is to generate a set of torque inputs such that the position tracking error of the transported object in the workspace converges asymptotically to zero. Formally, the control problem is to design the control input:

$$U = f(V_e, \dot{V}_e, X_o, V_o) \tag{5.10}$$

such that the following limits hold:
$\lim_{t\to\infty} \left\| X_o - X_o^d \right\| = 0, \lim_{t\to\infty} \left\| V_o - V_o^d \right\| = 0$
$\lim_{t\to\infty} \left\| F_{ie} - F_{ie}^d \right\| = bounded$

where, $X_o^d \in \mathbb{R}^6$, $V_o^d \in \mathbb{R}^6$ are the desired position and velocity of the object generated in the workspace $F_{ie}^d \in \mathbb{R}^6$ and $F_{ie} \in \mathbb{R}^6$ are the desired and measured internal forces.

5.4 Control design

5.4.1 Methodology

The overall control system is designed using the following steps:

- The required velocities of the object $V_o^r \in \mathbb{R}^6$ as well as the velocities of the end-effector $V_{ie}^r \in \mathbb{R}^6$ are first computed, and then the required velocity ${}^iV_B^r \in \mathbb{R}^{6n}$ of the n body-fixed frames ${}^iB_j$ illustrated in Figure 5.2 is calculated;
- The VDC approach is used to simplify the problem of adaptation of the parameters of the complete systems, where this problem is converted into a problem of estimation of the parameters of each subsystem. From the velocities computed in the first step, the estimated parameters are calculated;
- The control law of each mobile manipulator is finally designed.

5.4.2 Design

Step 1: The required velocity $V_o^r \in \mathbb{R}^6$ of the object is calculated based on the desired object velocity $V_o^d \in \mathbb{R}^6$:

$$\begin{cases} V_o^r = V_o^d + K_\lambda e_o \\ s_o = V_o^r - V_o \end{cases} \tag{5.11}$$

where $e_o = X_o^d - X_o$ is the position/orientation errors vector, K_λ is a scalar constant and $s_o \in \mathbb{R}^6$ is the sliding surface.

The desired velocity of the end-effector of each mobile manipulator $V_{ie}^d \in \mathbb{R}^6$ is calculated from

the desired velocity of the object $V_o^d \in \mathbb{R}^6$:

$$V_{ie}^d = J_{io}^T V_o^d \tag{5.12}$$

The derivative of the position error of the i-th end-effector is given by:

$$\dot{e}_i = V_{ie}^d - V_{ie} \tag{5.13}$$

Introducing the object velocity, (5.13) can be rewritten as:

$$\dot{e}_i = J_{io}^T (V_o^d - V_o) = J_{io}^T \dot{e}_o \tag{5.14}$$

Finally, the required velocity of the i-th end-effector is obtained based on (5.13), (5.14) and (5.1) as follows:

$$V_{ie}^r = V_{ie}^d + K_\lambda J_{io}^T e_o \tag{5.15}$$

Step 2: In this step, the goal is to virtually decompose (Zhu (2010)) the robotic system into several parts and open chains elements. Each part is a rigid body, and an open chain consists of a series of rigid links connected one by one. This decomposition is illustrated in Figure 5.2.

The transformation matrix of force/moment vectors from frame B to frame A is defined by:

$${}^A U_B = \begin{bmatrix} {}^A R_B & 0_{3\times 3} \\ S({}^A r_{AB}) {}^A R_B & {}^A R_B \end{bmatrix} \tag{5.16}$$

where ${}^A R_B \in \mathbb{R}^{3\times 3}$ is the rotation matrix between frames A and B, and $S({}^A r_{AB}) \in \mathbb{R}^{3\times 3}$ is a skew symmetric matrix built from the vector ${}^A r_{AB} \in \mathbb{R}^{3\times 3}$ linking the origins of frames A and B, expressed in the coordinates of frame A.

Assumption 5.1: In this paper, the manipulators are operating away from any singularity.

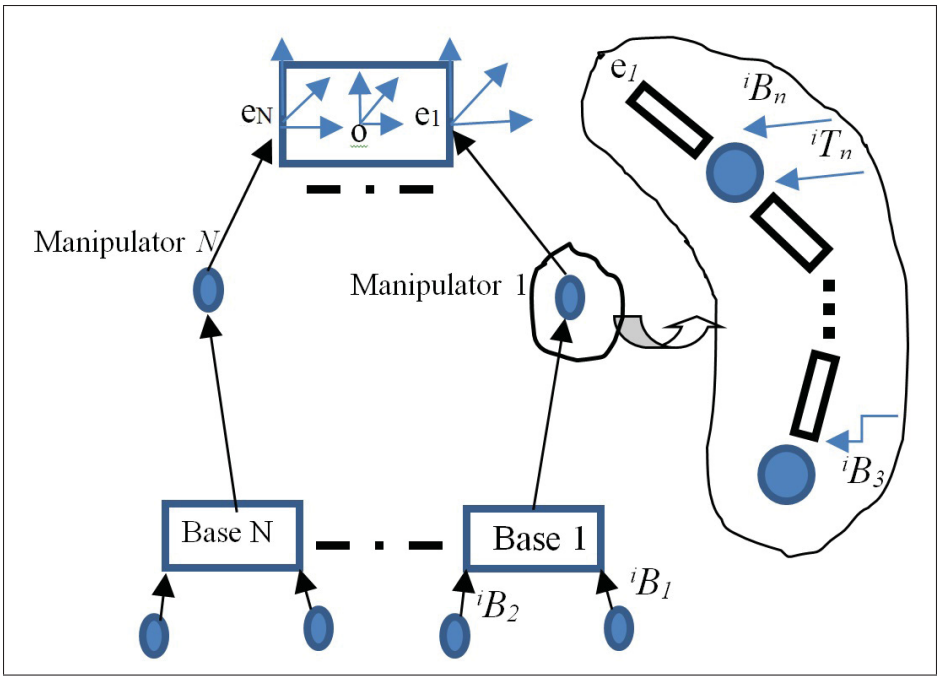

Figure 5.2 Virtual decomposition of N MMR handling a rigid object

The required velocity in any frame is given by:

$$^{i}V_{B}^{r} = J_{i}V_{ie}^{r} \tag{5.17}$$

with $^{i}V_{B}^{r} = \left[^{i}V_{B_1}^{rT} \quad \ldots \quad ^{i}V_{B_n}^{rT}\right]^{T}$ and $J_i \in \mathbb{R}^{6n\times n}$ being the Jacobian matrix. The dynamics of the object based on its required velocity are expressed in linear form by the following equation:

$$F_{o}^{*r} = M_{o}\dot{V}_{o}^{r} + C_{o}V_{o}^{r} + G_{o} = Y_{o}\theta_{o} \tag{5.18}$$

with $F_{o}^{*r} \in \mathbb{R}^{3}$ being the required object force, $\theta_o \in \mathbb{R}^{13}$ the vector of parameters, and $Y_o \in \mathbb{R}^{6\times 13}$ the dynamic regressor matrix.

The dynamics of the j-th rigid body of the i-th manipulator are given in linear form by the following equation:

$$^{i}F_{B_j}^{*r} = {}^{i}M_{B_j}{}^{i}\dot{V}_{B_j}^{r} + {}^{i}C_{B_j}{}^{i}V_{B_j}^{r} + {}^{i}G_{B_j} = {}^{i}Y_{B_j}{}^{i}\theta_{B_j} \tag{5.19}$$

with ${}^{i}M_{B_j} \in \mathbb{R}^{6\times6}$ being the matrix of inertial terms, ${}^{i}C_{B_j} \in \mathbb{R}^{6\times6}$ the matrix of centrifugal/-Coriolis terms, ${}^{i}G_{B_j} \in \mathbb{R}^{6}$ the vector related to gravity, ${}^{i}\theta_{B_j} \in \mathbb{R}^{13}$ the parameters' vector, and finally, ${}^{i}Y_{B_j} \in \mathbb{R}^{6\times13}$ the dynamic regressor matrix.

The vector of resulting forces/moments acting on the *j*-th rigid body is given by an iterative process (Zhu (2010)). We begin by computing the vector of forces at the different cutting points:

$$\begin{aligned} {}^{i}F^{r}_{B_n} &= {}^{i}F^{*r}_{B_n} \\ {}^{i}F^{r}_{B_{n-1}} &= {}^{i}F^{*r}_{B_{n-1}} + {}^{B_{n-1}}U_{B_n}\,{}^{i}F^{*r}_{B_n} \\ &\vdots \\ {}^{i}F^{r}_{B_1} &= {}^{i}F^{*r}_{B_1} + {}^{B_1}U_{B_2}\,{}^{i}F^{*r}_{B_2} + \ldots + {}^{B_{n-1}}U_{B_n}\,{}^{i}F^{*r}_{B_n} \end{aligned} \tag{5.20}$$

The general form is given by the following expression:

$${}^{i}F^{r}_{B_k} = {}^{i}F^{*r}_{B_k} + \sum_{j=k+1}^{n-1} {}^{B_j}U_{B_{j+1}}\,{}^{i}F^{*r}_{B_{j+1}} \tag{5.21}$$

with: $k = 1,..,n-1$.

Remark 5.2: The general form (5.21) clearly shows the advantages of using the VDC approach as compared to those based on the classical approach, such as in (Chen (2015); Zhao *et al.* (2016); Liu *et al.* (2016)), where, firstly, the whole dynamics of the system can easily be found based on the individual dynamics of each subsystem; secondly, the adaptation of the physical parameters is very simple and systematic, as mentioned in (Zhu *et al.* (1997)).

The control equation of the *i*-th mobile manipulator can be expressed based on the control equation of rigid body (5.19) and the forces in the different frames (5.20) by the following relation:

$${}^{i}M\dot{V}^{r}_{ie} + {}^{i}CV^{r}_{ie} + {}^{i}G = {}^{i}Q\,{}^{i}\theta \tag{5.22}$$

where ${}^{i}M = J_i^{T\,i}M_B J_i$, ${}^{i}C = J_i^{T\,i}M_B\dot{J}_i + J_i^{T\,i}C_B J_i$, ${}^{i}G = J_i^{T\,i}G_B$ and $J_i \in \mathbb{R}^{6n\times6}$ is the Jacobian matrix. Also, ${}^{i}M_B = Blockdiag({}^{i}M_{B_1},...,{}^{i}M_{B_n})$, ${}^{i}C_B = Blockdiag({}^{i}C_{B_1},...,{}^{i}C_{B_n})$ and ${}^{i}G_B = [{}^{i}G^{T}_{B_1},...,{}^{i}G^{T}_{B_n}]^{T}$

The control equation for the N mobile manipulator robots is designed as:

$$M\dot{V}_e^r + CV_e^r + G = Q\theta \tag{5.23}$$

with: $M = Blockdiag({}^1M, ..., {}^NM)$, $G = [{}^1G^T, ..., {}^NG^T]^T$, $C = Blockdiag({}^1C, ..., {}^NC)$, and $V_e^r = [V_{1e}^{rT}, ..., V_{Ne}^{rT}]^T$.

Since the physical parameters of the i-th mobile manipulator are unknown, using the estimate parameters of ${}^i\theta$ denoted ${}^i\hat{\theta}$, and adding the object, relation (5.23) is rewritten as:

$${}^i\hat{M}\dot{V}_{ie}^r + {}^i\hat{C}V_{ie}^r + {}^i\hat{G} = {}^iQ^i\hat{\theta} \tag{5.24}$$

We define the parameter estimation error as $\Delta\theta = {}^i\hat{\theta} - {}^i\theta$ From (5.13-5.16), we have:

$$\begin{cases} V_{ie}^r = V_{ie}^d + K_\lambda e_i \\ \dot{V}_{ie}^r = \dot{V}_{ie}^d + K_\lambda \dot{e}_i \\ s_i = V_{ie}^r - V_{ie} = \dot{e}_i + K_\lambda e_i \end{cases} \tag{5.25}$$

where $s_i \in \mathbb{R}^6$ is the sliding surface.

The control law of the i-th mobile manipulators is given by:

$${}^iU = {}^iU_p^r - {}^iU_f^r \tag{5.26}$$

where ${}^iU_p^r$ and ${}^iU_f^r$ are, respectively, the position and the force control laws. ${}^iU_p^r$ is given by:

$${}^iU_p^r = {}^iQ^i\hat{\theta} + {}^i\Gamma s_i \tag{5.27}$$

and the update law that is used to prove the global stability of the system is given by:

$${}^i\dot{\hat{\theta}} = {}^i\Gamma_\theta^{-T}{}^iQ^T s_i \tag{5.28}$$

where ${}^i\Gamma_\theta$ and ${}^i\Gamma$ are constant symmetric positive definite matrices, ${}^i\hat{\theta} = [{}^i\hat{\theta}_{B_1}^T, ..., {}^i\hat{\theta}_{B_n}^T]^T \in \mathbb{R}^{13n}$ being the estimate vector of the parameters.

Furthermore, ${}^iU_f^r$ is given by:

$$ {}^iU_f^r = F_{ie}^r = -(J_o(X_o))^+ F_o^{*r} - {}^iK_p({}^iF_I^d - {}^iF_I) \tag{5.29} $$

where ${}^iK_p$ is a constant symmetric positive definite matrix.

Expressing (5.24) for the N mobile manipulator robots gives:

$$ \hat{M}\dot{V}_e^r + \hat{C}V_e^r + \hat{G} = Q\hat{\theta} \tag{5.30} $$

The position control law of the entire system based on (5.27) is computed as follows:

$$ U_p^r = Q\hat{\theta} + \Gamma s \tag{5.31} $$

with: $\Gamma = Blockdiag({}^1\Gamma, .., {}^N\Gamma)$, $Q = Blockdiag({}^1Q, .., {}^NQ)$
$\hat{\theta} = [{}^1\hat{\theta}^T, ..., {}^N\hat{\theta}^T]^T$ and $s = [s_1^T, ..., s_N^T]^T$.
Furthermore, U_f^r is the force control law, and is given by:

$$ U_f^r = F_e^r \tag{5.32} $$

with: $F_e^r = [F_{1e}^{rT}, ..., F_{1e}^{rT}]^T$

Finally, the control law of the entire system is given as follows:

$$ U = U_p^r - U_f^r $$

$$ U = Q\hat{\theta} + \Gamma s - F_e^r \tag{5.33} $$

The block diagram in Fig. 5.3 shows the different control law calculation and implementation steps.

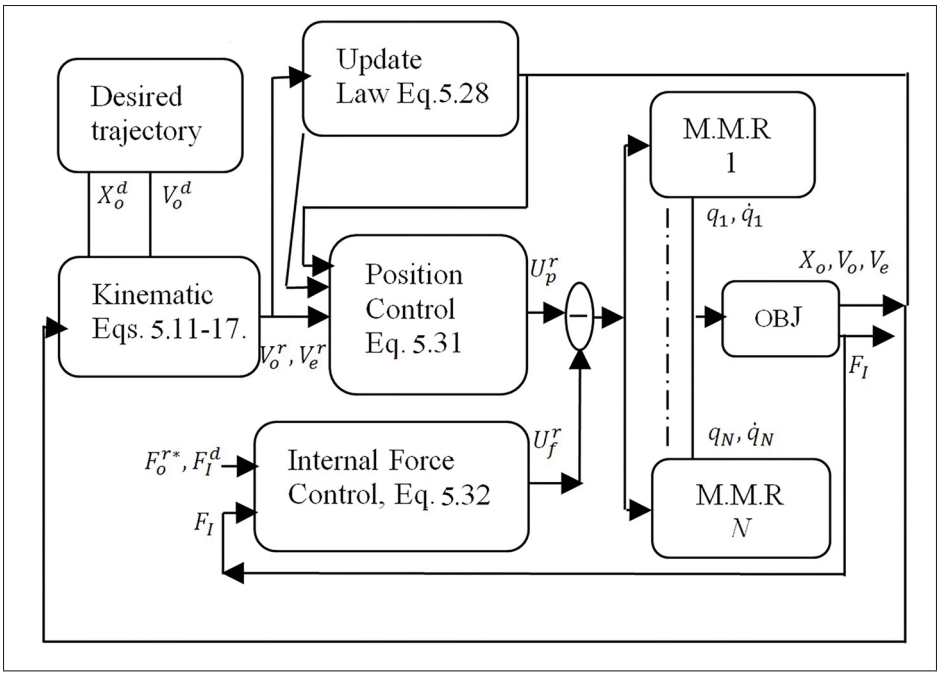

Figure 5.3 Adaptive control of N MMRs transporting a rigid object

5.4.3 Stability analysis

Remark 5.3: The global stability of the system using the VDC approach is proven through the virtual stability of each subsystem (Zhu *et al.* (1997); Zhu (2010)). Contrary to the original VDC stability and control, in this subsection, the stability analysis is proven based on an appropriate choice of a candidate Lyapunov function of the entire system.

To show the stability of the global system, we calculate the dynamic error of estimation parameters from equation (5.30) and (5.23) as follows:

$$\tilde{M}\dot{V}_e^r + \tilde{C}V_e^r + \tilde{G} = Q\Delta\theta \tag{5.34}$$

where $\begin{cases} \tilde{M} = \hat{M} - M \\ \tilde{C} = \hat{C} - C \\ \tilde{G} = \hat{G} - G \end{cases}$

and $\Delta\theta = \hat{\theta} - \theta$. Defining $\Delta F_e = F_e^r - F_e$, it follows from (5.4),(5.6) and (5.18) that

$$J_o \Delta F_e = -(M_o \dot{s}_o + C_o s_o) \tag{5.35}$$

with $s_o = V_o^r - V_o$.

To prove the stability, we consider the following Lyapunov function

$$V = \frac{1}{2} s^T M s + \frac{1}{2} \Delta\theta^T \Gamma_\theta \Delta\theta + \frac{1}{2} s_o^T M_o s_o \tag{5.36}$$

with $\Gamma_\theta = Blockdiag({}^1\Gamma_\theta, .., {}^N\Gamma_\theta)$.

The time derivative along the solution of relations (5.36) gives the following:

$$\begin{aligned} \dot{V} = s^T M \dot{s} + \tfrac{1}{2} s^T \dot{M} s + \Delta\dot{\theta}^T \Gamma_\theta \Delta\theta \\ + s_o^T M_o \dot{s}_o + \tfrac{1}{2} s_o^T \dot{M}_o s_o \end{aligned} \tag{5.37}$$

From (5.25), we know that, $s = V_e^r - V_e \Rightarrow \dot{s} = \dot{V}_e^r - \dot{V}_e$, and therefore, using the property 5.2, (5.37) gives:

$$\begin{aligned} \dot{V} = s^T (M\dot{V}_e^r - M\dot{V}_e) + \Delta\dot{\theta}^T \Gamma_\theta \Delta\theta + s_o^T M_o \dot{s}_o \\ + s^T (\tfrac{1}{2}(\dot{M} - 2C) + C) s + s_o^T (\tfrac{1}{2}(\dot{M}_o - 2C_o) + C_o) s_o \end{aligned} \tag{5.38}$$

Using (5.35), property 5.2 and the dynamics of the N MMRs (5.5), (5.38) gives:

$$\begin{aligned} \dot{V} = s^T \left(-U - F_e + CV_e + G + M\dot{V}_e^r\right) + s^T C s \\ + \Delta\dot{\theta}^T \Gamma_\theta \Delta\theta - s_o^T J_o \Delta F_e \end{aligned} \tag{5.39}$$

Further, a simple calculation using the control law (5.33), the control equation of the N MMRs (5.23), the equations (5.34,5.35) and the relation $s = J_o^T s_o$ yields:

$$\dot{V} = -s^T \Gamma s - s^T Q \Delta\theta + \Delta\dot{\theta} \Gamma_\theta \Delta\theta \tag{5.40}$$

Substituting the update control law (5.28), the relation (5.40) gives the following:

$$\dot{V} = -s^T \Gamma s \leq 0 \tag{5.41}$$

The system, including the trajectory is uniformly bounded, and as a result, V is a nonincreasing function, and therefore, s and $\Delta\theta$ are also bounded. Taking the time derivative (5.41) yields $\ddot{V} = -2s^T \Gamma \dot{s}$ since s and $\dot{s}$ are bounded. This implies that $\ddot{V}$ is bounded, and consequently, $\dot{V}$ is uniformly continuous. Since the desired trajectory is uniformly continuous, it implies that s_i and e_i are uniformly continuous as well. Thus, according to Barbalat's lemma, $\lim_{t\to\infty} \dot{V} = 0$ and therefore, $\lim_{t\to\infty} e_i = 0$.

5.5 Simulation results

Numerical simulations are carried out on two identical 6DoF MMRs handling a rigid object in coordination, as illustrated in Figure 5.4, and the parameters of both MMR and the object are given in Table 5.1 The desired trajectory of the center of gravity of the object is generated in

Table 5.1 System parameters

	Parameters
Object	$m_o = 1kg, I_o = 1kg.m^2$
Articulation: 1,2,3,4 (revolute)	$m_{1,2,3,4} = 1kg$, $I_{1,2,3,4} = 1kg.m^2$, $L_{1,2} = 1m$, $\quad L_{3,4} = 0.5m$,
Platform	$m_v = 6kg$, $I = 19kg.m^2$ $d = 1m$, $r = 1m$

the Cartesian space. Two examples of desired trajectories are used in these numerical simulations.In the first one, the object displacement is along the X-axis, the Y-axis and rotation along the Z-axis. In this case, there is no displacement along the Z-axis, and no rotation along the

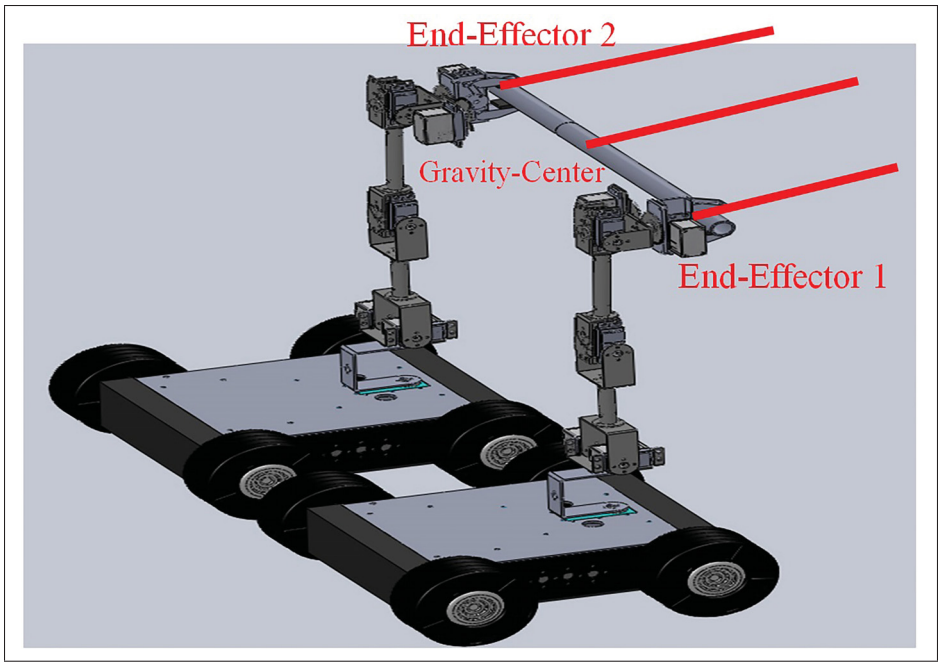

Figure 5.4 Two identical 6Dof mobile manipulators

X- and the Y-axes. The starting point is $P_o = (x_o, y_o, z_o, \beta) = (1, 0, 1, 0)$ and the final point is $P_f = (x_o, y_o, z_o, \beta) = (2, -0.5, 1, \frac{3\pi}{2})$.

In the second one, the object displacement is along the X-axis, with a sinusoidal trajectory along the Y-axis, the starting point is $P_o = (x_o, y_o, z_o, \beta) = (2, 0.5, 1, 0)$ and the final point is $P_f = (x_o, y_o, z_o, \beta) = (5, 0.7, 1, 0)$. The controls gains of the controller are chosen as ${}^i\Gamma = diag[250, 250, 250, 250]$, $K_p = diag(125)$ and $K_\lambda = 5$ the desired internal force vector F_I^d is parameterized by the Lagrangian multiplier vector $\lambda_I^d = \begin{bmatrix} \lambda_{Ix}^d & \lambda_{Iy}^d & \lambda_{Iz}^d \end{bmatrix}^T = \begin{bmatrix} 5 & 0 & 0 \end{bmatrix}^T$. The trajectory tracking are presented in Figure 5.5 and Figure 5.9. The simulation results in the Cartesian space are presented in Figure 5.6 and Figure 5.10. We can observe a good position and orientation tracking. The tracking of the internal forces along the XYZ positions and the moment along the Z-axis are presented in Figure 5.8 and Figure 5.12. As can be seen from the simulation results (Figure 5.7 and Figure 5.11), the objective of the trajectory tracking for a group of MMR, carrying a rigid object, is successfully realized.

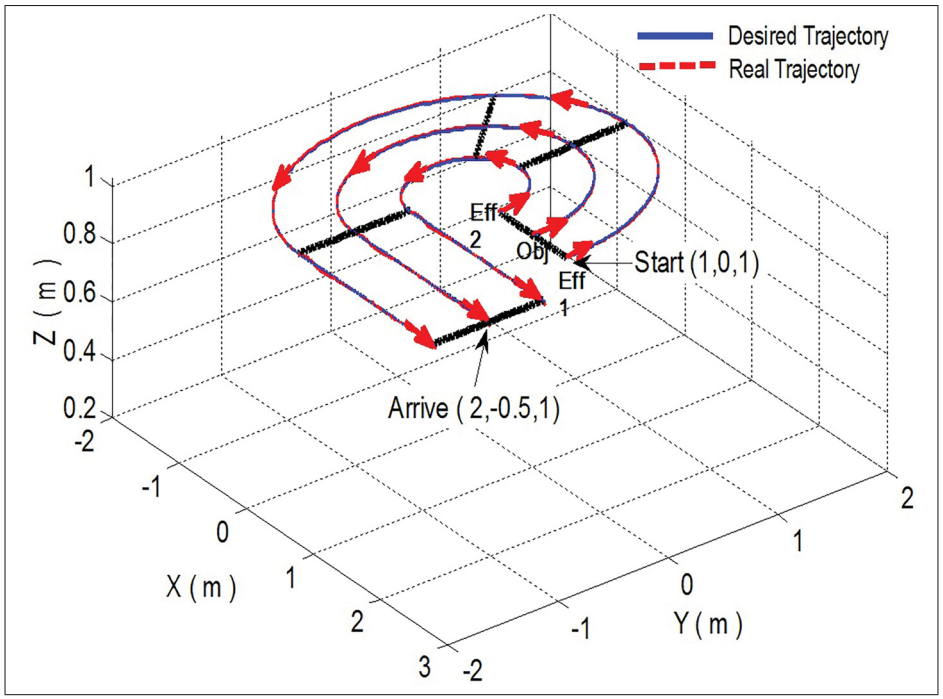

H

Figure 5.5 Desired and real trajectories of the object

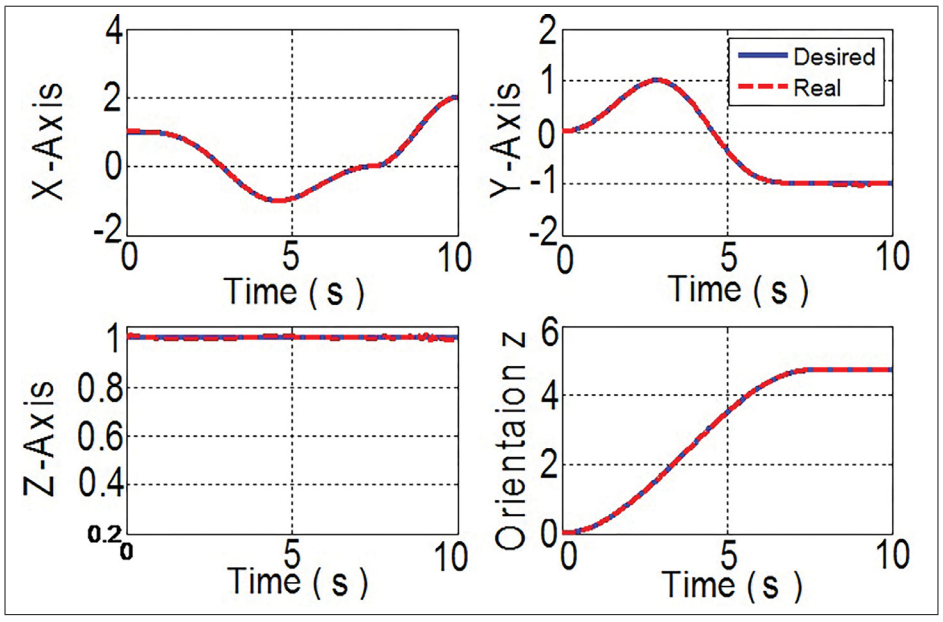

H

Figure 5.6 Trajectory tracking in Cartesian space: X-axis,Y- axis, Z-axis and orientation

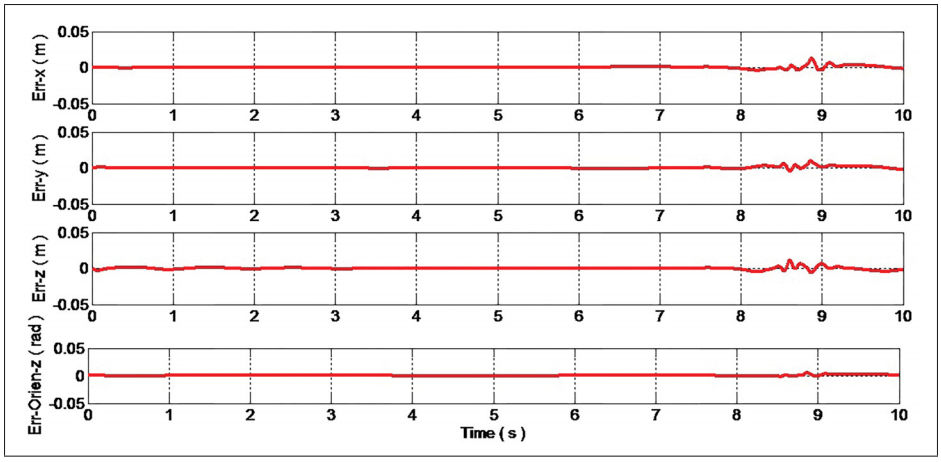

Figure 5.7 Positions errors

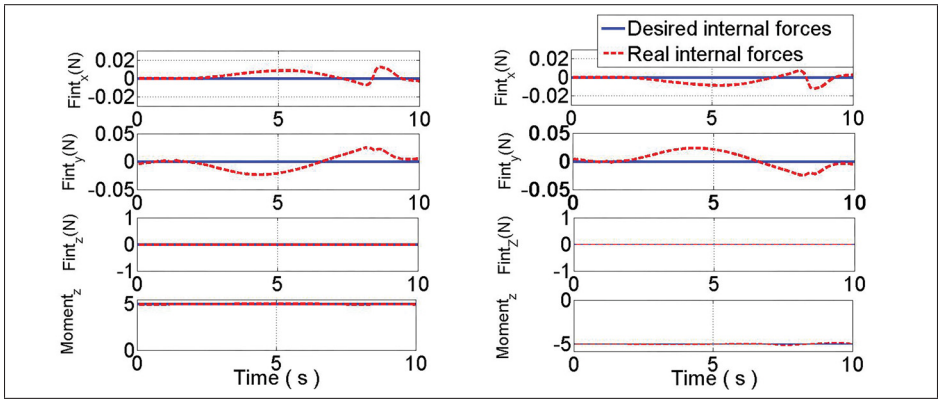

Figure 5.8 Desired and measured internal forces: (a) MMR 1, (b) MMR 2

In order to show the effect of the internal force control, two tests are performed on the second trajectory. In the first test, the position control is considered without taking into account the internal force. In the second test, the internal force control is introduced. Figure 5.9 shows that the position control is satisfactory in both cases. This confirms that the internal force does not affect the position of the object. However, as shown in Figure 5.13 a, the position control, without internal force control, does not ensure that the object will be properly handled. To move the object safely, the tracking of the internal force should be ensured, as shown in Figure 5.13b.

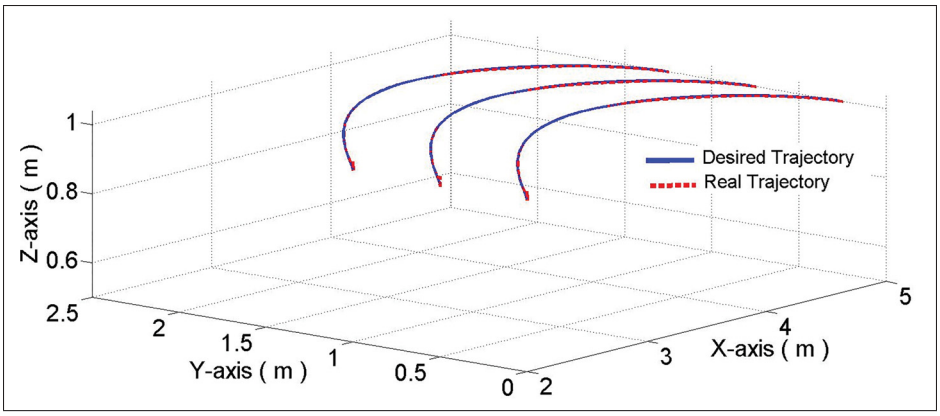

Figure 5.9 Trajectory of the object

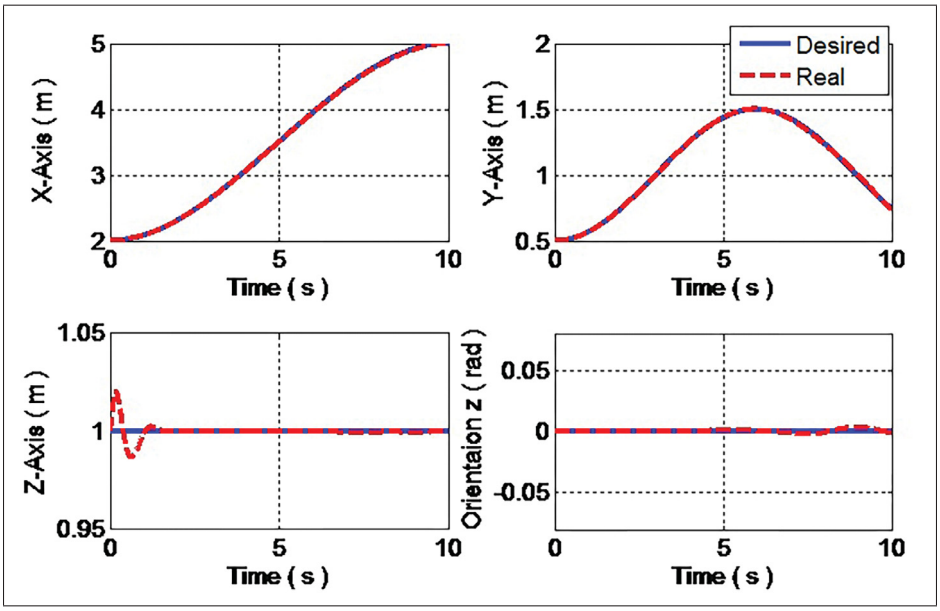

Figure 5.10 Trajectory tracking in Cartesian space:
X-axis,Y-axis, Z-axis and orientation

5.6 Experimental results

In this section, the proposed control scheme is implemented in real time on two identical mobile manipulator robots named Mob_ ETS. In this experimental test, a Zigbee technology communication is used between the application program implemented in Simulink Matlab® and the mobile manipulator robots. The adaptive control developed and simulated in the previ-

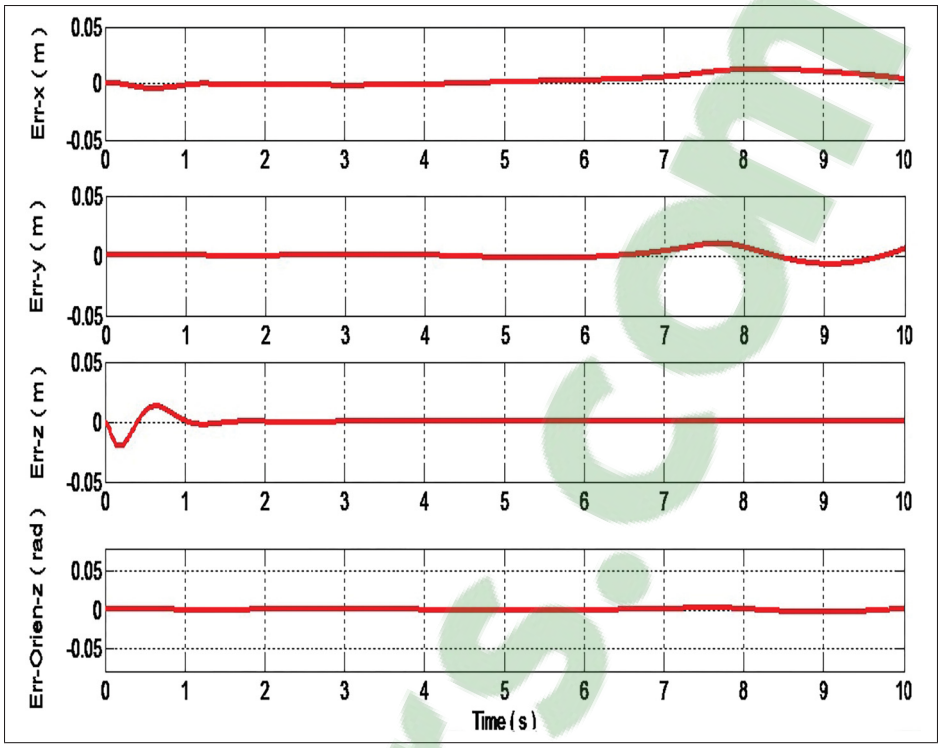

Figure 5.11 Positions errors

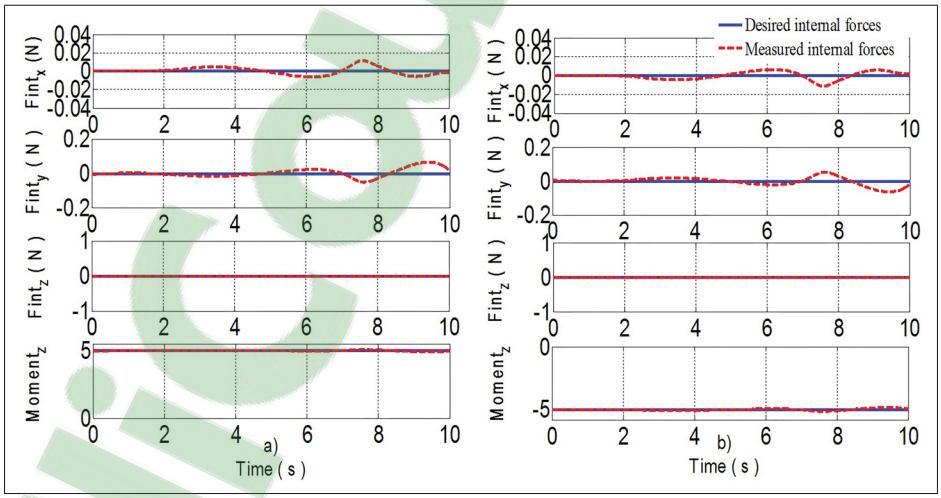

Figure 5.12 Desired and measured internal forces: (a) MMR 1, (b) MMR 2

ous section is implemented in real time using Real-Time Workshop (RTW) by Mathworks®. Since the external end-effector force is unavailable for measurement, in this section, we use an

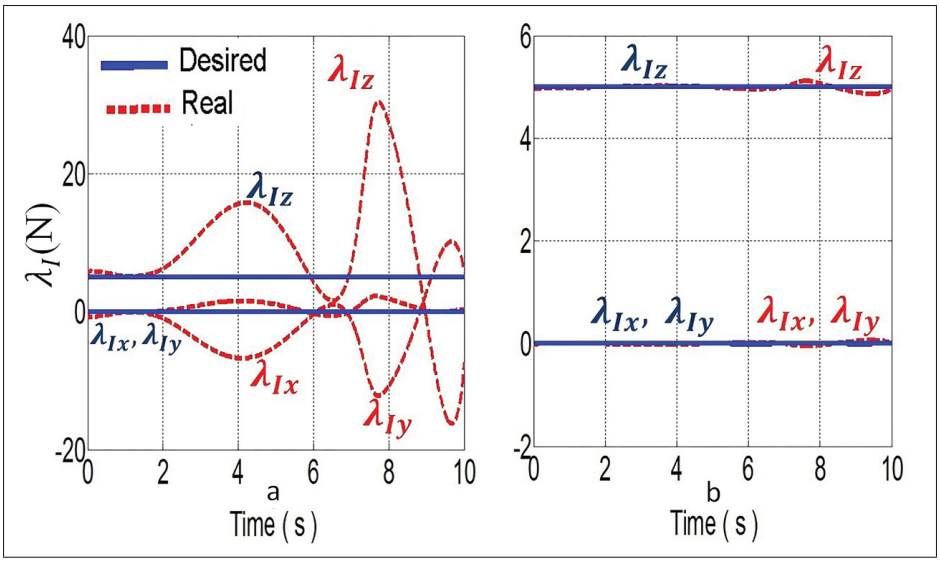

Figure 5.13 Desired and measured internal forces

end-effector observer proposed in Alcocer *et al.* (2003) for its estimation. Fig. 5.14 shows the complete structure design of the control.

The two wheels of the *j*-th mobile manipulator robot platform are actuated by two HN-GH12-2217Y DC motors (DC-12V-200RPM 30:1), and the angular positions are given using encoder sensors (E4P-100-079-D-H-T-B). All joints of the manipulator arm are actuated by Dynamixel motors (MX-64T).

The desired trajectory of the center of gravity of the object is generated in the Cartesian space. The object displacement is along the X-axis, with a sinusoidal trajectory along the Y-axis, The starting point $P_o = (x_o, y_o, z_o, \beta) = (0, -0.1, 0.42, 0)$ is and the final point is $P_f = (x_o, y_o, z_o, \beta) = (3, -0.1, 0.47, 0)$. The control gains of the controller are chosen to be ${}^i\Gamma = diag[50, 50, 50, 50]$, $K_p = diag(12)$ and $K_\lambda = 0.5$ and the desired internal force vector F_I^d is parametrized by the Lagrangian multiplier vector $\lambda_I^d = \begin{bmatrix} \lambda_{Ix}^d & \lambda_{Iy}^d & \lambda_{Iz}^d \end{bmatrix}^T = \begin{bmatrix} 1 & 0 & 0 \end{bmatrix}^T$. The sampling time is set at 0.015 second. The trajectory tracking is presented in Figure 5.15. The experimental results in the Cartesian space are presented in Figure 5.16. We can observe that there is a good position and orientation tracking. The results illustrated in Figures 5.16– 5.17 prove the effectiveness of the approach developed and simulated in the last section.

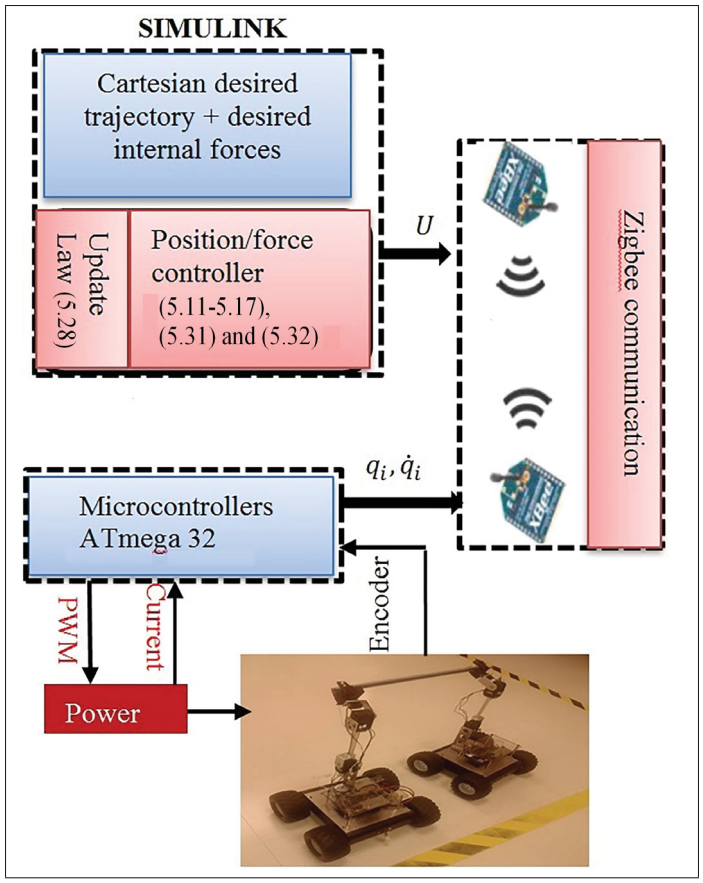

Figure 5.14 Real-time setup

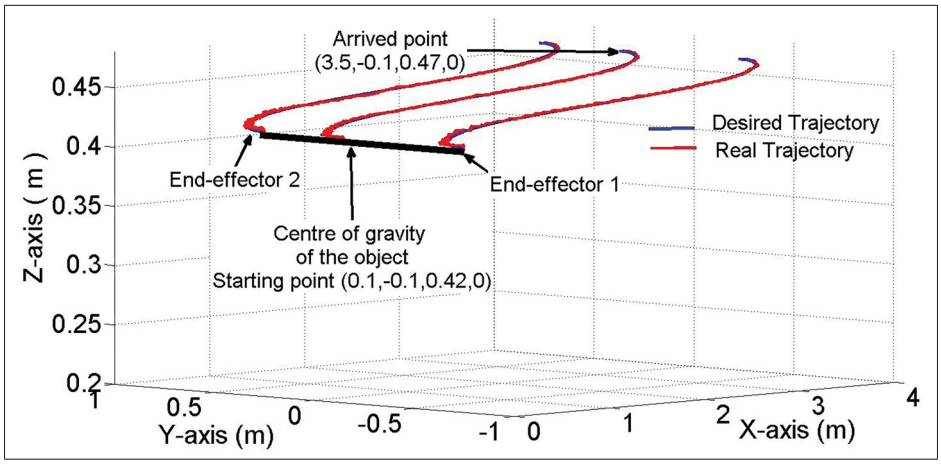

Figure 5.15 Desired and real trajectories of the object

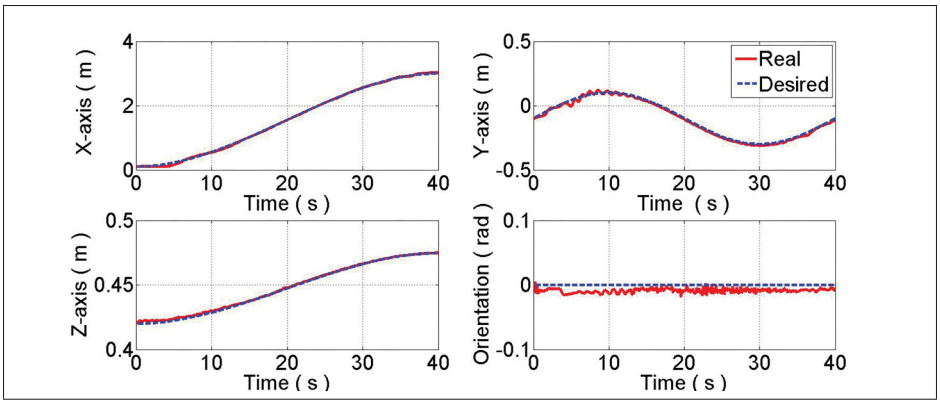

Figure 5.16 Trajectory tracking in Cartesian space:X-axis, Y-axis, Z-axis and orientation

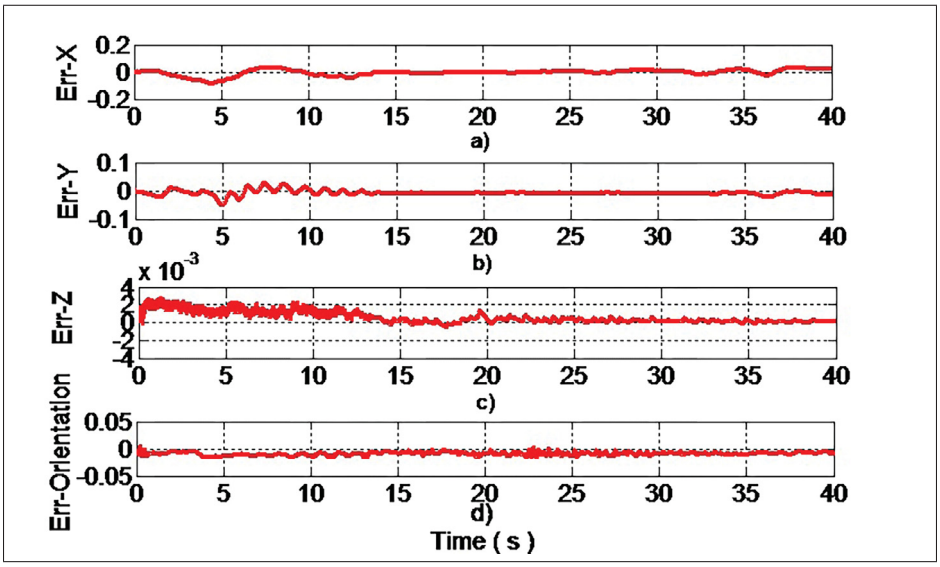

Figure 5.17 a) Error in X-axis, b) error in Y- axis, c) error in Z-axis and d) error in orientation

5.7 Conclusion

In this paper, a coordinated control scheme for multiple mobile manipulator robots transporting a rigid object in coordination has been presented. The desired trajectory of the object is generated in the workspace and the parameters of the handling object and the mobile manipulators are estimated online using the virtual decomposition approach. In this study, the external forces are considered available. The control law is designed based on an appropriate choice of

a Lyapunov function candidate, and the asymptotic stability is proved. The proposed control design ensures that the workspace position error converges to zero asymptotically and that the error of the internal force is bounded. The numerical simulation results show the effectiveness of the proposed control. The developed approach has been implemented in real time to show the validation of the theoretical development.

CHAPTER 6

ADAPTIVE BACKSTEPPING CONTROL OF MULTI-MOBILE MANIPULATORS HANDLING A RIGID OBJECT IN COORDINATION

Abdelkrim Brahmi[1], Maarouf Saad[1], Guy Gauthier[2], Wen-Hong Zhu[3]
and Jawhar Ghommam[4]

[1] Département of Electrical Engineering, École de Technologie Supérieure,
[2] Département of automated manufacturing Engineering, École de Technologie Supérieure,
1100 Notre-Dame Ouest, Montréal, Québec, Canada H3C 1K3
[3] Space Exploration,Canadian Space Agency,
6767 Route de l'Aéroport, Longueuil (St-Hubert), Québec, Canada J3Y 8Y9
[4] Research Unit on Mechatronics and Automation Systems,
Ecole National d'Ingenieurs de Sfax, BPW,3038 Sfax, Tunisia,

Accepted in the International Journal of Modelling, Identification and Control, January 13, 2018

Abstract

This paper presents an adaptive backstepping control scheme applied to a group of mobile manipulator robots transporting a rigid object in coordination. All the dynamic parameters of the robotic systems include the handled object and the mobile manipulators are assumed to be unknown but constant. The problem of uncertain parameter is resolved by using the virtual decomposition approach (VDC). This approach was originally applied to multiple manipulator robot systems. In this paper, the VDC approach is combined with backstepping control to ensure a good position tracking. The controller developed in this work ensures that the position error in the workspace converges to zero, and that the internal force error is bounded. The global stability of the entire system is proven based on the appropriate choice of Lyapunov function using virtual stability of each subsystem, based on the principle of the virtual work. An experimental validation is carried out for two mobile manipulators moving a rigid object in order to show the effectiveness of the proposed approach.

Keywords: Backstepping Control; Adaptive Control; Virtual decomposition Approach; Multiple mobile manipulator robots.

6.1 Introduction

The importance of having robots capable of locomotion and manipulation has fostered the design of the robot manipulator fixed on mobile platforms named mobile manipulator mobile (MMR). The most commonly knowns MMR include satellite arms, underwater robots in seabed exploration, and vehicles used in extra-planetary exploration. Cranes mounted on trucks are a typical example of mobile manipulator robots that are more or less automated. Notwithstanding their abilities of manipulation and locomotion, some tasks such as handling of heavy objects become unachievable by a single mobile manipulator robot, and require the cooperation of multiple mobile manipulator robots. This will render the control and design of the robotic system more complex. The complexity of the control of the mechanical system forming a closed kinematic chain mechanism resides in the fact that it imposes a set of kinematic constraints to coordinate the position and the velocity of the mobile manipulator. Hence the degree of freedom of the complete system is reduced. Further, the internal forces of the object produced by all mobile manipulators must be controlled. A restricted number of research works has been proposed to solve the problem of control of this category of robotic system which have a high degree of freedom and that are closely interconnected since all the mobile manipulator robot are rigidly attached to the object. The majority of published researches in this area have until now focused on three principal mechanisms of coordination: the decentralized control, the follower approach control leader and motion planning.

6.1.1 Previous Works

In the first approach, the complete system is considered to be in fact multiple subsystems, which simplifies the control design for each separate subsystem (Yan *et al.* (2014)). As an example of decentralized control applied to a group of holonomic mobile manipulators, in (Yohei *et al.* (2007)), a motion coordination control which does not use a torque/force sensor was proposed. In (Kosuge and Oosumi (1996); Hirata *et al.* (1999); Y. *et al.* (1999)) a control law based on the constraints at the contact points between the end-effectors of all mobile manipulators and the point representing the manipulated object was proposed in order to reduce the sensor noise

effect. A novel decentralized cooperative control, originally used to control a robot manipulator with a fixed base, and subsequently applied to control holonomic mobile manipulators, was proposed in (Khatib *et al.* (1996b); Park and Khatib (2008)), have been produced in this area. In (Shao *et al.* (2015)) a distributed control combined with observer state were designed for multi-agent robotic system.

In the second approach, one or several MMR are named as a leader capable of tracking a desired trajectory, while other members of the group follow leaders. This approach uses a very strong controller, and each robot in the group should be equipped with very sophisticated sensors in order to ensure adequate information exchange. Many contribution papers, such as (Chen and Li (2006); Z.-D. and K. (2004); Tang *et al.* (2009); Fujii *et al.* (2007); Du and Li (2012)) were proposed.

Finally, the third approach tackles the fact that the motion planning strategy to adopt is a critical problem in robotics, precisely in multi-robot systems as in (Mehrez *et al.* (2016)). Few research works have employed this approach, which is applied to multiple mobile manipulator robots in cooperation, with several robots transporting a single object in coordination, in a known/unknown environment. These studies include those presented in (Desai and Kumar (1997); Yamamoto and Fukuda (2002)). In (Desai and Kumar (1997)), an optimal trajectory was developed for two mobile manipulators pushing a common object to a known location. The authors in (Yamamoto and Fukuda (2002)) proposed a control law for multiple mobile manipulators moving a common object. Measurements of the dynamic manipulability and kinematic are given by taking into consideration collision avoidance. However, the dynamics of the object is ignored. In (Sun and Gong (2004a); LaValle (2006)), a planning approach based on genetic algorithms was proposed.

A multiple mobile manipulator system transporting an object is a typical example of this category of complex robotic systems. As result of the constraints imposed on the system forming a closed kinematic chain, the degrees of freedom of motion are often less than the number of actuators. In this case, it is not only the motion that needs to be controlled; the internal forces

should as well. To overcome these problems, a novel adaptive coordinated backstepping control based on the virtual decomposition approach applied to multiple mobile manipulators is proposed in this work.

6.1.2 Main contribution

All previous studies based on Lagrangian or Newton/Euler approaches require that the parameters of the system be well known. In practical terms, this is difficult, and the resulting model is generally uncertain. To solve the problem of modelling and dynamic control in the presence of uncertainty, some researchers have proposed an adaptive control approach (Karray and Feki (2014)). In (Abdelhedi and Derbel (2017)) an adaptive second order sliding mode control has been developed seeking to resolve the challenging problems of real systems reflected by the presence of these types of systems with a large degree of freedom, adapting the parameters using methods based on the full dynamics is very complicated due to the huge number of parameters involved. Others have proposed and intelligent adaptive control based on a neural networks scheme (Liu *et al.* (2014); Liu and Zhang (2013); Liu *et al.* (2013)) and a fuzzy logic approach (Mai and Wang (2014)). For instance, non-model-based techniques have been developed for a different type of mobile manipulator robot with dynamic parameter uncertainties. Another problem is that the dynamics of the whole system are complicated. Any change in the structure of the group requires a new dynamics modelling (removal of a faulty robot or addition of a new robot to the system).

Finally, some researchers proposed a different approaches of control applied to mobile manipulator robot to track a predefined trajectory. In (Fareh *et al.* (2017)), the author proposed a distributed controller applied to a 3Dof manipulator arm mounted on a nonholonomic mobile platform where the robot is decomposed into two subsystems including the mobile platform and the robot arm. A kinematic control was combined with the distributed control to control the robot. In (Karray and Feki (2017)), the author treat a tracking problem of mobile manipulator in which a feedback control was applied based on the fuzzy proportional-derivative control to generate a necessary torques. The author used a controller based on the dynamic models of

the manipulator and DC motors but in practice these dynamics are unknown. Differently to the cited works, a system comprised of many mobile manipulators holding an object constitutes one of the most important classes of robotic systems. The uncertainties, the high nonlinearity, and the tight kinematics and dynamics coupling characterising such systems greatly complicate the control problem and make it difficult to solve using the classical approaches explained earlier. To overcome these problems, we propose in this paper an adaptive decentralized approach based on an extension of the virtual decomposition control (VDC) methodology presented by (Zhu *et al.* (1997); Al-Shuka *et al.* (2014); Zhu (2010); C.O. *et al.* (2015)); this approach was originally designed for fixed-platform robotic systems with large degrees of freedom. It is simulated and implemented in real time to control a group of manipulator robots attached to a mobile platform, which are more complex than the manipulator robots. The difficulty with this category of robotic systems resides in the fact that not only must the coordination between robots in the system be controlled, but the coordination between the locomotion and manipulation of each manipulator mobile robot needs to be controlled independently. In contrast with what appears in the cited works, this paper enriches the body of knowledge in the field through the following contributions:

a. The proposed control schemes present several major advantages, with the main ones being that:

   - The individual dynamics of each subsystem make it much easier to obtain the dynamics of the whole system, whatever its degree of freedom;
   - They provide greater flexibility to the design of the control law, in addition to greatly simplifying the calculation of the dynamics system, even in the presence of a change in the system configuration, and;
   - They render the adaptation of the uncertain parameters very simple and systematic.

b. To solve the problem of parameter adaptation and modelling of systems using standard approaches, a VDC approach based on sliding mode control was previously proposed,

as explained earlier. In this paper, this approach (VDC) is combined with backstepping control to ensure a good workspace position tracking;

c. Finally, the global stability of the complete system is proven based on the appropriate choice of Lyapunov functions using the virtual stability of each subsystem, based on the principle of the virtual work. Contrary to the original VDC stability, in this paper, all parameters are estimated and considered completely unknown, with no known limit.

The rest of the paper is organized as follows. Section 6.2 presents the modelling of the system, while section 6.3 explains the control design. Simulation results are given in section 6.4. Section 6.5 presents an experimental validation of the developed approach. Finally, a conclusion is given in section 6.6.

6.2 Modeling and System Description

Figure 6.1 shows the holonomic manipulator arm mounted on nonholonomic mobile platform. where the manipulator has $\boldsymbol{p}$-DOF, the mobile platform has $\boldsymbol{m}$-DOF and the full robotic system has $\boldsymbol{n=m+p}$-DOF. Figure 6.1 shows the MMR with P_{ie} being the position/orientation vector of the j-th MMR end-effector.

Before presenting the adaptive backstepping control law developed based on the virtual decomposition approach, we start by stating a brief formulation of the kinematic and dynamic modelling of the i-th mobile manipulator robot and the handled object. In the VDC approach, the robotic system is decomposed into a graph consisting of multiple objects and open chains. An object is a rigid body, and open chains consist of a series of rigid links connected one by one by a hinge, and having certain degrees of freedom. The dynamic coupling between the subsystems can be represented by the flow of virtual power (FVP) at the cutting point. This refers to the principle of virtual work (Zhu *et al.* (1997); Al-Shuka *et al.* (2014); Zhu (2010)). This decomposition is illustrated in Figure 6.2.

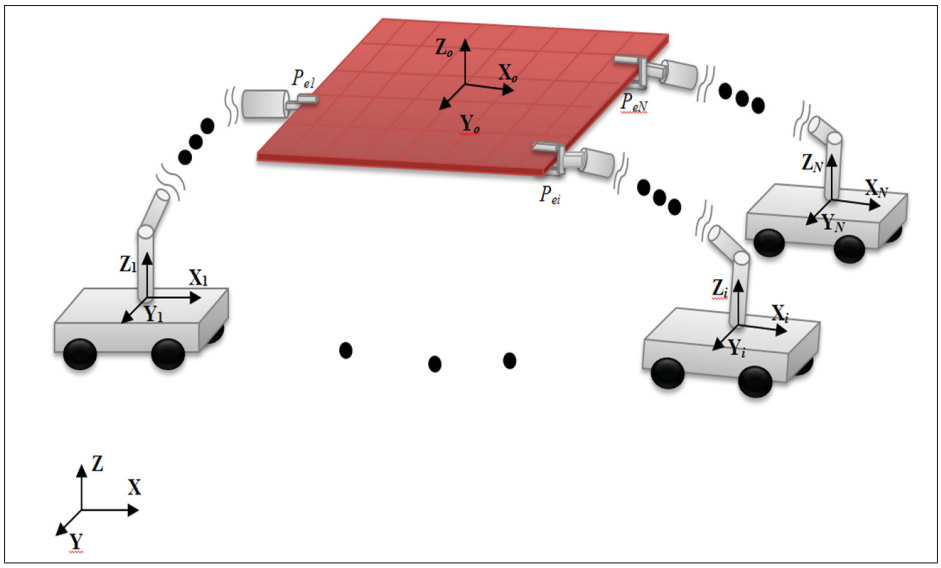

Figure 6.1 Multiple MMR handling a rigid object

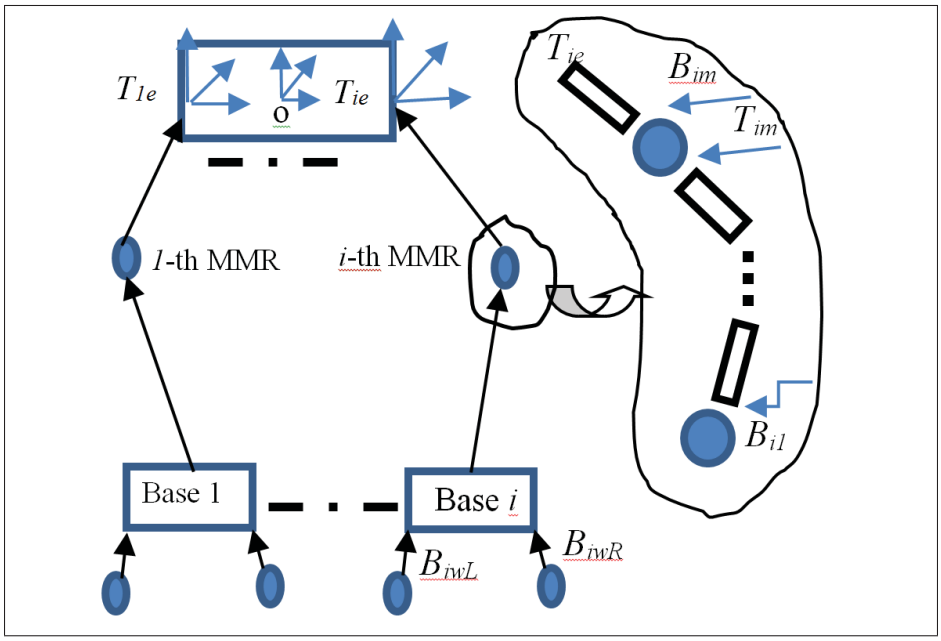

Figure 6.2 Virtual decomposition of the MMR

6.2.1 Kinematics and dynamics of the object

6.2.1.1 Kinematics model of the object

Since the frame o and T_{ie} for all $i \in \{1,N\}$ are rigidly attached, it follows that:

$$V_e = \begin{bmatrix} V_{1e} \\ . \\ . \\ . \\ V_{Ne} \end{bmatrix} = {}^{o}U_{T_e}^{T}\Gamma^{T}\,{}^{o}V = J_o\,{}^{o}V \tag{6.1}$$

where, ${}^{o}V = [v_o^T \; w_o^T]^T$ with v_o and w_o being the linear and angular velocities of the centre of gravity of the object respectively. $V_e = \begin{bmatrix} V_{1e}^T & . & . & . & V_{Ne}^T \end{bmatrix}^T$ are the velocities at the contact points between the end-effectors and the object , T_{ie} ,$i \in \{1,N\}$ and J_o is the jacobian matrix given as follows:

${}^{o}U_{T_e} = diag[{}^{o}U_{T_{1e}},...,{}^{o}U_{T_{ie}},...,{}^{o}U_{T_{Ne}}] \in \mathbb{R}^{6N\times 6N}$

$\Gamma = [I_6,...,I_6]^T \in \mathbb{R}^{6\times 6N}$

with, I_6 is the 6×6 identity matrix and the transformation matrix of force/moment and linear/angular velocity vectors from frame B to frame A is defined by:

$${}^{A}U_B = \begin{bmatrix} {}^{A}R_B & 0_{3\times 3} \\ \\ S({}^{A}r_{AB})\,{}^{A}R_B & {}^{A}R_B \end{bmatrix} \tag{6.2}$$

where ${}^{A}R_B$ is the rotation matrix between frames A and B, and $S({}^{A}r_{AB})$ is a skew symmetric matrix built from the vector ${}^{A}r_{AB}$ linking the origins of frames A and B, expressed in the coordinates of frame A.

6.2.1.2 Dynamics model of the object

The object handled by N mobiles manipulators is rigid. The equation of motion of the effort based on the linear parametrization form is given by the following equation:

$$ {}^{o}F = M_o(X_o)\,{}^{o}\dot{V} + C_o(X_o,\dot{X}_o)\,{}^{o}V + G_o(X_o) \tag{6.3} $$

where, v_o and w_o being respectively the linear and angular velocities of the object.${}^{o}F \in \mathbb{R}^6$ is the vector of forces applied on the object, $M_o \in \mathbb{R}^{6\times 6}$ is the mass matrix, $C_o \in \mathbb{R}^{6\times 6}$ represents the centrifugal and Coriolis matrix and $G_o \in \mathbb{R}^6$ is the vector of gravity.
The net force/moment vector is given by:

$$ {}^{o}F^* = \sum_{i=1}^{N} {}^{o}U_{T_{ie}}^{T}\,{}^{T_{ie}}F = \Gamma\,{}^{o}U_{T_e}\,{}^{T_e}F \tag{6.4} $$

where, ${}^{T_e}F = \begin{bmatrix} {}^{T_1 e}F^T & . & . & . & {}^{T_N e}F^T \end{bmatrix}^T$ denote the force/moment vectors in frame T_{ie} at the contact (cutting) point for $i \in \{1,N\}$. By introducing the internal force vector $F_{int} \in \mathbb{R}^{6\times N-1}$, the force/moment vectors at the contact point T_{ie} can be computed from (6.4) as:

$$ {}^{T_e}F = {}^{T_e}U_o \begin{bmatrix} \Phi_m & \Phi_f \end{bmatrix} \begin{bmatrix} {}^{o}F^* \\ F_{\text{int}} \end{bmatrix} \tag{6.5} $$

where ${}^{T_e}U_o = {}^{o}U_{T_e}^{-1}$ and the matrices $\Phi_m \in \mathbb{R}^{6N\times 6}$ and $\Phi_f \in \mathbb{R}^{6N\times(6N-6)}$ are governed by:

$$ \begin{cases} \Gamma\Phi_m = I_6 \\ \Gamma\Phi_f = 0 \end{cases} \tag{6.6} $$

Note that the matrix $\begin{bmatrix} \Phi_m & \Phi_f \end{bmatrix}$ is of full rank. There exists a matrix Ω that verifies:

$$ \begin{bmatrix} \Gamma \\ \Omega \end{bmatrix} = \begin{bmatrix} \Phi_m & \Phi_f \end{bmatrix}^{-1} \tag{6.7} $$

Therefore, the internal force coordinates can be calculated from (6.5) based on the force/moment at the N end-effectors as follows:

$$F_{\text{int}} = \Omega^{o} U_{T_e}{}^{T_e} F \tag{6.8}$$

6.2.2 Kinematics and Dynamics of the i-th Mobile Manipulator

Figure 6.3 shows the i-th holonomic manipulator arm attached to nonholonomic mobile platform where the manipulator has $\boldsymbol{p}$-DOF, the mobile platform has $\boldsymbol{m}$-DOF and the full robotic system has $\boldsymbol{n=m+p}$-DOF.

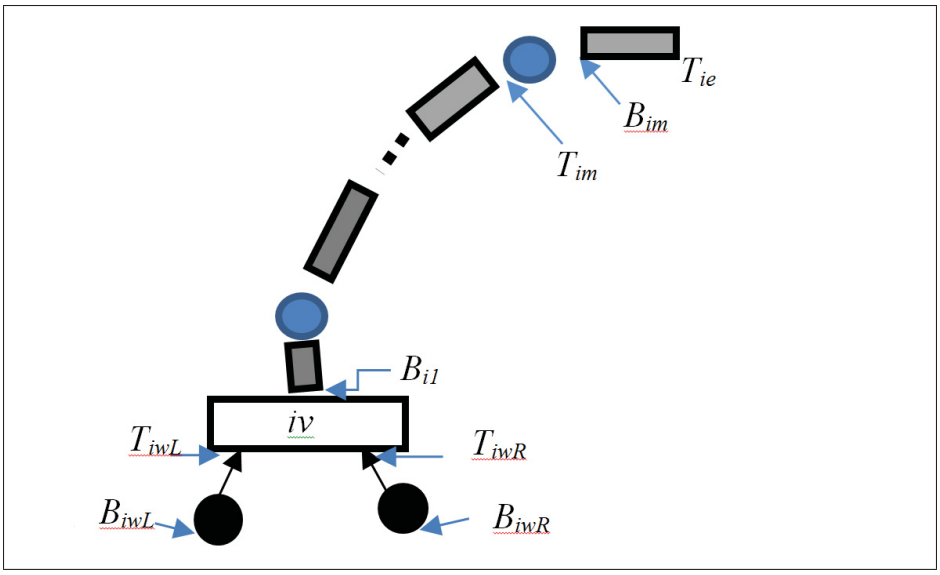

Figure 6.3 Virtual decomposition of the i-th MMR

6.2.2.1 Kinematics of the i-th mobile manipulator

The augmented linear/angular velocities vector of each frame B_{iwR} is defined as:
$V_{iB} = [\dot{q}_{ij}, V_{iv}, V_{B_{iwR}}^T, V_{B_{iwL}}^T, V_{B_{i1}}^T, ..., V_{B_{im}}^T]^T$.
where, $\dot{q}_{ij} = [\dot{q}_{iwR}, \dot{q}_{iwL}, \dot{q}_{i1} ..., \dot{q}_{im}]$ is the right/left wheels velocities and the j-th joint velocities

of the manipulator arm, $V_{B_{ij}} \in \mathbb{R}^6$ the linear and angular velocity vector of the corresponding frame B_{ij} , $V_{iv} \in \mathbb{R}^6$ is the linear/angular velocity vector of the mobile platform of the i-th mobile manipulator robot. In general, we can write the system in matrix form by using the Jacobian matrix:

$$\begin{cases} V_{iB} = J_{in}\dot{q}_{ij} \\ V_{ie} = J_{iq}\dot{q}_{ij} \end{cases} \tag{6.9}$$

where V_{ie} is the velocity at the contact points attached to the object and J_{in}, J_{iq} are the jacobian matrices.

6.2.2.2 Dynamics of the *i*-th mobile manipulator

The dynamics of the j-th rigid body of the i-th manipulator arm is given by the following equation:

$$F^*_{B_{ij}} = M_{B_{ij}}\dot{V}_{B_{ij}} + C_{B_{ij}}V_{B_{ij}} + G_{B_{ij}} \tag{6.10}$$

with, $M_{B_{ij}}$ being the matrix of inertial term, $C_{B_{ij}}$ the matrix of centrifugal/Coriolis term, $G_{B_{ij}}$ the vector related to the gravity and $j = wR, wL, 1, .., m$ represents the right/left wheels and the m joints of the arm manipulator. The dynamics of the mobile platform (object) is given by the following expression:

$$F^*_{iv} = M_{iv}\dot{V}_{iv} + C_{iv}V_{iv} + G_{iv} \tag{6.11}$$

with, M_{iv} being the matrix of inertial term, C_{iv} the matrix of centrifugal/Coriolis term, G_{iv} the vector related to the gravity. The vector of resulting forces / moments acting on the rigid body

is computed by an iterative process as follows:

$$\begin{aligned}
F_{B_{im}} &= F^*_{B_{im}} + {}^{B_{im}}U_{T_{ie}}{}^{T_{ie}}F \\
F_{B_{im-1}} &= F^*_{B_{im-1}} + {}^{B_{im-1}}U_{B_{im}}F_{B_{im}} \\
&\vdots \\
F_{iv} = F^*_{iv} &= {}^{iv}U_{T_{iwR}}F_{T_{iwR}} + {}^{iv}U_{T_{iwL}}F_{T_{iwL}} + {}^{iv}U_{B_{i1}}F_{B_{i1}} \\
F_{B_{iwR}} &= F^*_{B_{iwR}} + {}^{B_{iwR}}U_{T_{iwR}}F_{T_{iwR}} \\
F_{B_{iwL}} &= F^*_{B_{iwL}} + {}^{B_{iwL}}U_{T_{iwL}}F_{T_{iwL}}
\end{aligned} \tag{6.12}$$

The dynamics of the j-th joint actuator of the manipulator arm and that of the right/left driving motors of the platform are expressed based on the linear parameterization form by the following equation:

$$\begin{aligned}
\tau^*_{a_{ij}} &= J_{m_{ij}}\ddot{q}_{ij} + k^c_{ij}sign(\dot{q}_{ij}) \\
&= Y_{a_{ij}}\theta_{a_{ij}}
\end{aligned} \tag{6.13}$$

where, $J_{m_{ij}}$ denotes the moment of inertia of $j-th$ joint motor, $k^c_{ij} \in \mathbb{R}$ denotes the Coulomb friction coefficient, $Y_{a_{ij}} \in \mathbb{R}^{1\times 4}$ is the dynamic regressor matrix and $\theta_{a_{ij}} \in \mathbb{R}^4$ is known parameter vector, defined in (Zhu *et al.* (1997); Al-Shuka *et al.* (2014); Zhu (2010)) and is defined in (6.10),

Finally, from (6.10) and (6.13) the dynamics of the i-th mobile manipulator robot can be written as follows:

$$\tau_{a_{ij}} = \tau^*_{a_{ij}} + z^T F_{B_{ij}} \tag{6.14}$$

with, $z = [0\ 0\ 0\ 0\ 0\ 1]^T$ for the revolute joints and $z = [0\ 0\ 1\ 0\ 0\ 0]^T$ for the prismatic joints.

6.3 Control Design

6.3.1 Control problem statement

Before developing the design control, we introduce some assumptions to simplify the control formulation as follows:

Assumption 6.1: The desired object trajectory is assumed to be smooth, and there exists ε_1 , ε_2 and ε_3 such that

$$\left\| \frac{\partial X_o^d}{\partial x} \right\| \leq \varepsilon_1, \left\| \frac{\partial^2 X_o^d}{\partial x^2} \right\| \leq \varepsilon_2, \left\| \frac{\partial^3 X_o^d}{\partial x^3} \right\| \leq \varepsilon_3,$$

Assumption 6.2: The object is rigid and all end-effectors are attached rigidly to it. As a result, there is no relative motion between the end-effector and the object.

Assumption 6.3: The parameters of the object and the mobile manipulators are unknown but constant.

Assumption 6.4: All the joints velocities of the mobile manipulator robots are available for feedback as well as for the measurement of external forces.

The control objective is to generate a set of torque inputs such that the position's tracking error of the transported object in the workspace converges asymptotically to zero. Formally speaking, the control problem is to design the control input:

$$U = f\left(V_e, \dot{V}_e, X_o, {}^oV\right)$$

such that the following limits hold:

$$\lim_{t\to\infty} \left\| X_o - X_o^d \right\| = 0, \lim_{t\to\infty} \left\| {}^oV - {}^oV^d \right\| = 0$$

$$\lim_{t\to\infty} \left\| F_{int}^d - F_{int} \right\| = bounded.$$

where, $X_o^d \in \mathbb{R}^6, {}^oV^d \in \mathbb{R}^6$ are the desired position and velocity of the object generated in the workspace, $F_{int}^d \in \mathbb{R}^{6N}$ and $F_{int} \in \mathbb{R}^{6N}$are the desired and measured internal forces/moment coordinates.

6.3.2 Design

The parameters adaptation of the complete systems are obtained using the VDC approach, where this problem of adaptation is converted into a problem of estimation of the parameters of each subsystem. The different steps used in the design of the controller are discussed below.

Step 1: The goal in this step is to virtually decompose (Zhu *et al.* (1997); Al-Shuka *et al.* (2014); Zhu (2010)) and (Brahmi *et al.* (2013b)), the robotic system into several parts and open chain elements. Each part is a rigid body and open chain consists of a series of rigid links connected one by one. This decomposition is illustrated in Figure 6.2

Step 2: The desired velocities at contact point between the N end-effectors of the mobile manipulators ${V_e}^d \in \mathbb{R}^{6N}$ and the object ${}^oV^d \in \mathbb{R}^6$ are calculated from the desired velocity of the object :

$$ {V_e}^d = \begin{bmatrix} V_{1e}^d \\ . \\ . \\ . \\ V_{Ne}^d \end{bmatrix} = {}^oU_{T_e}^T \left(\Gamma^T {}^oV^d + \Omega^T K_f \left(\tilde{F}_{int}^d - \tilde{F}_{int} \right) \right) \tag{6.15} $$

where Γ, Ω are defined in (6.6)-(6.7), K_f is a diagonal positive definite matrix, $\tilde{F_{int}^d}$, $\tilde{F_{int}}$ are the filtered internal force/moment coordinates which are obtained as:

$$ \begin{cases} \dot{\tilde{F}}_{int}^d = \lambda_f \left(F_{int}^d - \tilde{F}_{int}^d \right) \\ \dot{\tilde{F}}_{int} = \lambda_f \left(F_{int} - \tilde{F}_{int} \right) \end{cases} \tag{6.16} $$

with λ_f being a diagonal positive definite matrix.

The required velocity in any frame B_{ij} is given by:

$$\begin{cases} V_{ie}^{d} = J_{iq}\dot{q}_{ij}^{d} \\ V_{iB}^{d} = J_{in}\dot{q}_{ij}^{d} \end{cases} \tag{6.17}$$

with $V_{iB}^{d} = [\dot{q}_{ij}^{d}, V_{iv}^{d}, V_{B_{iwR}}^{dT}, V_{B_{iwL}}^{dT}, V_{B_{i1}}^{dT}, ..., V_{B_{im}}^{dT}]^{T}$, $\dot{q}_{ij}^{d} = [\dot{q}_{iwR}^{d}, \dot{q}_{iwL}^{d}, \dot{q}_{i1}^{d}, .., \dot{q}_{im}^{d}]^{T}$, are the desired joint angular velocities and J_{iq}, J_{in} being the Jacobian matrix.

Step 3: In this step, the control design of the object is developed. The backstepping technique is used and can be presented as follows. Define the error variables for the object as follows:

$$\begin{cases} e_{1}^{o} = \left(X_{o} - X_{o}^{d}\right) \\ e_{2}^{o} = \left({}^{o}V - \alpha_{o}\right) \end{cases} \tag{6.18}$$

where α_o is the virtual input, to ensure the stability, this virtual input control is chosen as follows:

$$\alpha_{o} = {}^{o}V^{d} - K_{1}^{o}e_{1}^{o} \tag{6.19}$$

The control law of the object (6.3) based on the virtual input (6.19) and the linear parametrization form is given by the following expressions:

$$\begin{aligned} {}^{o}F^{*r} &= M_{o}\dot{\alpha}_{o} + C_{o}\alpha_{o} + G_{o} - e_{1}^{o} - K_{2}^{o}e_{2}^{o} \\ &= Y_{o}\theta_{o} - e_{1}^{o} - K_{2}^{o}e_{2}^{o} \end{aligned} \tag{6.20}$$

with, ${}^{o}F^{*r} \in \mathbb{R}^{6}$ being the required object force, $Y_o \in \mathbb{R}^{6\times 13}$ is the dynamic regressor matrix and $\theta_o \in \mathbb{R}^{13}$ is known parameter vector, defined in (Zhu *et al.* (1997); Al-Shuka *et al.* (2014); Zhu (2010)). The physical parameters of the object are considered unknown and need to be estimated, in which the estimated vector $\hat{\theta}_o$ is used and the required force/moment is obtained as follows:

$${}^{o}F^{*r} = Y_{o}\hat{\theta}_{o} - e_{1}^{o} - K_{2}^{o}e_{2}^{o} - K_{3}^{o}sign(e_{2}^{o}) \tag{6.21}$$

with $\dot{\hat{\theta}}_{o} = \rho Y_{o}s_{o}$ is the adaptation function, and is chosen to ensure system stability, $s_o = \left({}^{o}V^{d} - {}^{o}V\right)$, ρ, K_2^o, K_3^o are positive gains and Y_o is the dynamic regressor matrix, defined in

(Zhu *et al.* (1997); Al-Shuka *et al.* (2014); Zhu (2010)). The required force/moment vectors at the N end-effectors are computed from (6.20)-(6.21) based on (6.5) as follows:

$$ {}^{T_e}F^r = {}^{T_e}U_o \begin{bmatrix} \Phi_m & \Phi_f \end{bmatrix} \begin{bmatrix} {}^{o}F^{*r} \\ F^d_{\text{int}} \end{bmatrix} \tag{6.22} $$

Step 4: In this step, the control design of the i-th mobile manipulator is developed. The backstepping technique is used and can be presented as follows: Define error variables for the i-th mobile manipulator robot at the different cutting points as follows:

$$ \begin{cases} e_1^{B_{ij}} = z\left(q_{ij} - q_{ij}^d\right) \quad \text{and} \;\; e_1^{iv} = \left(x_{iv} - x_{iv}^d\right) \\ \\ e_2^{B_{ij}} = \left(V_{B_{ij}} - \alpha_{B_{ij}}\right) \;\; \text{and} \;\; e_2^{iv} = \left(V_{iv} - \alpha_{iv}\right) \end{cases} \tag{6.23} $$

where $\alpha_{B_{ij}}, \alpha_{iv}$ are a virtual inputs, to ensure the stability, these virtual inputs control are chosen as follows:

$$ \begin{cases} \alpha_{B_{ij}} = z\dot{q}_{ij}^d - K_1^{B_{ij}} e_1^{B_{ij}} - {}^{B_{ij}}U_{B_{ij}}^T V_{B_{ij}}, \\ \\ \alpha_{B_{iv}} = \dot{V}_{iv}^d - K_1^{iv} e_1^{iv} - \sum\limits_{j=w_R}^{w_L} {}^{iv}U_{B_{ij}}^T V_{B_{ij}} \end{cases} \tag{6.24} $$

The control law of the j-th rigid body (6.10)-(6.11) based the virtual inputs (6.24) and the linear parametrization form is given by the following expressions:

$$ \begin{cases} F_{B_{ij}}^{*r} = M_{B_{ij}}\dot{\alpha}_{B_{ij}} + C_{B_{ij}}\alpha_{B_{ij}} + G_{B_{ij}} - e_1^{B_{ij}} - K_2^{B_{ij}} e_2^{B_{ij}} \\ \qquad\quad = Y_{B_{ij}}\theta_{B_{ij}} - e_1^{B_{ij}} - K_2^{B_{ij}} e_2^{B_{ij}} \\ \\ F_{iv}^{*r} = M_{iv}\dot{\alpha}_{iv} + C_{iv}\alpha_{iv} + G_{iv} - e_1^{iv} - K_2^{iv} e_2^{iv} \\ \qquad\quad = Y_{iv}\theta_{iv} - e_1^{iv} - K_2^{iv} e_2^{iv} \qquad\qquad , \end{cases} \tag{6.25} $$

However, since the physical parameters of the j-th rigid body and the mobile platform are assumed unknown and need to be estimated, then the estimated vectors $\hat{\theta}_{B_{ij}}, \hat{\theta}_{iv}$ are used and

the required force/moment is obtained as follows:

$$\begin{cases} F_{B_{ij}}^{*r} = Y_{B_{ij}}\hat{\theta}_{B_{ij}} - e_1^{B_{ij}} - K_2^{B_{ij}} e_2^{B_{ij}} - K_3^{B_{ij}} sign(e_2^{B_{ij}}) \\ \\ F_{iv}^{*r} = Y_{iv}\hat{\theta}_{iv} - e_1^{iv} - K_2^{iv} e_2^{iv} - K_3^{iv} sign(e_2^{iv}) \end{cases} \tag{6.26}$$

where, $\dot{\hat{\theta}}_{B_{ij}} = \rho_{B_{ij}} Y_{B_{ij}}^T s_{B_{ij}}$, $\dot{\hat{\theta}}_{iv} = \rho_{iv} Y_{iv}^T s_{iv}$ are the adaptation functions, and are chosen to ensure system stability, $s_{B_{ij}} = (V_{B_{ij}}^d - V_{B_{ij}}), s_{iv} = (V_{iv}^d - V_{iv})$, and $\rho_{B_{ij}}, \rho_{iv}, K_2^{B_{ij}}, K_2^{iv}, K_3^{B_{ij}}, K_3^{iv}$ are positive gains. The vector of resulting forces/moments acting on the j-th rigid body is given by an iterative process (Zhu *et al.* (1997); Al-Shuka *et al.* (2014); Zhu (2010)) as in (6.12). We begin by computing the vector of forces at the different cutting points:

$$\begin{gathered} F_{B_{im}}^r = F_{B_{im}}^{*r} + {}^{B_{im}}U_{T_{ie}}{}^{T_{ie}}F^r \\ \\ F_{B_{im-1}}^r = F_{B_{im-1}}^{*r} + {}^{B_{im-1}}U_{B_{im}} F_{B_{im}}^{*r} \\ \vdots \\ F_{iv}^r = F_{iv}^{*r} = {}^{iv}U_{T_{iwR}} F_{T_{iwR}}^r + {}^{iv}U_{T_{iwL}} F_{T_{iwL}}^r + {}^{iv}U_{B_{i1}} F_{B_{i1}}^r \\ \\ F_{B_{iwR}}^r = F_{B_{iwR}}^{*r} + {}^{B_{iwR}}U_{T_{iwR}} F_{T_{iwR}}^r \\ \\ F_{B_{iwL}}^r = F_{B_{iwL}}^{*r} + {}^{B_{iwL}}U_{T_{iwL}} F_{T_{iwL}}^r \end{gathered} \tag{6.27}$$

The control equation of the j-th joint actuators of the mobile manipulator (6.14) based on its required velocity is expressed by the following expression:

$$\tau_{a_{ij}}^{*r} = J_{m_{ij}} \ddot{q}_{ij}^d + \xi\left(q_{ij}^d, \dot{q}_{ij}^d\right) = Y_{a_{ij}} \theta_{a_{ij}} \tag{6.28}$$

where, $\theta_{a_{ij}} \in \mathbb{R}^4$ is the parameters' vector of the j-th joint actuator, and $Y_{a_{ij}} \in \mathbb{R}^{1\times 4}$ is the dynamic regressor (row) vector, defined in (Zhu *et al.* (1997); Al-Shuka *et al.* (2014); Zhu (2010)). Since the physical parameters of the j-th actuator are unknown and need to be estimated, then

the estimated vector $\hat{\theta}_{a_{ij}}$ is used and the dynamic (6.19) becomes:

$$\tau_{a_{ij}}^{*r} = Y_{a_{ij}}\hat{\theta}_{a_{ij}} + K_{a_{ij}}\left(\dot{q}_{ij}^{d} - \dot{q}_{ij}\right) \tag{6.29}$$

where, $\dot{\hat{\theta}}_{a_{ij}} = \rho_{a_{ij}} Y_{a_{ij}}^{T} s_{a_{ij}}$ is the law adaptation function, and is chosen to ensure system stability, $s_{a_{ij}} = \left(\dot{q}_{ij}^{d} - \dot{q}_{ij}\right)$, and $\rho_{a_{ij}}$, $K_{a_{ij}}$ are positive gains.

Step 5: Finally, the *j*-th input control torque at the *i*-th mobile manipulator's joint is calculated based on the desired torque obtained from (6.29) $\tau_{a_{ij}}^{*r}$ and the required force at cutting point B_{ij}, $F_{B_{ij}^{r}}$ identified as:

$$\tau_{ij} = \tau_{a_{ij}}^{*r} + Z^{T} F_{ij}^{r} \tag{6.30}$$

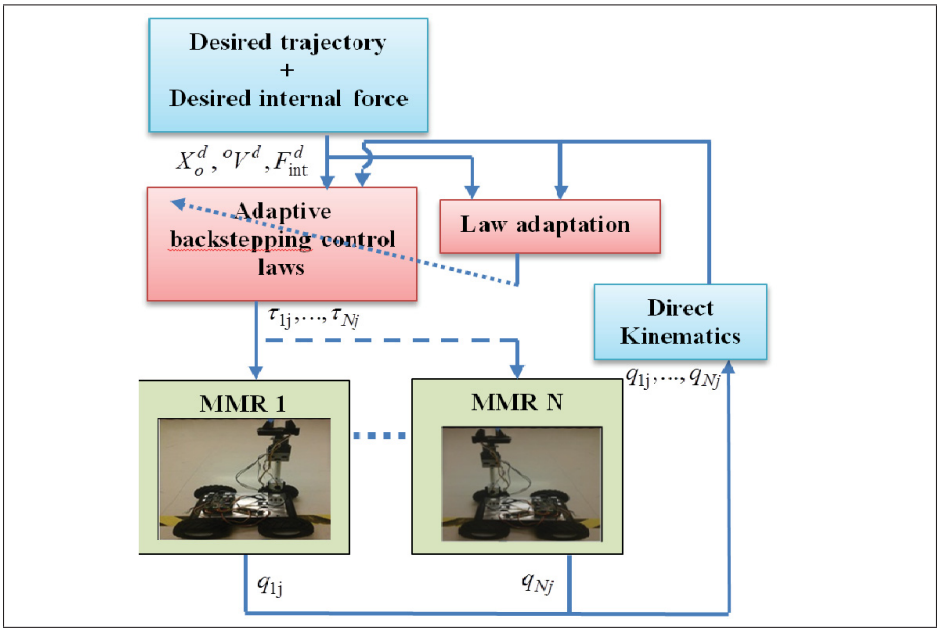

Figure 6.4 Adaptive coordinated control of N MMRs

Lemma 1: Consider the *j*-th rigid dynamics (6.10, 6.12) and the joint actuator dynamics (6.13), under the control design (6.21, 6.26, and 6.29) and the boundedness of the estimated parameters. The control objective is satisfied and the error tracking states are asymptotically stable.

Proof: Consider the Lyapunov function candidate:

$$V = V_o + \sum_{i=1}^{N} \left(\sum_{j=1}^{n} V_{ij} + \sum_{j=1}^{n} V_{a_{ij}} + V_{ip} \right) + V_f \tag{6.31}$$

where $V_o, V_{ij}, V_{a_{ij}}, V_{ip}, V_f$ are non-negative Lyapunov candidate functions related to the object, the j-th rigid link, the j-th joint , the mobile platform of the i-th mobile manipulator and the internal force respectively. These Lyapunov candidate functions are chosen as follows:

$$\begin{cases} V_o = \frac{1}{2} e_1^{oT} e_1^o + \frac{1}{2} e_2^{oT} M_o e_2^o + \frac{1}{2} \sum\limits_{k=1}^{13} \frac{\left(\theta_{ok} - \hat{\theta}_{ok}\right)^2}{\rho_{ok}} \\ V_{ij} = \sum\limits_{j=1}^{N} \left(\begin{array}{l} \frac{1}{2} e_1^{B_{ij}T} e_1^{B_{ij}} + \frac{1}{2} e_2^{B_{ij}T} M_{B_{ij}} e_2^{B_{ij}} \\ \\ + \frac{1}{2} \sum\limits_{k=1}^{13} \frac{\left(\theta_{B_{ijk}} - \hat{\theta}_{B_{ijk}}\right)^2}{\rho_{B_{ijk}}} \end{array} \right) \\ V_{a_{ij}} = \sum\limits_{j=1}^{N} \left(\begin{array}{l} \frac{1}{2} J_{m_{ij}} \left(\dot{q}_{ij}^d - \dot{q}_{ij} \right)^2 \\ \\ + \frac{1}{2} \sum\limits_{k=1}^{13} \frac{\left(\theta_{a_{ij}} - \hat{\theta}_{a_{ij}}\right)^2}{\rho_{a_{ij}}} \end{array} \right) \\ V_{ip} = \frac{1}{2} e_1^{iv} e_1^{iv} + \frac{1}{2} e_2^{iv} M_{iv} e_2^{iv} + \frac{1}{2} \sum\limits_{k=1}^{13} \frac{\left(\theta_{ivk} - \hat{\theta}_{ivk}\right)^2}{2} \\ V_f = \frac{1}{2} \left(\tilde{F}_{int}^d - \tilde{F}_{int} \right)^T K_f \lambda_f^{-1} \left(\tilde{F}_{int}^d - \tilde{F}_{int} \right) \end{cases} \tag{6.32}$$

where $\theta_{ok}, \hat{\theta}_{ok}, \theta_{B_{ijk}}, \hat{\theta}_{B_{ijk}}, \theta_{a_{ijk}}, \hat{\theta}_{a_{ijk}}, \theta_{ivk}$ and $\hat{\theta}_{ivk}$ are the k-th elements of the corresponding vector parameters. By knowing that, $e_2^{oT} sign(e_2^o) = \|e_2^o\|$, $e_2^{ivT} sign(e_2^{iv}) = \|e_2^{iv}\|$ and $e_2^{B_{ij}T} sign(e_2^{B_{ij}}) = \|e_2^{B_{ij}}\|$, using the definition of the virtual power and the choice of the parameter function adaptation as in (6.21) and (6.26); it is straightforward to prove that $\dot{V}$ is always decreasing and is given as follows:

$$\dot{V} = -(e_1^{oT} K_1^o e_1^o + e_2^{oT} K_2^o e_2^o + K_3^o \|e_2^o\|) - \sum_{j=1}^{N} \left[\begin{array}{c} \sum_{i=1}^{n} \left[\begin{array}{c} e_1^{B_{ij}T} K_1^{B_{ij}} e_1^{B_{ij}} + e_2^{B_{ij}T} K_2^{B_{ij}} e_2^{B_{ij}} + K_3^{B_{ij}} \|e_2^{B_{ij}} \| \\ + K_{a_{ij}} \left(\dot{q}_{ij}^d - \dot{q}_{ij} \right)^2 \end{array} \right] \\ \\ + (e_1^{ivT} K_1^{iv} e_1^{iv} + e_2^{ivT} K_2^{iv} e_2^{iv} + K_3^{iv} \|e_2^{iv}) \end{array} \right]$$

$$- \left(\tilde{F}_{int}^d - \tilde{F}_{int} \right)^T K_f \left(\tilde{F}_{int}^d - \tilde{F}_{int} \right) \tag{6.33}$$

The stability analysis shows that $\dot{V}$ is always decreasing and the system is asymptotically stable in the sense of Lyapunov.Using Barbalat's lemma (Spong *et al.* (2006)) we prove that the error tracking states are asymptotically stable. The reader can found the detailed proof stability in (Zhu *et al.* (1997); Al-Shuka *et al.* (2014); Zhu (2010)).

6.4 Experimental Results

The developed control scheme is tested experimentally in real time on two identical mobile manipulator robots named Mob-ETS localised in GREPCI laboratory. Figure 6.5 shows the complete structure design of the control. In this experimental test, a Zigbee technology communication is used between the mobile manipulator robots and the application program implemented in Simulink Matlab®. The adaptive backstepping control studied in the previous sections is implemented and compared with an existing control based on the computed torque approach in real time using Real-Time Workshop (RTW) of Mathworks®. Since the external end-effector force is unavailable for measurement, an end-effector observer proposed in (Alcocera *et al.* (2004)) is used to estimate it. The two wheels of the *j*-th mobile manipulator robot platform are actuated by two HN-GH12-2217Y DC motors (DC-12V-200RPM 30:1), and the angular positions are given using encoder sensors (E4P-100-079-D-H-T-B). All joints of the manipulator arm are actuated by Dynamixel motors (MX-64T). The control strategy was tested on 5-DOF mobile manipulator robot to track a desired trajectory in Cartesian space presented in Figure 6.6. The desired trajectory of the center of gravity of the object is generated in the Cartesian space. Two experimental tests of desired trajectories are used in this

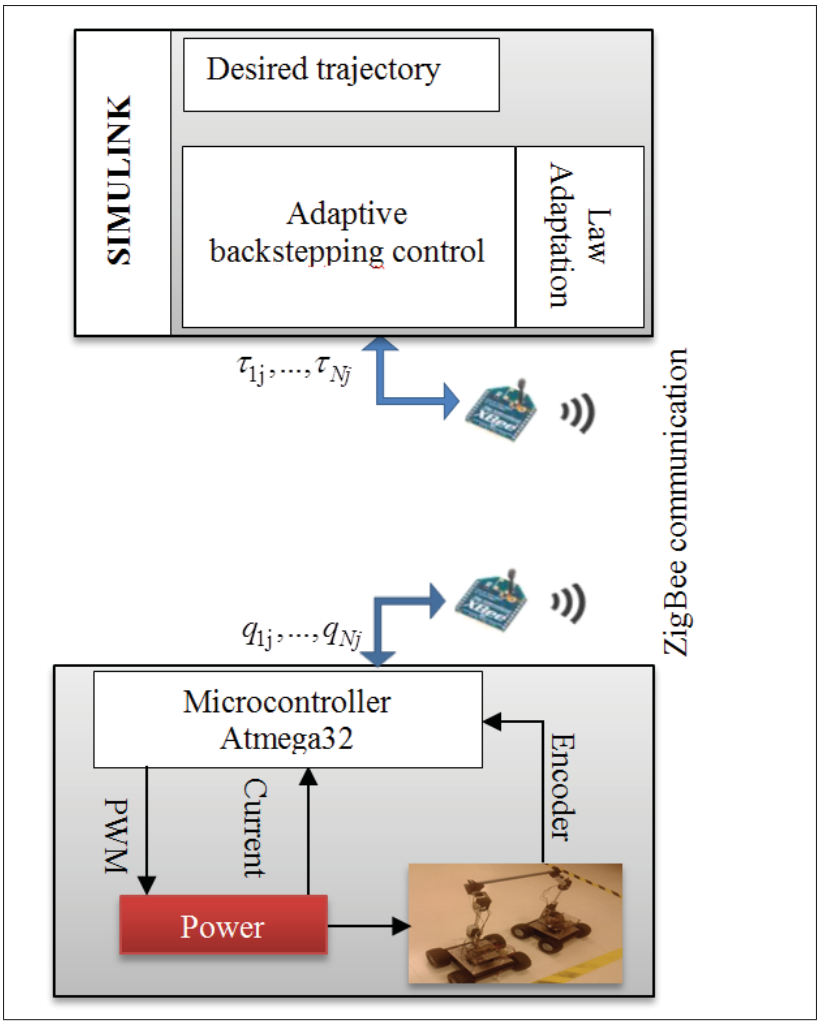

Figure 6.5 Real-time setup

implementation. In the first one, the object displacement is along the X-Y and the Z-axes with no rotation along these axes. The starting point is $P_e = (x_o, y_o, z_o, \beta_o) = (0.1, -0.1, 0.42, 0)$ the final point is $P_e = (x_o, y_o, z_o, \beta_o) = (3, 5, 0.47, 0)$, without end-effector orientation along X, Y or Z-axis. In the second one, the object displacement is along the X-axis, with a sinusoidal trajectory along the Y-axis, with the same starting and arrival points as in the first example. The trajectory tracking in the Cartesian space is presented in Figure 6.6 and Figure 6.7(a-b-c). It can be seen a good position tracking from Figure 6.7(a-b-c). This good tracking is confirmed by the related errors between the desired values and the real ones shown in Figure 6.7(d-e-f).

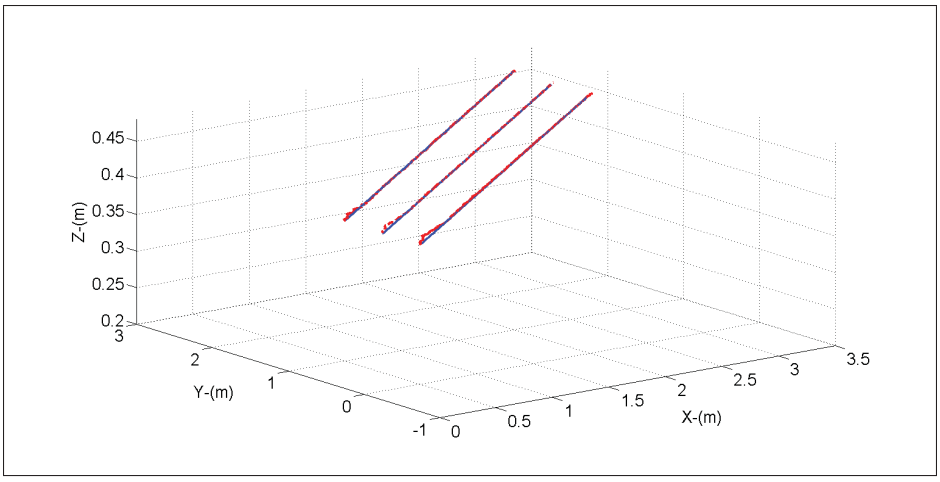

Figure 6.6 Desired and real trajectory of the object

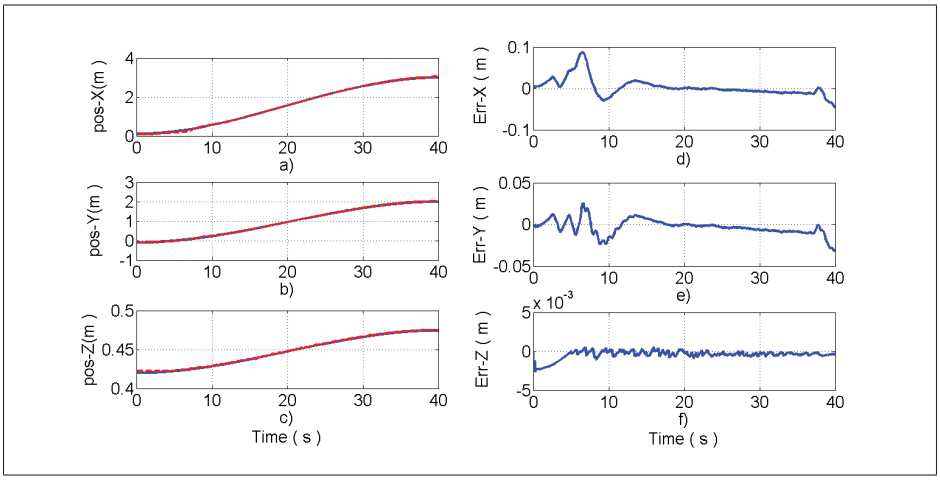

Figure 6.7 Tracking trajectory of x-position, (b) Tracking trajectory of y-position (c) Tracking trajectory of z-position, (d) Tracking error of x-position, (e) Tracking error of y-position (f) Tracking error of z- position

In the scenario 2, more complicate trajectory is used to show the effectiveness of the proposed adaptive control where object displacement is along the X-axis, with a sinusoidal trajectory along the Y-axis, with the same starting and arrival points as in the first example.

The trajectory tracking in the Cartesian space is showed in Figure 6.8 and Figure 6.9(a-b-c). It can be seen clearly a excellent position tracking from Figure 6.9(a-b-c). This good tracking is

proved and confirmed by the related errors between the desired values and the real ones shown in Figure 6.9(d-e-f).

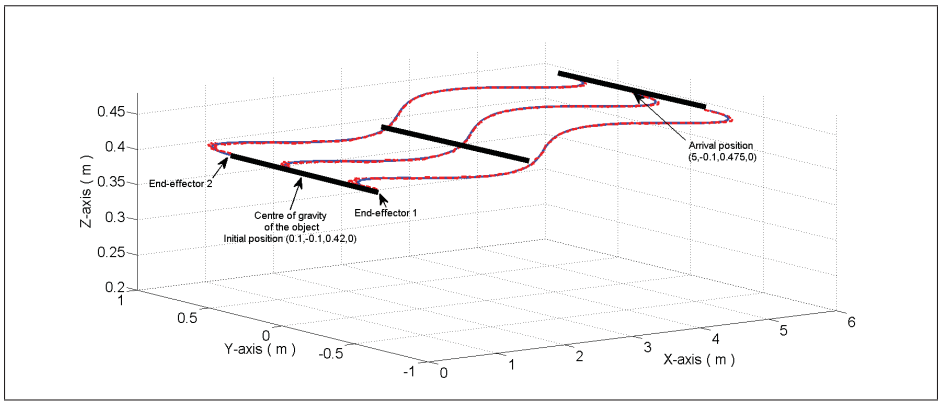

Figure 6.8 Desired and real trajectory of the object

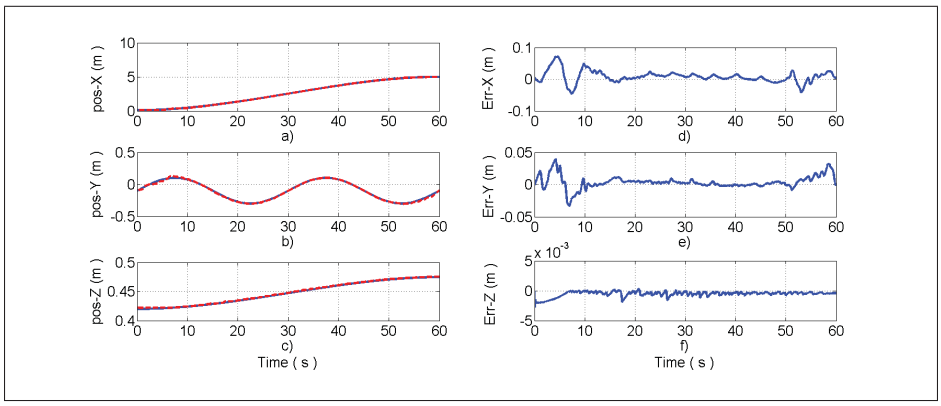

Figure 6.9 Tracking trajectory of x-position, (b) Tracking trajectory of y-position (c) Tracking trajectory of z-position, (d) Tracking error of x-position, (e) Tracking error of y-position (f) Tracking error of z- position

To show the performance of the developed adaptive backstepping control strategy, the computed torque (Slotine *et al.* (1991); Papadopoulos and Poulakakis (2000)) is implemented also for the same mobile manipulators. Figures 6.10-6.12 shows the obtained experimental results for the computed torque approach using the same second desired trajectory.

For comparison purposes, the robotic system is controlled by applying the computed torque method using the same second desired trajectory. The tracking of the position and orientation in the workspace is shown in Figure 6.10 and errors along the XYZ positions and the moment along the Z-axis are presented in Figure 6.11. Analysing the obtained experimental results showed in Figure 6.12, we can confirm that the resulting tracking errors of the proposed control strategy in this paper (dashed line) are smaller than those found using the computed torque method (solid line). This illustrates the performance and effectiveness of the adaptive backstepping control developed in this work.

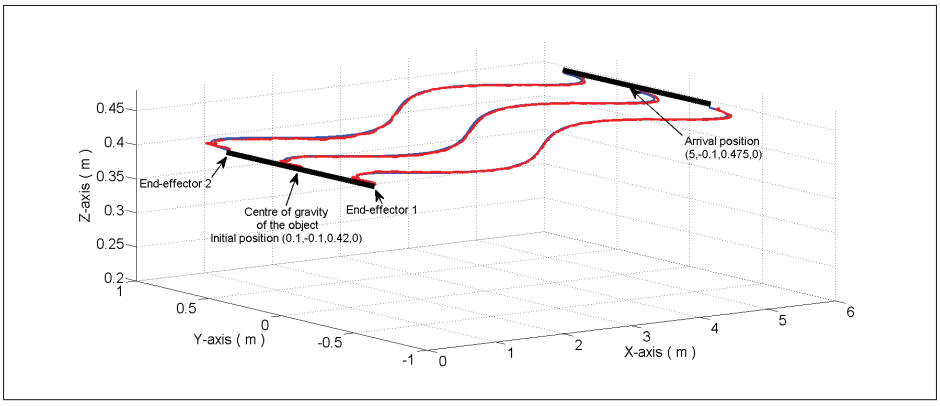

Figure 6.10 Desired and real trajectory of the object

6.5 Conclusion

In this paper, a novel adaptive coordinated backstepping control based on the virtual decomposition strategy was presented to control N mobile manipulator robots handling a rigid object in coordination to track desired trajectories generated in Cartesian space. The global stability of the complete system is proven based on the appropriate choice of Lyapunov functions using the virtual stability of each subsystem. The experimental results show the effectiveness of this proposed approach of control, where the tracking error of the desired trajectory in workspace converges to zero.

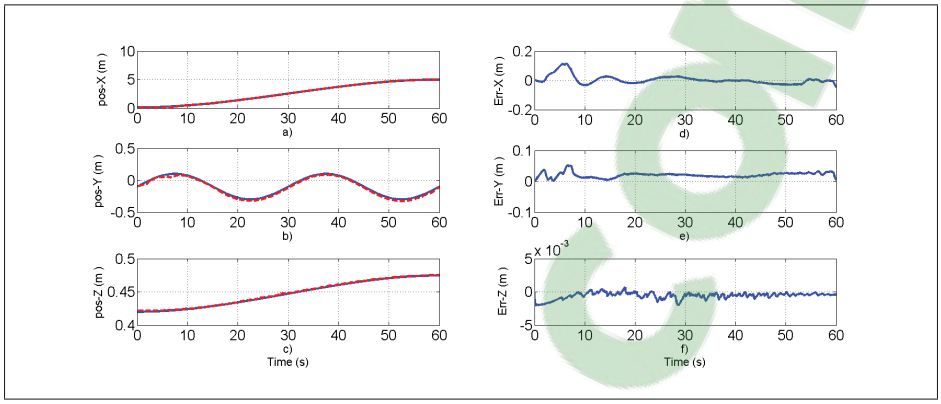

Figure 6.11 (a) Tracking trajectory of x-position, (b) Tracking trajectory of y-position (c) Tracking trajectory of z-position, (d) Tracking error of x-position, (e) Tracking error of y-position (f) Tracking error of z- position

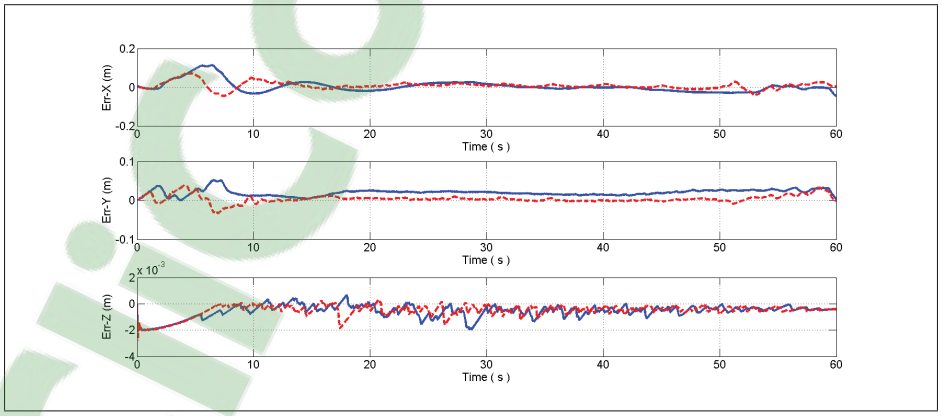

Figure 6.12 Errors: adaptive Backstepping control (dashed red line), computed torque (solid blue line)

CHAPTER 7

ADAPTIVE COORDINATED CONTROL OF MULTIPLE MOBILE MANIPULATORS BASED ON SLIDING MODE APPROACH

Abdelkrim Brahmi[1], Maarouf Saad[1], Guy Gauthier[2], Wen-Hong Zhu[3]
and Jawhar Ghommam[4]

[1] Département of Electrical Engineering, École de Technologie Supérieure,
[2] Département of automated manufacturing Engineering, École de Technologie Supérieure,
1100 Notre-Dame Ouest, Montréal, Québec, Canada H3C 1K3
[3] Space Exploration,Canadian Space Agency,
6767 Route de l'Aéroport, Longueuil (St-Hubert), Québec, Canada J3Y 8Y9
[4] Research Unit on Mechatronics and Automation Systems,
Ecole National d'Ingénieurs de Sfax, BPW,3038 Sfax, Tunisia,

Submitted to IEEE Transaction on Systems, Man, and Cybernetics: Systems, November ,2017

Abstract

This paper proposes an adaptive control for several mobile manipulator robots transporting a rigid object cooperatively under unknown parameters and disturbances. First, a global dynamic is developed for multiple mobile manipulators in coordination. It contains the dynamics of mobile manipulators, the dynamics of the object, and the geometric constraint between the end effector and the object. Next, we design an adaptive coordinated control based on a sliding mode approach in which the parameter uncertainties and the disturbance are estimated by an adaptive coordinated control technique. The proposed control ensures good tracking errors under which the errors converge to zero and the tracking error of the internal force stays bounded. Throughout this paper, the designed control law and a global stability analysis are carried out based on the appropriate choice of the candidate Lyapunov function. A numerical simulation and experimental validation are performed for two mobile manipulators transporting a rigid object to show the effectiveness of the developed control law.

Keywords: adaptive control; Multiple manipulator mobile robots; Coordinated control; Sliding mode approach.

7.1 Introduction

In recent years, mobile manipulators have attracted many researchers because of their combined manipulation and locomotion ability (Yamamoto and Yun (1996),Tanner *et al.* (2003), Furuno *et al.* (2003) and Andaluz *et al.* (2012)). In this paper, we consider a robotic manipulator attached to a nonholonomic mobile platform, which is used in large numbers of applications in modern factories. However, the difficulty with this category of robotic systems resides in the fact that the interaction motion between the manipulator, the mobile platform and the nonholonomic constraints must be considered in the control design. Some tasks, such as transporting heavy objects, are unachievable by only one mobile manipulator, and require cooperation among multiple mobile manipulators. This makes the design control of the robotic system more complex. The control of the mechanical system forming a closed kinematic chain mechanism is challenging to the extent that it imposes a set of kinematic constraints in coordinating the position and the velocity of the mobile manipulator. Multiple mobile manipulator systems transporting an object represent an excellent example of this category of complex robotic systems . As results of the constraints imposed on the system forming closed chain, is that the motion degrees of freedom is often less than the number of actuators. In this case, both the motion and the internal forces must be controlled. A limited number of research works have been proposed to solve the problem of controlling this class of robotic systems that have a high degree of freedom and are tightly interconnected. Many research works can be found in the literature to achieve the control of multiple mobile manipulators executing a tasks in coordination or cooperation under the hypothesis of known dynamics. As examples, in (Kosuge and Oosumi (1996),Hirata *et al.* (1999),Y. *et al.* (1999) and Papadopoulos and Poulakakis (2000)) several mobile manipulators carry a heavy and rigid object in cooperation in order to reduce the weight carried by each manipulator. In (Khatib *et al.* (1996a), Khatib *et al.* (1996b) and Park and Khatib (2008)), the authors propose an extension of four methods initially developed for manipulators attached on a fixed platform, and apply it to the control of mobile manipulator systems with a novel decentralized cooperative control . To date, most published research in this area has focused on three principal approaches of coordination: de-

centralized control (Kosuge and Oosumi (1996),Y. *et al.* (1999),Yohei *et al.* (2007),Zhijun *et al.* (2014) and Yan *et al.* (2014)), the follower-leader approach (Chen and Li (2006),Hirata *et al.* (2004c),Tang *et al.* (2009) and Fujii *et al.* (2007)) and the motion planing (Desai and Kumar (1997), Yamamoto and Fukuda (2002),Sun and Gong (2004a), LaValle (2006) and Latombe (2012)). However, these works rarely consider the parametric uncertainties of the robotics systems considered. In practice, the dynamic model of the resulting systems is generally uncertain. To solve the problem of modelling and dynamic control in the presence of uncertainties, some researchers have proposed intelligent adaptive approaches that are based on the neural network scheme (Liu *et al.* (2014), Liu and Zhang (2013) and Liu *et al.* (2013)), and fuzzy logic approach (Mai and Wang (2014), Zhijun *et al.* (2013) and Zhijun and Weidong (2008)). Motivated by the above observations, we develop an adaptive control to cope with coordinated multiple mobile manipulators in this paper. Based on what was accomplished in our previous work focused on the coordinate robot manipulators (Brahmi *et al.* (2016a)), we propose an novel adaptive control based on the sliding mode approach applied for multiple mobile manipulator robots handling rigid object cooperatively in the presence of parameters uncertainties. A global dynamics of an interconnected system including the dynamics of mobile manipulators, the dynamics of the object and the geometric constraint between the end effector and the handled object is developed for multiple mobile manipulator executing a task in coordination. Thereafter, we design a coordinated adaptive control in which the parameters uncertainties and the perturbations are estimated by the adaptive control techniques. The proposed control have two more important advantages: firstly, this controller ensures good tracking errors of the system under which these errors converge to zero and the tracking error of the internal force remains bounded under parameters uncertainties and disturbance. Secondly, the modified reaching law limits significantly the chartering. All through this paper, the designed control law and the global stability analysis are carried out based on the appropriate choice of the candidate Lyapunov function. The main contributions of this paper are summarized as follows:

a. An adaptive coordinated control based on the sliding mode approach is simulated and then applied in real time to group of mobile manipulator robots transporting a rigid ob-

ject. This controller ensures a good tracking of the desired trajectory/internal force under uncertainty of parameters and disturbance;

b. Contrary to the conventional sliding mode approach, in this paper, a novel reaching law based on the potential function is introduced to minimize the chatter;

c. The control design and the stability analysis are carried out based on the appropriate choice of the Lyapunov candidate function.

The rest of the paper is organized as follows. The systems modelling and description are explained in section 7.2. The main results of the adaptive control are described in section 7.3 and numerical simulation is presented in section 7.4. Experimental validation is given in section 7.5 and, finally, conclusion is given in section 7.6.

7.2 Modelling and System Description

Figure 7.1 shows the N manipulator robots mounted on nonholonomic mobile platforms. This section will briefly describe the kinematics and the dynamics models of the i-th MMR, the dynamic model for the handling object and then provides the dynamics of the entire system. We see that the different coordinate frames have been given for system modelling. With P_{ei} being the position/orientation vector of the i-th MMR effector, $X_oY_oZ_o$ is the handled object frame and XYZ is the inertial reference frame.

7.2.1 The Multiple Mobile Manipulator Dynamics

The dynamics of the i-th mobile manipulator in the articulated space is given by the following expression:

$$M_i(q_i)\ddot{q}_i + C_i(q_i,\dot{q}_i)\dot{q}_i + G_i(q_i) + p_i = E_i\tau_i + J_i^T f_i \tag{7.1}$$

where $M_i(q) \in \mathbb{R}^{n\times n}$ is the inertia matrix, $C_i(q_i,\dot{q}_i) \in \mathbb{R}^{n\times n}$ represent the Centrifugal and Coriolis terms, $G_i(q_i) \in \mathbb{R}^n$ is the vector of gravity, $q_i = \begin{bmatrix} q_{iv} & q_{ia} \end{bmatrix}^T \in \mathbb{R}^n$ with $q_{iv} \in \mathbb{R}^{n_v}$ and $q_{ia} \in \mathbb{R}^{n_a}$ are the coordinate generalized vector of the platform and the manipulator arm respectively, p_i

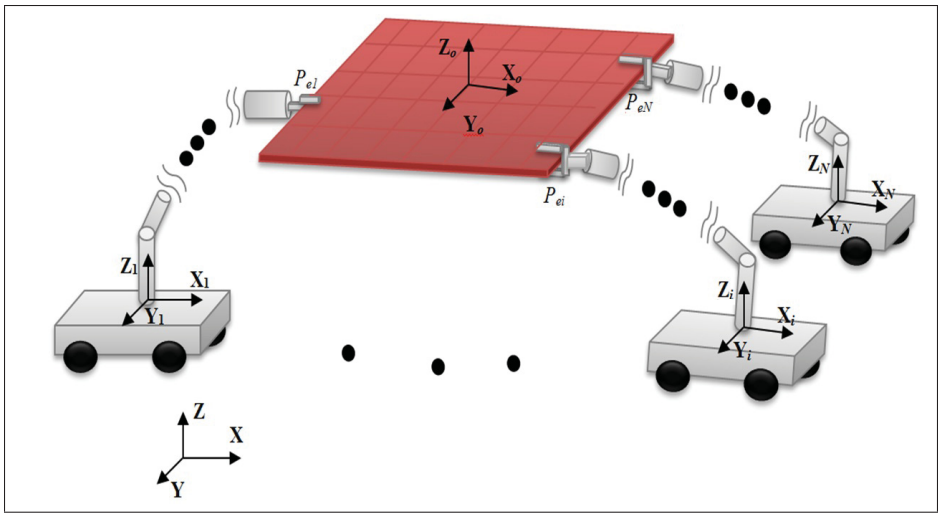

Figure 7.1 Multiple MMR handling a rigid object

is the external disturbance, $\tau_i \in \mathbb{R}^k$ the input torques and $E_i \in \mathbb{R}^{n\times k}$ is input transformation matrix. f_i is the vector of constraints forces corresponding to the holonomic and nonholonomic constraints and $J_i^T \in \mathbb{R}^{n\times n}$ is the Jacobian matrix and are represented as:

$$M_i = \begin{bmatrix} M_{iv} & M_{iva} \\ M_{iav} & M_{ia} \end{bmatrix}, C_i = \begin{bmatrix} C_{iv} & C_{iva} \\ C_{iav} & C_{ia} \end{bmatrix}, G_i = \begin{bmatrix} G_{iv} \\ G_{ia} \end{bmatrix}, p_i = \begin{bmatrix} p_{iv} \\ p_{ia} \end{bmatrix}, J_{ie} = \begin{bmatrix} A_i & 0 \\ J_{iv} & J_{ia} \end{bmatrix},$$

$$E_i = \begin{bmatrix} E_{iv} & 0 \\ 0 & E_{ia} \end{bmatrix}, f_i = \begin{bmatrix} f_{iv} \\ f_{ie} \end{bmatrix} \text{ and } \tau_i = \begin{bmatrix} \tau_{iv} \\ \tau_{ia} \end{bmatrix}.$$

As previously mentioned, the platform is subjected to non-holonomic constraints, in which the m independent velocity constraints are given as follows:

$$A_i(q_{iv})\dot{q}_{iv} = 0 \tag{7.2}$$

where $A_i(q_v)$ is the constraint matrix of the mobile platform. If we use a full rank matrix $R_i(q_{iv}) \in \mathbb{R}^{n_v\times(n-m)}$ as the basis for the null space of $A_i(q_{iv})$, we will obtain:

$$R_i^T(q_{iv})A_i^T(q_{iv}) = 0 \tag{7.3}$$

There exists an auxiliary input vector $\vartheta_{iv} \in \mathbb{R}^{n_v-m}$ that satisfies:

$$\dot{q}_{iv} = R_i(q_{iv})\dot{\vartheta}_{iv} \tag{7.4}$$

where m is the number of the non integrable and independent velocity constraints on the mobile platform. Let us define the vector $\eta_i = \begin{bmatrix} \vartheta_{iv} & q_{ia} \end{bmatrix}^T \in \mathbb{R}^{n-m}$, based on (7.4). The dynamics expression of the i-th mobile manipulator (7.1) can be given as follows:

$$M_i^1(\eta_i)\ddot{\eta}_i + C_i^1(\eta_i,\dot{\eta}_i)\dot{\eta}_i + G_i^1(\eta_i) + p_i^1 = E_i^1\tau_i + J_{ie}^T f_{ie} \tag{7.5}$$

where, $M_i^1 = \begin{bmatrix} R_i^T M_{iv} R_i & R_i^T M_{iva} \\ M_{iav} R_i & M_{ia} \end{bmatrix}$, $G_i^1 = \begin{bmatrix} R_i^T G_{iv} \\ G_{ia} \end{bmatrix}$, $C_i^1 = \begin{bmatrix} R_i^T M_{iv}\dot{R}_i + R_i^T C_{iv} R_i & R_i^T C_{iva} \\ M_{iav}\dot{R}_i + C_{iav} R_i & C_{ia} \end{bmatrix}$,
$J_{ie} = \begin{bmatrix} 0 & 0 \\ J_{iv} R_i & J_{ia} \end{bmatrix}$, $p_i^1 = \begin{bmatrix} R_i^T p_{iv} \\ p_{ia} \end{bmatrix}$, and $E_i^1 = \begin{bmatrix} R_i^T E_{iv} & 0 \\ 0 & E_{ia} \end{bmatrix}$.

The dynamics of the N mobile manipulator robots from (7.5) can be written as:

$$M\ddot{\eta} + C\dot{\eta} + G + P = E\tau + J_e^T F_e \tag{7.6}$$

where $M = diag(M_1^1,..,M_N^1) \in \mathbb{R}^{N(n-m)\times N(n-m)}$, $C = diag(C_1^1,..,C_N^1) \in \mathbb{R}^{N(n-m)\times N(n-m)}$, $G = [G_1^{1T},..,G_N^{1T}]^T \in \mathbb{R}^{N(n-m)}$, $F_e = [f_{1e}^T,..,f_{Ne}^T]^T$, $J_e^T = diag(J_{1e}^T,..,J_{Ne}^T) \in \mathbb{R}^{N(n-m)\times N(n-m)}$, $P = [p_1^{1T},..,p_N^{1T}]^T \in \mathbb{R}^{N(n-m)}$, $\eta = [\eta_1^{1T},..,\eta_N^{1T}]^T \in \mathbb{R}^{N(n-m)}$, and $E\tau = [(E_1\tau_1)^T,..,(E_N\tau_N)^T]^T \in \mathbb{R}^{N(n-m)}$.

7.2.2 Dynamics of Object

The object is rigidly handled by the N mobile manipulator robots. The coordinate center of gravity of object is denoted $x_o \in \mathbb{R}^{n_o}$ and its linear/angular velocity is denoted $V_o \in \mathbb{R}^{n_o}$. The dynamic expression is given by:

$$M_o(x_o)\dot{V}_o + C_o(x_o,V_o)V_o + G_o(x_o) = F_o \tag{7.7}$$

where $M_o \in \mathbb{R}^{n_o \times n_o}$ is the inertia matrix, $C_o \in \mathbb{R}^{n_o \times n_o}$ represent the Centrifugal and Coriolis terms, $G_o \in \mathbb{R}^{n_o}$ is the vector of gravity and $F_o \in \mathbb{R}^{n_o}$ is the vector of force applied to the object.

Remark 7.1: As in (Li *et al.* (2008)), in this paper, the degrees of freedom for each mobile manipulator robot are equal to the dimension of the task space coordinate of the object, that is, $n_o = n - m$, or that the mobile manipulator robot is non-redundant. The relationship between the end effector forces $F_e \in \mathbb{R}^{N(n-m)}$ and the object force $F_o \in \mathbb{R}^{n_o}$ is given by:

$$F_o = -J_o(x_o)^T F_e \tag{7.8}$$

The end effector force is decomposed into two orthogonal components: the first gives the internal force while the second contributes to the movement of the object. This representation is explained in (Li and Ge (2013)), and has the following form:

$$F_e = -J_o(x_o)^{T+} F_o - F_I \tag{7.9}$$

where $J_o(x_o)^{T+}$ is the pseudo-inverse of $J_o(x_o)^T \in \mathbb{R}^{n_o \times N(n-m)}$ given by $J_o(J_o^T J_o)^{-1}$ and $F_I = [F_{1I}^T, .., F_{NI}^T]^T \in \mathbb{R}^{N(n-m)}$ are the internal forces in the null space of J_o^T. These internal forces can be parametrized by the Lagrangian multiplier vector λ_I as follows:

$$F_I = \rho^T \lambda_I \tag{7.10}$$

where $\rho \in \mathbb{R}^{n_o \times N(n-m)}$ is the Jacobian matrix for the internal force, and satisfies the following property:

$$J_o^T \rho^T = 0 \tag{7.11}$$

multiplying both side of (7.9) by J_e^T we obtain:

$$J_e^T F_e = -\Im^T F_o - J_e^T F_I \tag{7.12}$$

where $\Im^T = J_e^T J_o(x_o)^{T+}$.

7.2.3 Total Dynamics

Let $V_{ie} \in \mathbb{R}^{(n-m)}$ denotes the linear/angular velocity of the i-th end effector. Then $\dot{\eta}_i \in \mathbb{R}^{(n-m)}$ is related to V_{ie} by the Jacobian matrix $J_{ie} \in \mathbb{R}^{(n-m)\times(n-m)}$ as:

$$V_{ie} = J_{ie}(\eta_{ie})\dot{\eta}_{ie} \tag{7.13}$$

and the relationship between V_o and V_{ie} is given by:

$$V_{ie} = J_{io}(x_o)V_o \tag{7.14}$$

From (7.13), the joint velocity of the N mobile manipulators is related to the linear/angular velocity of the end-effectors V_e by the following expression:

$$V_e = J_e(\eta)\dot{\eta} \tag{7.15}$$

The relationship between the end effector velocity of the N mobile manipulator robots (7.15) and the object based on (7.14) is given by:

$$V_e = J_o(x_o)V_o \tag{7.16}$$

where $J_e = blockdiag(J_{ie}) \in \mathbb{R}^{N(n-m)\times N(n-m)}$ and $J_o = [J_{1o}^T, .., J_{No}^T]^T \in \mathbb{R}^{N(n-m)\times n_o}$.

Assuming that all the robots acting on the object at the same time, yields:

$$V_o = J_o^+(x_o)V_e \tag{7.17}$$

Differentiating (7.17) with respect to time we obtain:

$$\dot{V}_o = J_o^+(x_o)\dot{V}_e + \frac{d(J_o^+(x_o))}{dt}Ve \tag{7.18}$$

Using (7.15) and (7.16), the dynamic model of the N mobile manipulator robots (7.6) coupled with the grasped object dynamics (7.7), based on (7.12), is given by:

$$M_e\dot{V}_e + C_eV_e + G_e + P = U - J_o^{T+}F_o - F_I \tag{7.19}$$

where $M_e = J_e^{+T}MJ_e^+$, $C_e = J_e^{+T}(M\dot{J}_e^+ + CJ_e^+)$, $G_e = J_e^{+T}G$ and $U = J_e^{+T}E\tau$.
Substituting the object dynamics (7.7) into (7.18) and using (7.10) and (7.17), the dynamics of the robotic systems (7.19) can be written as:

$$\mathbb{M}\dot{V}_e + \mathbb{C}V_e + \mathbb{G} + P = U - \rho^T\lambda_I \tag{7.20}$$

where $\mathbb{M} = M_e + J_o^{+T}M_oJ_o^+$, $\mathbb{G} = G_e + J_o^{+T}G_o$ and $\mathbb{C} = C_e + J_o^{+T}(M_o\dot{J}_o^+ + C_oJ_o^+)$.
The dynamic (7.20) has the following properties, that can be used in the control design and in the stability analysis.

Property 7.1: The matrix $\mathbb{M}$ is symmetric, positive definite and is bounded, i.e $\lambda_{min}I \leq \mathbb{M} \leq \lambda_{max}I$, with λ_{min}, λ_{max} denote the minimum and maximum eigenvalues of $\mathbb{M}$ and I is the identity matrix.

Property 7.2: The matrix $\dot{\mathbb{M}} - 2\mathbb{C}$ is skew-symmetric, that is, $x^T(\dot{\mathbb{M}} - 2\mathbb{C})x = 0$ for any vector $x \in \mathbb{R}^{(n-m)}$.

Property 7.3: All Jacobian matrices are uniformly continuous and uniformly bounded if X_e and x_o are uniformly continuous and uniformly bounded, respectively.

7.3 Control Design

Given an object desired trajectory x_{od} and a desired internal force F_{Id}, since the system is tightly coupled we can compute the corresponding desired end effector's position and velocity trajectories X_{ed}, V_{ed} from (7.16). Therefore, the control objective is to determine a control law

such that the following limits hold:

$$\lim_{t\to\infty}(\|x_o - x_{od}\|) = 0, \ \lim_{t\to\infty}(\|V_o - V_{od}\|) = 0$$

$$\lim_{t\to\infty}\|F_I - F_{Id}\| = bounded$$

where, $x_{od} \in \mathbb{R}^{n_o}$, $V_{od} \in \mathbb{R}^{n_o}$ are the desired position and velocity of the object generated in the workspace, $F_{Id} \in \mathbb{R}^{n_o}$ and $F_I \in \mathbb{R}^{n_o}$ are the desired and measured internal forces.

Assumption 7.1: The desired reference trajectory x_{od}, X_{ed} and their derivatives up to the third order are assumed to be bounded and uniformly continuous. The desired internal force is also bounded and uniformly continuous.

Let $e = X_e - X_{ed}$, $e_f = \lambda_I - \lambda_{Id}$, then the required internal force and velocity are given by

$$\lambda_{Ir} = \lambda_{Id} - K_\lambda e_f \tag{7.21}$$

$$V_{er} = V_{ed} - K_p e \tag{7.22}$$

$$s = V_e - V_{er} = \dot{e} + K_p e \tag{7.23}$$

with K_λ is a diagonal positive definite matrix, λ_{Id} is the internal force control, K_p is a positive definite gains matrix and V_{ed} is the desired velocity.

7.3.1 Coordinated Control

The control law can be given as:

$$U = A_m^T \psi_m - Ksign(s) - K_s s + J_e^T \rho^T \lambda_{Ir} \tag{7.24}$$

where $A_m = [\mathbb{M}\ \mathbb{C}\ \mathbb{G}\ P]^T$, $\psi_m = [\dot{V}_{er}\ V_{er}\ 1\ 1]^T$, K_s, K are positive gains matrices and $sign(s)$ is the signium function. Based on the terms given in the assumption 7.1, the dynamics expression

(7.20) can be given by the following:

$$\mathbb{M}\dot{s} = -A_m^T \psi_m + U - J_e^T \rho^T \lambda_I - \mathbb{C}s \tag{7.25}$$

Considering the Lyapunov candidate function as follows:

$$V = \frac{1}{2} s^T \mathbb{M} s \tag{7.26}$$

The first time derivative of V is given by:

$$\dot{V} = s^T \mathbb{M}\dot{s} + \frac{1}{2} s^T \dot{\mathbb{M}} s \tag{7.27}$$

$$\dot{V} = s^T (-A_m^T \psi_m + U - J_e^T \rho^T \lambda_I) \tag{7.28}$$

Considering the control law (7.24), using (7.17) under the properties 7.1, 7.2 and 7.3, the time derivative of (7.26) can be written as:

$$\begin{aligned} \dot{V} &= -s^T K_s s - K|s| \\ &\leq -\lambda_{min}(K_s) \|s\|^2 \leq 0 \end{aligned} \tag{7.29}$$

Based on assumption 7.1, V is a nonincreasing function, and therefore, s is also bounded. Taking the second derivative of V yields $\ddot{V} = -2s^T K_s \dot{s}$ since s and $\dot{s}$ are bounded, which implies that $\ddot{V}$ is bounded, and consequently, $\dot{V}$ is uniformly continuous. As the referenced trajectory is uniformly continuous, it implies that s and e are uniformly continuous likewise. Thereby, according to Barbalat's lemma $\lim_{t\to\infty} \dot{V} = 0$ and consequently $\lim_{t\to\infty} e = 0$.

Remark 7.2: This proposed control law of relation (7.24) requires a well-known of the dynamics of the robotic system and disturbances. In practice, the dynamics is uncertain and the disturbances are unknown, making the implementation of the above control law very complex and undesirable. Therefore, we propose an adaptive coordinated control scheme, as outlined in the next subsection.

7.3.2 Adaptive Coordinated Control

Assumption 7.2: There exist some finite positive constants, $a_i \geq 0, \quad 1 \leq i \leq 4$ and a finite positive constant $a_5 \geq 0$ such that $\forall X_e \in \mathbb{R}^n$, $\forall V_e \in \mathbb{R}^n$, $\|\mathbb{M}\| \leq a_1$, $\|\mathbb{C}\| \leq a_2 + a_3\|V_e\|$, $\|\mathbb{G}\| \leq a_4$ and $sup_{\geq 0}\|P\| \leq a_5$. Since $a_i \geq 0$ are considered unknown, the adaptive laws are then developed to estimate the unknown upper bounds. Let us consider the following control law:

$$U = -\sum_{i=1}^{5} \frac{s\hat{a}_i \psi_i^2}{\|s\|\psi_i + \delta_i} - K_s s - \frac{Ksign(s)}{H(s)} + \rho^T \lambda_{Ir} \tag{7.30}$$

where δ_i is a time-varying positive function, and converges to zeros as $t \to \infty$ and that satisfies: $\lim_{t\to\infty} \int_0^t \delta_i(r)dr = \alpha_i < \infty$, with α_i is a finite constant (Wang *et al.* (2004)) and $H(s)$ is given by the following expression:

$$H(s) = \beta + (1-\beta)h(|s|, 0, s_q) \tag{7.31}$$

where s_q is an upper limit positive constant, $0 < \beta < 1$ and $h(x,a,b)$ is referred to be a p-time differential bump function that satisfies the following properties (Do (2008),Do (2010)):

- $h(x,0,b) = 0, \quad \text{if } x \leq 0;$
- $h(x,0,b) = 1, \quad \text{if } x \geq b;$
- $0 < h(x,0,b) < 1, \quad \text{if } 0 < x < b;$
- $h(x,0,b)$ is p-time differentiable with respect to x;
- $\frac{\partial h(x,0,b)}{\partial x} > 0$ if $x \in (0,b)$.

Let $h(x,a,b)$ be defined as follows:

$$h(x,a,b) = \frac{\int_0^x g(\sigma)g(b-\sigma)d\sigma}{\int_0^b g(\sigma)g(b-\sigma)d\sigma}$$

where g is such that: $g(z) = 0$ if $z \leq 0$ and $g(z) = z^l$ if $z \geq 0$, and l is a positive constant integer.

Remark 7.3: The term $-\frac{Ksign(s)}{H(s)}$ is added to the proposed control law, unlike the controller proposed in (Wang *et al.* (2004)) and (Li *et al.* (2008)). Thus, a more robust control performance and fast convergence can be obtained when the system states are close to the surface $s = 0$.

From the definition of the potential function (7.31), one can see that if $|s|$ increases, $H(s)$ approaches β, and therefore, $\frac{K}{H(s)}$ converges to $\frac{K}{\beta}$, which is greater than K. This means that $\frac{K}{H(s)}$ increases in reaching phase, and consequently, the attraction of the sliding surface will be faster. On the other hand, if $|s|$ decreases, then $H(s)$ approaches one, and $\frac{K}{H(s)}$ converges to K. This means that, when the system approaches the sliding surface, $\frac{K}{H(s)}$ decreases progressively, which significantly minimizes the chattering. Consequently, the proposed law lets the controller to dynamically adjust to the changes in the switching function by making $\frac{K}{H(s)}$ vary between K and $\frac{K}{\beta}$.

Remark 7.4: If $h(|s|,0,s_q)$ is chosen to be equal to an exponential function, then the reaching law of (7.30) becomes identical to the ERL proposed in (Fallaha *et al.* (2011)). Therefore, the exponential reaching law becomes a particular case of the proposed approach.

Remark 7.5: In the case of $\beta = 1$, the reaching law of (7.30) becomes exactly the same control given in (7.24). Therefore, the conventional reaching law can be considered as a particular case of the proposed approach.

7.3.2.1 Stability analysis

The chosen Lyapunov candidate function can be given as:

$$V = \frac{1}{2}s^T\mathbb{M}s + \frac{1}{2}\tilde{A}_m^T\Gamma_a^{-1}\tilde{A}_m \tag{7.32}$$

where $\tilde{A}_m = A_m - \hat{A}_m$, $A_m = [a_1 \;\; a_2 \;\; a_3 \;\; a_4 \;\; a_5]^T$, $\hat{A}_m$ denotes the estimated constants of A_m, $\Gamma_a = diag(\gamma_1, .., \gamma_5)$ and $\gamma_i \geq 0$ are constants. The first time derivative of (7.32) is given by:

$$\dot{V} = s^T \mathbb{M}\dot{s} + \frac{1}{2} s^T \dot{\mathbb{M}} s + \tilde{A}_m^T \Gamma_a^{-1} \dot{\hat{A}}_m \tag{7.33}$$

Based on Assumption 7.2 , the dynamics model (7.20) and the closed loop (7.25), (7.33) can be simplified as follow:

$$\dot{V} \leq s^T (\|\mathbb{M}\|\|\dot{V}_e\| + \|\mathbb{C}\|\|V_e\| + \|\mathbb{G}\| + \|P\| + U - \rho^T \lambda_I) + \tilde{A}_m^T \Gamma_a^{-1} \dot{\hat{A}}_m \tag{7.34}$$

Using the control law (7.30) under Assumption 7.2, the first derivative (7.34) can be written as follows:

$$\begin{aligned} \dot{V} \leq & -s^T K_s s - K\|s\| + \sum_{i=1}^{5} \|s\| a_i \psi_i \\ & - \sum_{i=1}^{5} \frac{\|s\|^2 \hat{a}_i \psi_i^2}{\|s\| \psi_i + \delta_i} - \sum_{i=1}^{5} \tilde{a}_i \gamma_i^{-1} \dot{\hat{a}}_i \end{aligned} \tag{7.35}$$

Considering the update law as:

$$\dot{\hat{a}}_i = \gamma_i \left(\frac{\|s\|^2 \psi_i^2}{\|s\| \psi_i + \delta_i} - \gamma_i^{'} \hat{a}_i \right) \tag{7.36}$$

with $\gamma_i \geq 0$; $\gamma_i^{'} \geq 0$ and $\delta_i \geq 0$ verifying the following expressions:

$$\begin{cases} \int_0^\infty \gamma_i^{'}(r) dr = \alpha_{i\gamma'} < \infty \\ \\ \int_0^\infty \delta_i(r) dr = \alpha_{i\delta} < \infty \end{cases} \tag{7.37}$$

Substituting the update law (7.36) into (7.35) with some simplifications, we obtain:

$$\dot{V} \leq -s^T K_s s - K\|s\| + \sum_{i=1}^{5} \frac{\|s\| a_i \psi_i^2 \delta_i}{\|s\| \psi_i + \delta_i} - \sum_{i=1}^{5} \tilde{a}_i \gamma_i^{'} \hat{a}_i \tag{7.38}$$

$$\dot{V} \leq -s^T K_s s - K\|s\| + \sum_{i=1}^{5} a_i \delta_i - \sum_{i=1}^{5} \tilde{a}_i \gamma_i^{'} \hat{a}_i \tag{7.39}$$

$$\leq -s^T K_s s - K\|s\| - \sum_{i=1}^{5} \hat{a}_i \delta_i - \sum_{i=1}^{5} \tilde{a}_i \gamma_i^{'} (a_i - \tilde{a}_i)$$

$$\leq -s^T K_s s - K\|s\| + \sum_{i=1}^{5} a_i \delta_i - \sum_{i=1}^{5} \gamma_i^{'} \tilde{a}_i a_i + \sum_{i=1}^{5} \gamma_i^{'} \tilde{a}_i^2$$

$$\leq -s^T K_s s - K\|s\| + \sum_{i=1}^{5} a_i \delta_i - \sum_{i=1}^{5} \frac{1}{4} \gamma_i^{'} a_i^2$$

$$+ \sum_{i=1}^{5} \frac{1}{4} \gamma_i^{'} a_i^2 - \sum_{i=1}^{5} \gamma_i^{'} (\frac{1}{2} a_i - \tilde{a}_i)^2$$

$$\leq -s^T K_s s - K\|s\| + \sum_{i=1}^{5} a_i \delta_i + \sum_{i=1}^{5} \frac{1}{4} \gamma_i^{'} a_i^2$$

$$\leq -\lambda_{min}(K_s)\|s\|^2 + \sigma \tag{7.40}$$

Since $\sigma = \sum_{i=1}^{5} a_i \delta_i + \sum_{i=1}^{5} \frac{1}{4} \gamma_i^{'} a_i^2 \to 0$ as $t \to \infty$, from above, s converge to a small set containing the origin when $t \to \infty$.

Integrating both side of the inequality (7.38) we obtain:

$$V(t) - V(0) \leq \int_0^t (-s^T K_s s - K\|s\|) dr + \int_0^t (\sigma) dr \tag{7.41}$$

Since a_i is constant and by using (7.35), the above equation (7.41) can be rewritten as:

$$V(t) - V(0) \leq \int_0^t (-s^T K_s s - K\|s\|) dr$$

$$+ \sum_{i=1}^{5} a_i \int_0^t \delta_i dr + \sum_{i=1}^{5} \frac{1}{4} a_i^2 \int_0^t \gamma_i^{'} dr$$

$$V(t) - V(0) < -\int_0^t (s^T K_s s + K\|s\|) dr$$

$$+ \sum_{i=1}^{5} a_i \alpha_{i\delta} + \sum_{i=1}^{5} \frac{1}{4} a_i^2 \alpha_{i\gamma'} \tag{7.42}$$

Therefore V is bounded, consequently implies that $s \in L_\infty^m$. From (7.42) we obtain:

$$\int_0^t (s^T K_s s + K\|s\|)dr < V(0) - V(t) + A_m^T \alpha_\delta + A_m^T \alpha_{i\gamma'} A_m \tag{7.43}$$

Consequently $s \in L_2^{n-m}$. From (7.22) and (7.23), it can be proved that $e, \dot{e} \in L_\infty^{n-m}$. As $e, \dot{e} \in L_\infty$ was established, under Assumption 7.1, we can conclude that X_e, V_e, V_{er}, $\dot{V}_{er} \in L_\infty^{n-m}$ and $\dot{x}_o \in L_\infty^{n_o}$. Therefore, all terms on the right hand side of (7.25) are bounded, which implies that $\dot{s}$ and $\ddot{\eta}$ are also bounded. As results, we have $s \to 0$ as $t \to \infty$. Finally, it follows that $e_o, \dot{e}_o \to 0$ as $t \to \infty$.

To complete the proof of stability, substituting the control law (7.30) and (7.21) into the reduced order dynamic expression (7.20) yields:

$$\rho^T(\lambda_{Ir} - \lambda_I) = A_m \psi_m + \sum_{i=1}^{5} \frac{s\hat{a}_i \psi_i^2}{\|s\|\psi_i + \delta_i} + \frac{Ksign(s)}{H(s)} + K_s s$$

$$\rho^T e_f = (K_\lambda + I)^{-1} \mu \tag{7.44}$$

with $\mu = A_m \psi_m + \sum_{i=1}^{5} \frac{s\hat{a}_i \psi_i^2}{\|s\|\psi_i + \delta_i} + \frac{Ksign(s)}{H(s)} + K_s s$. All terms on the right hand side of (7.44) are bounded, therefore, the internal force tracking error are bounded, and can be adjusted by tuning the feedback gain K_λ

7.4 Simulation results

The numerical simulation is performed on two identical 4 DoF MMRs manipulating a rigid object in coordination. The block diagram in Fig 7.2 shows the different control law calculation and implementation steps. The parameters of the two robots and the object are summarized in Table 7.1.

The desired trajectory of the center of gravity of the object is given in the workspace where the trajectories of the two mobile manipulator robots are obtained by using the inverse kinematic of the robotic system (7.15). The desired trajectory for the object and the desired internal force

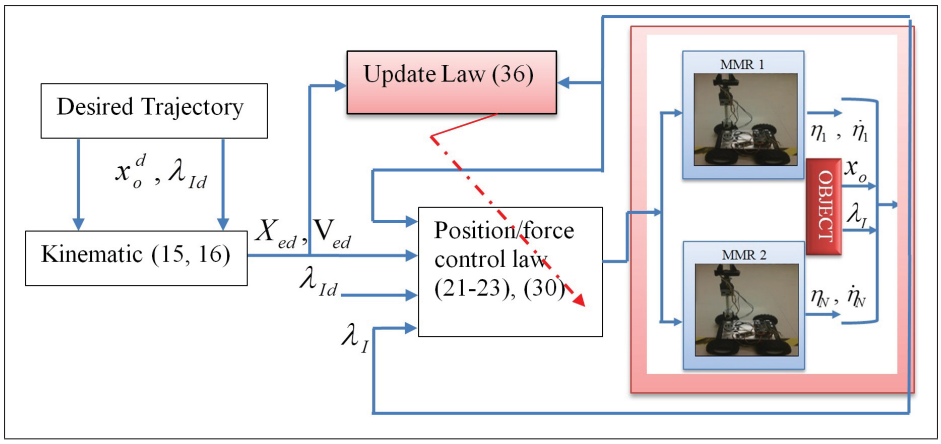

Figure 7.2 Adaptive control of N MMRs transporting a rigid object

Table 7.1 System parameters .

	Parameters
Object	$m_o = 1kg, I_o = 1kg.m^2$
Articulations:1,2,3,4 (rotoid)	$m_{1,2,3,4} = 1kg$, $I_{1,2,3,4} = 1kg.m^2$, $L_{1,2} = 1m$, $L_{3,4} = 0.5m$,
Platform	$m_v = 6kg$, $I = 19kg.m^2$ $d = 1m$, $r = 1m$

are chosen as:

$$\dot{x}_{od} = \begin{bmatrix} cos(sin(t)+\pi/2) \\ sin(sin(t)+\pi/2) \\ 0.0 \\ cos(t)+0.01cos(t) \end{bmatrix}, \lambda_{Id} = \begin{bmatrix} 5 \\ 0.0 \\ 0.0 \end{bmatrix}$$

The control gains of the controller are chosen as: $\gamma_i' = 0.8, K_p = 50, K_\lambda = 25, K_s = 50$, $\beta = 0.1$ and $K = 10$.

The workspace trajectory tracking is shown in Figure 7.3 and the simulation results in the Cartesian space is presented in Figure 7.4. From the two figures, we can observe a good tracking trajectory, and this result is confirmed by the result given in Figure 7.5 where the tracking error is acceptable. As can seen from the obtained results, the objective of the trajectory tracking of the handled object is successfully achieved.

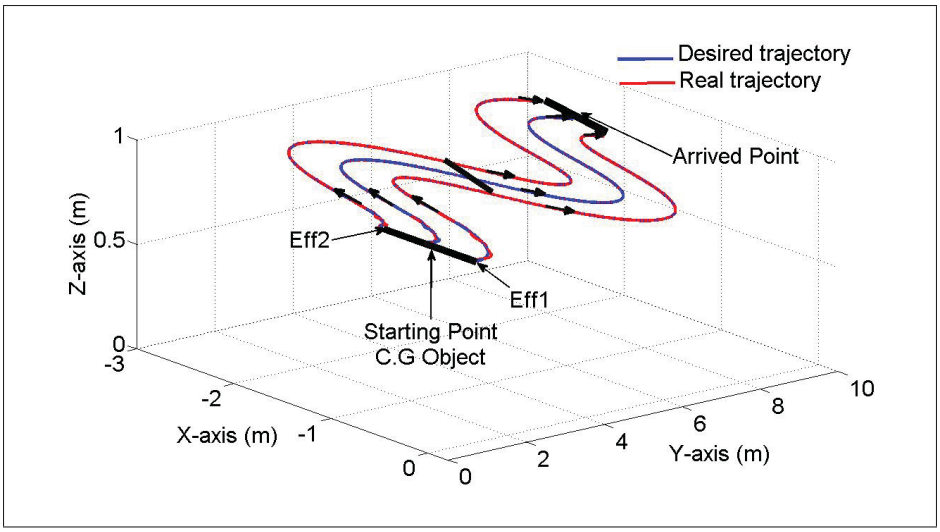

Figure 7.3 Desired and real trajectories of the object

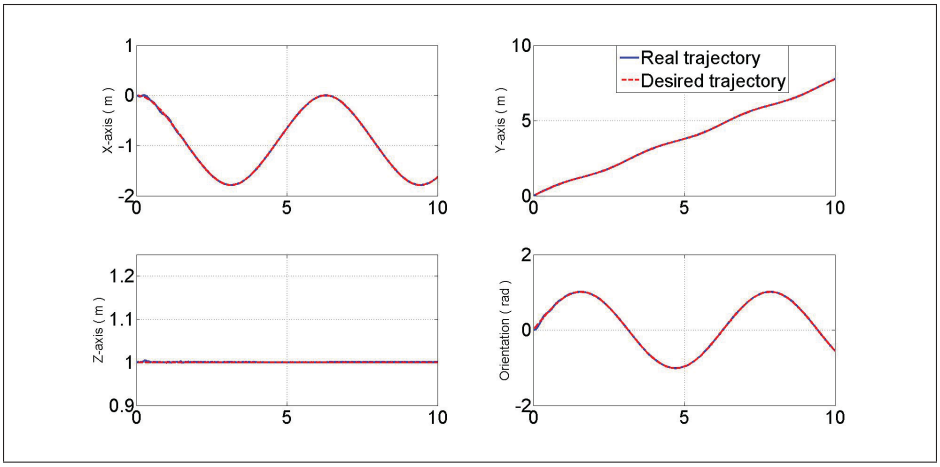

Figure 7.4 Trajectory tracking in Cartesian space:X-axis, Y- axis, Z-axis and orientation

To illustrate the advantages of our novel reaching proposed control law (7.30), we firstly compared this approach with a control law proposed in (Wang *et al.* (2004)), as well as with the conventional sliding mode. For comparison, the multi-mobile manipulators handling the object are controlled by applying the control law method proposed in (Wang *et al.* (2004)) using the same desired trajectory. The position tracking and orientation in the workspace are shown in Figure 7.6 and errors along the XYZ positions and the moment along the Z-axis are presented in Figure 7.7. According to the obtained results showed in Figure 7.7, the resulting tracking

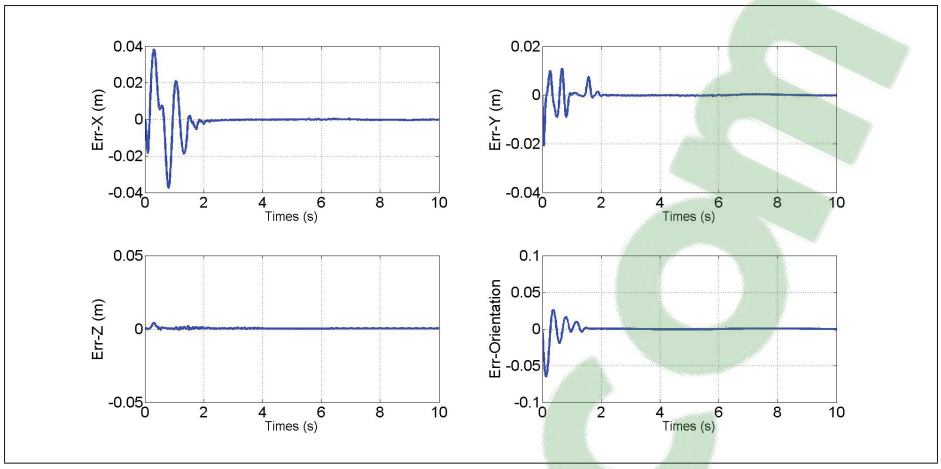

Figure 7.5 Error in X-axis, error in Y- axis, error in Z-axis and error in orientation

errors of the proposed control strategy (solid line) are smaller than those found using the control law method in (Wang *et al.* (2004)) (dashed line). This illustrates the effectiveness of the adaptive coordinated approach developed in this paper.

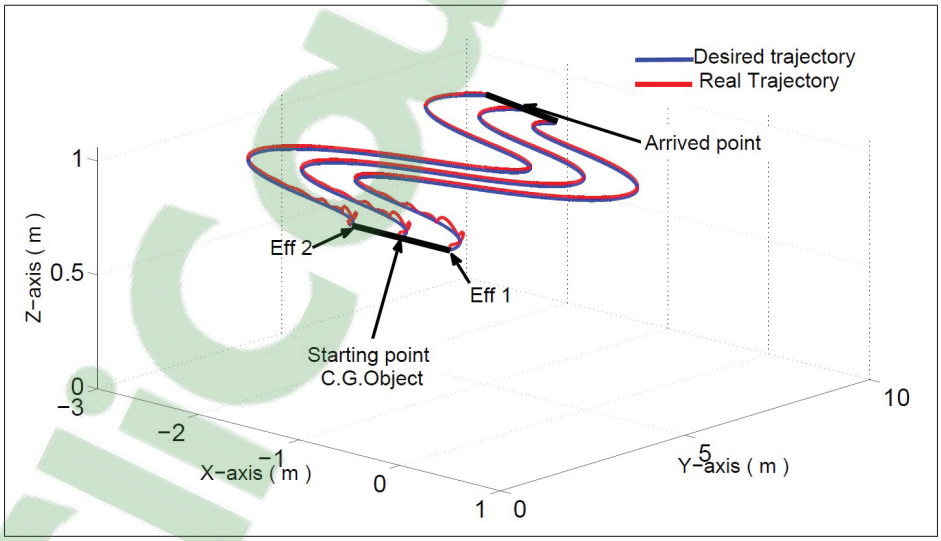

Figure 7.6 Desired and real trajectories of the object

For the second comparison, Figure 7.8. present the sliding surface obtained by the proposed control law and those obtained by the conventional sliding mode, as explained in the design

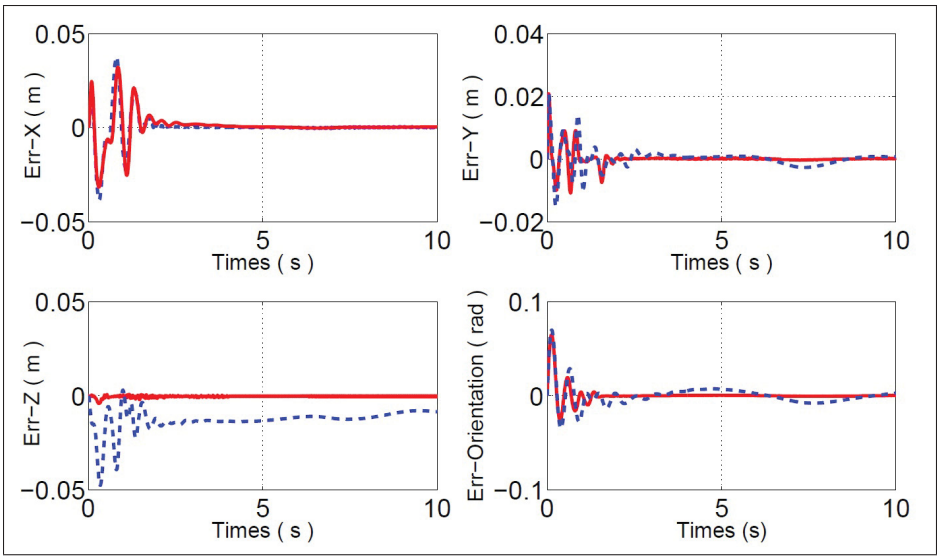

Figure 7.7 Errors: approach given in Wang (2004)(dashed blue line), proposed control law (solid red line)

control section. The results obtained in Figure 7.8-(a-b-c-d) compared to those in Figure 7.8-(e-f-g-h) clearly show that the proposed control law minimize the chattering when the sliding surface is close to zero.

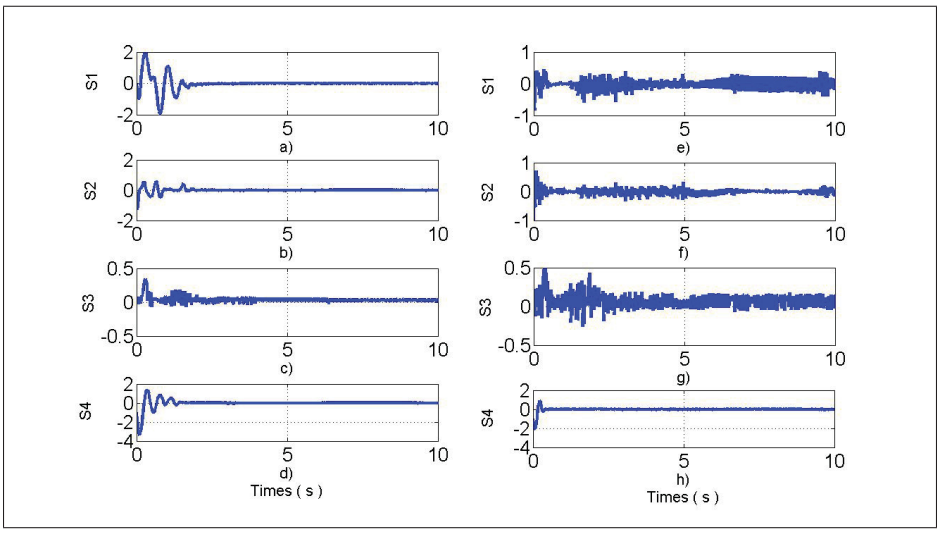

Figure 7.8 Sliding surfaces results: (a,b,c,d) with the proposed law; (e,f,g,h) with conventional sliding law

To validate the results obtained, the proposed controller was implemented in real time. In this test, two physical mobile manipulator robots were used to move a rigid object in coordination.

7.5 Experimental validation

In this section, the proposed control scheme is experimentally tested on two identical mobile manipulator robots named Mob_ETS. In this real-time implementation, a Zigbee communication is installed between the application program developed in Simulink Matlab® and the mobile manipulator robots. The robust adaptive control developed in the previous section is implemented in real-time by using Real Time Workshop (RTW) of Mathworks®. Figure 7.9 shows the entire structure design of the control and the hardware implementation. The two front wheels of the i-th mobile manipulator robot platform are actuated by two HN-GH12-2217Y DC motors (DC-12V-200RPM 30:1), and the angular positions are measured by using encoder sensors (E4P-100-079-D-H-T-B) where all joints of the manipulator arm are actuated by Dynamixel motors (MX-64T). The desired trajectory of the center of gravity of the object is generated in the workspace. In this experimental test, an example of the object trajectory is examined to show the effectiveness of the developed adaptive control law. In this case study, the object displacement is along X-, Y- and Z-axes. The starting point is $P_s = [x_o,\ y_o,\ z_o,\ \beta_o]^T = [0.1,\ -0.1,\ 0.42,\ 0]^T$ and the final point is $P_f = [x_o,\ y_o,\ z_o,\ \beta_o]^T = [4,\ 0,\ 0.48,\ 0]^T$. The control law gains and those of the update law are chosen to be $\gamma_i^{'} = 0.8, K_p = 7.5, K_\lambda = 1.5, K_s = 15$, $\beta = 0.1$ and $K = 5$. The desired internal force vector F_{Id} is parameterized by the Lagrangian multiplier vector $\lambda_{Id} = [\lambda_{Id_x},\ \lambda_{Id_y},\ \lambda_{Id_z}]^T = [1,\ 0,\ 0]^T$. The sampling time is set at 0.015 second.

The trajectory tracking is presented in Figure 7.10. The experimental results in the Cartesian space are presented in Figure 7.11. We can observe that there is a good position and orientation tracking. The results illustrated in Figures. 7.10-7.11, prove the effectiveness of the approach developed and simulated in the last section.

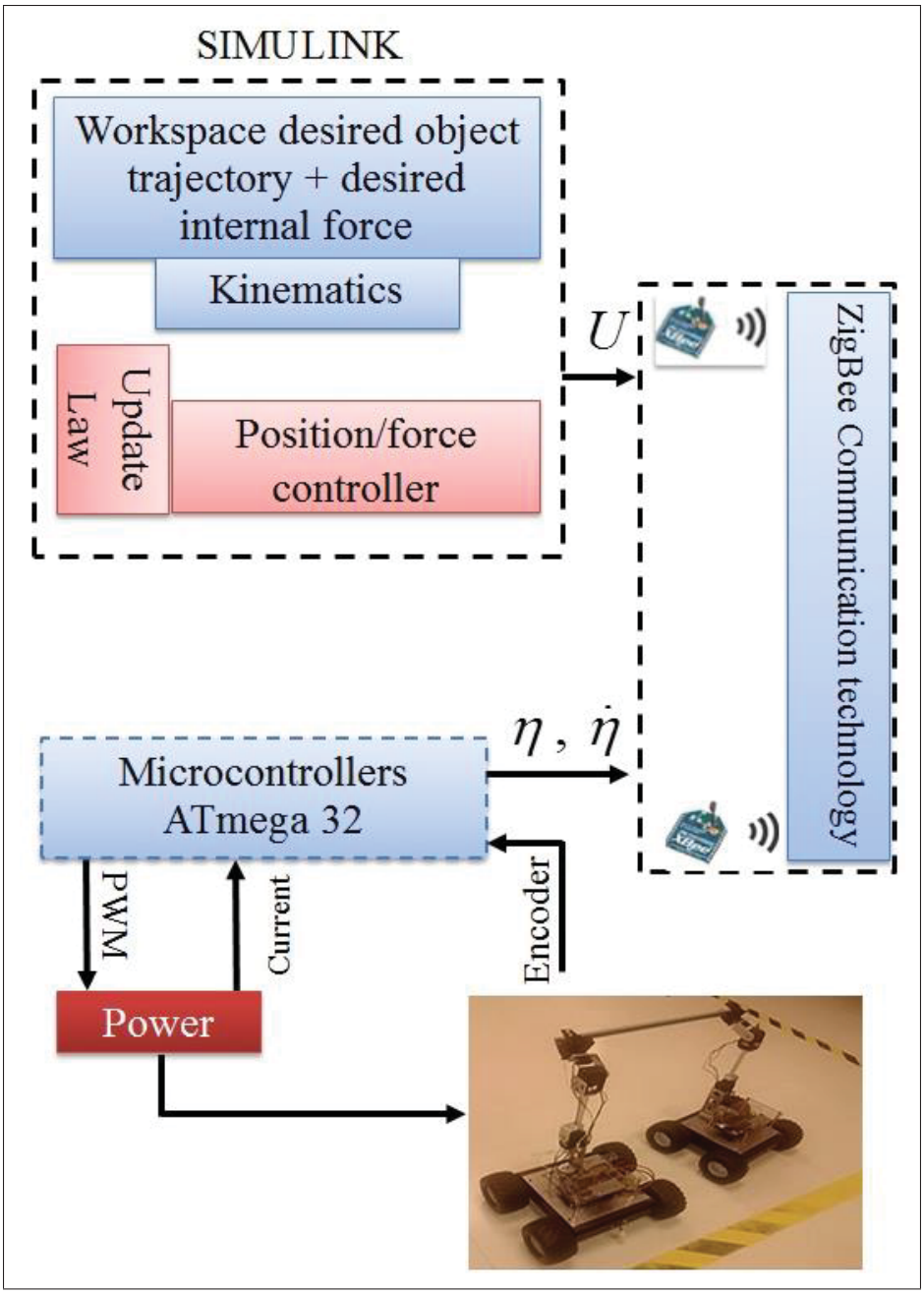

Figure 7.9 Real-time setup

7.6 Conclusion

In this paper, an adaptive coordinated control scheme for multiple mobile manipulator robots transporting a rigid object in coordination has been presented. The desired trajectory of the

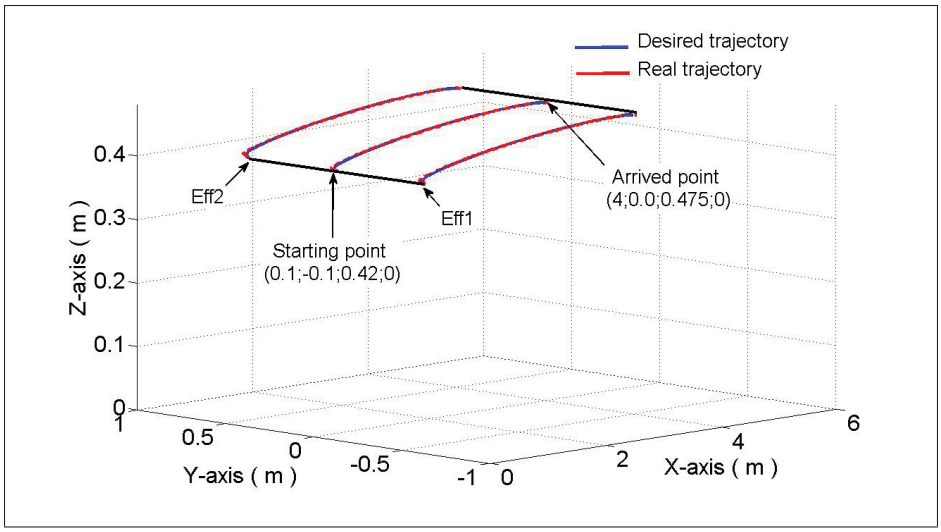

Figure 7.10 Desired and real trajectories of the object

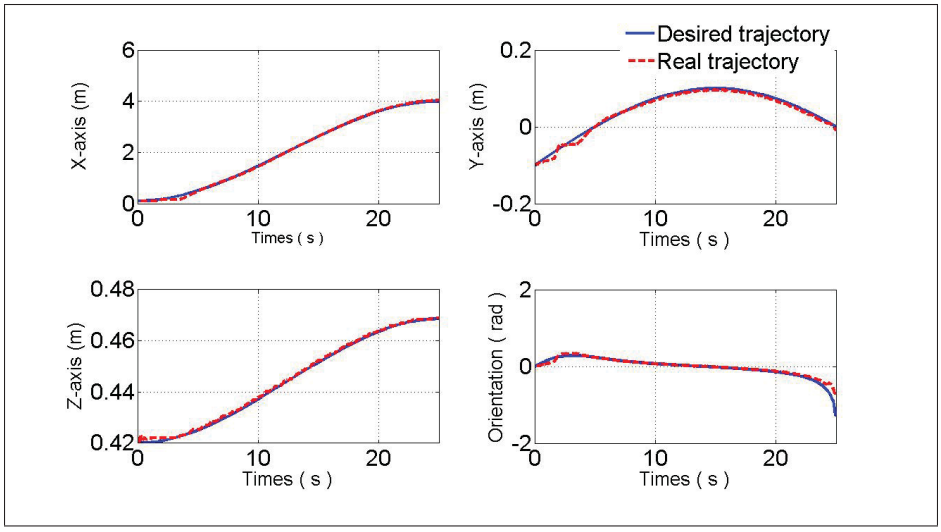

Figure 7.11 Trajectory tracking in Cartesian space:X-axis, Y- axis, Z-axis and orientation

object is generated in the workspace and the parameters of the handling object and the mobile manipulators are estimated on-line based on the adaptive update technique. The control law is designed based on the sliding mode approach combined with a potential function to reduce or limit the chatter phenomenon. An appropriate choice of a Lyapunov function candidate is used to prove the stability of the system. The proposed control design ensures that the workspace position error converges to zero asymptotically and that the error of the internal

force is bounded. The numerical simulation results show the effectiveness of the proposed control. The developed approach was implemented in real time to show the validity of the theoretical development.

CONCLUSION AND RECOMMENDATIONS

This thesis work was focused on developing a consistent control technique for a group of mobile manipulator robots executing a task in coordination. Different nonlinear controllers were simulated and experimentally applied to multiple mobile manipulator transporting a rigid object in coordination. To achieve all of the objectives of this thesis, as a first step, an experimental platform was developed and mounted in the laboratory of GREPCI-ETS to implement and validate the different designed control laws. In the second step, several adaptive coordinated motion/force tracking control were applied, ensuring that the desired trajectory can be tracked under parameter uncertainties and disturbances. The main results in this project can be summarized as follows:

- An adaptive coordinated control based on the virtual decomposition approach was modified and applied to an interconnected robotic systems; this approach was initially developed for manipulator arm mounted on fixed platform. In this work, this technique was combined with different nonlinear approaches such as the Lyapunov technique, the backstepping method and the potential function in the case of mobile robot formation control. All these proposed control schemes ensure a good tracking of the desired motion/force trajectory under unknown parameters of the mobile manipulators and the handled object. These parameters were firstly estimated by using the virtual decomposition approach, then by using the Lyapunov update function technique. The overall stability of the entire system was proved based on the virtual stability of each subsystem, the virtual work notions and the appropriate choice of the Lyapunov candidate function.

- An novel adaptive coordinate control based on the sliding mode approach combined with potential function was simulated numerically and implemented experimentally on the experimental platform developed in the laboratory, as explained above. Potential function was added to reduce or limit the chattering phenomenon. The proposed control law en-

sures that the workspace position error converges to zero asymptotically and that the error of the internal force is bounded. Stability of the robotic systems was proved by using the Lyapunov technique.

Finally, we can conclude that the developed control strategies guarantee a good desired motion/force tracking , compensate the parametric uncertainties of the interconnected robotic system and suppress the bounded disturbances.

Some limitations and problems can be raised in this thesis and can be considered as future work, since all the developed control schemes suppose that the environment is known and do not consider the presence of any obstacle. As recommendation for future work, we will consider more complex and unknown environment with static and dynamic obstacles. In this case an algorithm of obstacle avoidance should be combined with the proposed controller to give the robotic system more robustness. By considering these environments, the developed controllers will not be applied only in laboratory but will also be implemented on real industrial processes.

APPENDIX I

Elements in the regressor matrix Y_B and the parameters vector θ_B: Non-zero elements in the regressor matrix $Y_B \in R^{6x13}$ for the link linear parametrization:

$$Y_B(1,1) = \frac{d}{dt}({}^B v_r)(1) + {}^B v(5)\,{}^B v_r(3) - {}^B v(6)\,{}^B v_r(2) + {}^B g(1) \tag{AI-1}$$

$$Y_B(1,2) = -{}^B v(5)\,{}^B v_r(5) - {}^B v(6)\,{}^B v_r(6)) \tag{AI-2}$$

$$Y_B(1,3) = -\frac{d}{dt}({}^B v_r)(6) + {}^B v(5)\,{}^B v_r(4) \tag{AI-3}$$

$$Y_B(1,4) = \frac{d}{dt}({}^B v_r)(5) + {}^B v(6)\,{}^B v_r(4) \tag{AI-4}$$

$$Y_B(2,1) = \frac{d}{dt}({}^B v_r)(2) + {}^B v(6)\,{}^B v_r(1) - {}^B v(4)\,{}^B v_r(3) + {}^B g(2) \tag{AI-5}$$

$$Y_B(2,2) = \frac{d}{dt}({}^B v_r)(6) + {}^B v(4)\,{}^B v_r(5) \tag{AI-6}$$

$$Y_B(2,3) = -{}^B v(4)\,{}^B v_r(4) - {}^B v(6)\,{}^B v_r(5)) \tag{AI-7}$$

$$Y_B(2,4) = -\frac{d}{dt}({}^B v_r)(4) + {}^B v(6)\,{}^B v_r(5) \tag{AI-8}$$

$$Y_B(3,1) = \frac{d}{dt}({}^B v_r)(3) + {}^B v(4)\,{}^B v_r(2) - {}^B v(5)\,{}^B v_r(1) + {}^B g(3) \tag{AI-9}$$

$$Y_B(3,2) = -\frac{d}{dt}({}^B v_r)(5) + {}^B v(4)\,{}^B v_r(6) \tag{AI-10}$$

$$Y_B(3,3) = \frac{d}{dt}({}^B v_r)(4) + {}^B v(5)\,{}^B v_r(6) \tag{AI-11}$$

$$Y_B(3,4) = -{}^B v(4)\,{}^B v_r(4) - {}^B v(6)\,{}^B v_r(5)) \tag{AI-12}$$

$$Y_B(4,3) = Y_B(3,1) \tag{AI-13}$$

$$Y_B(4,4) = -Y_B(2,1) \tag{AI-14}$$

$$Y_B(4,6) = Y_B(3,3) \tag{AI-15}$$

$$Y_B(4,7) = -Y_B(2,4) \tag{AI-16}$$

$$Y_B(4,8) = Y_B(3,2) \tag{AI-17}$$

$$Y_B(4,9) = -Y_B(2,2) \tag{AI-18}$$

$$Y_B(4,10) = {}^B v(6)\,{}^B v_r(6) - {}^B v(5)\,{}^B v_r(5)) \tag{AI-19}$$

$$Y_B(4,11) = \frac{d}{dt}({}^B v_r)(4) + {}^B v(5)\,{}^B v_r(6) - {}^B v(6)\,{}^B v_r(5) \tag{AI-20}$$

$$Y_B(4,12) = -{}^B v(6)\,{}^B v_r(5) \tag{AI-21}$$

$$Y_B(4,13) = {}^B v(5)\,{}^B v_r(6) \tag{AI-22}$$

$$Y_B(5,2) = -Y_B(3,1) \tag{AI-23}$$

$$Y_B(5,4) = Y_B(1,1) \tag{AI-24}$$

$$Y_B(5,5) = -Y_B(3,2) \tag{AI-25}$$

$$Y_B(5,7) = Y_B(1,4) \tag{AI-26}$$

$$Y_B(5,8) = -Y_B(3,3) \tag{AI-27}$$

$$Y_B(5,9) = {}^B v(4)\,{}^B v_r(4) - {}^B v(6)\,{}^B v_r(6)) \tag{AI-28}$$

$$Y_B(5,10) = Y_B(1,3) \tag{AI-29}$$

$$Y_B(5,11) = {}^B v(6)\,{}^B v_r(4) \tag{AI-30}$$

$$Y_B(5,12) = \frac{d}{dt}({}^B v_r)(5) + {}^B v(6)\,{}^B v_r(4) - {}^B v(4)\,{}^B v_r(6) \tag{AI-31}$$

$$Y_B(5,13) = -{}^B v(4)\,{}^B v_r(6) \tag{AI-32}$$

$$Y_B(6,2) = Y_B(2,1) \tag{AI-33}$$

$$Y_B(6,3) = -Y_B(1,1) \tag{AI-34}$$

$$Y_B(6,5) = Y_B(2,2) \tag{AI-35}$$

$$Y_B(6,6) = -Y_B(1,3) \tag{AI-36}$$

$$Y_B(6,8) = {}^B v(5)\,{}^B v_r(5) - {}^B v(4)\,{}^B v_r(4)) \tag{AI-37}$$

$$Y_B(6,9) = Y_B(2,4) \tag{AI-38}$$

$$Y_B(6,10) = -Y_B(1,4) \tag{AI-39}$$

$$Y_B(6,11) = -{}^B v(5)\,{}^B v_r(4) \tag{AI-40}$$

$$Y_B(6,12) = {}^B v(4)\,{}^B v_r(5) \tag{AI-41}$$

$$Y_B(6,13) = \frac{d}{dt}({}^B v_r)(6) + {}^B v(4)\,{}^B v_r(5) - {}^B v(5)\,{}^B v_r(4) \tag{AI-42}$$

The vector of parameters $\theta_B \in R^{13}$ is given as follows:

$$\theta_B(1) = m_B \tag{AI-43}$$

$$\theta_B(2) = m_B\ {}^B r_{mx} \tag{AI-44}$$

$$\theta_B(3) = m_B\ {}^B r_{my} \tag{AI-45}$$

$$\theta_B(4) = m_B\ {}^B r_{mz} \tag{AI-46}$$

$$\theta_B(5) = m_B\ {}^B r_{mx}^2 \tag{AI-47}$$

$$\theta_B(6) = m_B\ {}^B r_{my}^2 \tag{AI-48}$$

$$\theta_B(7) = m_B\ {}^B r_{mz}^2 \tag{AI-49}$$

$$\theta_B(8) = m_B\ {}^B r_{mx}\ {}^B r_{my} - I_{Bxy} \tag{AI-50}$$

$$\theta_B(9) = m_B\ {}^B r_{mx}\ {}^B r_{mz} - I_{Bxz} \tag{AI-51}$$

$$\theta_B(10) = m_B\ {}^B r_{my}\ {}^B r_{mz} - I_{Byz} \tag{AI-52}$$

$$\theta_B(11) = I_{Bxx} \tag{AI-53}$$

$$\theta_B(12) = I_{Byy} \tag{AI-54}$$

$$\theta_B(13) = I_{Bzz} \tag{AI-55}$$

The following Y_{ai} vector and parameters vector θ_{ai} are defined:

$$Y_{ai} = \begin{bmatrix} \ddot{q}_{ai} & sign(\dot{q}_{ai}) & \dot{q}_{ai} & 1 \end{bmatrix} \tag{AI-56}$$

$$\theta_{ai} = \begin{bmatrix} J_{mai} & k_{cai}) & k_{vai} & c_{ai} \end{bmatrix} \tag{AI-57}$$

APPENDIX II

1. Dynamic and control of the link

The dynamics of the i-*th* rigid body is given in the linear form by the following equation:

$$F^*_{B_i} = M_{B_i}\dot{V}_{B_i} + C_{B_i}V_{B_i} + G_{B_i} = Y_{B_i}\theta_{B_i} \tag{AII-1}$$

where $M_{B_i} \in \mathbb{R}^{6\times6}$ is the matrix of inertial terms, $C_{B_i} \in \mathbb{R}^{6\times6}$ represent the matrix of centrifugal/Coriolis terms, $G_{B_i} \in \mathbb{R}^6$ is the vector related to the gravity.

The vector of resulting forces/moments acting on the rigid body is computed by an iterative process as follows.

$$\begin{aligned} F_{B_n} &= F^*_{B_n} \\ F_{B_{n-1}} &= F^*_{B_{n-1}} + {}^{B_{n-1}}U_{B_n}F_{B_n} \\ &\vdots \\ F_{B_1} &= F^*_{B_1} + {}^{B_1}U_{B_2}F^*_{B_2} + \ldots + {}^{B_1}U_{B_n}F_{B_n} \end{aligned} \tag{AII-2}$$

The dynamics of the i-*th* rigid body based on its required velocity $V^r_{B_i} \in \mathbb{R}^6$ is expressed in the linear form by the following equation:

$$F^{*r}_{B_i} = M_{B_i}\dot{V}^r_{B_i} + C_{B_i}V^r_{B_i} + G_{B_i} = Y_{B_i}\theta_{B_i} \tag{AII-3}$$

Since the physical parameters of the i-*th* rigid body are assumed to be unknown and should to be estimated, then the vector $\hat{\theta}_{B_i} \in \mathbb{R}^{13}$ is used and its equation of control becomes:

$$F^{*r}_{B_i} = Y_{B_i}\hat{\theta}_{B_i} + K_{B_i}(V^r_{B_i} - V_{B_i}) \tag{AII-4}$$

where, $\dot{\hat{\theta}}_{B_i} = \rho_{B_i}Y^T_{B_i}S_{B_i}$ is the parameters adaptation function, and is chosen to ensure system stability, $S_{B_i} = (V^r_{B_i} - V_{B_i})$ and $\rho_{B_i} \in \mathbb{R}^{13\times13}$ is diagonal positive matrix.

Let us consider the non-negative Laypunov candidate function as:

$$v_i = \frac{1}{2}(V_{B_i}^r - V_{B_i})^T M_{B_i}(V_{B_i}^r - V_{B_i}) + \frac{1}{2}\sum_{\gamma=1}^{13}\left(\theta_{i\gamma} - \hat{\theta}_{i\gamma}\right)^2/\rho_{i\gamma} \tag{AII-5}$$

where $\theta_{i\gamma}, \hat{\theta}_{i\gamma}$ denotes the γ-*th* element of $\theta_{i\gamma}$ and $\hat{\theta}_{i\gamma}$ respectively. $\rho_{i\gamma} > 0$ is a parameter update gain. Then based on dynamic of the i-*th* link (A II.1), (A II.2), its equation of control (A II.3),(A II-4) and the update control law given after (A II-4) , the first derivative along time is given by:

$$\dot{v}_i \leq -(V_{B_i}^r - V_{B_i})^T K_{B_i}(V_{B_i}^r - V_{B_i}) + (V_{B_i}^r - V_{B_i})^T (F_{B_i}^{*r} - F_{B_i}^*) \tag{AII-6}$$

Proof: Subtracting (A II-1) from (A II-4) gives:

$$F_{B_i}^{*r} - F_{B_i}^* = M_{B_i}(\dot{V}_{B_i}^r - \dot{V}_{B_i}) + C_{B_i}(V_{B_i}^r - V_{B_i}) + K_{B_i}(V_{B_i}^r - V_{B_i}) - Y_{B_i}(\theta_{B_i} - \hat{\theta}_{B_i}) \tag{AII-7}$$

Based on (A II-7) the time derivative of (A II-5) is given by the following expression:

$$\dot{v}_i = (V_{B_i}^r - V_{B_i})M_{B_i}(\dot{V}_{B_i}^r - \dot{V}_{B_i}) - \sum_{\gamma=1}^{13}(\theta_{B_{i\gamma}} - \hat{\theta}_{B_{i\gamma}})\frac{\dot{\hat{\theta}}_{i\gamma}}{\rho_{i\gamma}} \tag{AII-8}$$

$$\begin{aligned} &= -\left(V_{B_i}^r - V_{B_i}\right) K_{B_i}\left(V_{B_i}^r - V_{B_i}\right) + \left(V_{B_i}^r - V_{B_i}\right)^T \left(F_{B_i}^{*r} - F_{B_i}^*\right) \\ &\quad + \sum_{\gamma=1}^{13}\left(\theta_{B_{i\gamma}} - \hat{\theta}_{B_{i\gamma}}\right)\left[y_{i\gamma}(t)^T\left(V_{B_i}^r - V_{B_i}\right) - \frac{\dot{\hat{\theta}}_{i\gamma}}{\rho_{i\gamma}}\right] \end{aligned} \tag{AII-9}$$

Based on the update law we can prove that (Zhu (2010))

$$\left(\theta_{B_{i\gamma}} - \hat{\theta}_{B_{i\gamma}}\right)\left[y_{i\gamma}(t)^T\left(V_{B_i}^r - V_{B_i}\right) - \frac{\dot{\hat{\theta}}_{i\gamma}}{\rho_{i\gamma}}\right] \leq 0 \tag{AII-10}$$

To complete the prove of the stability, we can also prove that the following equality is given as follows:

$$\begin{aligned} \left(V_{B_i}^r - V_{B_i}\right)^T \left(F_{B_i}^{*r} - F_{B_i}^*\right) &= \left(V_{B_i}^r - V_{B_i}\right)^T \left(F_{B_i}^r - F_{B_i}\right) \\ &\quad - \left(V_{B_i}^r - V_{B_i}\right)^T \ {}^{B_i}U_{T_{i+1}}\left(F_{T_{i+1}}^r - F_{T_{i+1}}\right) \end{aligned}$$

$$= \left(V_{B_i}^r - V_{B_i}\right)^T \left(F_{B_i}^r - F_{B_i}\right) - \left(V_{T_{i+1}}^r - V_{T_{i+1}}\right)^T \left(F_{T_{i+1}}^r - F_{T_{i+1}}\right)$$

$$= p_{B_i} - p_{T_{i+1}} \tag{AII-11}$$

where p_{B_i}, p_{T_i} denote the virtual power flows at the cutting points (Figure 2.2).
Substituting (A II-11) into (A II-6) yields:

$$\dot{v}_i = -\left(V_{B_i}^r - V_{B_i}\right) K_{B_i} \left(V_{B_i}^r - V_{B_i}\right) + p_{B_i} - p_{T_{i+1}} \tag{AII-12}$$

2. Dynamic and control of the actuator

The dynamics of the i-*th* actuator can be expressed by the following dynamic:

$$\tau_{ai} = J_{m_{ai}} \ddot{q}_i + \xi(q_i, \dot{q}_i) \tag{AII-13}$$

where $\xi(q_i, \dot{q}_i)$ represents the friction and gravitation force / torque terms and J_{mai} is the moment of inertia of the motor driving this joint. According to the property of linearity in the parameters, this dynamic can be written in linear form as:

$$\tau_{ai} = Y_{ai} \theta_{ai} \tag{AII-14}$$

where, $\theta_{ai} \in \mathbb{R}^4$ are the column vectors of the dynamic parameters of the motor driving the i-*th* joint and $Y_{ai} \in \mathbb{R}^4$ are the dynamic regressor (row) vectors, also defined in the Appendix I.
The dynamics of the i-*th* joint actuator based on its required velocity q_i^r is expressed in the linear form by the following equation:

$$J_{m_{ai}} \ddot{q}_i^r + \xi(q_i^r, \dot{q}_i^r) = Y_{ai} \theta_{ai} \tag{AII-15}$$

Since the physical parameters of the i-*th* actuator are unknown and need to be estimated, then the vector $\hat{\theta}_{ai}$ is used and its dynamic becomes:

$$\tau_{ai}^r = Y_{ai} \hat{\theta}_{ai} + K_{ai}(\dot{q}_i^r - \dot{q}_i) \tag{AII-16}$$

where $\dot{\hat{\theta}}_{ai} = \rho_{ai} y_{ai}^T S_{ai}$ is the parameters adaptation function, and chosen to ensure system stability; $S_{ai} = \dot{q}_i^r - \dot{q}_i$, and ρ_{ai}, K_{ai} are positive gains. Y_{ai} is the dynamic regressor (row) vectors, defined in Appendix I (Zhu *et al.* (1997),Zhu (2010)).

Finally, the input control torque at the i-th articulation is calculated from the desired torque obtained from (AII-16) τ_i^r and the required force at cutting point B_i, identified $F_{B_i}^r$ as:

$$\tau_i = \tau_{ai}^r + Z^T F_{B^I}^r \tag{AII-17}$$

with $Z = [0\,0\,0\,0\,0\,1]^T$ for the revolute joints and $Z = [0\,0\,1\,0\,0\,0]^T$ for the prismatic joints. Let define the positive Laypunov candidate function as follow:

$$v_{ai} = \frac{1}{2} J_{m_{ai}} (\dot{q}_i^r - \dot{q}_i)^2 + \frac{1}{2} \sum_{i=1}^{4} \left(\theta_{ai\gamma} - \hat{\theta}_{ai\gamma}\right)^2 / \rho_{ai\gamma} \tag{AII-18}$$

where $\theta_{ai\gamma}, \hat{\theta}_{ai\gamma}$ denotes the γ-*th* element of $\theta_{ai\gamma}$ and $\hat{\theta}_{ai\gamma}$ respectively. $\rho_{ai\gamma} > 0$ is a parameter update gain. Then based on dynamic of the i-*th* actuator (AII-13), (AII-15), its equation of control (AII-16) and the update control law given after (AII-16) , the first derivative along time is given by:

$$\dot{v}_{ai} = -(\dot{q}_i^r - \dot{q}_i) J_{m_{ai}} (\ddot{q}_i^r - \ddot{q}_i) - \sum_{\gamma=1}^{4} \left(\theta_{ai\gamma} - \hat{\theta}_{ai\gamma}\right) \frac{\dot{\hat{\theta}}_{ai}}{\rho_{ai\gamma}} \tag{AII-19}$$

$$\dot{v}_{ai} \leq -K_{ai} (\dot{q}_i^r - \dot{q}_i)^2 + (\dot{q}_i^r - \dot{q}_i)(\tau_{ai}^r - \tau_{ai}) \tag{AII-20}$$

Proof: Subtracting (A II-13) from (A II-16) using the definition of Y_{ai} and θ_{ai} from Appendix I yields:

$$\begin{aligned} \tau_{ai}^r - \tau_{ai} = {} & J_{m_{ai}} (\ddot{q}_i^r - \ddot{q}_i) + (\xi(q_i^r, \dot{q}_i^r) - \xi(q_i, \dot{q}_i)) \\ & + K_{ai} (\dot{q}_i^r - \dot{q}_i) - Y_{ai}(t) \left(\theta_{ai} - \hat{\theta}_{ai}\right) \end{aligned} \tag{AII-21}$$

Based on the (A II-21) the time derivative of (A II-18) is obtained as follows:

$$\dot{v}_{ai} = (\dot{q}_i^r - \dot{q}_i) J_{m_{ai}} (\ddot{q}_i^r - \ddot{q}_i) - \sum_{\gamma=1}^{4} \left(\theta_{ai\gamma} - \hat{\theta}_{ai\gamma}\right) \frac{\dot{\hat{\theta}}_{ai\gamma}}{\rho_{ai\gamma}}$$

$$= -K_{ai}\left(\dot{q}_i^r - \dot{q}_i\right)^2 - k_{ci}\left[sign(\dot{q}_i^r) - sign(\dot{q}_i)\right]\left(\dot{q}_i^r - \dot{q}_i\right)$$
$$+ \sum_{\gamma=1}^{4}\left(\theta_{ai\gamma} - \hat{\theta}_{ai\gamma}\right)\left[y_{ai\gamma}(t) - \frac{\dot{\hat{\theta}}_{ai\gamma}}{\rho_{ai\gamma}}\right] + \left(\dot{q}_i^r - \dot{q}_i\right)\left(\tau_{ai}^r - \tau_{ai}\right) \quad \text{(AII-22)}$$

From the update law given after (A II-16)and based on what was explained in (Zhu (2010)), it follows that:

$$\left(\theta_{ai\gamma} - \hat{\theta}_{ai\gamma}\right)\left[y_{ai\gamma}(t) - \frac{\dot{\hat{\theta}}_{ai\gamma}}{\rho_{ai\gamma}}\right] \leq 0 \quad \text{(AII-23)}$$

we have also, the following relationship:

$$-k_{ci}\left[sign(\dot{q}_i^r) - sign(\dot{q}_i)\right]\left(\dot{q}_i^r - \dot{q}_i\right) \leq 0 \quad \text{(AII-24)}$$

Substituting (A II-17) into (A II-13) yields:

$$\left(\dot{q}_i^r - \dot{q}_i\right)\left(\tau_{ai}^r - \tau_{ai}\right) = -\left(\dot{q}_i^r - \dot{q}_i\right)Z^T\left(F_{B_i}^r - F_{B_i}\right) \quad \text{(AII-25)}$$

To complete the prove of the stability, we can also prove that the following equality is given as follows:

$$-\left(\dot{q}_i^r - \dot{q}_i\right)Z^T\left(F_{B_i}^r - F_{B_i}\right) = \left[\left(V_{B_i}^r - V_{B_i}\right) - {}^{T_i}U_{B_i}^T\left(V_{T_i}^r - V_{T_i}\right)\right]\left(F_{B_i}^r - F_{B_i}\right)$$

$$= -\left(V_{B_i}^r - V_{B_i}\right)\left(F_{B_i}^r - F_{B_i}\right)$$
$$+ \left(V_{T_i}^r - V_{T_i}\right)^{T_i}U_{B_i}^T\left(F_{B_i}^r - F_{B_i}\right)$$
$$= -p_{B_i} + p_{T_i} \quad \text{(AII-26)}$$

where p_{B_i}, p_{T_i} denote the virtual power flows at the cutting points (Figure2.2).
Substituting (A II-26) into (A II-20) yields:

$$\dot{v}_{ai} \leq -K_{ai}(\dot{q}_i^r - \dot{q}_i)^2 - p_{B_i} + p_{T_i} \quad \text{(AII-27)}$$

3. Stability of the entire system

Using the same procedure explained above, the non-negative Lyapunov candidate function of the complete system can be chosen as follows:

$$v = \sum_{i=1}^{n} v_i + \sum_{i=1}^{n} v_{ai} \tag{AII-28}$$

From (A II-12) and (A II-27) the first time derivative of (A II-28) is given by:

$$\dot{v} = -\sum_{i=1}^{n} \left(V_{B_i}^r - V_{B_i}\right)^T K_{B_i} \left(V_{B_i}^r - V_{B_i}\right) - \sum_{i=1}^{n} K_{ai} \left(\dot{q}_i^r - \dot{q}_i\right)^2 \tag{AII-29}$$

Since the two virtual power flows of a common frame at a common cutting points take the same magnitude with opposite signs, then these virtual power flows are washed-out in (A II-29).

BIBLIOGRAPHY

Abdelhedi, Fatma and Nabil Derbel. 2017. "Adaptive second order sliding mode control under parametric uncertainties: application to a robotic system". *International Journal of Modelling, Identification and Control*, vol. 27, n° 4, p. 332–341.

Al-Shuka, Hayder FN, B Corves and Wen-Hong Zhu. 2014. "Function approximation technique-based adaptive virtual decomposition control for a serial-chain manipulator". *Robotica*, vol. 32, n° 03, p. 375–399.

Alcocer, A, A Robertsson, A Valera and R Johansson. 2003. "Force estimation and control in robot manipulators". In *Proc. of the 7th IFAC Symp. Robot Control (SYROCO). Wrocław, Poland, September 2003*.

Alcocera, A., A. Robertssona, A. Valerac and R. Johanssona. 2004. "Force estimation and control in robot manipulators". In *A Proceedings Volume from the 7th IFAC Symposium: Robot Control 2003 (SYROCO'03).* p. 55. International Federation of Automatic Control.

Andaluz, Víctor H, Flavio Roberti, Marcos Toibero, Paulo Leica and Ricardo Carelli. 2012. *Adaptive Coordinated Cooperative Control of Multi-Mobile Manipulators*. INTECH Open Access Publisher.

Aranda, Miguel, Gonzalo López-Nicolás, Carlos Sagüés and Michael M Zavlanos. 2015. "Coordinate-free formation stabilization based on relative position measurements". *Automatica*, vol. 57, p. 11–20.

Baklouti, Faten, Sinda Aloui and Abdessattar Chaari. 2016. "Fuzzy sliding mode fault tolerant control for a class of perturbed nonlinear systems". *International Journal of Modelling, Identification and Control*, vol. 25, n° 4, p. 313–322.

Bennewitz, Maren, Wolfram Burgard and Sebastian Thrun. 2001. "Optimizing schedules for prioritized path planning of multi-robot systems". In *Proceedings 2001 ICRA , IEEE International Conference on Robotics and Automation,*. p. 271–276. IEEE.

Bolandi, Hossein and Amir Farhad Ehyaei. 2011. "A novel method for trajectory planning of cooperative mobile manipulators". *Journal of medical signals and sensors*, vol. 1, n° 1, p. 24.

Brahmi, A, Maarouf Saad, Guy Gauthier, Zhu Wen-Hong and J Ghommam. 2013a. "Adaptive control of multiple mobile manipulators transporting a rigid object". *In 2013 CCToMM Symposium on Mechanisms, Machines, and Mechatronics*.

Brahmi, A, M Saad, G Gauthier, B Brahmi, W-H Zhu and J Ghommam. 2016a. "Adaptive backstepping control of mobile manipulator robot based on virtual decomposition approach". In *8th International Conference on Modelling, Identification and Control (ICMIC'16)*. p. 707–712. IEEE.

Brahmi, Abdelkrim, Maarouf Saad, Guy Gauthier, Wen-Hong Zhu and Jawhar Ghommam. 2013b. "Real time control of ANAT robot manipulator using virtual decomposition approach". In *3rd International Conference on Systems and Control (ICSC'13)*. p. 962–967. IEEE.

Brahmi, Abdelkrim, Maarouf Saad, Guy Gauthier, Wen-Hong Zhu and Jawhar Ghommam. 2016b. "Adaptive control of mobile manipulator robot based on virtual decomposition approach". *Proceeding of the 13th International conference on informatics in Control, Automation and Robotics*, vol. 2, p. 254-261.

Brahmi, Abdelkrim, Maarouf Saad, Guy Gauthier, Wen-Hong Zhu and Jawhar Ghommam. 2017. "Tracking Control of Mobile Manipulator Robot Based on Adaptive Backstepping Approach". *International Journal of Digital Signals and Smart Systems*, p. Accepted.

Brock, Oliver, Oussama Khatib and Sriram Viji. 2002. "Task-consistent obstacle avoidance and motion behavior for mobile manipulation". In *Proceedings of the IEEE International Conference on Robotics and Automation, ICRA'02.* p. 388–393. IEEE.

Ceccarelli, Nicola, Mauro Di Marco, Andrea Garulli and Antonio Giannitrapani. 2008. "Collective circular motion of multi-vehicle systems". *Automatica*, vol. 44, n° 12, p. 3025–3035.

Chen, Gang. 2015. "Cooperative controller design for synchronization of networked uncertain Euler–Lagrange systems". *International Journal of Robust and Nonlinear Control*, vol. 25, n° 11, p. 1721–1738.

Chen, Xin and Yangmin Li. 2006. "Cooperative transportation by multiple mobile manipulators using adaptive NN control". In *International Joint Conference on Neural Networks, IJCNN'06.* p. 4193–4200. IEEE.

Chinelato, Caio Igor Gonçalves and Luiz de Siqueira Martins-Filho. 2013. "Control of cooperative mobile manipulators transporting a payload". In *International Congress of Mechanical Engineering (COBEM). ABCM*. p. 9943–9954.

C.O., Luna, Rahman M.H., Saad M., Maarouf, Archambault P.S. and Ferrer S.B. 2015. "Admittance-based upper limb robotic active and active-assistive movements". *International Journal of Advanced Robotic Systems*, vol. 12.

Craig, John J. 2005. *Introduction to robotics: mechanics and control*. Pearson Prentice Hall Upper Saddle River.

Dai, Gong-Bo and Yen-Chen Liu. 2016. "Distributed Coordination and Cooperation Control for Networked Mobile Manipulators". *IEEE Transactions on Industrial Electronics*.

Dai, Yanyan and Suk-Gyu Lee. 2012. "The leader-follower formation control of nonholonomic mobile robots". *International Journal of Control, Automation and Systems*, vol. 10, n° 2, p. 350–361.

Das, Aveek K, Rafael Fierro, Vijay Kumar, James P Ostrowski, John Spletzer and Camillo J Taylor. 2002. "A vision-based formation control framework". *IEEE transactions on robotics and automation*, vol. 18, n° 5, p. 813–825.

Desai, Jaydev P and Vijay Kumar. 1997. "Nonholonomic motion planning for multiple mobile manipulators". In *Proceedings., 1997 IEEE International Conference on Robotics and Automation,*. p. 3409–3414. IEEE.

Desai, J.P., J. Ostrowski and V. Kumar. 1998. "Controlling formations of multiple mobile robots". In *Proceedings of the IEEE International Conference on Robotics and Automation,*. p. 2864–2869. IEEE.

Do, K.D. 2008. "Formation tracking control of unicycle-type mobile robots with limited sensing ranges". *IEEE Transactions on Control Systems Technology*, vol. 16, n° 3, p. 527–538.

Do, K.D. 2010. "Control of nonlinear systems with output tracking error constraints and its application to magnetic bearings". *International Journal of Control*, vol. 83, n° 6, p. 1199–1216.

Du, H. and S. Li. 2012. "Finite-time cooperative attitude control of multiple spacecraft using terminal sliding mode control technique". *International Journal of Modelling, Identification and Control*, vol. 16, n° 4, p. 327–333.

Fallaha, C. J., M. Saad, H. Y. Kanaan and K. Al-Haddad. Feb 2011. "Sliding-Mode Robot Control With Exponential Reaching Law". *IEEE Transactions on Industrial Electronics*, vol. 58, n° 2, p. 600-610.

Fareh, Raouf, Abdelkrim Brahmi, Mohamad Saad, Maarouf Saad and Maamar Bettayeb. 2017. "Tracking control for non-holonomic mobile manipulator using decentralised control strategy". *International Journal of Modelling, Identification and Control*, vol. 28, n° 1, p. 58–69.

Farivarnejad, Hamed, Sean Wilson and Spring Berman. 2016. "Decentralized sliding mode control for autonomous collective transport by multi-robot systems". In *55th IEEE Conference on Decision and Control (CDC'16)*. p. 1826–1833. IEEE.

Fujii, Masakazu, Wataru Inamura, Hiroki Murakami, Kouji Tanaka and Kazuhiro Kosuge. 2007. "Cooperative control of multiple mobile robots transporting a single object with loose handling". In *IEEE International Conference on Robotics and Biomimetics, ROBIO'07*. p. 816–822. IEEE.

Fujimori, Atsushi, Hiroshi Kubota, Naoya Shibata and Yoshinari Tezuka. 2014. "Leader–follower formation control with obstacle avoidance using sonar-equipped mobile robots". *Proceedings of the Institution of Mechanical Engineers, Part I: Journal of Systems and Control Engineering*, vol. 228, n° 5, p. 303–315.

Furuno, Seiji, Motoji Yamamoto and Akira Mohri. 2003. "Trajectory planning of cooperative multiple mobile manipulators". In *Proceedings of the IEEE/RSJ International Conference on Intelligent Robots and Systems,*. p. 136–141. IEEE.

Gakuhari, Harunori, Songmin Jia, Yoshiro Hada and Kunikatsu Takase. 2004. "Real-time navigation for multiple mobile robots in a dynamic environment". In *IEEE Conference on Robotics, Automation and Mechatronics,*. p. 113–118. IEEE.

Ghommam, J, H Mehrjerdi and M Saad. 2013. "Robust formation control without velocity measurement of the leader robot". *Control Engineering Practice*, vol. 21, n° 8, p. 1143–1156.

Ghommam, Jawhar, Hasan Mehrjerdi, Maarouf Saad and Faiçal Mnif. 2010. "Formation path following control of unicycle-type mobile robots". *Robotics and Autonomous Systems*, vol. 58, n° 5, p. 727–736.

Ghommam, Jawhar, Hasan Mehrjerdi and Maarouf Saad. 2011. "Leader-follower based formation control of nonholonomic robots using the virtual vehicle approach". In *IEEE International Conference on Mechatronics (ICM'11),*. p. 516–521. IEEE.

Guozheng, Yan, Wang Yu and Lin Liangming. 2002. "The multiple robots path-planning based on dynamic programming". In *Proceedings of the 4th World Congress on Intelligent Control and Automation, 2002.* p. 1148–1152. IEEE.

Hekmatfar, Taher, Ellips Masehian and Seyed Javad Mousavi. 2014. "Cooperative object transportation by multiple mobile manipulators through a hierarchical planning architecture". In *Second RSI/ISM International Conference on Robotics and Mechatronics (ICRoM'14),*. p. 503–508. IEEE.

Hirata, Y., T. Sawada, Zhi-Dong Wang and K. Kosuge. Aug 2004a. "Leader-follower type motion control algorithm of multiple mobile robots with dual manipulators for handling a single object in coordination". In *Proceedings of the International Conference on Intelligent Mechatronics and Automation,*. p. 362-367.

Hirata, Yasuhisa, Kazuhiro Kosuge, Hajime Asama, Hayato Kaetsu and Kuniaki Kawabata. 1999. "Decentralized control of mobile robots in coordination". In *Proceedings of the IEEE International Conference on Control Applications,*. p. 1129–1134. IEEE.

Hirata, Yasuhisa, Youhei Kume, Takuro Sawada, Zhi-Dong Wang and Kazuhiro Kosuge. 2004b. "Handling of an object by multiple mobile manipulators in coordination based on caster-like dynamics". In *Proceedings of the IEEE International Conference on Robotics and Automation, ICRA'04.* p. 807–812. IEEE.

Hirata, Yasuhisa, Takuro Sawada, Zhi-Dong Wang and Kazuhiro Kosuge. 2004c. "Leader-follower type motion control algorithm of multiple mobile robots with dual manipulators for handling a single object in coordination". In *Proceedings of the International Conference on Intelligent Mechatronics and Automation,*. p. 362–367. IEEE.

Hollerbach, John M. 1980. "A recursive lagrangian formulation of maniputator dynamics and a comparative study of dynamics formulation complexity". *IEEE Transactions on Systems, Man, and Cybernetics*, vol. 10, n° 11, p. 730–736.

Iwamura, Makoto, Motoji Yamamoto and Akira Mohri. 2000. "A gradient-based approach to collision-free quasi-optimal trajectory planning of nonholonomic systems". In *Proceedings of the IEEE/RSJ International Conference on Intelligent Robots and Systems, (IROS'00).* p. 1734–1740. IEEE.

Jadbabaie, Ali, Jie Lin and A Stephen Morse. 2003. "Coordination of groups of mobile autonomous agents using nearest neighbor rules". *IEEE Transactions on automatic control*, vol. 48, n° 6, p. 988–1001.

Jean, J-H and L-C Fu. 1993. "An adaptive control scheme for coordinated multimanipulator systems". *IEEE Transactions on Robotics and Automation*, vol. 9, n° 2, p. 226–231.

Kang, Sung-Mo and Hyo-Sung Ahn. 2016. "Design and realization of distributed adaptive formation control law for multi-agent systems with moving leader". *IEEE Transactions on Industrial Electronics*, vol. 63, n° 2, p. 1268–1279.

Karray, Amal and Moez Feki. 2014. "Adaptive tracking control of a mobile manipulator actuated by DC motors". *International Journal of Modelling, Identification and Control*, vol. 21, n° 2, p. 193–201.

Karray, Amal and Moez Feki. 2017. "Controlling a mobile manipulator actuated by DC motors and a single phase H-bridge inverter". *International Journal of Modelling, Identification and Control*, vol. 28, n° 2, p. 125–134.

Khan, Muhammad Umer, Shuai Li, Qixin Wang and Zili Shao. 2016. "Formation Control and Tracking for Co-operative Robots with Non-holonomic Constraints". *Journal of Intelligent and Robotic Systems*, vol. 82, n° 1, p. 163–174.

Khatib, O. Mar 1985. "Real-time obstacle avoidance for manipulators and mobile robots". In *Proceedings. 1985 IEEE International Conference on Robotics and Automation*. p. 500-505.

Khatib, O, Kazu Yokoi, K Chang, Diego Ruspini, Robert Holmberg and Arancha Casal. 1996a. "Coordination and decentralized cooperation of multiple mobile manipulators". *Journal of Robotic Systems*, vol. 13, n° 11, p. 755–764.

Khatib, Oussama. 1986. "Real-time obstacle avoidance for manipulators and mobile robots". In *Autonomous robot vehicles*, p. 396–404. Springer.

Khatib, Oussama, Kazu Yokoi, K Chang, Diego Ruspini, Robert Holmberg and Arancha Casal. 1996b. "Vehicle/arm coordination and multiple mobile manipulator decentralized cooperation". In *Proceedings of the 1996 IEEE/RSJ International Conference on Intelligent Robots and Systems' 96, IROS 96,.* p. 546–553. IEEE.

Kosuge, Kazuhiro and Tomohiro Oosumi. 1996. "Decentralized control of multiple robots handling an object". In *Proceedings of the IEEE/RSJ International Conference on Intelligent Robots and Systems' IROS'96*. p. 318–323. IEEE.

Kosuge, Kazuhiro, Yasuhisa Hirata, Hajime Asama, Hayato Kaetsu and Kuniaki Kawabata. 1999. "Motion control of multiple autonomous mobile robots handling a large object in coordination". In *Proceedings of the IEEE International Conference on Robotics and Automation,*. p. 2666–2673. IEEE.

Kume, Yohei, Yasuhisa Hirata and Kazuhiro Kosuge. 2007. "Coordinated motion control of multiple mobile manipulators handling a single object without using force/torque sensors". In *IEEE/RSJ International Conference on Intelligent Robots and Systems, IROS'07*. p. 4077–4082. IEEE.

Kume, Youhei, Yasuhisa Hirata, Kazuhiro Kosuge, Hajime Asama, Hayato Kaetsu and Kuniaki Kawabata. 2001. "Decentralized control of multiple mobile robots transporting a single object in coordination without using force/torque sensors". In *Proceedings of the IEEE International Conference on Robotics and Automation, ICRA'01*. p. 3004–3009. IEEE.

Latombe, Jean-Claude. 2012. *Robot motion planning*. Springer Science & Business Media.

LaValle, Steven M. 2006. *Planning algorithms*. Cambridge university press.

Lawton, Jonathan RT, Randal W Beard and Brett J Young. 2003. "A decentralized approach to formation maneuvers". *IEEE Transactions on Robotics and Automation*, vol. 19, n° 6, p. 933–941.

Lewis, M Anthony and Kar-Han Tan. 1997. "High precision formation control of mobile robots using virtual structures". *Autonomous Robots*, vol. 4, n° 4, p. 387–403.

Li, Hao and Simon X Yang. 2003. "A behavior-based mobile robot with a visual landmark-recognition system". *IEEE/ASME transactions on mechatronics*, vol. 8, n° 3, p. 390–400.

Li, Huiping, Pan Xie and Weisheng Yan. 2016. "Receding horizon formation tracking control of constrained underactuated autonomous underwater vehicles". *IEEE Transactions on Industrial Electronics*.

Li, Xiaohai and Jizhong Xiao. 2005. "Robot formation control in leader-follower motion using direct Lyapunov method". *International Journal of Intelligent Control and Systems*, vol. 10, n° 3, p. 244–250.

Li, Z., S. S. Ge, M. Adams and W. S. Wijesoma. 2007. "Robust Adaptive Control of Cooperating Mobile Manipulators with Relative Motion". In *IEEE 22nd International Symposium on Intelligent Control*. p. 351-356.

Li, Zhijun and Shuzhi Sam Ge. 2013. *Fundamentals in Modeling and Control of Mobile Manipulators*. CRC Press.

Li, Zhijun and Chun-Yi Su. 2013. "Neural-adaptive control of single-master–multiple-slaves teleoperation for coordinated multiple mobile manipulators with time-varying communication delays and input uncertainties". *IEEE transactions on neural networks and learning systems*, vol. 24, n° 9, p. 1400–1413.

Li, Zhijun, Shuzhi Sam Ge and Zhuping Wang. 2008. "Robust adaptive control of coordinated multiple mobile manipulators". *Mechatronics*, vol. 18, n° 5, p. 239–250.

Li, Zhijun, Pey Yuen Tao, Shuzhi Sam Ge, Martin Adams and Wijerupage Sardha Wijesoma. 2009. "Robust adaptive control of cooperating mobile manipulators with relative motion". *IEEE Transactions on Systems, Man, and Cybernetics, Part B (Cybernetics)*, vol. 39, n° 1, p. 103–116.

Li, Zhijun, Chenguang Yang and Yong Tang. 2013. "Decentralised adaptive fuzzy control of coordinated multiple mobile manipulators interacting with non-rigid environments". *IET Control Theory and Applications*, vol. 7, n° 3, p. 397–410.

Liu, Haitao and Tie Zhang. 2013. "Neural network-based robust finite-time control for robotic manipulators considering actuator dynamics". *Robotics and Computer-Integrated Manufacturing*, vol. 29, n° 2, p. 301–308.

Liu, Xiangyu, Ping Zhang and Guanglong Du. 2016. "Hybrid adaptive impedance-leader-follower control for multi-arm coordination manipulators". *Industrial Robot: An International Journal*, vol. 43, n° 1, p. 112–120.

Liu, Xiaoyang, Nan Jiang, Jinde Cao, Shumei Wang and Zhengxin Wang. 2013. "Finite-time stochastic stabilization for BAM neural networks with uncertainties". *Journal of the Franklin Institute*, vol. 350, n° 8, p. 2109–2123.

Liu, Xiaoyang, Ju H Park, Nan Jiang and Jinde Cao. 2014. "Nonsmooth finite-time stabilization of neural networks with discontinuous activations". *Neural Networks*, vol. 52, p. 25–32.

Mai, Thang-Long and Yaonan Wang. 2014. "Adaptive-backstepping force/motion control for mobile-manipulator robot based on fuzzy CMAC neural networks". *Control Theory and Technology*, vol. 12, n° 4, p. 368–382.

Mbede, Jean Bosco, Shugen Ma, Y Toure, V Graefe and Lei Zhang. 2004. "Robust neuro-fuzzy navigation of mobile manipulator among dynamic obstacles". In *Proceedings of the IEEE International Conference on Robotics and Automation, ICRA'04,*. p. 5051–5057. IEEE.

Mehrez, O., Zyada Z., Abbas H.S. and Abo-Ismail A.A. 2016. "Non-prehensile manipulation planning of a three-rigid-link object using two cooperative robot arms". *International Journal of Modelling, Identification and Control*, vol. 26, n° 1, p. 19–31.

Mehrjerdi, Hasan, Jawhar Ghommam and Maarouf Saad. 2011. "Nonlinear coordination control for a group of mobile robots using a virtual structure". *Mechatronics*, vol. 21, n° 7, p. 1147–1155.

Ochoa Luna, Cristóbal, Mohammad Habibur Rahman, Maarouf Saad, Philippe S Archambault and Steven Bruce Ferrer. 2015. "Admittance-Based Upper Limb Robotic Active and Active-Assistive Movements". *International Journal of Advanced Robotic Systems*, vol. 12, n° 9, p. 117.

Ogren, P, N Egerstedt and Xiaoming Hu. 2000a. "Reactive mobile manipulation using dynamic trajectory tracking". In *Proceedingsof the IEEE International Conference on Robotics and Automation, ICRA'00.* p. 3473–3478. IEEE.

Ogren, P, L Petersson, M Egerstedt and X Hu. 2000b. "Reactive mobile manipulation using dynamic trajectory tracking: design and implementation". In *Proceedings of the 39th IEEE Conference on Decision and Control,.* p. 3001–3006. IEEE.

Pajak, Grzegorz, Iwona Pajak and Miroslaw Galicki. 2004. "Trajectory planning of multiple manipulators". In *Proceedings of the Fourth International Workshop on Robot Motion and Control, RoMoCo'04.* p. 121–126. IEEE.

Panagou, Dimitra, Dušan M Stipanović and Petros G Voulgaris. 2016. "Distributed coordination control for multi-robot networks using Lyapunov-like barrier functions". *IEEE Transactions on Automatic Control*, vol. 61, n° 3, p. 617–632.

Papadopoulos, E. and J. Poulakakis. 2000. "Planning and model-based control for mobile manipulators". In *Proceedings of the IEEE/RSJ International Conference on Intelligent Robots and Systems*. p. 1810–1815.

Park, Jaeheung and Oussama Khatib. 2008. "Robot multiple contact control". *Robotica*, vol. 26, n° 05, p. 667–677.

Peng, Zhaoxia, Guoguang Wen, Ahmed Rahmani and Yongguang Yu. 2015. "Distributed consensus-based formation control for multiple nonholonomic mobile robots with a specified reference trajectory". *International Journal of Systems Science*, vol. 46, n° 8, p. 1447–1457.

Petitti, Antonio, Antonio Franchi, Donato Di Paola and Alessandro Rizzo. 2016. "Decentralized motion control for cooperative manipulation with a team of networked mobile manipulators". In *IEEE International Conference on Robotics and Automation (ICRA'16),.* p. 441–446. IEEE.

Qian, Dianwei, Shiwen Tong, Jinrong Guo and SukGyu Lee. 2015. "Leader-follower-based formation control of nonholonomic mobile robots with mismatched uncertainties via integral sliding mode". *Proceedings of the Institution of Mechanical Engineers, Part I: Journal of Systems and Control Engineering*, vol. 229, n° 6, p. 559–569.

Ren, Wei and Randal Beard. 2004. "Decentralized scheme for spacecraft formation flying via the virtual structure approach". *Journal of Guidance, Control, and Dynamics*, vol. 27, n° 1, p. 73–82.

Sayyaadi, H and M Babaee. 2014. "Control of nonholonomic mobile manipulators for cooperative object transportation". *Scientia Iranica. Transaction B, Mechanical Engineering*, vol. 21, n° 2, p. 347.

Shao, Nuan, Huiguang Li, Xueli Wu and Guoyou Li. 2015. "Distributed containment control and state observer design for multi-agent robotic system". *International Journal of Modelling, Identification and Control*, vol. 23, n° 3, p. 193–203.

Shaw, Elaine, Hoam Chung, J Karl Hedrick and Shankar Sastry. 2007. "Unmanned helicopter formation flight experiment for the study of mesh stability". In *Cooperative Systems*, p. 37–56. Springer.

Siciliano, Bruno and Oussama Khatib. 2016. *Springer handbook of robotics*. Springer.

Slotine, J.J.E., W. Li et al. 1991. *Applied nonlinear control*. prentice-Hall Englewood Cliffs, NJ.

Spong, Mark W, Seth Hutchinson and Mathukumalli Vidyasagar. 2006. *Robot modeling and control*. Wiley New York.

Sugar, Thomas G and Vijay Kumar. 2002. "Control of cooperating mobile manipulators". *IEEE Transactions on robotics and automation*, vol. 18, n° 1, p. 94–103.

Sun, X. and D. Gong. 2004a. "Multi-robot moving path planning based on coevolutionary algorithm". In *Fifth World Congress on Intelligent Control and Automation*. p. 2231–2235.

Sun, Xiaoyan and Dunwei Gong. 2004b. "Multi-robot moving path planning based on coevolutionary algorithm". In *Fifth World Congress on Intelligent Control and Automation, WCICA 2004.* p. 2231–2235. IEEE.

Tan, Jindong and Ning Xi. 2001. "Unified model approach for planning and control of mobile manipulators". In *Proceedings of the IEEE International Conference on Robotics and Automation,ICRA'01.* p. 3145–3152. IEEE.

Tang, Chao, Chunquan Xu, Aiguo Ming and Makoto Shimojo. 2009. "Cooperative control of two mobile manipulators transporting objects on the slope". In *International Conference on Mechatronics and Automation, ICMA'09*. p. 2805–2810. IEEE.

Tanner, Herbert G, Kostas J Kyriakopoulos and NJ Krikelis. 1998. "Modeling of multiple mobile manipulators handling a common deformable object". *Journal of Robotic Systems*, vol. 15, n° 11, p. 599–623.

Tanner, Herbert G, Savvas G Loizou and Kostas J Kyriakopoulos. 2003. "Nonholonomic navigation and control of cooperating mobile manipulators". *IEEE Transactions on robotics and automation*, vol. 19, n° 1, p. 53–64.

Tzafestas, Costas S, Platon A Prokopiou and Spyros G Tzafestas. 1998. "Path planning and control of a cooperative three-robot system manipulating large objects". *Journal of intelligent and robotic systems*, vol. 22, n° 2, p. 99–116.

Vannoy, John and Jing Xiao. 2006. "Real-time adaptive mobile manipulator motion planning". In *IEEE/RSJ International Conference on Intelligent Robots and Systems,*. p. 10–10. IEEE.

Vannoy, John and Jing Xiao. 2007a. "Real-time tight coordination of mobile manipulators in unknown dynamic environments". In *IEEE/RSJ International Conference on Intelligent Robots and Systems, IROS'07.* p. 2513–2519. IEEE.

Vannoy, John and Jing Xiao. 2007b. "Real-time motion planning of multiple mobile manipulators with a common task objective in shared work environments". In *IEEE International Conference on Robotics and Automation,*. p. 20–26. IEEE.

Vargas-Jacob, Juan A, José J Corona-Sánchez and H Rodríguez-Cortés. 2016. "Experimental implementation of a leader-follower strategy for quadrotors using a distributed architecture". *Journal of Intelligent and Robotic Systems*, vol. 84, n° 1-4, p. 435–452.

Wang, YaoNan, ThangLong Mai and JianXu Mao. 2014. "Adaptive motion/force control strategy for non-holonomic mobile manipulator robot using recurrent fuzzy wavelet neural networks". *Engineering Applications of Artificial Intelligence*, vol. 34, p. 137–153.

Wang, ZP, SS Ge and TH Lee. 2004. "Robust motion/force control of uncertain holonomic/nonholonomic mechanical systems". *IEEE/ASME transactions on mechatronics*, vol. 9, n° 1, p. 118–123.

Wen, Guoguang, Zhaoxia Peng, Ahmed Rahmani and Yongguang Yu. 2014. "Distributed leader-following consensus for second-order multi-agent systems with nonlinear inherent dynamics". *International Journal of Systems Science*, vol. 45, n° 9, p. 1892–1901.

Wen, Guoguang, Yongguang Yu, Zhaoxia Peng and Ahmed Rahmani. 2016. "Distributed finite-time consensus tracking for nonlinear multi-agent systems with a time-varying reference state". *International Journal of Systems Science*, vol. 47, n° 8, p. 1856–1867.

Xiao, Hanzhen, Zhijun Li and C Chen. 2016. "Formation Control of Leader-Follower Mobile Robots Systems Using Model Predictive Control Based on Neuro-Dynamics Optimization". *IEEE Transaction on Industrial Electronics*, vol. 63, n° 9, p. 5752–5762.

Y., Hirata, Kosuge K., Hajime A., Hayato K. and Kuniaki K. 1999. "Motion control of multiple autonomous mobile robots handling a large object in coordination". In *Proceedings of the IEEE International Conference on Robotics and Automation,*. p. 2666–2673.

Yamamoto, Yoshio and Shinsuke Fukuda. 2002. "Trajectory planning of multiple mobile manipulators with collision avoidance capability". In *Proceedings of the IEEE International Conference on Robotics and Automation, ICRA'02.* p. 3565–3570. IEEE.

Yamamoto, Yoshio and Xiaoping Yun. 1996. "Effect of the dynamic interaction on coordinated control of mobile manipulators". *IEEE Transactions on Robotics and Automation*, vol. 12, n° 5, p. 816–824.

Yan, X.-G., Zhang Q., Spurgeon S.K., Zhu Q. and Fridman L.M. 2014. "Decentralised control for complex systems–an invited survey". *International Journal of Modelling, Identification and Control*, vol. 22, n° 4, p. 285–297.

Yin, Shen, Hongyan Yang and Okyay Kaynak. 2016. "Coordination Task Triggered Formation Control Algorithm for Multiple Marine Vessels". *IEEE Transactions on Industrial Electronics*.

Yohei, K., Yasuhisa H. and Kazuhiro K. 2007. "Coordinated motion control of multiple mobile manipulators handling a single object without using force/torque sensors". In *IEEE/RSJ International Conference on Intelligent Robots and Systems*. p. 4077–4082.

Yoshimura, Toshio. 2015. "Adaptive fuzzy backstepping control for MIMO uncertain discrete-time nonlinear systems using a set of noisy measurements". *International Journal of Modelling, Identification and Control*, vol. 23, n° 4, p. 336–345.

Yu, Junyan and Long Wang. 2012. "Group consensus of multi-agent systems with directed information exchange". *International Journal of Systems Science*, vol. 43, n° 2, p. 334–348.

Yu, Xiao and Lu Liu. 2016a. "Distributed formation control of nonholonomic vehicles subject to velocity constraints". *IEEE Transactions on Industrial Electronics*, vol. 63, n° 2, p. 1289–1298.

Yu, Xiao and Lu Liu. 2016b. "Distributed circular formation control of ring-networked nonholonomic vehicles". *Automatica*, vol. 68, p. 92–99.

Yu, Xiao and Lu Liu. 2017. "Cooperative control for moving-target circular formation of nonholonomic vehicles". *IEEE Transactions on Automatic Control*, vol. 62, n° 7, p. 3448–3454.

Z.-D., Wang and Kosuge K. 2004. "Leader-Follower type Motion Control Algorithm of Multiple Mobile Robots with Dual Manipulators for Handling a Single Object in Coordination".

Zhao, Dongya, Shaoyuan Li and Quanmin Zhu. 2016. "Adaptive synchronised tracking control for multiple robotic manipulators with uncertain kinematics and dynamics". *International Journal of Systems Science*, vol. 47, n° 4, p. 791–804.

Zheng, Ronghao, Yunhui Liu and Dong Sun. 2015. "Enclosing a target by nonholonomic mobile robots with bearing-only measurements". *Automatica*, vol. 53, p. 400–407.

Zheng, Taixiong and Xiangyang Zhao. 2006. "A novel approach for multiple mobile robot path planning in dynamic unknown environment". In *IEEE Conference on Robotics, Automation and Mechatronics,*. p. 1–5. IEEE.

Zhijun, L. and C. Weidong. 2008. "Adaptive neural-fuzzy control of uncertain constrained multiple coordinated nonholonomic mobile manipulators". *Engineering Applications of Artificial Intelligence*, vol. 21, n° 7, p. 985–1000.

Zhijun, L., Y. Chenguang and T. Yong. 2013. "Decentralised adaptive fuzzy control of coordinated multiple mobile manipulators interacting with non-rigid environments". *IET Control Theory and Applications*, vol. 7, n° 3, p. 397–410.

Zhijun, L., D. Shuming, S. Chun-Yi, L. Guanglin, Y. Zhangguo, L. Yanjun and M. Wang. 2014. "Decentralised adaptive control of cooperating Robotic manipulators with disturbance observers". *IET Control Theory and Applications*, vol. 8, n° 7, p. 515–521.

Zhu, Anmin and Simon X Yang. 2003. "Path planning of multi-robot systems with cooperation". In *Proceedings of the IEEE International Symposium on Computational Intelligence in Robotics and Automation,*. p. 1028–1033. IEEE.

Zhu, Wen-Hong. 2010. *Virtual Decomposition Control: Toward Hyper Degrees of Freedom Robots*. Springer Science & Business Media.

Zhu, Wen-Hong, Yu-Geng Xi, Zhong-Jun Zhang, Zeungnam Bien and Joris De Schutter. 1997. "Virtual decomposition based control for generalized high dimensional robotic systems with complicated structure". *IEEE Transactions on Robotics and Automation*, vol. 13, n° 3, p. 411–436.